ČESKÉ VYSOKÉ UČENÍ TECHNICKÉ V PRAZE, FAKULTA ELEKTROTECHNICKÁ

CZECH TECHNICAL UNIVERSITY IN PRAGUE, FACULTY OF ELECTRICAL ENGINEERING

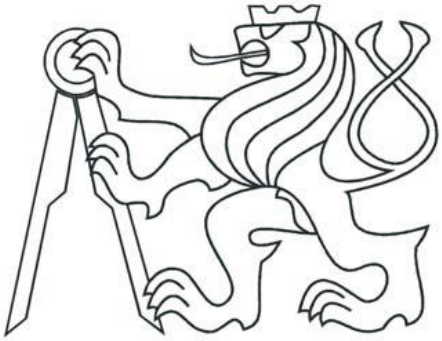

Habilitation Thesis

Recent Advanced Methods and Results in Distributed Cooperative Control

Nové pokročilé metody a výsledky v distribuovaném kooperativním řízení

assist. prof. **Kristian Hengster Movric,** PhD.

Prague, 2018

SUMMARY

The presented habilitation treatise takes the form of a collection of selected journal and conference papers published by the applicant in the recent five years. The unifying theme of distributed cooperative control can be seen as a common thread tying the whole collection together. Taken together, these present an author's contribution towards the current state-of-the-art in cooperative control. They bring interesting novel theoretical results and compelling applications, as well as open potential avenues of future research. In particular, the first chapters describe theoretical results for *homogeneous agents' state synchronization* and *heterogeneous agent output synchronization*. The following two chapters bring some applications to a compelling problem of distributed estimation and control, with specific focus on, but not limited to, distributed vibration reduction. Final chapter considers adaptation to yield completely distributed synchronization protocols.

A concise exposition of related recent results in distributed control of *homogeneous agents*, in Chapter 1, provides a wider framework for two immediate sequels. First of these, Chapter 2, brings technical details on state synchronization of homogeneous agents using *static output-feedback.* The following Chapter 3, on the other hand, extends the synchronizing region methods by considering *communication delays*. The fourth chapter, in contrast, considers general *heterogeneous agents*; providing conditions for output-synchronization and an L_2-bound in case of disturbances acting on the system. Building further on the revealed necessary and sufficient single-agents' conditions required for this, the fifth chapter casts output-synchronization and disturbance suppression in the form of graphical games.

On the applied side, Chapter 6 proposes networked observers that distributively fuse plant's estimates for control of large linear-time-invariant plants. If several measurements of differing reliability are available, one can further attempt *sensor fusion,* as discussed in Chapter 7. This then ideally improves on even the most precise measurements. The final Chapter 8 investigates adaptive consensus protocols, replacing the only remaining centralized piece of information required in the synchronizing region-based designs with dynamic adaptation. These results are applicable, in principle, to all synchronizing region based designs, which, in turn, makes them all fully distributed.

SOUHRN

Prezentovaný habilitační spis má formu souboru vybraných časopiseckých a konferenčních článků, které uchazeč publikoval v posledních pěti letech. Jednotící téma distribuovaného kooperativního řízení lze považovat za společnou nit spojující celou sbírku dohromady. Tyto články představují příspěvek autora k současnému stavu poznání v kooperativním řízení. Přinášejí zajímavé nové teoretické výsledky a slibné aplikace, stejně jako otevřené možnosti budoucího výzkumu. Zejména první kapitoly popisují teoretické výsledky pro synchronizaci stavu homogenních agentů a synchronizaci výstupu heterogenních agentů. Následující dvě kapitoly přinášejí některé aplikace k důležitému problému distribuovaného odhadu a řízení se zvláštním zaměřením na distribuované snížení vibrací. Závěrečná kapitola se zabývá adaptivními protokoly, které přináší úplnou distribuovanou synchronizaci.

Stručné představení souvisejících nedávných výsledků v distribuovaném řízení homogenních agentů v kapitole 1 poskytuje širší rámec pro dvě následující kapitoly. První z nich, kapitola 2, přináší technické detaily o synchronizaci stavu homogenních agentů pomocí statické výstupní zpětné vazby. Následující kapitola 3 na druhé straně rozšiřuje metody synchronizační oblasti o zahrnutí komunikačních zpoždění. Čtvrtá kapitola se naopak věnuje všeobecným heterogenním agentům a představuje podmínky pro výstupní synchronizaci a potlačení poruch působících na systém. Pátá kapitola na základě odhalených nezbytných a postačujících podmínek ukazuje synchronizaci výstupů a potlačení poruch v podobě grafických her.

V souvislosti s aplikacemi kapitola 6 navrhuje síťové pozorovatele, kteří slučují odhady stavů při řízení velkých lineárních časově invariantních systémů. Pokud je k dispozici několik měření rozdílné spolehlivosti, lze se pokusit o fúzi senzorů, jak je uvedeno v kapitole 7. Tím lze zlepšit i nejpřesnější měření. Závěrečná kapitola 8 zkoumá protokoly adaptivního konsenzu nahrazením jediného zbývajícího centralizovaného požadovaného údaje v návrzích založených na synchronizační oblasti dynamickou adaptací. Výsledky jsou v zásadě použitelné pro všechny návrhy založené na synchronizační oblasti, které tak všechny dělají plně distribuované.

Klíčová slova: kooperativní řízení, multiagentní systémy, distribuovaná zpětná vazba, synchronizace, synchronizační oblast, časová zpoždění, regulace výstupů, princip vnitřního modelu, distribuovaní pozorovatelé, fúze senzorů, protokoly adaptivního konsenzu

Key Words: cooperative control, multi-agent systems, distributed feedback, synchronization, synchronizing region, time-delays, output regulation, internal model principle, distributed observers, sensor fusion, adaptive consensus protocols.

CONTENTS

The presented habilitation treatise takes the form of a collection of selected SCI Expanded journal and conference papers published by the applicant in the recent five years. The unifying theme of distributed cooperative control can be seen as a common thread tying the whole collection together. Taken together, these papers present author's contribution towards the current state-of-the-art in cooperative control. They bring interesting novel results and compelling applications, as well as open a number of potential avenues of future research.

The presented papers are as follows:

ACKNOWLEDGMENTS

My sincere gratitude goes to all my colleagues and friends who directly and significantly contributed to specific papers collected in this habilitation treatise. In particular, first and foremost I wish here to thank prof. Ing. Michael Šebek dr.sc. for his continuing support and encouragement. No less am I indebted to doc. Zdenek Hurak and doc. Martin Hromčik for all their help and good advice in these past five years. Special thanks go to my fellow coauthors; dr. Farnaz Adib Yaghmaie, prof. ing. Tomaš Vyhlidal, PhD, prof. dr.sc. Sergej Čelikovski, as well as to Xueji Zhang, PhD, Štefan Knotek, the PhD candidates whom I had both the pleasure and honor to advise, and to MS. Martin Gurtner. Without their dedicated efforts many finer details of the work presented here would be absent. I am wholeheartedly looking forward to much future fruitful collaboration.

The research presented in this treatise was covered under the following grants:

-NSF grant ECCS-1405173, ONR grant N00014-13-1-0562, ONR grant N000141410718, grant W911NF-11-D-0001, China NNSF grant 61120106011, and China Education Ministry Project 111 (No. B08015),

-European social fund within the framework of realizing the project ''Support of inter-sectoral mobility and quality enhancement of research teams at Czech Technical University in Prague'', CZ.1.07/2.3.00/30.0034.

-Grant Agency of the Czech Technical University in Prague, Grant no. SGS14/182/OHK2/3T/ 12.

-ONR grant N00014-17-1-2239, China NSFC grant 61633007, the ATMRI-CAAS Project on Air Traffic Flow Management with the project reference number ATMRI: 2014-R7-SU

-European Regional Development Fund under the project Rob4Ind4.0 (reg. no. CZ.02.1.01/0.0/0.0/15 003/0000470).

-NRF BCA GBIC grant on Scalable and Smart Building Energy Management (NRF2015ENC-GBICRD001-057).

-Grant Agency of the Czech Technical University in Prague, grant No. SGS16/232/OHK3/3T/13

-Czech Granting Agency GAČR grant 16-25493Y

COPYRIGHT

INTRODUCTION

This treatise brings an overview of some recent advanced methods and results in distributed cooperative control. Classical control theory has a number of well-studied and time-proven design concepts; such as *optimal control theory*, the *Internal Model Principle* (IMP), H_∞ *control* for disturbances and the related *game theoretic formulations*. These were all originally applied to a system or a plant in a way which in hindsight we would now call *centralized*. With the growth in available computational power and a steady decrease in computer size and price, it became possible first to *decentralize* the controllers, and more recently to make them cooperate in a *distributed* manner. Surprisingly enough, the classical centralized theoretical concepts found their novel applications in this distributed domain as well, often in less-than-straightforward ways. Their familiar well-documented properties are since recently made to apply to autonomous single-agents, rather than the multi-agent system as a whole, allowing for designs which elegantly solve some of the canonical distributed control problems. This treatise particularly addresses the *state synchronization* problem for identical agents using distributed state and output-feedback, and the *output synchronization* problem for heterogeneous agents using distributed output-feedback, possibly under the effect of disturbances. Game theoretic formulations of N-player graphical games for state or output synchronization are mentioned together with their $2N$-player H_∞ counterparts, mirroring classical 2-player H_∞ game concepts.

A concise exposition of related recent results in distributed control of *homogeneous agents* is given first, providing a wider framework for two specific developments highlighted in the immediate sequels. This part originally appears published as a chapter in the book *Control of Complex System; Theory and Applications*, edited by Sarangapani Jaganathan and Kyriakos Vamvoudakis, in 2016. It specifically covers various applications of the fruitful *synchronizing region method* to problems encountered in analysis and design of distributed cooperative control. The synchronizing region method, in particular, relies heavily on conventional *optimal control* results and their more sofisticated variants, as well as on the classical *Lyapunov stability* theory. It, ideally, decouples the single-agent controller design from detailed properties of the communication graph topology. Two chapters following immediately bring specific technical results covered only briefly in this introductory general overview.

First of these, originally published in Elsevier's *Automatica*, (IF: 6.126, the main IFAC journal), in 2015, brings technical details on application of the synchronizing region method to state synchronization of homogeneous agents using *static output-feedback.* Restricting the choice of feedback to outputs only brings additional difficulties for the cooperative control design, as well as it somewhat restricts the type of graph topologies that allow for synchronization in the considered manner. The benefit, however, is a simple, time-invariant feedback guaranteeing distributed state synchronization and a finite H_∞ bound in presence of unmodelled disturbances. Developments of this chapter build on the earlier work on optimal output-feedback control and extend conventional results on distributed state-feedback to output-feedback settings. Specific contributions brought in the original paper are that the restrictive conditions in previously existing literature are removed to provide synchronizing controls for the general static output-feedback case, including non-passive systems and systems not satisfying any simplifying rank conditions. Applications are made to globally optimal designs including bounded L_2 gain synchronization, zero-sum games Nash equilibrium, and globally optimal control. Two similar conditions

on the local output measurement matrix and the global graph Laplacian are given that reveal the symmetry between local information restrictions due to output-feedback and global information restrictions due to the graph topology. A new class of digraphs is defined that satisfy this global condition. The structure of the guaranteed synchronization region for static output-feedback is studied and found to be a conical sector, not a right-half plane as found for the full state-feedback. A numerical example is provided that shows the applicability of these results in a case where previously existing results cannot be applied.

The following chapter, originally published in Elsevier's *Journal of the Franklin Institute*, (IF: 3.567), in 2015, takes into account *communication time-delays* which are realistically unavoidable in real-world distributed systems. It proves to be possible, using Razuminkhin-Lyapunov stability analysis, to apply the spirit of synchronizing region methods to systems with uniform time-delays, yielding delay dependent synchronizing regions that restrict the time-delay as well as the graph topologies allowing for synchronization. In particular, the delay-dependent synchronizing region is found to be bounded and shrinking with the growing time-delay. These results are applicable, in principle, to all distributed control cases analyzed originally as delay-free. Moreover, they reduce naturally to the familiar delay-free results when the bound on the delay is pushed to zero. Therefore, albeit somewhat conservative, results elaborated in this chapter present a natural extension of the conventional and more familiar synchronizing region concepts. As its first original contribution, this chapter brings together Razumikhin stability analysis and distributed cooperative control to extend the classical synchronizing region approach of delay-free distributed control to delay-dependent synchronizing regions applicable to agents with uniform control delay. The delay-dependent synchronizing region reduces effects of the communication graph topology to robust stability of a single-agent closed-loop system with delayed feedback. This concept first appeared in the context of oscillator synchronization. However, in contrast to earlier results, the approach proposed in this chapter accounts for realistic controllability properties of single-agents and provides a connection and comparison between the delay-free distributed feedback design and the familiar case of non-zero delays. Moreover, this chapter extends results on delays for cooperative control reported previously in the literature to LTI agents on directed graphs, and conventional synchronization results to the case of uniform delays. In contrast to earlier results, here are considered general directed, albeit constant, graph topologies and stability conditions are derived depending on single-agent system properties. Hence, stability analysis is scalable and does not involve considering the entire multi-agent system. The price to pay for that is the requirement to restrict one's attention to identical agents with uniform time-delays. As a second contribution, qualitative properties of delay-dependent synchronizing region, characterizing robust stability, are addressed. It is found that for non-zero delays the guaranteed delay-dependent synchronizing region is inherently bounded. Therefore one has a situation akin to discrete-time synchronization, and its bounded synchronizing region, elaborated in earlier work of the author. The nature of this sufficient condition is qualitatively similar to other results in the literature which give necessary and sufficient conditions for single-integrator consensus under delays. One finds here also the already mentioned tradeoff between fast synchronization and robustness to delays. A static cooperative synchronization control design procedure is given based on the guaranteed delay-dependent synchronizing region. The third contribution is in bringing stricter conditions for the stronger property of exponential cooperative stability with a

prescribed convergence rate. In that this paper extends delay-free results on convergence in the literature to agents with a uniform control-delay. Numerical example validates the proposed approach.

Considering a more general class of *heterogeneous agents*, treatment *via* synchronizing region methods is not directly applicable. Furthermore, the canonical distributed control problem appropriate for such multi-agent systems is output synchronization instead of state synchronization. Namely, the states of heterogeneous agents need not be commensurate to each other in any way, so aiming for their equality is generally ill posed. Outputs, on the other hand, if made to belong to the same vector space, can theoretically still synchronize. Following the seminal 2009 paper by Wieland, Sepulchre, Allgower, the *Internal Model Principle* is necessary and sufficient for achieving this goal. However, the Internal Model Principle further hints at an even more general geometrical structure of heterogeneous agents that may synchronize over general outputs. A paper published in the Wiley's *International Journal of Robust and Nonlinear Control* (IF: 3.856), in 2018, uses this insight to design distributed controls *via* LMIs for such generalized agents to guarantee output-synchronization and an L_2-bound in case of unmodelled disturbances acting on the system. These results are applicable to modelled disturbances as well, combining two complementary sets of geometrical requirements on single-agent structure. Developments of this chapter thus generalize the type of distributed feedback used for output synchronization as well as lift the specific assumptions on structure of the controller often used in earlier publications. Specifically, this chapter brings two main contributions. Firstly, it considers a group of heterogeneous agents in contrast to the homogeneous agents usually considered in previous publications. It assumes that the agents are subject to both modeled and unmodeled disturbances and aims to achieve H_∞ output regulation in comparison with previous results which do not consider unmodeled disturbances at all. Secondly, it allows the agents to communicate over a general class of switching graphs. In comparison, previously existing results in the literature usually did not consider switching graphs and the switching graphs, when considered, could change only over a set of topologies containing spanning trees. Those assumptions are not needed here. These two objectives are achieved using the simplest form of the controller; a static distributed output-feedback controller in a general framework without requiring limiting assumptions like acyclic graphs, or homogeneity or passivity of the single-agents.

Building further on the revealed necessary and sufficient geometrical structure of general heterogeneous agents required for output-synchronization over general outputs, the following chapter shows how output-synchronization and disturbance suppression problems can be cast in the form of $N/2N$ player graphical games. *Graphical games* were introduced in the literature, starting in 2010, to deal with homogeneous agent state synchronization and the corresponding L_2-bound, but as these novel results show, they are equally applicable in this broader context. Solution methods are based on *reinforcement learning* and *adaptive networks*, offering distributed on-line solutions to the derived game theoretic optimization problems. In particular, there are four main contributions of this chapter. It defines the novel concept of graphical games for heterogeneous agents as opposed to homogeneous agents hitherto considered in the literature. This allows one to achieve output regulation among heterogeneous agents. Graphical game for heterogeneous agents is considered in the literature already, however, the communication graph there is required to be acyclic (*i.e*. there are no loops in the graph). This restrictive assumption significantly simplifies the formulation and decouples the controller design of

each single-agent from the others. Furthermore, this chapter assumes that the agents are subject to unmodeled disturbances and defines an H_∞ graphical game for heterogeneous agents. The only previous reference pertaining to H_∞ control of multi-agent systems in the graphical game framework considers only homogeneous agents. Also, the H_∞ graphical game for heterogeneous agents results in coupled Hamilton-Jacobi-Bellman equations that are difficult to solve analytically. Hence, Reinforcement Learning is used and new actor-critic networks are developed to obtain solutions to these equations. In contrast, the actor-critic networks in the literature can be used only for homogeneous agents. Additionally, this chapter also brings an upper bound for the L_2-gain of output synchronization error with respect to unmodeled disturbances; in contrast to existing results, which do not calculate the upper bound but only contend its existence. These results hint at interesting possibilities for distributed MPC games, to name just one potential future direction of research.

On the more applied side of such purely theoretical developments, a recent boost in computational power paves the way to decentralization, distribution and development of real-world high performance networked systems consisting of various agents. Networking allowed for a new phenomenon of smart networks: *e.g.* Internet of Things, interconnecting smart devices all over the world and building smart ecosystems in public and private sphere: intelligent buildings, smart power grids, *etc*. The present is indeed witnessing an increasingly automated and networked world, where novel concepts of smart factories, cities, automated highways, *etc*. are leading us to a more intelligent future. With rapid advances and integration of computing, communication and smart sensing technologies, small-sized and low-cost sensing devices with embedded processing and communication capabilities are already being deployed in a wide range of environments. These technical achievements attract researchers to the emerging field of Networked Control Systems (NCS), and their synonymous Cyber-Physical Systems (CPS). These systems consist of agents networked by a communication topology, integrating two complementary fields: *control theory* and *graph theory*. Distributed NCSs find a wide range of applications in formation control of mobile robots, satellites, vehicles, energy generation in micro-grids, estimation by sensor networks, synchronization of coupled oscillators, describing agreement in human social networks, to name only a few.

The results, originally published in the IEEE *Transactions on Control Systems Technology,* (IF: 4.883), in 2017, particularly consider networked observers that fuse plant's state estimates for control purposes and associated controllers for large linear-time-invariant plants. The main motivation was to address pressing industrial concerns regarding vibration suppression in emerging smart materials and structures. Hence, specific target plants are large-scale flexible structures *e.g.* aircraft fuselages, truss bridges, lattice towers, *etc*. In order to satisfy the ever stricter environmental criteria manufacturers are looking into light-weight constructions that usually have decreased inherent vibration damping. Mechanical and structural vibrations are detrimental to the functioning and safety of these plants, hence effective vibration suppression is required in many cases. Thus arises the need for *smart materials* or *piezo-composites* that are able to do the task. In our framework, each agent has some or all of the following functions: *sensing, actuation, communication* and *information processing*. Presented results show a successful application of distributed estimation *via* cooperative consensus for each actuating agent to gain an estimate of the overall environment's state, which is then used for its control. Namely, every agent uses its own information together with information from its immediate neighbors to reach an

agreement on states with all the other agents in the network, called *consensus* or *synchronization*. Design of observers and controllers is a crucial problem for the considered plants. Each observer builds a part of *its* plant's state estimate based on *its* own *local measurements*, and the remaining part comes from the network. *Partial measurements* from different sensing agents are thus fused by the network through distributed communication. A distributed observer design is facilitated by the *synchronizing region* methodology for *pinning control*. Namely, the environment is considered as partially pinning into the network at the sensing nodes. Separation principle is found not to hold for this particular dynamic regulator architecture so care is required in designing observers and controllers to guarantee overall observer convergence and system stability. Controllers are designed *via* linear quadratic regulator (LQR) precepts to account for this fact in a flexible manner. The design conditions may be somewhat conservative, but one gains robustness to sensor failures and flexibility to network topology changes as an upshot. Specifically, the main contributions of this chapter are as follows. The communication graph topology is separated from the observer/controller design. Furthermore, the requirements on graph topology are relaxed from (connected) undirected graphs to more general directed graphs, compared with the previously existing results. Moreover, since the observer design is single-agent based, it leads to *flexibility* in terms of integrating additional sensors to the existent network and graceful degradation in case of communication link failures as long as connectivity requirements remain satisfied. These properties were not expected in the currently available literature.

Disturbances and uncertainties were at first not considered. However, notwithstanding compelling results, assuming measurements of *perfect accuracy*, albeit only partial, is naturally too strong a requirement for practical applications, even though it is satisfied in real-world cases to a fair degree, as indeed attested by physical experiments. Still, if several measurements of differing reliability are available, one can attempt *sensor fusion* taking into account the differing precisions of individual measurements, which is the topic of Chapter 7. This then ideally improves even on the most precise measurements. Although distributed Kalman filter developments, aiming to achieve these or similar ends, are already familiar in the literature, this discussion proposes a design of considerably simpler nature; one which is time invariant-thus simplifying implementation; does not require communication of variance matrices among different observers-thus reducing the communication load in the network; is generally suboptimal but nevertheless of satisfactory performance and robust to potential single-agent failures. Results clearly show appreciable disturbance suppression of the proposed design. These distributed observers can, of course, be used for control purposes along the lines of the previous chapter. The particular contributions of this chapter are in that it considers a more general communication topology than the previously proposed distributed observers. Moreover, the nodes implement a local Kalman filter to estimate the observable fraction of the plant state. Also, the nodes use information on process and measurement noises and apply information-weighted fusion to reach an agreement on the estimate of a plant state. Furthermore, the design and implementation of the proposed observer is fully distributed, in the sense that each node designs its local observer based on its own information and the information coming from its neighbors. In addition to that, the proposed design offers incorporation of redundant nodes or insertion of new communication links to the network to improve robustness to node or communication link failures.

The final Chapter 8 investigates possibilities of using adaptive consensus protocols on directed graph topologies in which the only remaining requirement for centralized information in the synchronizing region-based designs is avoided through adaptation of the *coupling constant*. In particular, the coupling constant in the synchronizing region designs, required by each single-agent, is often found to depend on the global graph topology, which is not known to each/any single-agent. Distributed adaptation protocols are supposed to, in a way, overcome this obstacle by providing that information to all single-agents dynamically. To put it simply, the local coupling gain of each agent is made to increase in dependence on its local neighborhood disagreement until synchronization is achieved. This may lead, however, to final coupling gains which are higher than those necessary for cooperative stability. Thus we propose the coupling gain decay to find the minimal level for the coupling gain values, achieving cooperative stability with a lower control effort. For directed graphs we stick to the simplest form of distributed feedback and avoid such nonlinear prescriptions as are proposed elsewhere in the literature. Preliminary results in this research direction were first presented on the 2016 *Necsys* conference, and 2017 *Process Control* conference. Work continues further on this topic. Results are applicable, in principle, to all designs based on the synchronizing region methods, which would, in turn, make them indeed fully distributed.

1. SYNCHRONIZING REGION APPROACH FOR IDENTICAL LINEAR TIME-INVARIANT AGENTS

Kristian Hengster-Movric and Michael Sebek, **Synchronizing Region Approach for Identical Linear Time-Invariant Agents**, *Control of Complex Systems - Theory and Applications*, Ch. 18, Elsevier, pp. 519-548, 2016.

This concise but comprehensive exposition of recent results in distributed control originally appears published as a chapter in the book *Control of Complex System; Theory and Applications*, edited by Sarangapani Jaganathan and Kyriakos Vamvoudakis. It specifically covers various applications of the fruitful synchronizing region method to problems encountered in analysis and design of distributed cooperative control of multi-agent systems. It serves to provide a general framework for the more specific developments given in the sequel. In particular, this part is immediately followed by two papers that first brought specific technical results covered only briefly in this first introductory chapter. Those are the synchronization of states in identical agents using static output-feedback, and synchronization of states in identical agents under tim-delays.

This chapter brings a selection of recent results in the field of identical system cooperative state synchronization. The presentation is by no means exhaustive, rather it focuses on a set of related results. Design methods are given herein for distributed synchronization control of continuous and discrete-time multi-agent systems on directed communication graphs. The graph topology properties generally complicate the design of synchronization controllers due to an interplay between the eigenvalues of the graph Laplacian matrix and the required stabilizing feedback gains. Methods surveyed here decouple the single-agent requirements from the detailed graph topology and bring control designs based on single-agent Riccati equations. Riccati equations are fairly familiar from conventional control theory where they find extensive applications, in particular in optimal linear quadratic regulator problems. Hence, stabilizing properties and robustness margins of feedback gains designed from their solutions are well known. Several conditions are given for state synchronization relying on relations of graph Laplacians' eigenvalues to various regions in the complex plane. Those regions depend on single-agent dynamics and solutions of appropriate Riccati equations. Distributed observation for agents networked on directed graphs is also investigated as a problem dual to multi-agent distributed synchronization. Cooperative observer design guaranteeing convergence of estimates of all agents to their actual states is proposed. This approach applies similarly to continous- and discrete-time systems. It is shown in particular that, in contrast to unbounded continuous-time synchronizing region, the discretetime synchronizing region is inherently bounded. Hence conditions for observer convergence and state synchronization in discrete-time are stricter than those in continuous-time. In the case of only outputs being available for feedback control the distributed static output-feedback (OPFB) control can be used. The synchronizing region of static OPFB control for continuous-time systems is exposed and found to be conical, unbounded but generally different in shape from the infinite right-half plane synchronizing region of distributed full state-feedback. Furthermore, multi-agent system synchronization under control signal delays is presented. All agents are assumed to have the same control delay. Delay-dependent synchronizing region is defined and methods are given guaranteeing its estimates. In the latter instance one must admit, in the present form, a considerable conservatism, which is a general feature inherent to simpler delay-dependent stability conditions. In principle less conservative methods can be applied following the same lines of reasoning. However, the presented delay-dependent estimate of a synchronizing region reduces naturally to that of delay-free system if the delay is set to zero. It is also shown that synchronizing region methods provide assessment of robustness to single-agent disturbances and uncertainties. Extension of the synchronizing region to H_∞ robustness in presence of disturbances is only briefly mentioned. As for single-agent uncertainties, being of the type that all agents remain identical, the amount of uncertainty restricts graph topologies that allow for synchronization.

Synchronizing Region Approach for Identical Linear Time-invariant Agents

Kristian Hengster Movric, Michael Sebek

Summary

This survey brings a selection of recent results in the field of identical system cooperative state synchronization. The presentation is by no means exhaustive, rather it focuses on a set of related results. Design methods are given herein for distributed synchronization control of continuous and discrete-time multi-agent systems on directed communication graphs. The graph topology properties generally complicate the design of synchronization controllers due to an interplay between the eigenvalues of the graph Laplacian matrix and the required stabilizing feedback gains. Methods surveyed here decouple the single-agent requirements from the detailed graph topology and bring control designs based on single-agent Riccati equations. Riccati equations are fairly familiar from conventional control theory where they find extensive applications, in particular in optimal linear quadratic regulator problems. Hence, stabilizing properties and robustness margins of feedback gains designed from their solutions are well known.

Several conditions are given for state synchronization relying on relations of graph Laplacians' eigenvalues to various regions in the complex plane. Those regions depend on single-agent dynamics and solutions of appropriate Riccati equations. Distributed observation for agents networked on directed graphs is also investigated as a problem dual to multi-agent distributed synchronization. Cooperative observer design guaranteeing convergence of estimates of all agents to their actual states is proposed. This approach applies similarly to continous- and discrete-time systems. It is shown in particular that, in contrast to unbounded continuous-time synchronizing region, the discrete-time synchronizing region is inherently bounded. Hence conditions for observer convergence and state synchronization in discrete-time are stricter than those in continuous-time. In the case of only outputs being available for feedback control the distributed static output-feedback (OPFB) control can be used. The synchronizing region of static OPFB control for continuous-time systems is exposed and found to be conical, unbounded but generally different in shape from the infinite right-half plane synchronizing region of distributed full state-feedback. Furthermore, multi-agent system synchronization under control signal delays is presented. All agents are assumed to have the same control delay. Delay-dependent synchronizing region is defined and methods are given guaranteeing its estimates. In the latter instance one must admit, in the present form, a considerable conservatism, which is a general feature inherent to simpler delay-dependent stability conditions. In principle less conservative methods can be applied following the same lines of reasoning. However, the presented delay-dependent estimate of a synchronizing region reduces naturally to that of delay-free system if the delay is set to zero.

It is also shown that synchronizing region methods provide assessment of robustness to single-agent disturbances and uncertainties. Extension of the synchronizing region to H_∞ robustness in presence of disturbances is only briefly mentioned. As for single-agent uncertainties, being of the type that all agents remain identical, the ammount of uncertainty restricts graph topologies that allow for synchronization.

I. INTRODUCTION

The last two decades have witnessed an increasing interest in multi-agent networked cooperative systems, inspired by natural occurrence of flocking and formation forming. In nature individual creatures act only according to locally available, nearest neighbor information [1], however the group as a whole succeeds in accomplishing global goals, *e.g.* predator evasion in a heard or school, or conserving energy in avian formations. These concepts and decision schemes are applied in engineering for control of spacecraft formations, unmanned aerial vehicles, mobile robots, distributed sensor networks *etc*. [2]. The canonical control problem there is *consensus* or *synchronization* of all agents' states. Early work with networked cooperative systems in continuous and discrete-time is presented in [3],[4],[5],[6],[7]. These papers generally refer to consensus without a leader, where the final synchronized state depends on precise initial conditions of all agents. By adding a command generator that pins to a group of other agents one can obtain synchronization to a command trajectory for all initial conditions using a virtual leader [5], which is also termed *pinning control* [8],[9]. We name this here the *cooperative tracker problem*. Necessary and sufficient conditions for synchronization are given by the *master stability function* and the related concept of the *synchronizing region* in [9],[10],[11]. The synchronizing region method crystalized over time as a versatile and robust tool for analysis and design of cooperative control systems. For continuous-time systems it guarantees synchronization [9],[12],[13] using optimal state-feedback derived from the continuous-time Riccati equation. It is shown that Riccati feedback gain at each node yields an unbounded right-half plane synchronizing region in the

complex plane. For discrete-time systems the guaranteed synchronizing region is inherently bounded which leads to stricter synchronizability conditions. There the discrete-time Riccati equation serves, in some sense, to maximize the synchronizing region, [14], [16] .

In multi-agent setting, the problems of cooperative observer convergence and synchronization are related by a duality concept for distributed systems on directed graphs, [15]. It is also shown that cooperative control design and cooperative observer design can both be approached by decoupling the effects of graph structure from the feedback gain design *via* Riccati-based procedure. Sufficient conditions are given guaranteeing observer convergence.

Lacking the full state-feedback, the static output-feedback (OPFB) cooperative synchronization control design is possible under certain stipulations. Usually one treats output-feedback control problems by observers, *i.e.* dynamic OPFB, thus increasing the order of dynamics, but static OPFB, when feasible, offers a simpler solution. Synchronizing region estimate for distributed static OPFB control of continuous-time agents is exposed and found to be a conical sector in the complex plane. This is to be contrasted with the infinite right-half plane synchronizing region of the full state-feedback, [17].

Considering practical means of distributed control *e.g.* wireless communication, dedicated busses, networked control, delays in information signals from neighboring agents are unavoidable, [4]. In realistic applications one is interested in effects these delays have on cooperative stability, *i.e.* the robustness of cooperative stability to delays. Generally well behaved system, robust to disturbances, may be sensitive to feedback delays, which can lead to poor performance and even result in loss of stability. Guaranteeing robustness of cooperative stability to delays is therefore important for all practical implementations of multi-agent distributed control. Some early papers on cooperative consensus, *e.g.* [4], address the problem of delayed signals from the neighbors. For discrete-time synchronization, delays are treated using stochastic matrices [21]. For continuous-time [4],[18],[19] introduce a uniform delay in one-dimensional single-integrator agents on undirected graphs. More recent work [18] extends [4] to directed graphs, introducing the delay margin and a responsible eigenvalue concept.

One way to extend both early [4] and more recent results on delays [18] to general continuous-time identical LTI agents on directed graphs is offered by the theory of retarded functional differential equations (RFDEs), [19]. Essential question is that of single-agent stability. In a search for simple and flexible stability conditions the delay-dependent criteria based on Razumikhin theorem, present a good choice. Here we are concerned with identical LTI agents, all having the same (*uniform*), constant control delay. The simplifying assumption of uniform delays is standard in the literature [4],[18],[19]. A static cooperative synchronization control design is presented based on the estimated delay-dependent synchronizing region. Stricter conditions for the stronger property of exponential cooperative stability with a prescribed convergence rate are also given. These results extend delay-free conditions for convergence in [13] to agents with a uniform control delay.

The synchronizing region concept, robust by merits of its definition, also offers means to guarantee robustness of multi-agent system cooperative stability to external disturbances and uncertainties in single-agent systems. For external disturbances one applies the H_∞ approach [20], leading to an $\mathcal{L}_2$ bound of the synchronization errors with respect to acting disturbances. For single-agent uncertainties one assumes that agents remain identical. Non-identical, *i.e. heterogeneous* agents, require methods other than those offered by the synchronizing region, which are not considered here. Considering the single-agent uncertainties closely it is found that those produce different effects depending on which part of the single-agent system they occur in. The combined effect is found to be qualitatively similar to that occurring with static OPFB. Greater magnitudes of uncertainties in single-agent systems ostensibly lead to stricter conditions on graph Laplacian matrix eigenvalues.

The outline of this survey is as follows; Section II brings graph theory preliminaries and notational conventions. Section III introduces the considered systems' dynamics, defines the control goals and specifies the forms of cooperative signals used. Section IV forms the main part of the survey. First it defines synchronizing regions bringing necessary and sufficient conditions for cooperative stability. Then it provides Lyapunov estimates of those synchronizing regions yielding sufficient conditions for cooperative stability and motivating the pertaining design schemes. Section V briefly addresses robustness of multi-agent systems to external disturbances and single-agent uncertainties by synchronizing region methodology, and Section VI brings the conclusions.

II. GRAPH PROPERTIES AND NOTATION

Consider a graph $\mathcal{G} = (\mathcal{V}, \mathcal{E})$ with a nonempty finite set of N nodes $\mathcal{V} = \{v_1, \cdots, v_N\}$ and a set of edges $\mathcal{E} \subseteq \mathcal{V} \times \mathcal{V}$. It is assumed that the graph is simple, *i.e.* there are no repeated edges or self-loops. Directed graphs are considered, and

This publication is supported by the Czech Granting Agency GAČR grant 16-25493Y.

information propagates through the graph along the edges. Two nodes v_j, v_k connected by an edge $(v_j, v_k) \in \mathcal{E}$ are termed *parent* node v_k and *child* node v_j, *i.e.* the edge leaves the parent node and connects into the child node. Denote the adjacency matrix as $E = [e_{ij}]$ with $e_{ij} > 0$ if $(v_i, v_j) \in \mathcal{E}$ and $e_{ij} = 0$ otherwise. Note that diagonal elements satisfy $e_{ii} = 0$. The set of neighbors of node v_i is $\mathcal{N}_i = \{v_j : (v_i, v_j) \in \mathcal{E}\}$, *i.e.* set of nodes with edges connecting into v_i. Define the in-degree matrix as a diagonal matrix, $D = diag(d_1 \dots d_N)$, with $d_i = \sum_j e_{ij}$, the (weighted) in-degree of node i. Define the graph Laplacian matrix as $L = D - E$, which has all row sums equal to 0.

A *directed path* is a sequence of edges joining two nodes. A graph is said to be *strongly connected* if any two nodes can be joined by a directed path. Node is termed *isolated* if it has no incoming edges. Hence in strongly connected graphs there are no isolated nodes. A *directed tree* is a subgraph containing a single node v_0, isolated in that subgraph, such that all other nodes in the subgraph except v_0 have only one parent and are joined to v_0 by a directed path. Node v_0 is called a *root node*. A graph is said to contain a directed *spanning tree* if there exists a directed tree containing every node in $\mathcal{V}$. The Laplacian matrix L has a simple zero eigenvalue if and only if its directed graph contains a spanning tree.

For a matrix $Q = Q^T \geq 0$ a square root, $Q^{1/2}$, is a matrix satisfying $(Q^{1/2})^T Q^{1/2} = Q$. We denote its matrix transpose as $Q^{T/2}$. Complex conjugation of a scalar $\sigma \in \mathbb{C}$ is denoted by an over bar $\overline{\sigma} \in \mathbb{C}$. The abbreviations *a.s.* and *e.s.* stand for asymptotic and exponential stability respectively.

III. SYSTEM DYNAMICS AND CONTROL GOAL

This section introduces single-agent dynamics considered in this survey. Control goals are defined and the used cooperative signals are specified. Given a graph $\mathcal{G}(\mathcal{V}, \mathcal{E})$, endow each of its N nodes with a state vector $x_i \in \mathbb{R}^n$ and a control input $u_i \in \mathbb{R}^m$. Consider at each node the dynamics, *i.e.* state evolution, given by a continuous-time differential equation,

$$\dot{x}_i(t) = Ax_i(t) + Bu_i(t), \tag{1}$$

or by a discrete-time difference equation,

$$x_i(k+1) = Ax_i(k) + Bu_i(k). \tag{2}$$

With control signal delays the single-agent dynamics in continuous-time is instead of (1) described by a single-delay retarded functional differential equation

$$\dot{x}_i(t) = Ax_i(t) + Bu_i(t-\tau). \tag{3}$$

The treatment of control delays in discrete-time is considerably simpler, with dynamics described by a variant of difference equation (2) where $u(k)$ is replaced by $u(k-l)$, $l > 0$, [21].

Let the output relations with $y_i \in \mathbb{R}^p$ be given as

$$y_i(t) = Cx_i(t), \quad y_i(k) = Cx_i(k). \tag{4}$$

Assume that (A, B) is stabilizable, (A, C) detectable, B has full column rank m, C has full row rank, p; hence there are no redundant control inputs nor redundant measurement outputs. Consider also a leader node, control node, or command generator, following the autonomous dynamics in continuous-time

$$\dot{x}_0(t) = Ax_0(t), \tag{5}$$

or in discrete-time

$$x_0(k+1) = Ax_0(k), \tag{6}$$

with $x_0 \in \mathbb{R}^n$. For instance, if $n = 2$ and matrix A has pure imaginary eigenvalues then the reference trajectory is harmonically oscillating. Let the leader have the same output relation as (4), $y_0 = Cx_0 \in \mathbb{R}^p$.

Then for the above one has the following,

Control goal: The *cooperative tracker* or *synchronization problem* is to select the control signals u_i for agent *i*, such that the states at all nodes asymptotically synchronize to the state of the control node, that is, $\lim_{t\to\infty}\|x_i(t) - x_0(t)\| = 0, \forall i$, in continuous-time or $\lim_{k\to\infty}\|x_i(k) - x_0(k)\| = 0, \forall i$ in discrete-time. These requirements must be fulfilled for all initial conditions $x_i(0)$.

3.1. Continuous and Discrete-time Cooperative Tracker

Considering the continuous-time multi-agent systems (1) and (5), define the local neighborhood tracking errors

$$e_i = \sum_{j\in N_i} e_{ij}(x_j - x_i) + g_i(x_0 - x_i) \tag{7}$$

where pinning gain $g_i \geq 0$ is nonzero if node v_i can sense the state of the control node (5). The intent is that only a small percentage of nodes have $g_i > 0$, yet all nodes should synchronize through distributed communication to the trajectory of the control node using local neighbor control protocols, [8]. It is assumed that at least one pinning gain is nonzero. Note that the local neighborhood tracking error represents the information available to agent *i* for control purposes. Choose the input of agent i as the weighted local control protocol

$$u_i = cKe_i, \tag{8}$$

where $c \in \mathbb{R}^+$ is a coupling gain to be detailed later. Then, the closed-loop dynamics of individual agents (1) are

$$\dot{x}_i(t) = Ax_i(t) + cBKe_i(t). \tag{9}$$

Considering the discrete-time multi-agent systems (2) and (6), the same local neighborhood tracking errors (7) are used for synchronization control, however they are weighted differently, [16]. Choose the input of agent i as the weighted local control protocol

$$u_i = c(1 + d_i + g_i)^{-1}Ke_i, \tag{10}$$

where $c \in \mathbb{R}^+$ is a coupling gain to be detailed later. Then, the closed-loop dynamics of individual agents (2) are

$$x_i(k+1) = Ax_i(k) + c(1 + d_i + g_i)^{-1}BKe_i(k). \tag{11}$$

The multi-agent systems (9) and (11) in total state-space form read

$$\dot{x}(t) = (I_N \otimes A - c(L + G) \otimes BK)(x(t) - \overline{x}_0(t)), \tag{12}$$

$$x(k+1) = (I_N \otimes A - c(I + D + G)^{-1}(L + G) \otimes BK)(x(k) - \overline{x}_0(k)), \tag{13}$$

where $x = \begin{bmatrix} x_1^T & \cdots & x_N^T \end{bmatrix}^T \in \mathbb{R}^{Nn}$, $\overline{x}_0 = \begin{bmatrix} x_0^T & \cdots & x_0^T \end{bmatrix}^T \in \mathbb{R}^{Nn}$ and $G = diag(g_1, \ldots, g_N)$ is the diagonal matrix of pinning gains. Introducing the synchronization error,

$$\delta_i = x_i - x_0, \tag{14}$$

one obtains the closed-loop dynamics in total state-space form as

$$\dot{\delta}(t) = (I_N \otimes A - c(L + G) \otimes BK)\delta(t), \tag{15}$$

in continuous-time and

$$\delta(k+1) = (I_N \otimes A - c(I + D + G)^{-1}(L + G) \otimes BK)\delta(k), \tag{16}$$

in discrete-time. Asymptotic stability of closed-loop synchronization error systems (15) and (16) guarantees cooperative synchronization. Hence the continuous and discrete-time stability of system matrices

$$I_N \otimes A - c(L+G) \otimes BK \,, \tag{17}$$

$$I_N \otimes A - c(I+D+G)^{-1}(L+G) \otimes BK \,, \tag{18}$$

determine the synchronization of multi-agent systems (9) and (11).

3.2. Discrete-time Cooperative Observer

With the availability of only outputs for feedback control one can proceed with the design of output dynamic controllers. The first step in that direction is to design cooperative observers with $\hat{x}_i(k)$ estimating states of agents $x_i(k)$ given measurements of their outputs $y_j(k)$. Only the discrete-time systems are presented here, but the same considerations and design methods are applicable *mutatis mutandis* to continuous-time case, [13].

Given an estimated output $\hat{y}_i = C\hat{x}_i$ at node *i*, define the *local output error*

$$\tilde{y}_i = y_i - \hat{y}_i \,. \tag{19}$$

To construct an observer that takes into account information from the neighbors of node *i*, define the *local neighborhood output disagreement*

$$\varepsilon_i = \sum_j e_{ij}(\tilde{y}_j - \tilde{y}_i) + g_i(\tilde{y}_0 - \tilde{y}_i) \,, \tag{20}$$

where the observer pinning gains are $g_i \geq 0$, with $g_i > 0$ only for a small percentage of nodes that have direct measurements of the output error $\tilde{y}_0$ of the control node. With the total output $y = \left[y_1^T \;\; \dots \;\; y_N^T \right]^T \in \mathbb{R}^{pN}$, the total output disagreement error $\varepsilon(k) \in \mathbb{R}^{pN}$ is

$$\varepsilon(k) = -(L+G) \otimes I_m \tilde{y}(k) + (L+G) \otimes I_m \underline{1} \tilde{y}_0(k) \,. \tag{21}$$

Throughout this subsection it is assumed that $x_0 = \hat{x}_0 \Rightarrow \tilde{y}_0 \equiv 0$, *i.e.* the control node's state is accurately known. Exemption from that assumption would require a separate observer for the leader's states that fulfills the above assumption asymptotically. Define the *distributed observer* dynamics

$$\hat{x}_i(k+1) = A\hat{x}_i(k) + Bu_i(k) - c(1+d_i+g_i)^{-1} F \varepsilon_i(k) \,. \tag{22}$$

where F is an observer gain matrix and c a coupling gain, to be detailed later. The total distributed observer dynamics then takes the form

$$\hat{x}(k+1) = I_N \otimes A\hat{x}(k) + I_N \otimes Bu(k) + c(I+D+G)^{-1}(L+G) \otimes F\tilde{y}(k)$$

$$\hat{x}(k+1) = \left[I_N \otimes A - c\left(I+D+G\right)^{-1}\left(L+G\right) \otimes FC \right] \hat{x}(k) + I_N \otimes Bu(k) + c\left(I+D+G\right)^{-1}\left(L+G\right) \otimes Fy(k)$$

Define the *i-th state observer error*

$$\eta_i(k) = x_i(k) - \hat{x}_i(k) \,,$$

where $x_i(k)$ follows dynamics (2). The total state-space observer error $\eta = \left[\eta_1^T \;\; \dots \;\; \eta_N^T \right]^T \in \mathbb{R}^{nN}$ follows the discrete-time dynamics

$$\eta(k+1) = \left[I_N \otimes A - c(I+D+G)^{-1}(L+G) \otimes FC \right] \eta(k) \,. \tag{23}$$

The total observer system matrix

$$I_N \otimes A - c(I + D + G)^{-1}(L + G) \otimes FC \tag{24}$$

determines the observer estimate $\hat{x}_i$ dynamics with respect to the true state x_i. The goal is asymptotic observer convergence for all distributed observers, *i.e.* $\eta \to 0$. It should be noted that the pinning terms in the local neighborhood output disagreement mean pinning with zero. Comparing this with the cooperative tracker setup a brief explanation is required. Pinning with zero here serves the purpose of making a fixed zero reference, which is needed for convergence of all observers' estimates, directly available to some particular observers. The remaining observers rely on relative measurements only, thus receiving information on the fixed zero reference in a distributed way.

3.3. Static Distributed Output-feedback Cooperative Tracker

Let the multi-agent systems be given as (1),(4) and (5). Define the *local neighborhood output error*

$$e_{yi} = \sum_j e_{ij}(y_j - y_i) + g_i(y_0 - y_i), \tag{25}$$

where $g_i > 0$ only for a few nodes having direct measurements of the leader's output $y_0(t)$. The feedback control signal for agent *i* is chosen as a linear distributed static OPFB

$$u_i = cKe_{yi}, \tag{26}$$

where $c > 0$ is the coupling gain and K is the local OPFB gain matrix. Standard cooperative control approaches assume distributed control in terms of state neighborhood error (7), or construct dynamic controllers in terms of output disagreement (20). By contrast this subsection studies distributed static OPFB of the form (26). In total state-space form, the local neighborhood output error (25) reads

$$e_y = -(L + G) \otimes C\delta, \tag{27}$$

where $e_y = \begin{bmatrix} e_{y1}^T & \cdots & e_{yN}^T \end{bmatrix}^T \in \mathbb{R}^{Np}$. Define as before, *i.e.* by stacking single-agent vectors, all other total quantities. The total state-space form of the distributed OPFB (26) is then

$$u = -c(L + G) \otimes KC\delta. \tag{28}$$

Note that expression (27) reflects the restrictions on the information available for distributed static OPFB control. Matrix C specifies the local single-agent restrictions due to OPFB, while $L + G$ specifies the information restrictions on a coarser scale due to limited communication. Both local and global restrictions appear in the kronecker product (27) in a symmetric manner.

Feedback (26) gives closed-loop single-agent systems (1) as

$$\dot{x}_i = Ax_i + cBKCe_i, \tag{29}$$

which yields the multi-agent system dynamics in total state-space form

$$\dot{x} = (I_N \otimes A)x - c(L + G) \otimes BKC\delta. \tag{30}$$

The total dynamics of synchronization errors follows readily as

$$\dot{\delta} = (I_N \otimes A - c(L + G) \otimes BKC)\delta. \tag{31}$$

Hence cooperative stability under distributed OPFB is determined by asymptotic stability of the system matrix in (31),

$$I_N \otimes A - c(L + G) \otimes BKC. \tag{32}$$

3.4. Multi-agent Systems with Uniform Control Delays

This subsection describes the single-agents and the total multi-agent system dynamics under uniform time-delays in control signal, [19]. Let the single-agent dynamics be given as a continuous-time LTI system with a fixed control signal delay $\tau \geq 0$,

$$\dot{x}_i(t) = Ax_i(t) + Bu_i(t-\tau), \tag{33}$$

where $x_i \in \mathbb{R}^n, u_i \in \mathbb{R}^m \ \forall i$ are the states and inputs. Let there be an autonomous leader given by (5). The delay $\tau \geq 0$ is taken to be constant and same for all agents, *i.e. uniform*. Though this need not be true in more realistic models, having different delays for different agents makes them, strictly speaking, not identical as dynamical systems. The assumption on uniform delays is a standard simplifying assumption [4],[19], and it is crucial for the following development.

With the local neighborhood error (7) let the control signal for agent *i* be calculated as a linear feedback of the local neighborhood error (8), where K is the local linear feedback gain matrix, and $c > 0$ is the coupling gain, to be detailed later. This gives the closed-loop single-agent dynamics

$$\dot{x}_i(t) = Ax_i(t) + cBKe_i(t-\tau). \tag{34}$$

Introducing the synchronization error (14) one has in total state-space form

$$\dot{x}(t) = (I_N \otimes A)x(t) - c(L+G) \otimes BK\delta(t-\tau), \tag{35}$$

where $x = \begin{bmatrix} x_1^T & \cdots & x_N^T \end{bmatrix}^T \in \mathbb{R}^{Nn}$, $\delta = \begin{bmatrix} \delta_1^T & \cdots & \delta_N^T \end{bmatrix}^T \in \mathbb{R}^{Nn}$. The total synchronization error system is then given as

$$\dot{\delta}(t) = (I_N \otimes A)\delta(t) - c(L+G) \otimes BK\delta(t-\tau). \tag{36}$$

Equation (36) is a linear retarded functional differential equation (RFDE), of the form

$$\dot{\delta}(t) = \overline{A}\delta(t) + \overline{A}_d\delta(t-\tau), \tag{37}$$

whose asymptotic stability guarantees synchronization.

IV. SUFFICIENT CONDITIONS FOR SYNCHRONIZATION

This section first brings definitions of synchronizing regions for systems presented in Section III, and the pertaining necessary and sufficient conditions for cooperative synchronization, [10],[13],[15],[16]. Then it provides Lyapunov estimates of these synchronizing regions yielding sufficient conditions for cooperative stability. Those sufficient conditions in turn lead to design procedures.

4.1. Synchronizing Regions and Cooperative Stability Conditions

Two lemmas are given below providing a simplification crucial in designing local feedback gains K and motivating definitions of synchronizing regions. Lemma 1 is presented without a proof, as proofs of its parts are readily found in the literature. The proof is however provided for Lemma 2 as it is not as straightforward as that of Lemma 1 and not as readily available.

Lemma 1. [9],[13],[15],[16]. The structured matrix $I_N \otimes A - c\Gamma \otimes B$ is Hurwitz if and only if all the matrices $A - c\lambda_j B$ are Hurwitz, where λ_j are the eigenvalues of Γ.

Hence the relevant matrices in (17),(18),(24) and (32) are Hurwitz if and only if

1. $A - c\lambda_j BK$

is continuous-time asymptotically stable for all λ_j eigenvalues of $L+G$

2. $A - c\lambda_j BK$

is discrete-time asymptotically stable for all λ_j eigenvalues of $(I + D + G)^{-1}(L + G)$,

3. $A - c\lambda_j FC$

is discrete-time asymptotically stable for all λ_j eigenvalues of $(I + D + G)^{-1}(L + G)$,

4. $A - c\lambda_j BKC$

is continuous-time asymptotically stable for all λ_j eigenvalues of $L + G$. ■

Lemma 1 applies to continuous-time and discrete-time cooperative state-feedback control (1,2.), discrete-time cooperative observer design (3.) and continuous-time static OPFB control design (4.). Lemma 2 brings an analogous result for distributed state-feedback in case of uniform control delays.

Lemma 2. [19]. The trivial solution of system (36), $\delta(t) \equiv 0$, is asymptotically stable if and only if the trivial solutions of systems

$$\dot{y}(t) = Ay(t) - c\lambda_j BKy(t - \tau), \tag{38}$$

each having an order of a single-agent system, where λ_j are the eigenvalues of the graph matrix $(L+G)$, are asymptotically stable $\forall j$.

Proof: The stability of (38) is determined by the transcendental transfer function matrix,

$$\left[sI_{Nn} - (I_N \otimes A) + c(L+G) \otimes BKe^{-s\tau} \right]^{-1}. \tag{39}$$

The frequency domain expression (39) needs to be asymptotically stable; a property depending on the roots of the pertaining characteristic quasipolynomial,

$$\Delta(s) = \det\left[sI_{Nn} - (I_N \otimes A) + c(L+G) \otimes BKe^{-s\tau} \right]. \tag{40}$$

Knowing that linear transformations do not change the determinant of a matrix one can use a coordinate transformation $T \otimes I_n$ in (40), where $T^{-1}(L+G)T = \Lambda$ is an upper triangular matrix, thereby simplifying the problem considerably. Whence one obtains

$$\begin{aligned} &\det\left[sI_{Nn} - (I_N \otimes A) + c(L+G) \otimes BKe^{-s\tau} \right] \\ &= \det\left[(T \otimes I_n)^{-1}(sI_{Nn} - (I_N \otimes A) + c(L+G) \otimes BKe^{-s\tau})(T \otimes I_n) \right] \\ &= \det\left[sI_{Nn} - I_N \otimes A + c\Lambda \otimes BKe^{-s\tau} \right] \\ &= \prod_j \det\left[sI_n - A + c\lambda_j BKe^{-s\tau} \right], \end{aligned} \tag{41}$$

where λ_j are the eigenvalues of Λ, equaling the eigenvalues of the graph matrix $(L+G)$. Therefore, each factor in the product (41), $\det(sI_n - A + c\lambda_j BKe^{-s\tau})$, must be asymptotically stable. This requirement is equivalent to the asymptotic stability of the trivial solution for a set of linear RFDEs

$$\dot{y}(t) = Ay(t) - c\lambda_j BKy(t - \tau). \tag{42}$$

Systems (42) are in the form of (37) but have the order of a single-agent dynamics, *i.e. n*. ■

The proof of Lemma 2 uses a detour in the frequency domain but the result pertains to time domain, and as such it shall be used. This is in contrast with many treatments of delays in the literature using frequency domain stability criteria, *e.g.* the Nyquist criterion, but more along the lines of methods guaranteeing a synchronizing region. In fact, conclusions of Lemma 1 for continuous-time cases can be considered as special cases of Lemma 2 with zero delay. Note that Lemma 1 and 2 provide necessary and sufficient conditions for cooperative stability. Both Lemma 1 and 2

rely on appropriate state transformations reducing the cooperative stability of high-order total dynamics to asymptotic stability of a set of lower-order systems. This reduced problem is then addressed by the synchronizing region approach.

The following definitions, motivated by Lemma 1 and 2, are required for subsequent development.

Definition 1. Given matrices (A, B), the *synchronizing region* for a matrix pencil

$$A - \sigma B \tag{43}$$

is a set given by $S_c = \{\sigma \in \mathbb{C} : A - \sigma B \text{ is } a.s.\}$. ■

Definition 2. Given a complex retarded functional differential equation (38) the *delay-dependent synchronizing region* is a subset of the complex plane $\mathbb{C}$ depending on the delay τ,

$$S_c(\tau) = \{\sigma \in \mathbb{C} : Ay(t) + \sigma A_d\, y(t-\tau)\ a.s.\}. \quad ■$$

Remark 1. The appropriate notions of stability used in Definition 1 and 2 depend on the particular system considered. Definitions for continuous and discrete-time synchronizing regions applicable here are given in [13],[15],[16],[17]. Furthermore, the actual matrix B in matrix pencil (43) one has the control over depends on whether one has full-state or only output-feedback and is different in controller and observer designs. Hence according to Lemma 1 and 2, conditions for cooperative stability in each case reduce to having all the relevant graph matrix eigenvalues scaled by an appropriate value of the coupling gain $c > 0$ into the pertaining synchronizing region. The goal is then to design the local feedback gain matrices K, F that in some way maximize the synchronizing region, thus facilitating cooperative stabilization.

In order to assess a synchronizing region one resorts to its guaranteed estimates. Sufficient conditions guaranteeing synchronizing region estimates for matrix pencils (43) are based on Lyapunov methods and evaluation of the following single-agent Lyapunov quadratic forms,

$$(A - \sigma B)^{\dagger} P + P(A - \sigma B), \tag{44}$$

in continuous-time [12],[13],[17], and

$$(A - \sigma B)^{\dagger} P (A - \sigma B) - P, \tag{45}$$

in the discrete-time [16]. The presence of time-delays requires similar albeit more involved approach using Lyapunov-Razumikhin functions instead of Lyapunov functions. The following theorems bring sufficient conditions and design schemes guaranteeing synchronization for a wide class of communication graphs. Some details of the Lyapunov-Razumikhin approach are only briefly sketched, the interested reader being referred to [19] for a more detailed exposition.

4.2. Discrete-time Cooperative Tracker Distributed Control Design

The following two Theorems bring design methods for distributed control gains K that guarantee discrete-time multi-agent system synchronization.

Theorem 1. [16]. **H_∞-Riccati Inequality Design for Synchronization.** Given systems (2) and (6), with protocol (10), assume that the interaction graph contains a spanning tree with at least one pinning gain that connects into a root node. Then the eigenvalues of the graph matrix $(I + D + G)^{-1}(L + G)$, $\Lambda_i > 0, \forall i$. If there exists an $\omega \in \mathbb{R}$ such that

$$\delta(\omega) := \max_{j \in \{1,\ldots,N\}} |1 - \omega\Lambda_j| < \delta_c, \tag{46}$$

where δ_c is obtained by

$$\delta_c = \sup_{\delta > 0} \{\delta \mid \exists P > 0 \text{ s.t. } P > A^T PA - (1-\delta^2) A^T PB (B^T PB)^{-1} B^T PA\} \tag{47}$$

then there exists a $P > 0$ solving

$$P > A^T PA - (1-\delta^2) A^T PB(B^T PB)^{-1} B^T PA. \tag{48}$$

with $\delta = \delta(\omega)$. Moreover, the control gain $K = (B^T PB)^{-1} B^T PA$, and coupling gain $c = \omega$ guarantee synchronization.

Proof: Denote $\delta_j = 1 - \omega\Lambda_j$. It is found that

$$P - (A - \omega\Lambda_j BK)^\dagger P(A - \omega\Lambda_j BK) = P - A^T PA + (1 - |\delta_j|^2) A^T PB(B^T PB)^{-1} B^T PA \geq P - A^T PA + (1-\delta^2) A^T PB(B^T PB)^{-1} B^T PA > 0.$$

where † denotes complex conjugate transpose. Thus, it follows from the single-agent discrete-time Lyapunov inequality that $\rho(A - \omega\Lambda_j BK) < 1$, hence is discrete-time stable. The rest of the proof follows from Lemma 1, [16]

■

Remark 2. For the single-input case, *i.e.*, $\mathrm{rank}(B)=1$, the sufficient condition given in Theorem 1 is also necessary, [16]. The importance of Theorem 1 is in showing that cooperative feedback design based on the Riccati inequality allows for separation of the single-agent feedback gain design from the detailed properties of the communication graph topology, as long as the graph contains a spanning tree with a nonzero pinning gain into a root node. Specifically, it reveals that if Riccati-based design is used for the feedback K at each node, then synchronization is guaranteed for a class of communication graphs whose graph matrix eigenvalues satisfy condition (46). This condition is appealing because it allows for a disentanglement of the properties of individual agents' feedback gains, as reflected by δ_c, and the graph topology, described by Λ_k, relating these through an inequality.

Theorem 2. [16] H_2-**Riccati Design for Synchronization.** Given systems (2),(6), with protocol (10), assume that the interaction graph contains a spanning tree with at least one pinning gain nonzero that connects into the root node. Then the eigenvalues of the graph matrix $(I + D + G)^{-1}(L + G)$, Λ_i, satisfy $\Lambda_i > 0, \forall i$. Let $P > 0$ be a solution of the single-agent discrete-time Riccati-like equation

$$A^T PA - P + Q - A^T PB(B^T PB)^{-1} B^T PA = 0 \tag{49}$$

for some prescribed $Q = Q^T > 0$. Define

$$r := \left[\sigma_{\max}(Q^{-T/2} A^T PB(B^T PB)^{-1} B^T PAQ^{-1/2}) \right]^{-1/2}. \tag{50}$$

Then protocol (10) guarantees synchronization of multi-agent systems (11) for some K if there exists a covering circle $C(c_0, r_0)$ of the graph matrix eigenvalues Λ_k, $k = 1 \ldots N$ such that

$$\frac{r_0}{c_0} < r. \tag{51}$$

Moreover, if condition (51) holds then the feedback gain matrix

$$K = (B^T PB)^{-1} B^T PA \tag{52}$$

and the coupling gain

$$c = \frac{1}{c_0} \tag{53}$$

guarantee state synchronization.

Proof: The synchronizing region for the choice of K given in Theorem 2, (52) contains the open circle $C(1, r)$. This is seen by choosing the state-feedback gain matrix as (52), with $P > 0$ solving equation (49); one has

$$A^T PA - P + Q - K^T \left(B^T PB \right) K = 0 \cdot$$

From this equation one obtains by completing the square

$$A^T PA - P + Q - K^T B^T PBK = (A - BK)^T P(A - BK) - P + Q = 0 .$$

Therefore, given the single-agent quadratic Lyapunov function $V(y) = y^T Py$, $y \in \mathbb{R}^n$, the choice of feedback gain stabilizes the system (A, B). A synchronizing region estimate can be found from the condition

$$(A - \sigma BK)^\dagger P(A - \sigma BK) = (A - \mathrm{Re}\,\sigma BK)^T P(A - \mathrm{Re}\,\sigma BK) + \mathrm{Im}^2\,\sigma (BK)^T PBK < P ,$$

where † denotes complex conjugate transpose (Hermitian adjoint), $\sigma \in \mathbb{C}$. Therefore from the above one has

$$\begin{aligned}
&(A - \sigma BK)^\dagger P(A - \sigma BK) - P \\
&= A^T PA - P - 2\,\mathrm{Re}\,\sigma K^T (B^T PB)K + \mathrm{Re}^2\,\sigma (BK)^T PBK + \mathrm{Im}^2\,\sigma (BK)^T PBK \\
&= A^T PA - P - (1 - |\sigma - 1|^2)(BK)^T PBK = -Q + K^T (B^T PB)K - (1 - |\sigma - 1|^2)(BK)^T PBK \\
&= -Q + |\sigma - 1|^2 K^T B^T PBK
\end{aligned} .$$

This implies stability if

$$Q - |\sigma - 1|^2 K^T B^T PBK > 0 ,$$

which gives a simple bounded complex region, more precisely a part of the complex gain margin region

$$Q > |\sigma - 1|^2 K^T B^T PBK \Rightarrow 1 > |\sigma - 1|^2 \sigma_{\max}(Q^{-T/2}(BK)^T P(BK)Q^{-1/2}) .$$

This is an open circle $C(1, r)$ specified by

$$|\sigma - 1|^2 < \frac{1}{\sigma_{\max}(Q^{-T/2}K^T B^T PBKQ^{-1/2})} .$$

Furthermore, expressing K as the H_2 Riccati equation state-feedback completes this part of the proof. Now, given a circle $C(1, r)$, centered at 1 of radius *r*, contained in the synchronizing region S of matrix pencil $A - \sigma BK$, and the properties of dilation (homothety), assuming there exists a directed spanning tree in the graph with a nonzero pinning gain into a root node, it follows that synchronization is guaranteed if all eigenvalues Λ_k are contained in a circle $C(c_0, r_0)$ similar with respect to homothety to a circle concentric with and contained within $C(1, r)$.

The center of the covering circle c_0 can be taken on the real axis due to symmetry and the radius equals $r_0 = \max_k |\Lambda_k - c_0|$. Taking these as given, one should have

$$\frac{r_0}{c_0} < \frac{r}{1} . \tag{54}$$

If this equation is satisfied then choosing $c = 1/c_0$ maps with homothety the covering circle of all eigenvalues $C(c_0, r_0)$ into a circle $C(1, r_0/c_0)$ concentric with and, for $r > r_0/c_0$, contained in the interior of the circle $C(1, r)$.

■

If there exists a solution $P > 0$ to Riccati equation (49), B must have full column rank. Assuming B has full column rank, there exists a positive definite solution P to (49) only if (A, B) is stabilizable.

Remark 3. (Comparison of H_∞- and H_2-Riccati designs for synchronization) By comparing (50) to (46) it is seen that a similar role is played by δ_c in Theorem 1 and r in Theorem 2. The latter can be explicitly computed using (50), but it depends on the selected *Q*. On the other hand, δ_c is found by numerical LMI techniques, [16]. Further, in Theorem 1, $\omega \in \mathbb{R}$ plays a role analogous to $1/c_0$ in Theorem 2. Theorem 1 relies on analysis based on the

circle $C(1,\delta_c)$, whereas Theorem 2 uses $C(1,r)$. Both circles are contained in the synchronizing region of the respective designed feedbacks.

More importantly, Theorem 2 gives synchronization conditions in terms of the radius *r* easily computed as (50) in terms of an H_2 Riccati equation solution. Computing the radius δ_c used in Theorem 1 must be generally done *via* an LMI. However, the condition in Theorem 1 is milder than that in Theorem 2. That is, $C(1,r)$ is generally contained in $C(1,\delta_c)$, so that systems that fail to meet the condition of Theorem 2 may yet be found synchronizable when tested according to the condition in Theorem 1.

4.3. Discrete-time Cooperative Observer Design

Having addressed the problem of cooperative stabilization in Subsection 4.2, we now consider the dual problem of cooperative estimation. Cooperative estimators and observers find their use, among other applications, in dynamic cooperative controllers designed to guarantee state synchronization, [15]. The following theorem is based on observer Riccati equation and brings a result dual to that of Theorem 2.

Theorem 3. [15]. **Riccati Design of Distributed Observer Gains.** Given systems (22) assume the interaction graph contains a spanning tree with at least one pinning gain that connects into the root node. Let $P>0$ be a solution of the single-agent discrete-time observer Riccati equation

$$APA^T - P + Q - APC^T (CPC^T)^{-1} CPA^T = 0, \tag{55}$$

where $Q = Q^T > 0$. Choose the observer gain matrix as

$$F = APC^T (CPC^T)^{-1}. \tag{56}$$

Define

$$r_{obs} := \left[\sigma_{\max} (Q^{-T/2} APC^T (CPC^T)^{-1} CPA^T Q^{-1/2}) \right]^{-1/2}. \tag{57}$$

Then the observer errors (23) are asymptotically stable if there exists a covering circle $C(c_0, r_0)$ of the graph matrix $(I+D+G)^{-1}(L+G)$ eigenvalues Λ_k, $k=1...N$ such that

$$\frac{r_0}{c_0} < r_{obs}. \tag{58}$$

If (58) holds then the coupling gain

$$c = \frac{1}{c_0} \tag{59}$$

makes the observer error dynamics (23) stable. ■

The proof follows similarly as that of Theorem 2, [15].

4.4. Continuous-time Cooperative Tracker Distributed Static OPFB Design

Under special conditions on single-agent systems it is possible to achieve cooperative stabilization by static distributed OPFB. Considerations lead to distributed design of static output-feedbacks, thereby avoiding the need for dynamic cooperative controllers.

Definition 3. Given matrices (A, B, C), and the static OPFB gain K, the *synchronizing region for static OPFB* is a set given by $S_y = \{\sigma \in \mathbb{C} : A - \sigma BKC \text{ is } a.s.\}$. ■

Theorem 4. [17]. Let the multi-agent system be given by (1), (4) and (5). Let the graph have a spanning tree with at least one pinning gain connecting to a root node. Choose the distributed static OPFB control (26), where the OPFB gain K satisfies the single-agent output Riccati-type equation

$$A^T P + PA + Q - PBR^{-1}B^T P + M^T R^{-1} M = 0 \tag{60}$$

for some $Q = Q^T > 0$, $R = R^T > 0$, $R = R^T > 0$, together with

$$KC = R^{-1}(B^T P + M). \tag{61}$$

In addition let the inequality

$$C^T K^T RKC - C^T K^T M - M^T KC \geq 0 \tag{62}$$

be satisfied. Then the guaranteed synchronizing region for static OPFB is a conical sector in the complex plane.

Proof: Let the following abbreviations be introduced

$$a := \lambda_{\min>0}(Q^{-T/2} C^T K^T RKC Q^{-1/2}), \tag{63}$$

$$b := \lambda_{\min>0}(Q^{-T/2}(C^T K^T RKC - C^T K^T M - M^T KC)Q^{-1/2}) \tag{64}$$

$$f := \lambda_{\max}(jQ^{-T/2}(M^T KC - C^T K^T M)Q^{-1/2}) \tag{65}$$

where $\lambda_{\min>0}$ denotes the smallest eigenvalue on the complement of the kernel.

Take the single-agent quadratic Lyapunov function $V(x) = x^\dagger Px$, $x \in \mathbb{C}^n$, for the complex matrix pencil $A - \sigma BKC$. The dagger † denotes the Hermitian adjoint. The positive definite real matrix, $P = P^T$, is chosen as a solution of the output Riccati-type equation (60). The time-derivative of this Lyapunov function is determined by the quadratic form of a Hermitean matrix

$$(A - \sigma BKC)^\dagger P + P(A - \sigma BKC) = A^T P + PA - \overline{\sigma} C^T K^T B^T P - \sigma PBKC,$$

which, by completing the squares, reads

$$A^T P + PA + (\sigma KC - R^{-1}(B^T P + M))^\dagger R(\sigma KC - R^{-1}(B^T P + M)) - |\sigma|^2 C^T K^T RKC + \overline{\sigma} C^T K^T M + \sigma M^T KC - C^T K^T RKC.$$

The choice of the OPFB satisfying (61) makes this expression equal to

$$A^T P + PA + |\sigma - 1|^2 C^T K^T RKC - |\sigma|^2 C^T K^T RKC + \overline{\sigma} C^T K^T M + \sigma M^T KC - C^T K^T RKC.$$

Using the single-agent output Riccati-type equation (60) gives

$$= -Q - (B^T P + M)^T R^{-1}(B^T P + M) - M^T R^{-1} M + PBR^{-1}B^T P + (1 - 2\,\mathrm{Re}\,\sigma) C^T K^T RKC + \overline{\sigma} C^T K^T M + \sigma M^T KC.$$

The sufficient condition guaranteeing asymptotic stability is then

$$-Q - (B^T P + M)^T R^{-1}(B^T P + M) - M^T R^{-1} M + PBR^{-1}B^T P + (1 - 2\,\mathrm{Re}\,\sigma) C^T K^T RKC + \overline{\sigma} C^T K^T M + \sigma M^T KC < 0,$$

allowing assessment of the synchronizing region for static OPFB in $\mathbb{C}$. This expression is equivalent to

$$-Q - |\sigma|^2 C^T K^T RKC + |\sigma - 1|^2 C^T K^T RKC + (\overline{\sigma} - 1) C^T K^T M + (\sigma - 1) M^T KC < 0. \tag{66}$$

With $|\sigma - 1|^2 - |\sigma|^2 = (1 - 2\,\mathrm{Re}\,\sigma)$ (66) becomes

$$-Q - (2\,\mathrm{Re}\,\sigma - 1) C^T K^T RKC + (\mathrm{Re}\,\sigma - 1)(C^T K^T M + M^T KC) + j\,\mathrm{Im}\,\sigma (M^T KC - C^T K^T M) < 0.$$

After straightforward manipulations condition (66) reads

$$
\begin{aligned}
&-I - \mathrm{Re}\,\sigma(Q^{-T/2}C^T K^T RKCQ^{-1/2}) \\
&-(\mathrm{Re}\,\sigma - 1)Q^{-T/2}(C^T K^T RKC - C^T K^T M - M^T KC)Q^{-1/2} + \mathrm{Im}\,\sigma(jQ^{-T/2}(M^T KC - C^T K^T M)Q^{-1/2}) < 0
\end{aligned}
\tag{67}
$$

Inequality (67) is certainly satisfied for $\mathrm{Re}\,\sigma \geq 1$ if

$$
\begin{aligned}
&-1 - \mathrm{Re}\,\sigma\lambda_{\min>0}(Q^{-T/2}C^T K^T RKCQ^{-1/2}) \\
&-(\mathrm{Re}\,\sigma - 1)\lambda_{\min>0}(Q^{-T/2}(C^T K^T RKC - C^T K^T M - M^T KC)Q^{-1/2}) + \left|\mathrm{Im}\,\sigma\right|\lambda_{\max}(jQ^{-T/2}(M^T KC - C^T K^T M)Q^{-T/2}) < 0
\end{aligned}
\tag{68}
$$

Note here that even though the last matrix term in (67) is antisymmetric it cannot be disregarded for the evaluation of the quadratic form. This is so because *j* multiplying it makes it Hermitian, and one has complex vector spaces here. Namely, the proof of Lemma 1 uses a coordinate transformation that is generally complex. This matrix has a special property that its eigenvalues appear as $\pm\lambda \in \mathbb{R}$, which is seen by complex conjugating the eigenvalue-eigenvector relation. Hence the absolute value of $\mathrm{Im}\,\sigma$ is needed in (68) compared to (67).

With the introduced abbreviations and shorthand notation, $v := \mathrm{Re}\,\sigma, w := \mathrm{Im}\,\sigma$, a guaranteed synchronizing region for OPFB is described as $v \geq 1$ and

$$
|w| < \left[1 - b + (a+b)v\right]/f\ , \tag{69}
$$

which describes a conical sector in the complex plane. This completes the proof. ■

Corollary 1. If $M = 0$ one recovers the synchronizing region characteristic of the full state-feedback [12],[13], described by the matrix inequality

$$
-Q + (1 - 2\,\mathrm{Re}\,\sigma)C^T K^T RKC < 0\,.
$$

However, given the prescribed output measurement matrix C in (27), the choice $M = 0$ generally cannot be made, [17]. That is, there may exist $M \neq 0$ such that (61) holds, *i.e.* $K^* C = R^{-1}(B^T P + M)$, yet $K^* C = R^{-1}B^T P$ fails to hold. ■

As in all cases hitherto presented with a guaranteed OPFB synchronizing region cooperative stability is achieved by scaling all the graph matrix eigenvalues into that region by an appropriate choice of a coupling gain $c > 0$. With the synchronizing region having the form of a conical sector one finds a restriction on the argument of the complex eigenvalues of the graph matrix. As a special case of OPFB, with $C = I_n, M = 0$, the proof of Theorem 4 reproduces the well-known continuous-time full state-feedback unbounded right half-plane synchronizing region[1], [13]. It should be emphasized that the cooperative stability conditions presented here are only sufficient, being based on Lyapunov estimates of guaranteed synchronizing regions, while Lemma 1 and 2 give necessary and sufficient conditions.

4.5. Delayed Control Cooperative Tracker Design

This subsection brings an application of the synchronizing region methodology to asymptotic and exponential cooperative stability of multi-agent systems having a uniform time-delay in control signals. Full state distributed feedback is considered for simplicity. Investigating such systems is the first step in tackling the effects of time-delays on cooperative stability. Although in realistic systems the assumption of uniform delays seems restrictive it is nonetheless frequently adopted for the sake of simplicity and feasibility of analysis.

4.5.1. Asymptotic Delay-dependent Cooperative Stability

As variants of Lyapunov stability analysis applicable to time-delay systems are not considered generally familiar the basic results on Lyapunov-Razumikhin stability conditions are given in the following theorem. Those results are then specialized to linear retarded functional differential equations (RFDE) and quadratic Lyapunov-Razumikhin functions, which are subsequently applied to complex RFDE (38) to guarantee delay-dependent synchronizing region estimate.

---

[1] It is mainly for this reason that the conventional continuous-time full-state distributed feedback cooperative tracker is not treated separately to parallel its discrete-time counterpart in Subsection 4.2.

Theorem 5. (*Lyapunov-Razumikhin stability theorem,* [19]). Let α, β, γ be class $\mathcal{K}$ functions, and let $p(s) > s \ \forall s > 0$ be a scalar continuous non-decreasing function. If there exists a continuous function $V(x): \mathbb{R}^n \to \mathbb{R}$ such that for some $k > 0$, for all $x_t \in \mathcal{C}$ satisfying $V(x_t(\vartheta)) \le k, \ \forall \vartheta \in [t-\tau, t]$, one has $\alpha(\|x\|) \le V(x) \le \beta(\|x\|)$,

$$\frac{d}{dt} V(x(t)) \le -\gamma(\|x(t)\|), \ \text{if } V(x(\vartheta)) < p(V(x(t)), \forall \vartheta \in [t-\tau, t],$$

then the trivial solution $x(t) \equiv 0$ of the considered RFDE is uniformly asymptotically stable. Furthermore, the set in $\mathcal{C}$ where $V(x_t(\vartheta)) \le k, \ \forall \vartheta \in [t-\tau, t]$ is an invariant subset in the region of attraction in the space $\mathcal{C}$. ■

Based on Theorem 5 sufficient conditions for asymptotic stability depending on delays are derived for the special case of linear single-delay complex RFDE having the form (37) or (38). The Lyapunov-Razumikhin functions appearing in Theorem 5 are modified to accommodate for the fact that the system is complex. State vectors x are allowed to be complex and the dagger † denotes the Hermitian adjoint, *i.e.* transposition and complex conjugation. Real $P = P^T > 0$ then give real-valued single-agent quadratic Lyapunov-Razumikhin functions, $V(x) = x^\dagger P x > 0, \ x \in \mathbb{C}^n$.

Theorem 6. (*Lyapunov-Razumikhin delay-dependent result for the complex equation,* [19]). Let there exist real positive definite symmetric matrices $P, P_1, P_2 > 0$, and a constant $\tau_0 > 0$ so that the following conditions are satisfied

$$P_1^{-1} < P, \ P_2^{-1} < P, \tag{70}$$

$$(A + \sigma A_d)^\dagger P + P(A + \sigma A_d) + \tau_0 |\sigma|^2 P A_d A P_1 A^T A_d^T P + \tau_0 |\sigma|^4 P A_d^2 P_2 (A_d^2)^T P + 2\tau_0 P < 0. \tag{71}$$

Then, for given $\sigma \in \mathbb{C}$, the trivial solution, $x(t) \equiv 0$, of equation

$$\dot{x}(t) = Ax(t) + \sigma A_d x(t-\tau) \tag{72}$$

is uniformly asymptotically stable for $0 \le \tau \le \tau_0$. ■

Lyapunov-Razumikhin delay-dependent sufficient stability conditions of Theorem 6 in turn provide a guaranteed estimate of the delay-dependent synchronizing region when applied to single-agent complex RFDE (72).

Theorem 7. [19]. Let (A, B) be stabilizable. Choose the local feedback gain as

$$K = R^{-1} B^T P, \tag{73}$$

with $P > 0$ a real symmetric solution of the single-agent algebraic matrix equation

$$A^T P + PA + Q - PBR^{-1} B^T P + \tau_0 (P A_d A P_1 A^T A_d^T P + P A_d^2 P_2 (A_d^2)^T P + 2P) = 0. \tag{74}$$

where $A_d = -BK = -BR^{-1} B^T P$, $Q > 0$ and $P_1 > 0, P_2 > 0$ symmetric matrices chosen to satisfy

$$P_1^{-1} < P, \ P_2^{-1} < P.$$

Then the single-agent closed-loop system, given by $A + A_d = A - BK$, is asymptotically stable with the delay margin τ_0 and the guaranteed synchronizing region estimate for delay margin τ is determined by inequalities

$$\operatorname{Re} \sigma > 1/2, \tag{75}$$

$$(1 - 2\operatorname{Re}\sigma) Q^{-T/2} P B R^{-1} B^T P Q^{-1/2} + Q^{-T/2} ((\tau |\sigma|^2 - \tau_0) P A_d A P_1 A^T A_d^T P + (\tau |\sigma|^4 - \tau_0) P A_d^2 P_2 (A_d^2)^T P + 2(\tau - \tau_0) P) Q^{-1/2} < I. \tag{76}$$

Proof: If the real positive definite symmetric solution of (71) exists, with the feedback gain (70), the closed-loop system matrix $A + A_d = A - BR^{-1}B^T P$ satisfies

$$(A - BR^{-1}B^T P)^T P + P(A - BR^{-1}B^T P) + \tau_0 (PA_d AP_1 A^T A_d^T P + PA_d^2 P_2 (A_d^2)^T P + 2P) = -Q - PBR^{-1}B^T P < 0,$$

guaranteeing stability of the closed-loop single-agent system ($\sigma = 1$) with the delay margin τ_0. The synchronizing region for the delay margin τ, generally different than τ_0, follows as

$$\begin{aligned}
&(A - \sigma BR^{-1}B^T P)^\dagger P + P(A - \sigma BR^{-1}B^T P) + \tau(|\sigma|^2 PA_d AP_1 A^T A_d^T P + |\sigma|^4 PA_d^2 P_2 (A_d^2)^T P + 2P) \\
&= A^T P + PA - 2\,\mathrm{Re}\,\sigma (PBR^{-1}B^T P) + \tau(|\sigma|^2 PA_d AP_1 A^T A_d^T P + |\sigma|^4 PA_d^2 P_2 (A_d^2)^T P + 2P) \\
&= -Q + (1 - 2\,\mathrm{Re}\,\sigma) PBR^{-1}B^T P - \tau_0 (PA_d AP_1 A^T A_d^T P + PA_d^2 P_2 (A_d^2)^T P + 2P) + \tau(|\sigma|^2 PA_d AP_1 A^T A_d^T P + |\sigma|^4 PA_d^2 P_2 (A_d^2)^T P + 2P) \\
&= -Q + (1 - 2\,\mathrm{Re}\,\sigma) PBR^{-1}B^T P + ((\tau|\sigma|^2 - \tau_0) PA_d AP_1 A^T A_d^T P + (\tau|\sigma|^4 - \tau_0) PA_d^2 P_2 (A_d^2)^T P + 2(\tau - \tau_0) P)
\end{aligned}$$

For stability the above matrix expression needs to be negative definite, which is equivalent to

$$-I + (1 - 2\,\mathrm{Re}\,\sigma) Q^{-T/2} PBR^{-1}B^T PQ^{-1/2} + Q^{-T/2} ((\tau|\sigma|^2 - \tau_0) PA_d AP_1 A^T A_d^T P + (\tau|\sigma|^4 - \tau_0) PA_d^2 P_2 (A_d^2)^T P + 2(\tau - \tau_0) P) Q^{-1/2} < 0.$$

Condition (74) guarantees single-agent stability with delay margin τ_0 when delays τ are neglected. This concludes the proof. ■

Note that a real positive definite solution to (74) surely exists under the conditions of the Theorem for the delay margin τ_0 sufficiently small, as it equals the solution of the ARE with the Q matrix appropriately redefined by subtracting the resulting term multiplied by τ_0. For sufficiently small τ_0 the Q matrix thus redefined is still positive definite.

Corollary 2. [19]. Let (A, B) be stabilizable. Choose the local feedback gain as

$$K = R^{-1}B^T P, \tag{77}$$

with $P > 0$ a real symmetric solution of the single-agent algebraic Riccati equation

$$A^T P + PA + Q - PBR^{-1}B^T P = 0, \tag{78}$$

where $Q = Q^T > 0$. Choose symmetric matrices $P_1 > 0, P_2 > 0$ satisfying $P_1^{-1} < P, P_2^{-1} < P$. Then the guaranteed estimate of the delay-dependent synchronizing region $S_c(\tau)$ is determined by inequalities

$$\mathrm{Re}\,\sigma > 1/2, \tag{79}$$

$$(1 - 2\,\mathrm{Re}\,\sigma) Q^{-T/2} PBR^{-1}B^T PQ^{-1/2} + \tau Q^{-T/2} \left[|\sigma|^2 PBKAP_1 A^T K^T B^T P + |\sigma|^4 P(BK)^2 P_2 (K^T B^T)^2 P + 2P \right] Q^{-1/2} < I. \tag{80}$$

■

Building on a guaranteed delay-dependent synchronizing region estimate of Theorem 7 and Corollary 2, the following result brings a design prescription for state-synchronization under delayed distributed state-feedback.

Theorem 8. [19]. Let the graph contain the spanning tree with pinning to a root node. Choose the local feedback matrix as the Riccati gain of Corollary 2. Then the multi-agent system (35) synchronizes for the choice of

$$c \geq \frac{1}{2 \min \mathrm{Re}\,\lambda(L + G)}, \tag{81}$$

if the delay margin τ satisfies the condition

$$(1-2\,\mathrm{Re}\,c\lambda_j)Q^{-T/2}PBR^{-1}B^TPQ^{-1/2}+\tau Q^{-T/2}\left[\left|c\lambda_j\right|^2 PBKAP_1A^TK^TB^TP+\left|c\lambda_j\right|^4 P(BK)^2P_2(K^TB^T)^2P+2P\right]Q^{-1/2}<I, \quad (82)$$

for all $c\lambda_j$. ■

4.5.2. Exponential Delay-dependent Cooperative Stability

Conditions for exponential cooperative stability are presented here as a strengthening of asymptotic cooperative stability conditions of Subsection 4.5.1.

Definition 4. Given a complex retarded functional differential equation (38), the *delay-dependent synchronizing region for exponential stability* with a prescribed convergence rate $a\in\mathbb{R}^+$ is a subset of the complex plane $\mathbb{C}$ depending on the delay τ,

$$S_c(\tau,a)=\left\{\sigma\in\mathbb{C}: Ay(t)+\sigma A_d y(t-\tau)\ e.s.\right\}, \quad (83)$$

with exponential stability characterized by the prescribed convergence rate a. ■

A sufficient condition for asymptotic stability with exponential convergence rate for RFDEs based on Razumikhin stability functions is detailed in the following theorem, (ibid [19]).

Theorem 9. (*Lyapunov-Razumikhin exponential stability result*) Let the conditions of Theorem 5 be satisfied with $\lambda\|x\|^p=\alpha(\|x\|)$ for some $\lambda>0,\ p\in\mathbb{R},\ p\geq 1,\ \gamma>0$, and

$$\frac{d}{dt}V(x(t))\leq-\gamma V(x(t))\ \ if\ V(x(\vartheta))<V(x(t))e^{\gamma\tau},\ \forall\vartheta\in\left[t-\tau,t\right]. \quad (84)$$

Then the trivial solution $x(t)\equiv 0$ of the considered RFDE is exponentially stable with convergence rate γ/p. ■

Linear delay differential systems, *e.g.* (37), have the spectrum-determined growth property. Therefore in case of exponential stability the convergence rate is determined by the spectral abscissa. Theorem 9 applied to (37) provides a Lyapunov-Razumikhin bound on the spectral abscissa. The following result guarantees exponential stability with a prescribed convergence rate in dependence of delays for the complex RFDE, [19]. It is considered a stricter version of Theorem 6.

Theorem 10. [19]. (*Lyapunov-Razumikhin delay dependent exponential stability result for the complex equation*). Let there exist real positive definite symmetric matrices $P,P_1,P_2>0$, and a constant $\tau_0>0$ so that the following conditions are satisfied

$$P_1^{-1}<P,\ P_2^{-1}<P,$$

$$(A+\sigma A_d)^\dagger P+P(A+\sigma A_d)+\tau_0\left|\sigma\right|^2 PA_dAP_1A^TA_d^TP+\tau_0\left|\sigma\right|^4 PA_d^2P_2(A_d^2)^TP+2\tau_0e^{2\gamma\tau_0}P<-\gamma P \quad (85)$$

where $\gamma\in\mathbb{R}^+$. Then, for given $\sigma\in\mathbb{C}$, the trivial solution, $y(t)\equiv 0$, of equation

$$\dot{y}(t)=Ay(t)+\sigma A_d y(t-\tau)$$

is exponentially stable for $0\leq\tau\leq\tau_0$, with convergence rate $\gamma/2$.

Proof: Follows from Theorem 9 and Theorem 6. With the quadratic Lyapunov-Razumikhin function one has $p=2$ in Theorem 9. Provisions (84) of Theorem 9 on the interval $\left[t-2\tau,t\right]$; $V(x(\vartheta))<V(x(t))e^{2\gamma\tau}\ \ \forall\vartheta\in\left[t-2\tau,t\right]$ yield the inequality

$$\frac{d}{dt}V(x(t))\leq x^\dagger(t)\left[(A+\sigma A_d)^\dagger P+P(A+\sigma A_d)+\tau\left|\sigma\right|^2 PA_dAP_1A^TA_d^TP+\tau\left|\sigma\right|^4 PA_d^2P_2(A_d^2)^TP+2\tau e^{2\gamma\tau}P\right]x(t).$$

By condition (85) of the Theorem, for $0 \le \tau \le \tau_0$

$$\frac{d}{dt}V(x(t)) \le -\gamma V(x(t)),$$

thus, according to Theorem 9, completing the proof. ■

Exponential stability of the transformed model with prescribed convergence rate, used to derive the stability condition (85), is sufficient to guarantee the same for the original system, [19]. Exponential stability with a prescribed convergence rate is stronger than asymptotic stability; hence synchronizing region satisfying the prescribed exponential convergence rate is contained in the asymptotic stability synchronizing region for the same time-delay,

$$S_c(\tau, a) \subseteq S_c(\tau).$$

Due to exponential terms the exponential synchronizing region estimate (85) strongly depends on the values of delay τ and the prescribed convergence rate a. As Theorem 10 shows, the inclusion property with respect to decreasing delays holds naturally for prescribed convergence exponential stability synchronizing region estimates (85). Furthermore the synchronizing region for greater convergence rates a is necessarily contained in that for smaller ones,

$$S_c(\tau, a_1) \subseteq S_c(\tau, a_2) \text{ for } a_1 \ge a_2.$$

These considerations reflect the robustness of exponential stability with respect to delays. Design methodology of Theorem 8 is equally applicable to synchronizing region with a prescribed exponential convergence rate. One only needs to consider the single-agent algebraic matrix equation

$$A^T P + PA + Q - PBR^{-1}B^T P + \tau_0 (PA_d A P_1 A^T A_d^T P + PA_d^2 P_2 (A_d^2)^T P + 2e^{2\gamma\tau_0} P) = -\gamma P$$

guaranteeing exponential stability for the single-agent system, instead of asymptotic stability guaranteed by (74). Then an estimate of the synchronizing region for exponential stability with the same convergence rate a but possibly different delays τ follows similarly as in Theorem 7 from the single-agent matrix inequality

$$-Q + (1 - 2\,\mathrm{Re}\,\sigma) PBR^{-1}B^T P + (\tau|\sigma|^2 - \tau_0) PA_d A P_1 A^T A_d^T P + (\tau|\sigma|^4 - \tau_0) PA_d^2 P_2 (A_d^2)^T P + 2(\tau e^{2\gamma\tau} - \tau_0 e^{2\gamma\tau_0}) P < 0$$

It should be remarked that for delay-free case, $\tau = 0 = \tau_0$, the above results naturally reduce to ones presented in preceding subsections, *i.e.* those not considering time-delays, leading to unbounded synchronizing regions.

If all the diagonal blocks in (41), *i.e.* all the systems (42), are exponentially stable with a prescribed convergence rate, as guaranteed by the delay-dependent synchronizing region, then the original system (36) shares the same convergence property. Therefore synchronization is guaranteed with a prescribed exponential convergence rate if all the graph matrix eigenvalues are scaled into the pertaining synchronizing region by an appropriate coupling gain.

V. ROBUST SYNCHRONIZING REGION FOR DISTURBANCES AND UNCERTAIN SYSTEMS

Design of cooperative controls robust to external disturbances and single-agent uncertainties can also be approached *via* synchronizing region methodology. This section brings H_∞-synchronizing regions for robustness to disturbances and synchronizing regions for uncertain agents.

5.1. H_∞-Synchronizing Regions

Reference [20] introduces a concept of an H_∞-synchronizing region for agents

$$\dot{x}_i = Ax_i + Bu_i + D\omega_i,$$

acted upon by external disturbances ω_i. Regulated outputs are $z_i = N^{-1}C\sum_{j=1}^{N}(x_i - x_j)$ and those signals are related to the total synchronization error. Graph topology is assumed undirected and the distributed state-feedback (8) is used. An appropriate state transformation of the total multi-agent system dynamics leads to considering systems of the form

$$\dot{\hat{x}}_i = (A - c\lambda_i BK)\hat{x}_i + D\hat{\omega}_i$$
$$\hat{z}_i = C\hat{x}_i$$

which are required to be asymptotically stable in absence of disturbances, and to have an H_∞-bound on output $\hat{z}_i$ with respect to disturbance $\hat{\omega}_i$ less than γ for all relevant eigenvalues of the graph matrix, λ_i. This motivates the interest in system

$$\dot{\zeta}_i = (A - \sigma BK)\zeta_i + D\omega_i$$
$$z_i = C\zeta_i$$

that defines the H_∞-synchronizing region, $\sigma \in \mathbb{R}$, for undirected graphs. Then an H_∞ Riccati inequality

$$A^T P + PA - \delta PBB^T P + \gamma^{-2} PDD^T P + C^T C < 0$$

for any $\delta > 0$ is used to provide a guaranteed H_∞-synchronizing region estimate and to subsequently construct the single-agent feedback gain

$$K = \frac{1}{2} B^T P .$$

This feedback gain in distributed state-feedback (8) guarantees an $\mathcal{L}_2$ bound less than γ for all regulated outputs z_i with respect to disturbances if the coupling gain $c > 0$ is chosen such that all relevant graph matrix eigenvalues λ_i satisfy $c\lambda_i \geq \delta$. For more details on H_∞-synchronizing regions the interested reader is referred to [20].

5.2. Synchronizing Regions for Uncertain Agents

For single-agent uncertainties, assume bounded yet otherwise unknown uncertainties in the system matrix A, denoted by δA, and in the input-to-state coupling matrix B, denoted likewise by δB. For clarity, only distributed state-feedback is presented here. Consider the guaranteed synchronizing region estimate for an uncertain matrix pencil $(A + \delta A, B + \delta B)$ with feedback gain K,

$$A + \delta A - \sigma(B + \delta B)K .$$

The single-agent Lyapunov stability condition is constructed as

$$(A + \delta A)^T P + P(A + \delta A) - \sigma P(B + \delta B)K - \overline{\sigma} K^T (B + \delta B)^T P < 0 .$$

Choosing the state-feedback gain as designed for the certain part of single-agent system (A, B),

$$K = R^{-1} B^T P ,$$

where $P > 0$ is a real symmetric solution of the single-agent algebraic Riccati equation,

$$A^T P + PA - PBR^{-1} B^T P = -Q ,$$

leads to the stability requirement

$$A^T P + PA + \delta A^T P + P\delta A - \sigma PBR^{-1} B^T P - \sigma P\delta BR^{-1} B^T P - \overline{\sigma} PBR^{-1} B^T P - \overline{\sigma} PBR^{-1} \delta B^T P < 0$$
$$\Rightarrow A^T P + PA - 2\,\mathrm{Re}\,\sigma PBR^{-1} B^T P + \delta A^T P + P\delta A - \sigma P\delta BR^{-1} B^T P - \overline{\sigma} PBR^{-1} \delta B^T P$$

$$= -Q + (1 - 2\,\mathrm{Re}\,\sigma)PBR^{-1}B^T P + (\delta A^T P + P\delta A) - (\sigma P\delta BR^{-1}B^T P + \overline{\sigma} PBR^{-1}\delta B^T P)$$

$$= -Q + (1 - 2\,\mathrm{Re}\,\sigma)PBR^{-1}B^T P + (\delta A^T P + P\delta A)$$

$$- \mathrm{Re}\,\sigma(P\delta BR^{-1}B^T P + PBR^{-1}\delta B^T P) - j\,\mathrm{Im}\,\sigma(P\delta BR^{-1}B^T P - PBR^{-1}\delta B^T P) < 0$$

It is seen from the above expression that uncertainties δA contribute terms independent of σ which can be robustly taken care of by sufficiently large $\mathrm{Re}\,\sigma$. Note that for a fixed solution P a magnitude bound on δA gives a constant bounded indefinite term. Hence, due to δA uncertainties, the shape of a guaranteed synchronizing region remains qualitatively the same. However, uncertainties δB contribute terms depending on σ, with $\mathrm{Re}\,\sigma, \mathrm{Im}\,\sigma$ multiplying Hermitian matrices. Comparing this matrix expression with that for constant OPFB, (67), leads one to conclude that the guaranteed robust synchronizing region has a conical form; the uncertainties in B change the shape of guaranteed synchronizing region qualitatively as well, (*c.f.* proof of Theorem 4). So, the greater the magnitude of uncertainties δB, the narrower a guaranteed synchronizing region estimate in the complex plane.

It is worth emphasizing here yet again that this is only a sufficient and not a necessary stability condition, hence one operates with guaranteed synchronizing region estimates rather than exact synchronizing regions.

VI. CONCLUSIONS

This research summary reviews some methods of cooperative stability analysis and control design for various identical-agent multi-agent system state-synchronization problems. Cooperative state-feedback, observer design, static OPFB, and delayed state-feedback are addressed. The common tread is the synchronizing region approach; separating the detailed graph topology from single-agent dynamics and thus guaranteeing robustness and flexibility. This versatile approach crystallized in the past few years into a useful analysis and design tool. It is shown in this survey, for the first time to the knowledge of the authors, that this methodology is also applicable to uncertain single-agent systems. Single-agent uncertainties are found to restrict the graph topologies that allow for robust synchronization in terms of magnitudes of uncertainties.

References

[1] Vicsek, T., Czirok, A., Ben E., Jacob, I., Cohen, & Schochet, O. (1995) Novel type of phase transitions in a system of self-driven particles," Phys. Rev. Lett., 75, pp. 1226–1229.

[2] Olfati-Saber, R., Fax, J. A., & Murray, R. (2007). Consensus and Cooperation in Networked Multi-Agent Systems (invited paper). *Proceedings of the IEEE*, 95(1), pp. 215-233.

[3] Tsitsiklis, J. (1984). Problems in Decentralized Decision Making and Computation. Ph.D. dissertation, Dept. Elect. Eng. and Comput. Sci., MIT, Cambridge, MA.

[4] Olfati-Saber, R., & Murray, R.M. (2004). Consensus problems in networks of agents with switching topology and time-delays. *IEEE Transactions on Automatic Control*, 49(9), pp. 1520-1533.

[5] Jadbabaie, A., Lin, J., & Morse, A. (2003). Coordination of groups of mobile autonomous agents using nearest neighbour rules. *IEEE Transactions on Automatic Control*, 48(6), pp. 988–1001.

[6] Fax, J.A., & Murray, R. M. (2004), Information Flow and Cooperative Control of Vehicle Formations. *IEEE Transactions on Automatic Control*, 49(9), pp. 1465-1476.

[7] Ren, W., & Beard, R.W. (2005). Consensus seeking in multiagent systems under dynamically changing interaction topologies. *IEEE Transactions on Automatic Control*, 50, pp. 655–661,

[8] Wang, X. F., & Chen, G. (2002). Pinning control of scale free dynamical networks. *Physica A*, 310, pp. 521-531.

[9] Li, Z., Duan, Z., Chen, G., & Huang, L. (2010). Consensus of multiagent systems and synchronization of complex networks: a unified viewpoint. *IEEE Transactions on Circuits and Systems I, Reg. Papers,* 57(1), pp. 213–224.

[10] Pecora, L. M., & Carroll, T. L. (1998). Master Stability Functions for Synchronized Coupled Systems. *Physical Review Letters*, 80(10), pp. 2109-2112.

[11] Duan, Z., Chen, G., & Huang, L. (2009). Disconnected synchronized regions of complex dynamical networks. *IEEE Transactions on Automatic Control*, 54(4), pp. 845–849.

[12] Tuna, S. E. (2008). LQR-based coupling gain for synchronization of linear systems. *arXiv:0801.3390v1 [math.OC]*.

[13] Zhang, H., & Lewis, F. L. (2011). Optimal Design for Synchronization of Cooperative Systems: State Feedback, Observer and Output Feedback, *IEEE Transactions on Automatic Control*, 56(8), pp. 1948-1953

[14] Elia, N. & Mitter, S.K. (2001). Stabilization of linear systems with limited information, IEEE Transactions on Automatic Control, 46(9), pp. 1384-1400.

[15] Hengster-Movric, K., Lewis, F.L. (2012). Cooperative observers and regulators for discrete-time multiagent systems. *International Journal of Robust and Nonlinear Control*; DOI: 10.1002/rnc.2840

[16] Hengster-Movric, K., You, K., Lewis, F.L & Xie, L. (2012). Synchronization of Discrete-time Multi-agent Systems on graphs using Riccati Design. *Automatica,* 49(2). pp. 414-423.

[17] Hengster-Movric, K., Lewis, L. (2015). Distributed Static Output-feedback Control for State Synchronization in Networks of Identical LTI Agents, *Automatica*, 53, pp. 282-290.

[18] Sipahi R, Qiao W. (2010) Responsible eigenvalue concept for the stability of a class of single-delay consensus dynamics with fixed topology, *IET Control Theory and Applications*; DOI: 10.1049/iet-cta.2010.0202

[19] Hengster-Movric, K., Lewis, F., Šebek, M., Vyhlidal, T. (2015). Cooperative Synchronization Control for Agents with Control Delays: A Synchronizing Region Approach, *Journal of the Franklin Institute*, DOI: 10.1016/j.jfranklin.2015.02.011.

[20] Li, Z., Duan, Z., Chen, G. (2010) H_∞ Consensus Regions of Multi-agent Systems, *Proceedings of the 29th Chinese Control Conference*, July 29-31, 2010, Bejing, China

[21] Tanner, H.G., Christodoulakis, D.K. (2005) State synchronization in local-interaction networks is robust with respect to time delays, *2005 and 2005 European Control Conference. CDC-ECC '05. 44th IEEE Conference on Decision and Control,* 12-15 Dec. 2005. pp. 4945–4950. DOI: 10.1109/CDC.2005.1582945

2. DISTRIBUTED STATIC OUTPUT-FEEDBACK CONTROL FOR STATE SYNCHRONIZATION OF MULTI-AGENT SYSTEMS

Kristian Hengster-Movric, Frank L. Lewis**,** Michael Sebek, **Distributed Static Output-feedback Control for State Synchronization of Multi-agent Systems**, *Automatica* 53 (2015), pp. 282–290.

This paper, published in Elsevier's *Automatica*, (IF: 6.126, the main IFAC journal), in 2015, brings technical details on the application of the synchronizing region to state synchronization of multi-agent systems comprised of homogeneous agents using static output-feedback. Restricting the choice of feedback to outputs brings additional difficulties for the design of the cooperative control, as well as it somewhat restricts the type of graph topologies that allow for synchronization in this manner. The benefit is a simple, time-invariant feedback guaranteeing distributed state synchronization and H_∞-bound in case of disturbances.

This paper studies state synchronization of multi-agent systems with disturbances using distributed static output-feedback (OPFB) control. The bounded L_2 gain synchronization problem using distributed static OPFB is defined and solved. The availability of only output measurements restricts the local controls design, while the communication graph topology restricts global information flow among the agents. It is shown here that these two types of restriction can be dealt with in a symmetric manner and lead to two similar conditions guaranteeing the existence of bounded L_2 gain static OPFB. One condition is on the output measurement matrix on a local scale, and the other on the graph Laplacian matrix on a global scale. Under additional conditions a distributed two-player zero-sum game using static OPFB is also solved and leads to distributed Nash equilibrium on the communication graph. As a special case the static OPFB globally optimal control is given. A new class of digraphs satisfying the above condition on the graph Laplacian is studied. The synchronizing region for distributed static OPFB control is exposed and found to be conical, different than the infinite right-half plane synchronizing region for distributed state feedback.

Automatica 53 (2015) 282–290

Contents lists available at ScienceDirect

Automatica

journal homepage: www.elsevier.com/locate/automatica

Brief paper

Distributed static output-feedback control for state synchronization in networks of identical LTI systems☆

Kristian Hengster-Movric [a,1], Frank L. Lewis [b], Michael Sebek [a]

[a] Department of Control Engineering, Czech Technical University in Prague, Czech Republic

[b] University of Texas at Arlington Research Institute, 7300 Jack Newell Blvd., S, Ft. Worth, TX 76118, USA

ARTICLE INFO

Article history:
Received 29 June 2013
Received in revised form
16 July 2014
Accepted 18 November 2014
Available online 26 January 2015

Keywords:
Multi-agent systems
Distributed control
Synchronization
Synchronizing region
Static output-feedback
H_∞-control
Cooperative two-player zero-sum game
Optimal control

ABSTRACT

This paper studies state synchronization of multi-agent systems with disturbances using distributed static output-feedback (OPFB) control. The bounded L_2 gain synchronization problem using distributed static OPFB is defined and solved. The availability of only output measurements restricts the local controls design, while the communication graph topology restricts global information flow among the agents. It is shown here that these two types of restriction can be dealt with in a symmetric manner and lead to two similar conditions guaranteeing the existence of bounded L_2 gain static OPFB. One condition is on the output measurement matrix on a local scale, and the other on the graph Laplacian matrix on a global scale. Under additional conditions a distributed two-player zero-sum game using static OPFB is also solved and leads to distributed Nash equilibrium on the communication graph. As a special case the static OPFB globally optimal control is given. A new class of digraphs satisfying the above condition on the graph Laplacian is studied. The synchronizing region for distributed static OPFB control is exposed and found to be conical, different than the infinite right-half plane synchronizing region for distributed state feedback.

1. Introduction

Standard approaches to output-feedback (OPFB) synchronization of multi-agent systems on graphs employ dynamic OPFB compensators, or static OPFB assuming some extra conditions simplifying the problem. This paper is concerned with the general static OPFB synchronization problem on graphs. Solutions are sought that optimize certain globally defined performance measures. Conditions on the local output measurement matrix and on the global graph Laplacian are given that are similar; these reveal the structure of the interactions between local measurement limitations and global graph communication limitations. A numerical example is given showing the power of the new approach in providing static OPFB synchronization where existing methods cannot apply.

The last two decades have witnessed an increasing interest in multi-agent networked cooperative systems, Baillieul and Antsaklis (2007), Fax and Murray (2004), Jadbabaie, Lin, and Morse (2003), Li, Duan, Chen, and Huang (2010), Olfati-Saber, Fax, and Murray (2007), Olfati-Saber and Murray (2003, 2004), Schenato, Sinopoli, Franceschetti, Poolla, and Sastry (2007), Tsitsiklis (1984) and Wang and Chen (2002). Early work, Fax and Murray (2004), Olfati-Saber et al. (2007), Olfati-Saber and Murray (2003, 2004), Ren and Beard (2005) and Tsitsiklis (1984), refers to consensus without a leader. By adding a command generator leader that pins to a group of agents one can obtain synchronization to a reference trajectory; this is termed pinning control (Chen, Liu, & Lu, 2007; Hengster-Movric, You, Lewis, & Xie, 2012; Sorrentino, di Bernardo, Garofalo, & Chen, 2007; Wang & Chen, 2002; Zhang & Lewis, 2011). We call this the *cooperative tracker problem*. There all the agents synchronize to the leader's reference trajectory. Necessary and sufficient conditions for synchronization to the leader are given by the master stability function approach (Pecora & Carroll, 1998), and the related concept of synchronizing region (Duan, Chen, & Huang, 2009; Sorrentino et al., 2007; Tuna, 2008; Wang & Chen, 2002). This guarantees local stability. Global results are obtained by contraction analysis, *i.e.* incremental stability (Lohnmiller & Slotine, 1997; Pavlov, Pogromski, van de Wouv, & Nijmeijer, 2004; Russo, di Bernardo, & Sontag, 2013). For linear systems, however, local

☆ The material in this paper was not presented at any conference. This paper was recommended for publication in revised form by Associate Editor Dimos V. Dimarogonas under the direction of Editor Frank Allgöwer.

E-mail addresses: kristian.hengster-movric@mavs.uta.edu (K. Hengster-Movric), Lewis@uta.edu (F.L. Lewis), michael.sebek@fel.cvut.cz (M. Sebek).

[1] Tel.: +420 224 357 488; fax: +420 224 918 646.

http://dx.doi.org/10.1016/j.automatica.2014.12.015
0005-1098/

and global stabilities coincide; hence the synchronizing region approach yields global results. Pinning control papers often assume a special inner coupling matrix that simplifies the design (Chen et al., 2007; Duan et al., 2009; Liu, 2011; Sorrentino et al., 2007; Wang & Chen, 2002) and disregards the controllability properties of single-agent systems. For nonlinear systems special autonomous dynamics is assumed (*e.g.* QUAD) (Chen et al., 2007; Liu, 2011), to guarantee synchronization.

For state-feedback synchronization of linear time-invariant (LTI) systems, an approach given in Li et al. (2010), Tuna (2008) and Zhang and Lewis (2011) uses locally optimal feedback derived from the algebraic Riccati equation. Such control guarantees an unbounded right-half plane synchronizing region. Hence, state synchronization is achieved under mild conditions on the directed communication graph topology, utilizing stabilizability properties of individual agents.

If the entire agents' states are not available one can use the dynamic OPFB, as detailed in Hengster-Movric and Lewis (2012), Li, Duan, and Chen (2011); Li et al. (2010), Scardovi and Sepulchre (2009), You and Xie (2011) and Zhang and Lewis (2011). There, observer-based dynamic cooperative regulators are used to guarantee state synchronization under single-agent stabilizability and detectability. The approach in Wieland, Sepulchre, and Allgower (2011) uses a reference model based design to extend these results to heterogeneous LTI networks. There, identical reference generators communicate their full states and synchronize. Such local reference signals are then tracked by agents.

In the case of dynamic OPFB control, necessary and sufficient conditions for the existence of stabilizing regulators are agent's stabilizability and detectability. The static OPFB cooperative control problem is considerably more involved than distributed dynamic OPFB design. It is known that for the single-agent case, static OPFB control depends on deep structural geometric properties of the dynamics (Syrmos, Abdallah, Dorato, & Grigoriadis, 1997; Wonham, 1985, chap. 4). Generally, individual agent's stabilizability and detectability is not sufficient for existence of stabilizing static OPFB controls and there exist no closed-form formulae for stabilizing or optimal static OPFB gains. The 1997 survey paper (Syrmos et al., 1997) gives static OPFB solutions in terms of coupled Riccati and Lyapunov equations. In Lewis, Vrabie, and Syrmos (2012) static OPFB solutions are given in terms of two coupled Riccati equations. In Gadewadikar, Lewis, and Abu-Khalaf (2006); Gadewadikar, Lewis, Xie, Kučera, and Abu-Khalaf (2007) necessary and sufficient conditions for static OPFB bounded L_2 gain control are given in terms of a generalized Riccati equation and an extra condition in terms of the measurement matrix.

In Chopra and Spong (2006) static OPFB synchronization was provided for passive systems. In Scardovi and Sepulchre (2009) dynamic OPFB synchronization was considered. A result was also given there that provides static OPFB designs for passive systems. In Ma and Zhang (2010) static OPFB synchronization controls rely on a rank condition that simplifies the problem so that necessary and sufficient conditions are local stabilizability and detectability.

The approaches in Li et al. (2010), Tuna (2008) and Zhang and Lewis (2011) provide guaranteed synchronization using locally optimal state feedback design at each agent. Globally optimal design for state feedback cooperative control that optimizes performance measures that depend on all the agent dynamics has been considered in many papers (Borelli & Keviczky, 2008; Cao & Ren, 2010; Dunbar & Murray, 2006; Hengster-Movric & Lewis, 2014; Jovanovic, 2005; Qu, Simaan, & Doug, 2009; Vamvoudakis & Lewis, 2011). The common difficulty, however, is that globally optimal control solutions are generally not distributed, so that each agent's control depends not only on its neighbors in the graph (Cao & Ren, 2010; Hengster-Movric & Lewis, 2014; Qu et al., 2009). To have a distributed control that is optimal in some sense it is possible *e.g.* to consider each agent optimizing its own, local, performance index. This is done for receding horizon control in Dunbar and Murray (2006), implicitly in Zhang and Lewis (2011), and for distributed games on graphs in Vamvoudakis and Lewis (2011), where the notion of optimality is Nash equilibrium. In the case of agents with identical LTI dynamics, Borelli and Keviczky (2008) presents a suboptimal state feedback design that is distributed on the graph topology.

An H_∞-control approach to cooperative synchronization is detailed in Li, Duan, and Chen (2010), where an LMI-based design is used to achieve synchronization and disturbance rejection. That work, Li et al. (2010), uses cooperative full state feedback. The H_∞-synchronizing region is defined as a generalization of the conventional synchronizing region (Duan et al., 2009; Li et al., 2010; Zhang & Lewis, 2011) and LMI conditions are given for it to be unbounded on the real line.

In this paper we study static OPFB cooperative control designs that consider global performance measures. The bounded L_2 gain synchronization problem using distributed static OPFB is defined and solved. Under additional conditions a distributed two-player zero-sum game using static OPFB is also solved and leads to distributed Nash equilibrium on the communication graph. As a special case the static OPFB globally optimal control is given. Requiring solutions of these static OPFB control problems to be distributed imposes a condition on the graph topology. A new class of digraphs satisfying that condition is studied. The guaranteed synchronizing region for distributed static OPFB control is exposed and found to be different than the infinite right-half plane synchronizing region for distributed state feedback. A numerical example is given that shows the power of the new approach in providing static OPFB synchronization where existing methods cannot do so.

The contributions of this paper are as follows. Restrictive conditions in Ma and Zhang (2010) and Scardovi and Sepulchre (2009) and other existing works are removed to provide synchronizing controls for the general static OPFB case, including non-passive systems and systems not satisfying simplifying rank conditions. Applications are made to globally optimal designs including bounded L_2 gain synchronization, zero-sum games Nash equilibrium, and globally optimal control. Two similar conditions on the local output measurement matrix and the global graph Laplacian are given that reveal the symmetry between local information restrictions due to OPFB and global information restrictions due to the graph topology. A new class of digraphs is defined that satisfy the global condition. The structure of the guaranteed synchronization region for static OPFB is studied and found to be a conical sector, not a right-half plane as for full state feedback. A numerical example is provided that shows the applicability of these new results in a case where existing results such as Ma and Zhang (2010) and Scardovi and Sepulchre (2009) cannot be applied.

Section 2 gives basic concepts and notation. Section 3 defines and solves the distributed bounded L_2 gain synchronization problem by static OPFB. Section 4 solves the static OPFB distributed zero-sum game problem and the globally optimal control problem. Section 5 finds that the guaranteed synchronizing region for static OPFB is conical. Section 6 brings a numerical example that can be solved by the approach in this paper and not by other existing approaches. Section 7 concludes the paper.

2. Graph properties and synchronization

This section presents elements of the algebraic graph theory and defines the synchronization problem using static OPFB distributed control.

Consider a graph, $\mathcal{G} = (\mathcal{V}, \mathcal{E})$, with a nonempty finite set of N vertices, $\mathcal{V} = \{v_1, \ldots, v_N\}$, and a set of edges $\mathcal{E} \subseteq \mathcal{V} \times \mathcal{V}$. It is

assumed that the graph is simple, *i.e.* there are no repeated edges or self-loops. Directed graphs are considered, and information propagates through the graph along the edges. Denote the connectivity matrix as $E = [e_{ij}]$ with $e_{ij} > 0$ if $(v_j, v_i) \in \mathcal{E}$ and $e_{ij} = 0$ otherwise. Note that diagonal elements satisfy $e_{ii} = 0$. The set of neighbors of node v_i is $\mathcal{N}_i = \{v_j : (v_j, v_i) \in \mathcal{E}\}$, *i.e.* the set of nodes with arcs coming into v_i. Define the degree matrix as a diagonal matrix, $H = \text{diag}(h_1 \dots h_N)$, with $h_i = \sum_j e_{ij}$, the (weighted) in-degree of node i. Define the graph Laplacian matrix as $L = H - E$, which has all row sums equal to zero.

A *directed path* is a sequence of edges joining two vertices. A graph is said to be *strongly connected* if any two vertices can be joined by a directed path. A graph is said to contain a directed *spanning tree* if there exists a vertex, v_0, such that every other vertex in $\mathcal{V}$ can be reached from v_0 following a directed path. Such a vertex, v_0, is called a root node. The Laplacian matrix L has a simple zero eigenvalue if and only if the directed graph contains a spanning tree.

For a matrix $Q = Q^T \geq 0$ a square root, $Q^{1/2}$, is a matrix satisfying $(Q^{1/2})^T Q^{1/2} = Q$. We denote its matrix transpose as $Q^{T/2}$. Complex conjugation of a scalar $\sigma \in \mathbb{C}$ is denoted by an over bar $\bar{\sigma} \in \mathbb{C}$.

The multi-agent system under consideration is comprised of N identical agents and a leader, having linear time-invariant (LTI) dynamics. Let the leader system be given as

$$\begin{aligned} \dot{x}_0 &= Ax_0, \\ y_0 &= Cx_0, \end{aligned} \tag{1}$$

and the agents as

$$\begin{aligned} \dot{x}_i &= Ax_i + Bu_i + Dd_i, \\ y_i &= Cx_i. \end{aligned} \tag{2}$$

The d_i are disturbance signals acting on agents, assumed sufficiently regular for the unique solution of (2) to exist.

Note that matrix A may not be stable. Therefore, the autonomous command generator (1) describes many reference trajectories of interest including periodic trajectories, ramp-type trajectories, *etc.*, Hengster-Movric and Lewis (2012).

Define the *local neighborhood output error*

$$e_{yi} = \sum_j e_{ij}(y_j - y_i) + g_i(y_0 - y_i) \tag{3}$$

where $g_i \geq 0$ are the pinning gains, with $g_i > 0$ only for a few nodes having direct measurements of the leader's output, Wang and Chen (2002). The feedback control signal for agent i is chosen as a linear distributed static OPFB

$$u_i = cKe_{yi}, \tag{4}$$

where $c > 0$ is the coupling gain and K is the local OPFB gain matrix. The expression

$$e_i = \sum_j e_{ij}(x_j - x_i) + g_i(x_0 - x_i), \tag{5}$$

is the *local (state) neighborhood error*, Wang and Chen (2002) and Zhang and Lewis (2011). Let $\delta_i = x_i - x_0$ be the synchronization error. Globally one has $\delta = col(\delta_1, \dots, \delta_N)$, so the local neighborhood error equals

$$e = -(L + G) \otimes I_n \delta, \tag{6}$$

where $G = \text{diag}(g_1 \dots g_N)$ is the diagonal matrix of pinning gains. Standard cooperative control approaches assume distributed control in terms of state neighborhood error (5), or construct dynamic observers in terms of OPFB (3). By contrast this paper studies distributed static OPFB of the form (4).

In this paper we assume that the graph contains a spanning tree, with at least one non-zero pinning gain connecting into a root node. Then the matrix $(L + G)$ is nonsingular, Fax and Murray (2004), therefore, $e = 0 \Leftrightarrow \delta = 0$.

Globally, the local neighborhood output error (3) is

$$e_y = -(L + G) \otimes C\delta, \tag{7}$$

where $e_y = col(e_{y1}, \dots, e_{yN})$. Define similarly other global quantities. The global form of the distributed OPFB (4) is

$$u = -c(L + G) \otimes KC\delta. \tag{8}$$

Note that expression (7) reflects the restrictions on the information available for distributed static OPFB control. Matrix C specifies the local agent restrictions due to OPFB, while $L + G$ specifies the information restrictions on a coarser scale due to limited communication. Both local and global restrictions appear in (7) in a symmetric manner.

Definition 1. The *distributed synchronization control problem* for a multi-agent system (2), with a leader (1), is to find distributed feedback controls, u_i, for agents, that guarantee $\lim_{t\to\infty} \|\delta_i(t)\| = 0$, $\forall i$. We call this the *cooperative tracker problem*.

Feedback (4) gives closed loop single-agent system as

$$\dot{x}_i = Ax_i + cBKCe_i + Dd_i, \tag{9}$$

which yields the dynamics of the multi-agent system in global form

$$\dot{x} = (I_N \otimes A)x - c(L + G) \otimes BKC\delta + (I_N \otimes D)d, \tag{10}$$

where global vectors x, d are defined similarly as δ. The synchronization error global dynamics follows as

$$\dot{\delta} = (I_N \otimes A - c(L + G) \otimes BKC)\delta + (I_N \otimes D)d. \tag{11}$$

For the structured system (11) one has the following property of the system matrix, crucial in simplifying the distributed feedback control design.

Lemma 1 (*Fax & Murray, 2004* and *Li et al., 2010*)**.** *The matrix $I_N \otimes A - c(L+G) \otimes BKC$ is Hurwitz if and only if all the matrices $A - c\lambda_j BKC$ are Hurwitz, where λ_j are the eigenvalues of $(L + G)$.* ■

Lemma 1 connects stability properties of (11) to robust stabilization of a single-agent system. The conditions of Lemma 1 can be guaranteed by locally optimal state feedback design at each agent (Li et al., 2010; Tuna, 2008; Zhang & Lewis, 2011). It has not been established how these conditions can be guaranteed by distributed static OPFB design. We will do so in Section 3.

3. Distributed bounded L_2 gain static output-feedback

This section presents the cooperative bounded L_2 gain problem and reviews a result for static OPFB of single-agent systems. Main result Theorem 1 is given that solves the cooperative bounded L_2 gain problem using distributed static OPFB. It is found that in keeping with the symmetry revealed in (7), symmetric conditions must hold on the local output measurement matrix C and the global graph matrix $L + G$.

3.1. Formulation of the cooperative H_∞-control Problem

The dynamics (11) of the synchronization error δ for a general control u is

$$\begin{aligned} \dot{\delta} &= (I_N \otimes A)\delta + (I_N \otimes B)u + (I_N \otimes D)d, \\ y &= (I_N \otimes C)\delta. \end{aligned} \tag{12}$$

The output y of (12) has been redefined as compared to (2) bearing in mind its use in the control law (8). Given system (12), define the *performance output*, Gadewadikar et al. (2006), as

$$\|z(t)\|^2 = \delta^T Q \delta + u^T R u,$$

for some positive definite symmetric matrices $Q > 0, R > 0$ whose structure is detailed later. It is assumed without loss of generality that the matrix C has full row rank. The system L_2 *gain* is said to be bounded or attenuated by γ if, for all L_2 disturbances $d(t)$

$$\frac{\int_0^\infty \|z(t)\|^2\, dt}{\int_0^\infty \|d(t)\|_T^2\, dt} = \frac{\int_0^\infty (\delta^T Q \delta + u^T R u) dt}{\int_0^\infty d(t)^T T d(t) dt} \leq \gamma^2. \tag{13}$$

Remark 1. Note that a weighting matrix $T > 0$ is introduced in (13), which generalizes the form of the L_2 gain as compared to standard single-agent H_∞-control, Gadewadikar et al. (2006, 2007) where $T = I$. This is required in the analysis of H_∞-control for cooperative multi-agent systems as detailed in the proof of Theorem 1.

Definition 2. Given a multi-agent system, the *bounded synchronization L_2 gain (H_∞-synchronization) problem* for the distributed static OPFB is to find the distributed static OPFB control such that the closed-loop multi-agent system reaches synchronization in absence of disturbances, and that synchronization L_2 gain is bounded as in (13) for all L_2 disturbances.

For any LTI system

$$\begin{aligned} \dot{\delta} &= \bar{A}\delta + \bar{B}u + \bar{D}d, \\ y &= \bar{C}\delta, \end{aligned} \tag{14}$$

to design a static OPFB control, $u = -\bar{K}y = -\bar{K}\bar{C}\delta$, guaranteeing that L_2 gain is bounded as in (13), one proceeds as follows, Gadewadikar et al. (2006). Define the performance criterion

$$J(\delta, \bar{K}, d) = \int_0^\infty (\delta^T (Q + \bar{C}^T \bar{K}^T R \bar{K} \bar{C})\delta - \gamma^2 d^T T d) dt. \tag{15}$$

The main result of Gadewadikar et al. (2006) states that necessary and sufficient conditions for existence of the H_∞ static OPFB control for general LTI systems, with $Q = Q^T \geq 0$, are: $(\bar{A}, \bar{B})$ stabilizable, $(\bar{A}, Q^{1/2})$ detectable, and there exist matrices $\bar{K}^*, \bar{M}$ such that

$$\bar{K}^* \bar{C} = R^{-1}(\bar{B}^T P + \bar{M}), \tag{16}$$

where $P = P^T > 0$ is a solution to the generalized Riccati-type equation (the HJI equation)

$$P\bar{A} + \bar{A}^T P + Q - P\bar{B}R^{-1}\bar{B}^T P + \bar{M}^T R^{-1}\bar{M} + \gamma^{-2} P \bar{D} T^{-1} \bar{D}^T P = 0. \tag{17}$$

The matrix $\bar{M}$ in (16) provides additional design freedom needed for OPFB stabilization. Note that (16) may not hold if $\bar{M} = 0$. That is, given matrix $\bar{C}$, there may be no solution to (17) with $\bar{M} = 0$ such that $\bar{K}^* \bar{C} = R^{-1}\bar{B}^T P$.

3.2. Cooperative output-feedback control for bounded L_2 gain

The existence of the solution to the bounded L_2 gain synchronization problem for system (12) in the form of the cooperative distributed static OPFB control (4) is detailed in the following main theorem. This result shows how to design a distributed static OPFB of the form (8) that guarantees a bounded L_2 gain (13). The key is to realize that in distributed control on graphs, the matrices in (14) are specially structured so that

$$\begin{aligned} \bar{A} &= I_N \otimes A, \qquad \bar{B} = I_N \otimes B, \\ \bar{C} &= I_N \otimes C, \qquad \bar{D} = I_N \otimes D. \end{aligned} \tag{18}$$

Moreover, since the multi-agent distributed systems are structured as in (12), the global static OPFB feedback gain has the structure $K_1 \otimes K_2$, commensurate with Eq. (7).

Theorem 1. *Let the synchronization error dynamics with disturbances acting upon agents be given in global form as (12). Let the graph have a spanning tree with at least one non-zero pinning gain connecting to a root node. Suppose there exist symmetric positive definite matrices P_1, P_2, and matrices M_2, K_2 satisfying*

$$P_1 = cR_1(L + G) \tag{19}$$

$$\begin{aligned} &A^T P_2 + P_2 A + Q_2 - P_2 B R_2^{-1} B^T P_2 \\ &\quad + \gamma^{-2} P_2 D D^T P_2 + M_2^T R_2^{-1} M_2 = 0 \end{aligned} \tag{20}$$

for some $Q_2 = Q_2^T > 0$, $R_1 = R_1^T > 0$, $R_2 = R_2^T > 0$, and coupling gain $c > 0$, together with

$$K_2^* C = R_2^{-1}(B^T P_2 + M_2). \tag{21}$$

Then the cooperative control

$$u^* = -c(L + G) \otimes K_2^* C \delta, \tag{22}$$

guarantees a synchronization L_2 gain bounded as in (13) by γ, where matrices Q, R, T are structured as

$$R = R_1 \otimes R_2, \tag{23}$$

and either

i. $T = P_1 \otimes I = cR_1(L + G) \otimes I$ *with*

$$\begin{aligned} Q &= c^2 (L + G)^T R_1 (L + G) \otimes (Q_2 + A^T P_2 \\ &\quad + P_2 A + \gamma^{-2} P_2 D D^T P_2) \\ &\quad - cR_1(L + G) \otimes (A^T P_2 + P_2 A + \gamma^{-2} P_2 D D^T P_2) \\ &> 0 \end{aligned} \tag{24}$$

or

ii. $T = R_1 \otimes I$ *with*

$$\begin{aligned} Q &= c^2 (L + G)^T R_1 (L + G) \otimes (Q_2 + A^T P_2 + P_2 A) \\ &\quad - cR_1(L + G) \otimes (A^T P_2 + P_2 A) > 0. \end{aligned} \tag{25}$$

Proof. Let the OPFB control for (12) be structured as

$$u = \bar{K}(I_N \otimes C)\delta = K_1 \otimes K_2 C \delta.$$

The Hamiltonian for system (14) with the performance criterion (15) and the quadratic value function, $V(\delta) = \delta^T P \delta$, equals

$$\begin{aligned} H &= \delta^T (P(\bar{A} - \bar{B}\bar{K}\bar{C}) + (\bar{A} - \bar{B}\bar{K}\bar{C})^T P)\delta + \delta^T P \bar{D} d \\ &\quad + d^T \bar{D}^T P \delta + \delta^T (Q + \bar{C}^T \bar{K}^T R \bar{K} \bar{C})\delta - \gamma^2 d^T T d. \end{aligned} \tag{26}$$

Stationarity condition gives the worst case disturbance d^*

$$\frac{\partial H}{\partial d} = 0 \Rightarrow d^* = \gamma^{-2} T^{-1} \bar{D}^T P \delta. \tag{27}$$

With such a disturbance the Hamiltonian becomes

$$\begin{aligned} H &= \delta^T (P(\bar{A} - \bar{B}\bar{K}\bar{C}) + (\bar{A} - \bar{B}\bar{K}\bar{C})^T P)\delta \\ &\quad + \gamma^{-2} \delta^T P \bar{D} T^{-1} \bar{D}^T P \delta + \delta^T (Q + \bar{C}^T \bar{K}^T R \bar{K} \bar{C})\delta. \end{aligned}$$

This quadratic form is determined by the matrix

$$\begin{aligned}&P(\bar{A}-\bar{B}\bar{K}\bar{C})+(\bar{A}-\bar{B}\bar{K}\bar{C})^TP+Q\\&\quad+\bar{C}^T\bar{K}^TR\bar{K}\bar{C}+\gamma^{-2}P\bar{D}T^{-1}\bar{D}^TP\\&=\bar{A}^TP+P\bar{A}+Q+\gamma^{-2}P\bar{D}T^{-1}\bar{D}^TP-P\bar{B}R^{-1}\bar{B}^TP\\&\quad+(\bar{K}\bar{C}-R^{-1}\bar{B}^TP)^TR(\bar{K}\bar{C}-R^{-1}\bar{B}^TP)\\&=\bar{A}^TP+P\bar{A}+Q+\gamma^{-2}P\bar{D}T^{-1}\bar{D}^TP\\&\quad-P\bar{B}R^{-1}\bar{B}^TP+\bar{M}^TR^{-1}\bar{M}.\end{aligned}\tag{28}$$

The last line is obtained from the requirement on the OPFB gain, $\bar{K}^*\bar{C}=R^{-1}(\bar{B}^TP+\bar{M})$, for some matrix $\bar{M}$. By the output Riccati-type equation, (17), (28) equals zero identically, *i.e.*

$$H(\delta,\nabla V,\bar{K}^*,d^*)=0.\tag{29}$$

The system (12) is structured, (18). Its structured value function is given by the matrix $P=P_1\otimes P_2$. With the matrix R of the Theorem and similarly structured general $T=T_1\otimes T_2$, $\bar{M}=M_1\otimes M_2$ one finds the matrix (28) equal to

$$\begin{aligned}&(I_N\otimes A^T)(P_1\otimes P_2)+(P_1\otimes P_2)(I_N\otimes A)+Q\\&\quad+\gamma^{-2}(P_1\otimes P_2)(I_N\otimes D)(T_1^{-1}\otimes T_2^{-1})(I_N\otimes D^T)(P_1\otimes P_2)\\&\quad-(P_1\otimes P_2)(I_N\otimes B)(R_1^{-1}\otimes R_2^{-1})(I_N\otimes B^T)(P_1\otimes P_2)\\&\quad+(M_1^T\otimes M_2^T)(R_1^{-1}\otimes R_2^{-1})(M_1\otimes M_2).\end{aligned}$$

Choosing $T_2=I$, of an appropriate dimension, one has $T=T_1\otimes I$ and

$$\begin{aligned}&P_1\otimes(A^TP_2+P_2A)+Q+\gamma^{-2}P_1T_1^{-1}P_1\otimes P_2DD^TP_2\\&\quad-P_1R_1^{-1}P_1\otimes P_2BR_2^{-1}B^TP_2+M_1^TR_1^{-1}M_1\otimes M_2^TR_2^{-1}M_2.\end{aligned}\tag{30}$$

For the OPFB gain one has

$$\begin{aligned}\bar{K}\bar{C}&=(K_1\otimes K_2)(I_N\otimes C)=K_1\otimes K_2C\\&=(R_1^{-1}\otimes R_2^{-1})(P_1\otimes B^TP_2+M_1\otimes M_2)\\&=c(L+G)\otimes K_2^*C,\end{aligned}\tag{31}$$

which is satisfied for $M_1=P_1$, by the global topology condition, (19), and the local OPFB condition, (21).

Nothing in the conditions for OPFB, (19), (21), specifies the matrix T_1. Choosing $T_1=P_1>0$, with $M_1=P_1$ in (30) gives

$$\begin{aligned}&P_1\otimes(A^TP_2+P_2A)+Q+\gamma^{-2}P_1P_1^{-1}P_1\otimes P_2DD^TP_2\\&\quad-P_1R_1^{-1}P_1\otimes P_2BR_2^{-1}B^TP_2+P_1R_1^{-1}P_1\otimes M_2^TR_2^{-1}M_2\\&=P_1\otimes(A^TP_2+P_2A+\gamma^{-2}P_2DD^TP_2)+Q\\&\quad-P_1R_1^{-1}P_1\otimes(P_2BR_2^{-1}B^TP_2-M_2^TR_2^{-1}M_2).\end{aligned}$$

If the Q matrix is taken to be

$$\begin{aligned}Q&=P_1\otimes(Q_2-P_2BR_2^{-1}B^TP_2+M_2^TR_2^{-1}M_2)\\&\quad+Q_1\otimes(P_2BR_2^{-1}B^TP_2-M_2^TR_2^{-1}M_2),\end{aligned}\tag{32}$$

the global output Riccati-type equation, (17), decouples as

$$\begin{aligned}&P_1\otimes(A^TP_2+P_2A+\gamma^{-2}P_2DD^TP_2+Q_2\\&\quad-P_2BR_2^{-1}B^TP+M_2^TR_2^{-1}M_2)\\&\quad+(Q_1-P_1R_1^{-1}P_1)\otimes(P_2BR_2^{-1}B^TP_2-M_2^TR_2^{-1}M_2)=0.\end{aligned}$$

That is certainly satisfied if

$$\begin{aligned}&Q_1=P_1R_1^{-1}P_1,\\&A^TP_2+P_2A+Q_2-P_2BR_2^{-1}B^TP_2\\&\quad+\gamma^{-2}P_2DD^TP_2+M_2^TR_2^{-1}M_2=0.\end{aligned}$$

Alternatively, the choice $T_1=R_1$ gives the equation

$$\begin{aligned}&P_1\otimes(A^TP_2+P_2A)+Q+P_1R_1^{-1}P_1\otimes(\gamma^{-2}P_2DD^TP_2-P_2BR_2^{-1}B^TP_2\\&\quad+M_2^TR_2^{-1}M_2)=0,\end{aligned}$$

which decouples similarly with the choice of

$$\begin{aligned}Q&=P_1\otimes(Q_2-P_2BR_2^{-1}B^TP_2+M_2^TR_2^{-1}M_2+\gamma^{-2}P_2DD^TP_2)\\&\quad+Q_1\otimes(P_2BR_2^{-1}B^TP_2-M_2^TR_2^{-1}M_2-\gamma^{-2}P_2DD^TP_2)\end{aligned}\tag{33}$$

or equivalently

$$Q=-P_1\otimes(A^TP_2+P_2A)+Q_1\otimes(Q_2+A^TP_2+P_2A),\tag{34}$$

where $Q_1=P_1R_1^{-1}P_1=c^2(L+G)^TR_1(L+G)$. The global topology condition (19), used in (32), (33), gives (24), (25).

Hence, with the choice of the structure for matrices Q, R, P, T detailed in the theorem, one has the global output algebraic Riccati-type equation decoupled into local and global parts. Thus the conditions on the graph topology and the local OPFB gain guarantee that the global output Riccati-type equation is satisfied.

The Hamiltonian for the general LTI system evaluated at the specified control, $\bar{K}^*$, and disturbance signals, d^* is identically zero, (29). The original Hamiltonian then equals

$$\begin{aligned}H(\delta,\nabla V,\bar{K},d)&=H(\delta,\nabla V,\bar{K}^*,d^*)+\delta^T(-P\bar{B}(\bar{K}\bar{C}-R^{-1}\bar{B}^TP)\\&\quad-\bar{C}^T\bar{K}^T(\bar{B}^TP-R\bar{K}\bar{C})-\bar{M}^TR^{-1}\bar{M})\delta-\underbrace{\gamma^{-2}\delta^TP\bar{D}T^{-1}\bar{D}^TP\delta}_{\gamma^2d^{*T}Td^*}\\&\quad+\underbrace{\delta^TP\bar{D}d}_{\gamma^2d^{*T}Td}+d^T\bar{D}^TP\delta-\gamma^2d^TTd\\&=\delta^T(-P\bar{B}(\bar{K}\bar{C}-R^{-1}\bar{B}^TP)-\bar{C}^T\bar{K}^T(\bar{B}^TP-R\bar{K}\bar{C})\\&\quad-\bar{M}^TR^{-1}\bar{M})\delta-\gamma^2(d-d^*)^TT(d-d^*).\end{aligned}\tag{35}$$

Recalling that

$$H(\delta,\nabla V,\bar{K},d)=\frac{dV}{dt}+\delta^T(Q+\bar{C}^T\bar{K}^TR\bar{K}\bar{C})\delta-\gamma^2d^TTd,$$

choosing $\bar{K}=\bar{K}^*$ leads to

$$\begin{aligned}&\frac{dV}{dt}+\delta^T(Q+\bar{C}^T\bar{K}^TR\bar{K}\bar{C})\delta-\gamma^2d^TTd\\&\quad=-(d-d^*)^TT(d-d^*)\le0.\end{aligned}$$

Upon integration, $\forall T>0$, one finds

$$\begin{aligned}&V(\delta(T))-V(\delta(0))\\&\quad+\int_0^T(\delta^T(Q+\bar{C}^T\bar{K}^{*T}R\bar{K}^*\bar{C})\delta-\gamma^2d^TTd)dt\le0.\end{aligned}$$

The rest of the proof follows similarly as in Gadewadikar et al. (2006). ■

It is interesting to note that not only the control (22) is distributed, respecting the graph topology, so is the worst case disturbance, (27), for both choices of T in (24), (25).

Remark 2. Global condition (19) refers to the graph topology $L+G$. Local conditions (20), (21) refer to the local static OPFB restrictions due to C. These global and local conditions appear in (19), (21), respectively, in a similar way. This is due to the symmetry in the global and local information restrictions embodied in (7).

Conditions (24), (25), that the matrix Q be positive definite, are not trivial. For those to be satisfied, in case (i) one must have $c>0$ sufficiently large and

$$Q_2+A^TP_2+P_2A+\gamma^{-2}P_2DD^TP_2\ge0.\tag{36}$$

Then the first term in (24) can dominate the second term except on its kernel, as determined by kernel of (36). According to Eq. (20), (36) is equivalent to

$$P_2BR_2^{-1}B^TP_2 - M_2^TR_2^{-1}M_2 \geq 0, \tag{37}$$

which is a condition on M_2. Since $R_2 > 0$, (37) implies that $\ker(B^TP_2) \subseteq \ker M_2$. Also, condition (37) can be written as

$$C^TK_2^TR_2K_2C - C^TK_2^TM_2 - M_2^TK_2C \geq 0. \tag{38}$$

Similarly in case (ii), one needs $c > 0$ sufficiently large and

$$Q_2 + A^TP_2 + P_2A \geq 0, \tag{39}$$

which by (20) is equivalent to

$$P_2BR_2^{-1}B^TP_2 - \gamma^{-2}P_2DD^TP_2 - M_2^TR_2^{-1}M_2 \geq 0. \tag{40}$$

The expression (40) is a condition on the size of M_2, D. For (40) to hold it is necessary that (37) *i.e.* (38) holds. Also, (40) necessarily implies that $\ker(B^TP_2) \subseteq \ker(D^TP_2)$. Both conditions (37), (40) hold if $M_2 = 0, D = 0$. If (37), (40) do hold, choosing the coupling gain c sufficiently large makes the matrix Q positive definite. Namely on the kernel of the first term in (24), (25), as determined by kernels of (36) or (39), the second term in matrix Q, (24), (25), equals

$$cR_1(L+G) \otimes Q_2 = P_1 \otimes Q_2 > 0.$$

Hence by condition (19) one has $Q > 0$. Note that the global topology condition (19) and the local condition (38) are both required for this.

Remark 3. The control design in (20), (21) is distributed at each agent and so is the implementation (22). We consider the global optimal problem using static OPFB. As such, the global performance index naturally depends on the graph topology through the weights (24), (25). It also requires the global property (19). Our approach in Theorem 1 clearly decouples the distributed nature of the problem, arising from OPFB constraints due to matrix C, and the global information restrictions due to the graph topology $L+G$. See the comments following (8).

Remark 4. A new class of digraphs which satisfy condition (19) is required. In particular, this class of digraphs admits a distributed solution to an appropriately defined global optimal control problem, Hengster-Movric and Lewis (2014). The topological condition for global optimality of the distributed control (22) is (19),

$$R_1(L+G) = P_1, \tag{41}$$

where $R_1 = R_1^T > 0$, $L+G$ is a nonsingular M-matrix, and $P_1 = P_1^T > 0$. The existence of a matrix $R_1 > 0$ satisfying (41), is detailed in the following theorem.

Theorem 2. *Let $L+G$ be a graph matrix. Then there exists a positive definite symmetric matrix $R_1 = R_1^T > 0$ such that $R_1(L+G) = P_1$ is a symmetric positive definite matrix if and only if $L+G$ has a diagonal Jordan form.*

Proof is given in Hengster-Movric and Lewis (2014). ■

4. Distributed two-player zero-sum games and globally optimal output-feedback

This section provides solutions for two special applications of the static OPFB design in Theorem 1. First we present and solve distributed two-player zero-sum games using static OPFB. Then we consider the special case of cooperative globally optimal control.

4.1. Distributed two-player zero-sum games

Let the multi-agent system be given by (12). The system (12) has two inputs, hence the theory of the two-player zero-sum games (Basar & Olsder, 1999; Lewis et al., 2012) is applicable.

Given a performance criterion, $J(x(0), u, d)$, and a dynamical system with two inputs, u, d, the two-player zero-sum game puts the control input u and the disturbance input d at odds with one another. The objective of the control is to minimize the performance criterion J, while the objective of the disturbance is to maximize it. For games in general, the concept of Nash equilibrium is of central importance (Basar & Olsder, 1999; Lewis et al., 2012).

Definition 3. Given a performance criterion, $J(x(0), u, d)$, the policies u^*, d^* are in a Nash equilibrium if

$$J(x(0), u^*, d) \leq J(x(0), u^*, d^*) \leq J(x(0), u, d^*).$$

According to the Nash condition, if both players are at equilibrium, (u^*, d^*), then (u^*, d^*) provides a unique game-theoretic saddle point solution. That is the value of the performance criterion at the Nash equilibrium, $V(x_0) = J(x_0, u^*, d^*)$, satisfies

$$V^*(x_0) = \min_u \max_d J(x(0), u, d) = \max_d \min_u J(x(0), u, d).$$

The main result of this section is presented as the following corollary to Theorem 1.

Corollary 1. *Let the conditions of Theorem 1 be satisfied. Let the matrix M_2 additionally satisfy*

$$C^T(K_2 - K_2^*)^TR_2(K_2 - K_2^*)C + M_2^T(K_2 - K_2^*)C + C^T(K_2 - K_2^*)^TM_2 \geq 0, \tag{42}$$

for any $K_2 \neq K_2^*$. Then the control (22) and the worst case disturbance (27) are the solutions of the distributed two-player zero-sum game with the performance index

$$J(\delta_0, u, d) = \int_0^\infty (\delta^TQ\delta + u^TRu - \gamma^2d^TTd)dt, \tag{43}$$

where matrices Q, R, T are structured as in Theorem 1.

Proof. Follows the same starting lines as the proof of Theorem 1. Here we start from the expression (35)

$$\begin{aligned} H(\delta, \nabla V, K, d) = &-\gamma^2(d-d^*)^T(d-d^*) \\ &+ \delta^T(-P\bar{B}(\bar{K}\bar{C} - R^{-1}\bar{B}^TP) \\ &- \bar{C}^T\bar{K}^T(\bar{B}^TP - R\bar{K}\bar{C}) - \bar{M}^TR^{-1}\bar{M})\delta. \end{aligned}$$

One has the game-theoretic saddle point if the matrix $\bar{M}$ is chosen such that, Gadewadikar et al. (2006),

$$-P\bar{B}(\bar{K}\bar{C} - R^{-1}\bar{B}^TP) - \bar{C}^T\bar{K}^T(\bar{B}^TP - R\bar{K}\bar{C}) - \bar{M}^TR^{-1}\bar{M} \geq 0.$$

Since $\bar{K}^*\bar{C} = R^{-1}\bar{B}^TP + R^{-1}\bar{M}$, this can be written as

$$\bar{C}^T(\bar{K} - \bar{K}^*)^TR(\bar{K} - \bar{K}^*)\bar{C} + \bar{M}^T(\bar{K} - \bar{K}^*)\bar{C} + \bar{C}^T(\bar{K} - \bar{K}^*)^T\bar{M} \geq 0. \tag{44}$$

This is clearly satisfied in the special case of $\bar{M} = 0$.

Given that, as in the proof of Theorem 1, $\bar{K} = K_1 \otimes K_2$, $\bar{K}^* = K_1 \otimes K_2^*$, since K_1 is fixed by the graph topology $L+G$, the general condition (44) for the purposes of this Theorem reduces to

$$\begin{aligned} &(I_N \otimes C^T)K_1^T \otimes (K_2 - K_2^*)^T(R_1 \otimes R_2)K_1 \otimes (K_2 - K_2^*)(I_N \otimes C) \\ &+ (M_1^T \otimes M_2^T)K_1 \otimes (K_2 - K_2^*)(I_N \otimes C) \\ &+ (I_N \otimes C^T)K_1^T \otimes (K_2 - K_2^*)^T(M_1 \otimes M_2) > 0. \end{aligned}$$

With $M_1 = P_1$ and (19) one obtains

$$P_1R_1^{-1}P_1 \otimes (C^T(K_2 - K_2^*)^TR_2(K_2 - K_2^*)C + M_2^T(K_2 - K_2^*)C + C^T(K_2 - K_2^*)^TM_2).$$

The first term is positive definite and equal to $P_1R_1^{-1}P_1 = c^2(L + G)^TR_1(L + G)$, by condition (19) of Theorem 1. Positive semi-definiteness of the second term guarantees the positive semi-definiteness of the entire expression. Therefore, if M_2 can be chosen such that

$$C^T(K_2 - K_2^*)^TR_2(K_2 - K_2^*)C + M_2^T(K_2 - K_2^*)C + C^T(K_2 - K_2^*)^TM_2 \geq 0,$$

then (44) is positive semidefinite. This implies that if the local OPFB K_2^*C is the solution of the local game-theoretic problem, Gadewadikar et al. (2006), then, given the global topology condition, (19), the same holds for the global problem. ■

Condition (42) is crucial when compared to conditions of Theorem 1. It implies the weaker local condition (38) (just set $K_2 = 0$ in (42)). (42) guarantees that the Hamiltonian be positive definite with respect to deviations of OPFB gain from that proposed in Theorem 1. Hence the performance criterion (43) is a proper game-theoretic performance criterion having a game-theoretic saddle point, Gadewadikar et al. (2006). Namely a saddle point in the Hamiltonian implies a game-theoretic saddle point of the performance criterion, Gadewadikar et al. (2006) and Lewis et al. (2012). Note that condition (19) is also needed here.

4.2. Cooperative globally optimal output-feedback

When the effects of the disturbances are absent, *i.e.* $D = 0$ in (12), the game-theoretic problem of Section 4.1 reduces to the globally optimal control problem for OPFB, Lewis et al. (2012). This result is presented as a second corollary to Theorem 1.

Corollary 2. *Let the conditions of Theorem 1 and Corollary 1 be satisfied for $d \equiv 0$ and $D \equiv 0$. Then the control (22) is optimal with respect to the performance index*

$$J(\delta_0, u) = \int_0^\infty (\delta^TQ\delta + u^TRu)dt, \tag{45}$$

where the matrices Q, R are given by (23), and

$$Q = c^2(L + G)^TR_1(L + G) \otimes (Q_2 + A^TP_2 + P_2A) - cR_1(L + G) \otimes (A^TP_2 + P_2A) > 0, \tag{46}$$

for the coupling gain $c > 0$ sufficiently large. ■

The proof is analogous to the proof of Corollary 1, noting that $d \equiv 0, D \equiv 0$ make the choice of T in Theorem 1 immaterial, and both variants for Q presented there reduce to a single choice, (46). Local condition (42) of Corollary 1 guarantees optimality and (46).

Note that if the graph does not contain the spanning tree, with at least one non-zero pinning gain connecting to a root node, then, with all other conditions of Corollary 2 satisfied, one has optimality, with positive semidefinite Q in (45). This implies convergence to the kernel of Q. The existence of a spanning tree, *i.e.* the non-singularity of the graph matrix, $L + G$, is necessary for state synchronization.

Remark 5. Remark 2 applies also here. The conditions on c for synchronization in Corollary 2, are more than sufficient, and presume both global and local conditions (19), (38). Global condition is discussed in detail in Remark 4. However, removing the global requirements of Sections 3 and 4 removes condition (19), leaving weaker conditions for synchronization. In that case the local condition (38) remains a sufficient condition, as detailed in Section 5.

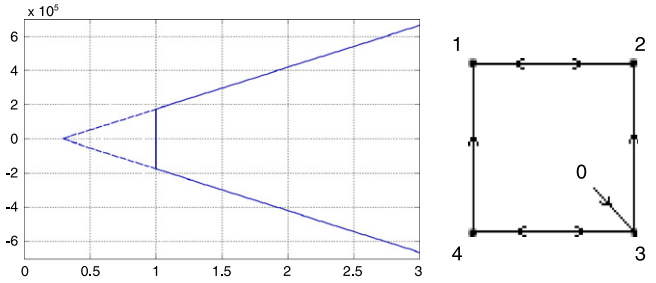

Fig. 1. a. Synchronizing region for static OPFB. b. The graph.

5. Synchronizing region for output-feedback

This section studies the guaranteed synchronizing region for static OPFB and finds it to be a conical region as shown in Fig. 1(a), Section 6, as opposed to the unbounded right-half plane for full state feedback cooperative control (Li et al., 2010; Zhang & Lewis, 2011). In the following it is taken that $d \equiv 0$, $D \equiv 0$, and subscript '2' of local quantities is omitted for simplicity.

Let the local OPFB gain K for an LTI system defined by matrices (A, B, C) satisfy conditions (20), (21) for some matrix M. Then the closed loop system matrix A-BKC is Hurwitz, Gadewadikar et al. (2006).

Definition 4. Given matrices (A, B, C), and the static OPFB gain K, the *synchronizing region for static OPFB* is a set given by $S_y = \{\sigma \in \mathbb{C} : A - \sigma BKC \text{ is stable}\}$.

Hence, according to Lemma 1 the system matrix in (11) is stable if and only if all the scaled graph matrix eigenvalues, $c\lambda_j$, are in the synchronizing region for static OPFB of the matrix pencil

$$A - \sigma BKC. \tag{47}$$

Making the choice of K (20), (21), guarantees the synchronizing region for static OPFB as shown below.

Theorem 3. *Let the multi-agent system be given by (1), (2), where $D \equiv 0, d \equiv 0$. Let the graph have a spanning tree with at least one non-zero pinning gain connecting to a root node. Choose the distributed static OPFB control (4), where the OPFB gain, K, satisfies (20), (21). In addition let the inequality (38) be satisfied. Then the guaranteed synchronizing region for static OPFB is the conical sector in the complex plane.*

Proof. Let the following abbreviations be introduced

$$a := \lambda_{\min>0}(Q^{-T/2}C^TK^TRKCQ^{-1/2}), \tag{48}$$

$$b := \lambda_{\min>0}(Q^{-T/2}(C^TK^TRKC - C^TK^TM - M^TKC)Q^{-1/2}) \tag{49}$$

$$f := \lambda_{\max}(jQ^{-T/2}(M^TKC - C^TK^TM)Q^{-1/2}) \tag{50}$$

where $\lambda_{min>0}$ denotes the smallest eigenvalue on the complement of the kernel.

Take the quadratic Lyapunov function, $V(x) = x^\dagger Px$, for the complex system matrix (47). The dagger $\dagger$ denotes the hermitian adjoint. The positive definite real matrix, $P = P^T$, is chosen as a solution of the output Riccati-type equation (20). The time derivative of this Lyapunov function is determined by the quadratic form of a hermitian matrix

$$(A - \sigma BKC)^\dagger P + P(A - \sigma BKC) = A^TP + PA - \bar{\sigma}C^TK^TB^TP - \sigma PBKC,$$

which, by completing the squares, reads

$$A^TP + PA + (\sigma KC - R^{-1}(B^TP + M))^\dagger R(\sigma KC - R^{-1}(B^TP + M)) - |\sigma|^2 C^TK^TRKC + \bar{\sigma}C^TK^TM + \sigma M^TKC - C^TK^TRKC.$$

The choice of the OPFB satisfying (21) makes this expression equal to

$$A^TP + PA + |\sigma - 1|^2 C^TK^TRKC - |\sigma|^2 C^TK^TRKC + \bar{\sigma}C^TK^TM + \sigma M^TKC - C^TK^TRKC.$$

Using the output Riccati-type equation, (20), gives

$$= -Q - (B^TP + M)^TR^{-1}(B^TP + M) - M^TR^{-1}M + PBR^{-1}B^TP + (1 - 2\mathrm{Re}\,\sigma)C^TK^TRKC + \bar{\sigma}C^TK^TM + \sigma M^TKC.$$

The sufficient condition guaranteeing stability is then

$$-Q - (B^TP + M)^TR^{-1}(B^TP + M) - M^TR^{-1}M + PBR^{-1}B^TP + (1 - 2\mathrm{Re}\,\sigma)C^TK^TRKC + \bar{\sigma}C^TK^TM + \sigma M^TKC < 0,$$

allowing the assessment of the synchronizing region for static OPFB in $\mathbb{C}$. This expression is equivalent to

$$-Q - |\sigma|^2 C^TK^TRKC + |\sigma - 1|^2 C^TK^TRKC + (\bar{\sigma} - 1)C^TK^TM + (\sigma - 1)M^TKC < 0. \quad (51)$$

With $|\sigma - 1|^2 - |\sigma|^2 = (1 - 2\mathrm{Re}\,\sigma)$ (51) becomes

$$-Q - (2\mathrm{Re}\,\sigma - 1)C^TK^TRKC + (\mathrm{Re}\,\sigma - 1)(C^TK^TM + M^TKC) + j\mathrm{Im}\,\sigma(M^TKC - C^TK^TM) < 0.$$

After straightforward manipulations condition (51) reads

$$-I - \mathrm{Re}\,\sigma(Q^{-T/2}C^TK^TRKCQ^{-1/2}) - (\mathrm{Re}\,\sigma - 1)Q^{-T/2}(C^TK^TRKC - C^TK^TM - M^TKC)Q^{-1/2} + \mathrm{Im}\,\sigma(jQ^{-T/2}(M^TKC - C^TK^TM)Q^{-1/2}) < 0. \quad (52)$$

Inequality (52) is certainly satisfied for $\mathrm{Re}\,\sigma \geq 1$ if

$$-1 - \mathrm{Re}\,\sigma\lambda_{\min>0}(Q^{-T/2}C^TK^TRKCQ^{-1/2}) - (\mathrm{Re}\,\sigma - 1)\lambda_{\min>0}(Q^{-T/2}(C^TK^TRKC - C^TK^TM - M^TKC)Q^{-1/2}) + |\mathrm{Im}\,\sigma|\,\lambda_{\max}(jQ^{-T/2}(M^TKC - C^TK^TM)Q^{-T/2}) < 0. \quad (53)$$

Note here that even though the last matrix term in (52) is antisymmetric it cannot be disregarded for the evaluation of the quadratic form. This is so because j multiplying it makes it hermitian, and one has complex vector spaces here. Namely, the proof of Lemma 1 uses a coordinate transformation that is generally complex. This matrix has a special property that its eigenvalues appear as $\pm\lambda \in \mathbb{R}$, which is seen by complex conjugating the eigenvalue–eigenvector relation. Hence the absolute value of $\mathrm{Im}\,\sigma$ is needed in (53) compared to (52).

With the introduced abbreviations and shorthand notation, $x := \mathrm{Re}\,\sigma$, $y := \mathrm{Im}\,\sigma$, a guaranteed synchronizing region for OPFB is described as $x \geq 1$ and

$$|y| < [1 - b + (a + b)x]/f, \quad (54)$$

which is a conical sector in the complex plane. This completes the proof. ■

Remark 6. If $M = 0$ one recovers the synchronizing region characteristic of the full state feedback (Li et al., 2010; Zhang & Lewis, 2011) defined by

$$-Q + (1 - 2\mathrm{Re}\,\sigma)C^TK^TRKC < 0.$$

However, given the prescribed output measurement matrix C in (2), the choice $M = 0$ generally cannot be made, Gadewadikar et al. (2006). That is, there may exist $M \neq 0$ such that (21) holds, *i.e.* $K^*C = R^{-1}(B^TP + M)$, yet $K^*C = R^{-1}B^TP$ fails to hold.

Remark 7. The work in Li et al. (2010) presents conditions in terms of LMI for state feedback synchronizing region in $\mathbb{R}$ to be unbounded. The structure of the synchronizing region for static OPFB in $\mathbb{C}$ is not revealed in that work. In Theorem 3 we show it is a conical sector, (54). Such form of the synchronizing region imposes constraints on the graph matrix eigenvalues similar to those presented in Hengster-Movric et al. (2012) for discrete-time systems.

6. Numerical example

A numerical example is presented here for which distributed static OPFB can be designed using the approach in this paper, but not by other approaches existing in the literature. Note that this system is not passive hence (Scardovi & Sepulchre, 2009) cannot be applied. Also it does not satisfy the rank condition (13) in Ma and Zhang (2010), so that cannot be used either.

Consider a multi-agent system (1), (2), with matrices

$$A = \begin{bmatrix} 0 & 1 \\ 1 & -1 \end{bmatrix}, \qquad B = I_2, \qquad C = \begin{bmatrix} 1 & 0.6 \end{bmatrix}, \qquad D = 0.$$

Note that A is unstable but stabilizable. The solution of the equation, (20), with matrices $Q = I_2$, $R = 0.5I_2$ and

$$M = \begin{bmatrix} 0 & 0.1444 \\ 0 & -0.3348 \end{bmatrix} \quad \text{is } P = \begin{bmatrix} 0.8561 & 0.3693 \\ 0.3693 & 0.5563 \end{bmatrix}.$$

The OPFB gain (21) given by this P is $K = [1.7122 \quad 0.7386]^T$ which, with the chosen M, satisfies (38). In this case the choice of $M \neq 0$ is necessary. That is $KC = R^{-1}B^TP$ fails to hold. The synchronizing region for OPFB, (54), is determined by the coefficients $a = 2.3644$, $b = 2.3645$, $f = 5.372 * 10^{-5}$, depicted in Fig. 1(a). The graph topology is given by $L = [2\ -1\ 0\ -1; -1\ 2\ -1\ 0; 0\ 0\ 1\ -1; 0\ 0\ -1\ 1]$, $G = \mathrm{diag}(0, 0, 1, 0)$, (Fig. 1(b)), satisfying (19) with $R_1 = [1\ 0\ 1\ -2; 0\ 1\ -2\ 0; 1\ -2\ 11.4\ -3.8; -2\ 0\ -3.8\ 8.6] > 0$, and $c = 2.7$.

7. Conclusions

This paper examines distributed static OPFB control for state synchronization of identical LTI agents. Disturbances are assumed to act on the agents. The cooperative bounded L_2 gain problem using static OPFB is defined and solved. A stronger condition affords a solution of the distributed two-player zero-sum game. The distributed globally optimal OPFB control problem is solved as a special case. Conditions are found guaranteeing global optimality w.r.t. a quadratic performance criterion. The notion of synchronizing region is extended to static OPFB.

Acknowledgments

This work is supported by NSF grant ECCS-1405173, ONR grant N00014-13-1-0562, ONR grant N000141410718, grant W911NF-11-D-0001, China NNSF grant 61120106011, and China Education Ministry Project 111 (No. B08015), European social fund within the framework of realizing the project "Support of inter-sectoral mobility and quality enhancement of research teams at Czech Technical University in Prague", CZ.1.07/2.3.00/30.0034.

References

Baillieul, J., & Antsaklis, P. J. (2007). Control and communication challenges in networked real-time systems (invited paper). *Proceedings of IEEE*, *95*(1), 9–28.
Basar, T., & Olsder, G. J. (1999). *Dynamic noncooperative game theory*. Society for Industrial and Applied Mathematics.

Borelli, F., & Keviczky, T. (2008). Distributed LQR design for identical dynamically decoupled systems. *IEEE Transactions on Automatic Control*, *53*(8), 1901–1912.
Cao, Y., & Ren, W. (2010). Optimal linear-consensus algorithms: an LQR perspective. *IEEE Transactions on Systems, Man and Cybernetics*, *40*(3), 819–830.
Chen, T., Liu, X., & Lu, W. (2007). Pinning complex networks by a single controller. *IEEE Transactions on Circuits and Systems*, *54*(6), 1317–1326.
Chopra, N., & Spong, M. (2006). Passivity-based control of multi-agent systems. In *Advances in robot control* (pp. 107–134). Springer.
Duan, Z., Chen, G., & Huang, L. (2009). Disconnected synchronized regions of complex dynamical networks. *IEEE Transactions on Automatic Control*, *54*(4), 845–849.
Dunbar, W. B., & Murray, R. M. (2006). Distributed receding horizon control for multi-vehicle formation stabilization. *Automatica*, *42*(4), 549–558.
Fax, J. A., & Murray, R. M. (2004). Information flow and cooperative control of vehicle formations. *IEEE Transactions on Automatic Control*, *49*(9), 1465–1476.
Gadewadikar, J., Lewis, F. L., & Abu-Khalaf, M. (2006). Necessary and sufficient conditions for H_∞ static output-feedback control. *Journal of Guidance, Control, and Dynamics*, *29*(4), 915–920.
Gadewadikar, J., Lewis, F. L., Xie, L., Kučera, V., & Abu-Khalaf, M. (2007). Parametrization of all stabilizing H_∞ static state-feedback gains: application to output-feedback design. *Automatica*, *43*, 1597–1604.
Hengster-Movric, K., & Lewis, F. L. (2012). Cooperative observers and regulators for discrete-time multiagent systems. *International Journal of Robust and Nonlinear Control*, http://dx.doi.org/10.1002/rnc.2840.
Hengster-Movric, K., & Lewis, F. L. (2014). Cooperative optimal control for multi-agent systems on directed graph topologies. *IEEE Transactions on Automatic Control*, *59*(3), 769–774.
Hengster-Movric, K., You, K., Lewis, F. L., & Xie, L. (2012). Synchronization of discrete-time multi-agent systems on graphs using Riccati design. *Automatica*, *49*(2), 414–423.
Jadbabaie, A., Lin, J., & Morse, A. (2003). Coordination of groups of mobile autonomous agents using nearest neighbour rules. *IEEE Transactions on Automatic Control*, *48*(6), 988–1001.
Jovanovic, M. R. (2005). On the optimality of localized distributed controllers. In *American control conference, June 8–10, Portland, OR, USA* (pp. 4583–4588).
Lewis, F. L., Vrabie, D., & Syrmos, V. L. (2012). *Optimal control* (3rd ed.). John Wiley & Sons.
Li, Z., Duan, Z., & Chen, G. (2010). H_∞ consenus regions of multi-agent systems. In *Proceedings of the 29th Chinese control conference, July 29–31, Beijing, China*.
Li, Z., Duan, Z., & Chen, G. (2011). Consensus of discrete-time linear multi-agent systems with observer-type protocols. *Discrete and Continuous Dynamical Systems, Series B*, *16*(2), 489–505.
Li, Z., Duan, Z., Chen, G., & Huang, L. (2010). Consensus of multiagent systems and synchronization of complex networks: a unified viewpoint. *IEEE Transactions on Circuits and Systems. I. Regular Papers*, *57*(1), 213–224.
Liu, X. (2011). Cluster synchronization for for linearly coupled complex networks. *Journal of Industrial and Management Optimization*, *7*(1), 87–101.
Lohnmiller, W., & Slotine, J. -J. E. (1997). On contraction analysis for nonlinear systems, NSL-961001.
Ma, C. Q., & Zhang, J. F. (2010). Necessary and sufficient conditions for consensusability of linear multi-agent systems. *IEEE Transactions on Automatic Control*, *55*(5), 1263–1268.
Olfati-Saber, R., Fax, J. A., & Murray, R. (2007). Consensus and cooperation in networked multi-agent systems (invited paper). *Proceedings of the IEEE*, *95*(1), 215–233.
Olfati-Saber, R., & Murray, R. M. (2003). Consensus protocols for networks of dynamic agents. In *Proceedings of American control conference* (pp. 951–956).
Olfati-Saber, R., & Murray, R. M. (2004). Consensus problems in networks of agents with switching topology and time-delays. *IEEE Transactions on Automatic Control*, *49*(9), 1520–1533.
Pavlov, A., Pogromski, A., van de Wouv, N., & Nijmeijer, H. (2004). Convergent dynamics, a tribute to Boris Pavlovich Demidovich. *Systems & Control Letters*, *52*, 257–261.
Pecora, L. M., & Carroll, T. L. (1998). Master stability functions for synchronized coupled systems. *Physical Review Letters*, *80*(10), 2109–2112.
Qu, Z., Simaan, M., & Doug, J. (2009). Inverse optimality of cooperative control for networked systems. In *Joint 48th IEEE conference on decision and control and 28th Chinese control conference, Shanghai, PR China, December 16–18*.
Ren, W., & Beard, R. W. (2005). Consensus seeking in multiagent systems under dynamically changing interaction topologies. *IEEE Transactions on Automatic Control*, *50*, 655–661.
Russo, G., di Bernardo, M., & Sontag, E. D. (2013). A contraction approach to the hierarchical analysis and design of networked systems. *IEEE Transactions on Automatic Control*, *58*(5), 1328–1331.
Scardovi, L., & Sepulchre, R. (2009). Synchronization in networks of identical linear systems. *Automatica*, *45*, 2557–2562.
Schenato, L., Sinopoli, B., Franceschetti, M., Poolla, K., & Sastry, S. (2007). Foundations of control and estimation over lossy networks. *Proceedings of the IEEE*, *91*(1), 163–187.
Sorrentino, F., di Bernardo, M., Garofalo, F., & Chen, G. (2007). Controllability of complex networks via pinning. *Physical Review E*, *75*(4), 046103.
Syrmos, V. L., Abdallah, C. T., Dorato, P., & Grigoriadis, K. (1997). Static output feedback: a survey. *Automatica*, *33*(2), 125–137.
Tsitsiklis, J. (1984). *Problems in decentralized decision making and computation*. (Ph.D. dissertation), Cambridge, MA: Dept. Elect. Eng. and Comput. Sci., MIT.
Tuna, S. E. (2008). LQR-based coupling gain for synchronization of linear systems. arXiv:0801.3390v1 [math.OC].
Vamvoudakis, K. G., & Lewis, F. L. (2011). Policy iteration algorithm for distributed networks and graphical games. In *50th IEEE conference on decision and control and European control conference, CDC-ECC, Orlando, FL, USA*.
Wang, X. F., & Chen, G. (2002). Pinning control of scale free dynamical networks. *Physica A*, *310*, 521–531.
Wieland, P., Sepulchre, R., & Allgower, F. (2011). An internal model principle is necessary and sufficient for linear output synchronization. *Automatica*, *47*, 1068–1074.
Wonham, M. (1985). *Linear multivariable control, a geometric approach* (3rd ed.) (pp. 86–97). Spriger Verlag, 85.
You, K., & Xie, L. (2011). Coordination of discrete-time multi-agent systems via relative output-feedback. *International Journal of Robust and Nonlinear Control*, *21*, http://dx.doi.org/10.1002/rnc.1659.
Zhang, H., & Lewis, F. L. (2011). Optimal design for synchronization of cooperative systems: state feedback, observer and output-feedback. *IEEE Transactions on Automatic Control*, *56*(8), 1948–1953.

Kristian Hengster-Movric was born in Zagreb, Croatia, in 1986. He enrolled in the College of Electrical Engineering and Computing at The University of Zagreb in 2004 and received the M.S. degree in the Automatics in 2009. The Ph.D. was conferred by The University of Texas at Arlington, in 2013. He received the second place prize N.M. Stelmakh Outstanding Student Research award, and obtained The Deans Fellowship in the same year. Kristian is currently at the Czech Technical University in Prague in a capacity of a postdoctoral fellow at the Department of Control Engineering, Faculty of Electrical Engineering. Research interests include dynamical systems and control theory applied to complex, multi-agent systems and distributed systems control.

Frank L. Lewis, Fellow IEEE, Fellow IFAC, Fellow UK Institute of Measurement & Control, PE Texas, UK Chartered Engineer, is Distinguished Scholar Professor, Distinguished Teaching Professor, and Moncrief-O'Donnell Chair at The University of Texas at Arlington Research Institute. He obtained the Bachelor's Degree in Physics/EE and the MSEE at Rice University, the M.S. in Aeronautical Engineering from Univ. W. Florida, and the Ph.D. at Ga. Tech. He works in feedback control, intelligent systems, distributed control systems, and sensor networks. He is author of 6 US patents, 250 journal papers, 360 conference papers, 15 books, 44 chapters, and 11 journal special issues. He received the Fulbright Research Award, NSF Research Initiation Grant, ASEE Terman Award, Int. Neural Network Soc. Gabor Award 2009, UK Inst Measurement & Control Honeywell Field Engineering Medal 2009. Received Outstanding Service Award from Dallas IEEE section selected as Engineer of the Year by Ft. Worth IEEE Section. Listed in Ft. Worth Business Press Top 200 Leaders in Manufacturing. Received the 2010 IEEE Region 5 Outstanding Engineering Educator Award and the 2010 UTA Graduate Dean's Excellence in Doctoral Mentoring Award. Elected to UTA Academy of Distinguished Teachers 2012. He served on the NAE Committee on Space Station in 1995. He is an elected Guest Consulting Professor at South China University of Technology and Shanghai Jiao Tong University. Founding Member of the Board of Governors of the Mediterranean Control Association. Helped win the IEEE Control Systems Society Best Chapter Award (as Founding Chairman of DFW Chapter), the National Sigma Xi Award for Outstanding Chapter (as President of UTA Chapter), and the US SBA Tibbets Award in 1996 (as Director of ARRI's SBIR Program).

Michael Sebek was born in Prague, Czechoslovakia, in 1954. He obtained the Ing. (M.Sc.) degree in electrical engineering with distinction from the Czech Technical University in Prague in 1978, the C.Sc. (Ph.D.) degree in control engineering and the Dr.Sc. degree in control theory from the Czech Academy of Sciences in 1981 and 1995, respectively. Since 1979, he has been with the Institute of Information Theory and Automation, Prague, most recently as the Head of the Department of Control Theory. Currently, he is the Head of the Control Engineering Department of the Czech Technical University in Prague. He is also the CEO of PolyX Ltd., producer of the Polynomial Toolbox for Matlab. He held visiting positions at the Strathclyde University, Glasgow, UK (1986); University of Twente, NL (1990–91); and at the ETH Zurich, CH (1994–95).

The research interests of M. Sebek include linear control and systems theory, robust control, network and n-D systems, numerical methods and software. He published well over 200 research papers and developed several successful software packages. He has led numerous national and international research projects. Within IFAC, he was a Council member (2008–14) and the General Chair of the 16th World Congress in Prague 2005. Currently, he is a member of the IFAC Awards Committee.

3. COOPERATIVE SYNCHRONIZATION CONTROL FOR AGENTS WITH CONTROL DELAYS: A SYNCHRONIZING REGION APPROACH

Kristian Hengster-Movric, Frank L. Lewis, Michael Sebek, Tomas Vyhlidal, **Cooperative synchronization control for agents with control delays: A synchronizing region approach**, *Journal of the Franklin Institute*, 2015

This paper, published in Elsevier's *Journal of the Franklin Institute*, (IF: 3.567), in 2015, takes into account communication time-delays which are realistically unavoidable in real-world distributed multi-agent systems. It proves to be possible, using the Razuminkhin-Lyapunov stability analysis, to apply the spirit of the synchronizing region methods to systems with uniform time-delays, yielding a delay-dependent synchronizing region that restricts the maximal value of the time-delay as well as the graph topologies allowing for synchronization under the considered delays. These results are applicable, in principle, to all cases analyzed as being delay-free, and they indeed reduce to the familiar delay-free results when the upper bound on the delays is pushed to zero. Therefore, albeit somewhat conservative, the results elaborated in this part present a natural extension of the familiar synchronizing region concepts to the realistic case of having time-delays.

This chapter investigates multi-agent system synchronization in presence of control signal time-delays. Agents are assumed to be identical linear time-invariant systems, interacting on a directed graph topology, all having the same control time-delay. Distributed control of multi-agent systems is complicated by the fact that the communication graph topology interplays with single-agent dynamics. Here a design method based on a synchronizing region is given that decouples the design of local feedback gains from the detailed properties of graph topology. Such extension of the synchronizing region concept to agents with delays is rigorously justified. Delay-dependent synchronizing region is defined and methods are given guaranteeing its estimates. Qualitative properties of delay-dependent synchronizing regions and implications for control design are discussed. It is found that these regions are inherently bounded which restricts the graphs that allow for synchronization under delayed communication. Stronger property of exponential stability with a prescribed convergence rate is presented as a special case.

Available online at www.sciencedirect.com

ScienceDirect

Journal of the Franklin Institute 352 (2015) 2002–2028

Journal *of* The Franklin Institute

www.elsevier.com/locate/jfranklin

Cooperative synchronization control for agents with control delays: A synchronizing region approach ☆

Kristian Hengster-Movric[a,*], Frank L. Lewis[b], Michael Šebek[a,d], Tomáš Vyhlídal[c,d]

[a]*Department of Control Engineering, Faculty of Electrical Engineering, Czech Technical University in Prague, Czech Republic*

[b]*UTARI, University of Texas at Arlington, United States*

[c]*Department of Instrumentation and Control Engineering, Faculty of Mechanical Engineering, Czech Technical University in Prague, Czech Republic*

[d]*CIIRC, Czech Technical University in Prague, Czech Republic*

Received 12 July 2014; received in revised form 19 December 2014; accepted 16 February 2015
Available online 25 February 2015

Abstract

This paper investigates multi-agent system synchronization in the presence of control signal delays. Agents are assumed to be identical linear time-invariant systems, interacting on a directed graph topology, all having the same control delay. Distributed control of multi-agent systems is complicated by the fact that the communication graph topology interplays with single-agent dynamics. Here a design method based on a synchronizing region is given that decouples the design of local feedback gains from the detailed properties of graph topology. Such extension of the synchronizing region concept to agents with delays is rigorously justified. Delay-dependent synchronizing region is defined and methods are given guaranteeing its estimates. Qualitative properties of delay-dependent synchronizing regions and implications for control design are discussed. It is found that these regions are inherently

☆This work is supported by the European social fund within the framework of realizing the project "Support of inter-sectoral mobility and quality enhancement of research teams at Czech Technical University in Prague", CZ.1.07/2.3.00/30.0034, the NSF Grant ECCS-1405173, ONR Grant N00014-13-1-0562, ONR Grant N000141410718, Grant W911NF-11-D-0001, China NNSF Grant 61120106011, and China Education Ministry Project 111 (No. B08015). The fourth author was supported by the Grant Agency of the Czech Technical University in Prague, Grant no. SGS14/182/OHK2/3T/12.

*Correspondence to: Czech Technical University in Prague, FEL, Karlovo Namesti 13E, 121 35, Praha 2, Czech Republic.

E-mail address: hengskri@fel.cvut.cz (K. Hengster-Movric).

http://dx.doi.org/10.1016/j.jfranklin.2015.02.011

bounded which restricts the graphs that allow for synchronization under delayed communication. Stronger property of exponential stability with a prescribed convergence rate is presented as a special case.

1. Introduction

The last two decades have witnessed an increasing interest in multi-agent network cooperative systems, inspired by natural occurrence of flocking and formation forming [1–12]. Early work with networked cooperative systems in continuous and discrete-time is presented in [1–6]. Those papers generally refer to the consensus problem without a leader, where the final consensus value is determined by initial conditions. Necessary and sufficient conditions for distributed systems to synchronize were given. On the other hand, by adding a leader that pins to a group of agents one can have synchronization to a command trajectory through pinning control [7,13], for all initial conditions. We term this the *cooperative tracking problem*. Most early papers consider one-dimensional agents, in continuous-time usually single-integrators. These results are extended to general linear time-invariant (LTI) agents in [6,12,13,15]. Synchronization using dynamic compensators or output-feedback is considered in [8,13,14].

For identical LTI agents without delays, the synchronizing region concept [8,10,13] greatly simplifies the design of local distributed feedback gains [12,13,15]. The synchronizing region approach, originally introduced in the context of oscillator synchronization [10], reduces effects of the graph topology on the multi-agent system dynamics to robust stability of a single-agent closed-loop system. Inspired in part by [7,10], the considerations in [12,13] show *via* single-agent Lyapunov stability estimates that a distributed state-feedback, derived from a local algebraic Riccati equation, guarantees synchronization for a broad class of communication graphs. Developments of [9] additionally consider synchronization with prescribed exponential convergence rate using the same single-agent approach.

Considering practical means of distributed control *e.g.* networked control, dedicated busses and wireless communication, delays in information signals from neighboring agents are unavoidable [3]. In realistic applications one is interested in effects those delays have on cooperative stability, or differently put, in robustness of cooperative stability to delays. Generally well behaved system, robust to disturbances, may be sensitive to feedback delays, which can lead to poor performance and even loss of stability. Guaranteeing robustness to delays is therefore important for all practical implementations of multi-agent distributed control. Some early papers on cooperative consensus [1,3,5] address the problem of delayed information from the neighbors. For discrete-time synchronization, delays are treated in [28] using stochastic matrices. For continuous-time, [1,3] introduce a uniform delay in one-dimensional single-integrator agents on undirected graphs. More recent work [17] extends the approach of [1,3] to directed graph topologies, introducing the delay margin and a responsible eigenvalue concept.

One way to extend the early results on delays [1,3] and more recent [17] to general continuous-time identical LTI agents on directed graphs is offered by the theory of retarded functional differential equations (RFDEs) [24]. Essential question is that of guaranteeing single-agent stability. Lyapunov–Krasovskii and Lyapunov–Razumikhin theorems are extensively used to reach stability conclusions for RFDEs [16,18,19,21,22,24,25]. The former theorem uses functionals and allows for necessary and sufficient stability conditions, while the latter uses functions, thus avoiding the need for,

generally complicated, functional time derivatives. Krasovskii result is more general, but Razumikhin result applies more easily to systems with time-varying or even uncertain delays [25]. Furthermore, Razumikhin stability function provides a connection to classical Lyapunov methods of delay-free systems. Those theorems furnish delay-independent and delay-dependent stability results [16,25]. Delay-independent results essentially rely on robustness of delay-free part of a system to any type of disturbance, including delayed signals. A brief reflection reveals that delay-independent stability results tend to be overly conservative, as information on the actual delay is not used and delayed signals are always treated as detrimental disturbances. In contrast, delay-dependent results allow the treatment of delayed stabilizing feedback [25]. Both Krasovskii and Razumikhin delay-dependent stability results are well known in the literature [18,21,25]. Hence in a search for simple and flexible stability conditions the delay-dependent results based on Razumikhin theorem [16,21] present a good choice. Nevertheless, Razuminkin delay-dependent stability criteria show considerable conservatism and reducing this conservatism is a topic of current research.

Different approaches to general synchronization under delays are present in the literature. To name just a few [32–35] make use of Lyapunov–Krasovskii functionals. Results given in [32] use Krasovskii functionals to derive quite involved stability criteria. Stability conditions are expressed in a centralized manner in that stability depends jointly on single-agent systems as well as the graph topology. The proposed dynamic synchronization control is obtained there in a centralized way. Similarly, [33] motivated by neural networks expresses stability criteria for synchronization of multi-agent systems by large LMIs whose size increases with an increasing number of agents, a difficulty admitted candidly by authors themselves. Both [32] and [33] assume inputs acting directly on all agents' states, which is not generally the case with realistic agents. In comparison [34] treats a fairly general class of systems, random switching stochastic systems with time varying communication topology and uncertainties, *via* H_∞ robust control. Krasovskii functionals are used in a centralized way to guarantee robust stochastic stability. Master-slave synchronization for systems with mixed neutral and discrete time-delays is analyzed in [35] again *via* Krasovskii functionals. Systems considered in [34,35] are treated as a whole; no attention is paid to the distributed implementation of controls. Existing work also deals with nonlinear agents [29] and heterogeneous agent output synchronization [30] under mild assumptions on delays and graph topology, but considering only undirected graphs and basing stability analysis on the system as a whole, which is in contrast with the philosophy of scalable conditions depending on single-agent systems [10,13,17]. The simpler case of identical LTI agents with uniform delay allows for simpler, distributed, stability criteria.

This paper is concerned with identical LTI agents, all having the same (*uniform*), constant, control signal delay. If delays were allowed to differ in different agents those would no longer be identical as dynamical systems. The simplifying assumption on uniform delays is standard in the literature [1,3,17]. The underlying communication graph is assumed directed. This paper as its first contribution brings together Razumikhin stability analysis and distributed cooperative control to extend the classical synchronizing region approach of delay-free distributed control to delay-dependent synchronizing region applicable to agents with uniform control delay. The delay-dependent synchronizing region reduces effects of the communication graph topology to robust stability of a single-agent closed-loop system with delayed feedback. This concept first appeared in context of oscillator synchronization in [20], along the lines of [10]. In contrast to [20] the approach proposed in this paper accounts for controllability properties of single-agents and provides a connection and comparison between the delay-free distributed feedback design [13] and the case of nonzero delays. Moreover this paper extends results on delays for cooperative control reported in [1,3] to LTI agents on directed graphs, and synchronization results of [12,13] to the case of uniform

delays. In contrast to [29,30,32–35], here are considered general directed, albeit constant, graph topologies and stability conditions are derived depending on single-agent systems. Hence stability analysis is scalable and does not involve the entire multi-agent system. The price for that is restricting consideration to identical agents with uniform time delays. As a second contribution qualitative properties of the delay-dependent synchronizing region, characterizing robust stability, are addressed. It is found that for nonzero delays the guaranteed delay-dependent synchronizing region is inherently bounded. Therefore one has a situation similar to the discrete-time synchronization problem [15], and its bounded synchronizing region. The nature of this sufficient condition is qualitatively similar to the result in [3] which gives necessary and sufficient conditions for single-integrator consensus under delays. One finds here also a tradeoff between fast synchronization and robustness to delays similar to that mentioned in [1,3]. A static cooperative synchronization control design procedure is given based on the guaranteed delay-dependent synchronizing region. The third contribution is in bringing stricter conditions for stronger property of exponential cooperative stability with a prescribed convergence rate. In that this paper extends delay-free results on convergence in [9] to agents with a uniform control delay. Numerical example validates the proposed approach.

The paper is organized as follows. Section 2 gives graph properties and notation. Section 3 presents the multi-agents system dynamics and defines the control problem. Section 4 applies the appropriately modified classical delay-dependent stability results to guarantee the delay-dependent synchronizing region. Section 5 addresses the main problem of cooperative control design for systems having a control delay. Section 6 brings a strengthening of results in Sections 4 and 5 to exponential stability with a prescribed convergence rate. Section 7 relates general conditions of Section 5 to a familiar special case of single-integrator agents on undirected graphs. A numerical example of the proposed design is presented in Section 8, and conclusions are given in Section 9.

2. Graph properties

Consider a graph $\mathcal{G}=(\mathcal{V},\mathcal{E})$ with N vertices $\mathcal{V}=\{v_1,\cdots,v_N\}$ and a set of edges or arcs $\mathcal{E}\subseteq\mathcal{V}\times\mathcal{V}$. It is assumed that the graph is simple, *i.e.* there are no repeated edges or self-loops $(v_i,v_i)\notin\mathcal{E},\ \forall i$. Mostly directed graphs are considered. Denote the connectivity matrix as $E=[e_{ij}]$ with $e_{ij}>0$ *if* $(v_j,v_i)\in\mathcal{E}$ and $e_{ij}=0$ otherwise. The set of neighbors of node v_i is denoted as $\mathcal{N}_i=\{v_j:(v_j,v_i)\in\mathcal{E}\}$, *i.e.* the set of nodes with arcs coming into v_i. Define the degree matrix as $D=\mathrm{diag}(d_1\ldots d_N)$ with $d_i=\sum_j e_{ij}$ the (weighted) degree of node i (*i.e.* the ith row sum of E). Define the graph Laplacian matrix as $L=D-E$. A *path* from node v_{i_1} to node v_{i_k} is a sequence of edges $(v_{i_1},v_{i_2}),(v_{i_2},v_{i_3}),\ldots,(v_{i_{k-1}},v_{i_k})$, with $(v_{i_{j-1}},v_{i_j})\in\mathcal{E}$ or $(v_{i_j},v_{i_{j-1}})\in\mathcal{E}$ for $j\in\{2,\ldots,k\}$. A *directed path* is a sequence of edges $(v_{i_1},v_{i_2}),(v_{i_2},v_{i_3}),\ldots,(v_{i_{k-1}},v_{i_k})$, with $(v_{i_{j-1}},v_{i_j})\in\mathcal{E}$ for $j\in\{2,\ldots,k\}$. The graph is said to be *connected* if every two vertices can be joined by a path. A graph is said to be *strongly connected* if every two vertices can be joined by a directed path. The graph is said to contain a (directed) *spanning tree* if there exists a vertex, v_0, such that every other vertex in $\mathcal{V}$ can be connected to v_0 by a (directed) path starting from v_0. Such a special vertex is then called a root node. The Laplacian matrix L has a simple zero eigenvalue if and only if the undirected graph is connected, or the directed graph contains a spanning tree.

For any matrix A, $\sigma_{min}(A)$, $\sigma_{max}(A)$ denote the minimal and maximal singular values of A respectively. For a positive semi-definite symmetric matrix A, $\lambda_{>0\ min}(A)$ denotes the minimal nonzero eigenvalue. The abbreviation *a.s.* stands for asymptotic stability, and *e.s.* for exponential stability.

3. System dynamics and problem statement

This section describes the single-agent dynamics and the global dynamics of the entire multi-agent system. An appropriate state transformation reduces the cooperative stability of global dynamics to asymptotic stability of a set of RFDEs. Such a reduced problem is addressed by the synchronizing region. Let the single-agent dynamics be given by an LTI system with control signal delay, $\tau \geq 0$

$$\dot{x}_i(t) = Ax_i(t) + Bu_i(t-\tau), \tag{1}$$

where $x_i \in R^n$, $u_i \in R^m$ $\forall i$ are the states and inputs. Let there be an autonomous leader dynamics given as

$$\dot{x}_0(t) = Ax_0(t) \tag{2}$$

with $x_0 \in R^n$. The delay τ is taken to be constant and same for all agents. Though this needs not be true in more realistic models, having different delays for different agents make them, strictly speaking, not identical as dynamical systems. The assumption on uniform delays is a standard simplifying assumption [1,3,17] and it is crucial for the following development.

The distributed cooperative synchronization control problem is to find controls u_i depending on x_i, $x_{j\in\mathcal{N}_i}$ such that as $t\to\infty$, $\|x_i - x_0\| \to 0$, $\forall i$. Define the local neighborhood error

$$e_i = \sum_j e_{ij}(x_j - x_i) + g_i(x_0 - x_i), \tag{3}$$

where $g_i \geq 0$ are the pinning gains, which are nonzero only for those nodes that have a direct connection to the leader [7,13]. Let the control signal for agent i be calculated as a linear feedback of the local neighborhood error

$$u_i(t) = cKe_i(t), \tag{4}$$

where K is the local linear feedback gain matrix to be detailed later, and $c>0$ is the coupling gain. This gives the closed loop single-agent dynamics

$$\dot{x}_i(t) = Ax_i(t) + cBKe_i(t-\tau). \tag{5}$$

Introducing the synchronization error, $\delta_i = x_i - x_0$, one has in global form

$$\dot{x}(t) = (I_N \otimes A)x(t) - c(L+G) \otimes BK\delta(t-\tau), \tag{6}$$

where $x = \left[x_1^T \ldots x_N^T\right]^T \in R^{Nn}$, $\delta = \left[\delta_1^T \ldots \delta_N^T\right]^T \in R^{Nn}$, and $G = \mathrm{diag}(g_1 \ldots g_N)$ is the diagonal matrix of pinning gains. The global synchronization error system is then given as

$$\dot{\delta}(t) = (I_N \otimes A)\delta(t) - c(L+G) \otimes BK\delta(t-\tau). \tag{7}$$

Eq. (7) is a linear retarded functional differential equation (RFDE), of the form

$$\dot{\delta}(t) = \overline{A}\delta(t) + \overline{A}_d\delta(t-\tau). \tag{8}$$

Existence of solutions to the Cauchy problem for Eq. (8) is guaranteed by the Schauder fixed point theorem and uniqueness follows from Lipschitz continuity of the functional defining the dynamics [24]. The Lipschitzean property is here fulfilled by virtue of linearity. Linearity of Eq. (8) also ensures the boundedness of the dynamics functional [16].

Instead of analyzing the global system (7), following the lines of synchronizing region approach [10,13] the following Lemma provides a simplification useful in designing local feedback gains K.

Lemma 1. The trivial solution of system (7) is asymptotically stable if and only if the trivial solutions of systems

$$\dot{y}(t) = Ay(t) - c\lambda_j BKy(t-\tau),$$

each having an order of a single agent, where λ_i are the eigenvalues of the graph matrix $(L+G)$, are asymptotically stable, $\forall j$.

Proof. The stability of Eq. (7) is determined by the transcendental transfer function matrix

$$[sI_{Nn} - (I_N \otimes A) + c(L+G) \otimes BKe^{-s\tau}]^{-1}. \tag{9}$$

The frequency domain expression (9) needs to be asymptotically stable, a property determined by the roots of the pertaining characteristic quasipolynomial

$$\Delta(s) = \det[sI_{Nn} - (I_N \otimes A) + c(L+G) \otimes BKe^{-s\tau}]. \tag{10}$$

Knowing that linear transformations do not change the determinant of a matrix one can use a coordinate transformation $T \otimes I_n$ in Eq. (10), where $T^{-1}(L+G)T = \Lambda$ is an upper triangular matrix, thereby simplifying the problem considerably. Whence one obtains

$$\begin{aligned}
&\det[sI_{Nn} - (I_N \otimes A) + c(L+G) \otimes BKe^{-s\tau}] \\
&\quad = \det\left[(T \otimes I_n)^{-1}(sI_{Nn} - (I_N \otimes A) + c(L+G) \otimes BKe^{-s\tau})(T \otimes I_n)\right] \\
&\quad = \det[sI_{Nn} - I_N \otimes A + c\Lambda \otimes BKe^{-s\tau}] \\
&\quad = \prod_j \det\left[sI_n - A + c\lambda_j BKe^{-s\tau}\right],
\end{aligned} \tag{11}$$

where λ_j are the eigenvalues of Λ, equaling the eigenvalues of the graph matrix $(L+G)$. Therefore, each factor in the product (11), $\det(sI_n - A + c\lambda_j BKe^{-s\tau})$, must be asymptotically stable. This requirement is equivalent to the asymptotic stability of the trivial solution for a set of linear RFDEs

$$\dot{y}(t) = Ay(t) - c\lambda_j BKy(t-\tau). \tag{12}$$

Systems (12) are in the form of Eq. (8) but have the order of a single-agent dynamics, *i.e.* n.

The proof of Lemma 1 uses a detour in the frequency domain but the result pertains to time domain, and as such it shall be used. This is in contrast with many treatments of delays in the literature using frequency domain stability criteria, *e.g.* the Nyquist criterion [27,17], but more along the lines of [7,12,13], as detailed in Section 4.

Bearing the synchronizing region concept in sight [10,11,13], it is advantageous to separate the dependence from the, generally complex, scaled eigenvalues $c\lambda_j$ of the graph matrix $(L+G)$ and instead consider the complex RFDE

$$\dot{y}(t) = Ay(t) + \sigma A_d y(t-\tau), \tag{13}$$

where $\sigma \in C$, $A_d = -BK$. Note that Eq. (12) describes a dynamical system generally in an n-dimensional complex vector space, C^n. The need for complex state vectors arises due to the triangularizing coordinate transformation T used in proof of Lemma 1, that is generally complex, and the generally complex eigenvalues of the graph matrix, λ_j. Because of the latter $\sigma \in C$ is required in Eq. (13). Hence Eq. (13) is clearly an equation defined on a complex vector space C^n, in contrast to Eq. (1) defined on R^n. This necessary generalization creates no difficulties as the standard Lyapunov techniques to be employed (*c.f.* Section 4) are straightforwardly applicable to systems with complex states [9].

The robust stability of Eq. (13) with respect to σ motivates the following definition.

Definition 1. Given a complex retarded functional differential Eq. (13) the delay-dependent synchronizing region is a subset of the complex plane C depending on the delay τ

$$S_c(\tau) = \{\sigma \in C : Ay(t) + \sigma A_d y(t-\tau)\ a.s.\}.$$

Delay-dependent synchronizing region is introduced in [20] for oscillator synchronization, following the lines of [10]. Those papers, however, do not consider the controllability properties of individual systems.

Given system matrices (A, B) the delay-dependent synchronizing region is determined by the choice of local feedback matrix K. Then the cooperative stability of the entire multi-agent system, *i.e.* $\delta \to 0$, in the presence of a uniform delay $\tau \geq 0$, is guaranteed if and only if there exists a coupling gain $c > 0$ such that $c\lambda_j \in S_c(\tau),\ \forall j$. The control design proceeds by first designing the local feedback matrix K and then the coupling gain $c > 0$ that scales all the graph matrix eigenvalues into the delay-dependent synchronizing region.

The following result presents an important property of the graph matrix $(L + G)$ related to the underlying graph topology. This fact is well known in the literature hence the proof is omitted [7,13,26].

Lemma 2. If the graph has a spanning tree with at least one nonzero pinning gain connecting to a root node then the graph matrix $(L + G)$ is nonsingular with all the eigenvalues in the right half-plane.

4. Stability results for the complex linear RFDE

This section extends the classical stability conditions for RFDEs to the complex RFDE (13) providing a guaranteed delay-dependent synchronizing region. For that purpose the classical stability results for RFDE (8) are first presented and then applied, *mutatis mutandis*, to Eq. (13).

Theorem 1. (*Lyapunov–Razumikhin theorem* [16,19,25]). Let α, β, γ be class $\mathcal{K}$ functions, and let $p(s) > s\ \forall s > 0$ be a scalar continuous non-decreasing function. If there exists a continuous function $V(x) : R^n \to R$ such that for some $k > 0$, for all $x_t \in \mathcal{C}$ satisfying $V(x_t(\vartheta)) \leq k,\ \forall \vartheta \in [t-\tau, t]$, one has

$$\alpha(\|x\|) \leq V(x) \leq \beta(\|x\|)$$

$$\frac{d}{dt}V(x(t)) \leq -\gamma(\|x(t)\|),\ \text{ if } V(x(\vartheta)) < p(V(x(t))),\ \forall \vartheta \in [t-\tau, t]$$

then the trivial solution $x(t) \equiv 0$ is uniformly asymptotically stable. Furthermore, the set in $\mathcal{C}$ where $V(x_t(\vartheta)) \leq k,\ \forall \vartheta \in [t-\tau, t]$ is an invariant subset in the region of attraction in the space $\mathcal{C}$.

Based on Theorem 1 sufficient conditions for asymptotic stability are derived for the special case of linear single-delay RFDE having the form (8).

Theorem 2. (*Lyapunov–Razumikhin delay-dependent result* [16,21]). Let there exist positive definite symmetric matrices $P, P_1, P_2 > 0$, and a constant $\tau_0 > 0$. Let the following conditions be satisfied:

$$P_1^{-1} < P,\ \ P_2^{-1} < P, \tag{14}$$

$$(A+A_d)^T P + P(A+A_d) + \tau_0 P A_d A P_1 A^T A_d^T P + \tau_0 P A_d^2 P_2 (A_d^2)^T P + 2\tau_0 P < 0. \tag{15}$$

Then the trivial solution $x(t) \equiv 0$ of the equation

$$\dot{x}(t) = Ax(t) + A_d x(t-\tau)$$

is uniformly asymptotically stable for $0 \le \tau \le \tau_0$.

Now we extend the result of Theorem 2 to RFDE (13) in order to obtain estimates of the synchronizing region $S_c(\tau)$. The Lyapunov–Razumikhin functions appearing in Theorem 2 are modified to accommodate for the fact that the system (13) is complex. State vectors x are allowed to be complex and the dagger † denotes the hermitian adjoint, *i.e.* transposition and complex conjugation. With real $P = P^T > 0$ this gives real valued quadratic Lyapunov–Razumikhin functions

$$V(x) = x^\dagger P x > 0. \tag{16}$$

The substitution $A_d \mapsto \sigma A_d$, $A_d^T \mapsto (\sigma A_d)^\dagger = \overline{\sigma} A_d^T$ in Theorem 2 is rigorously justified as follows.

Theorem 3. (*Lyapunov–Razumikhin delay-dependent result for the complex equation*). Let there exist real positive definite symmetric matrices $P, P_1, P_2 > 0$, and $\tau_0 > 0$. Let the following conditions be satisfied:

$$P_1^{-1} < P, \quad P_2^{-1} < P, \tag{17}$$

$$(A+\sigma A_d)^\dagger P + P(A+\sigma A_d) + \tau_0 |\sigma|^2 P A_d A P_1 A^T A_d^T P + \tau_0 |\sigma|^4 P A_d^2 P_2 (A_d^2)^T P + 2\tau_0 P < 0. \tag{18}$$

Then, for given $\sigma \in C$, the trivial solution, $x(t) \equiv 0$, of Eq. (13) is uniformly asymptotically stable for $0 \le \tau \le \tau_0$.

Proof. First it should be observed that since the solution $x(t)$ is continuously differentiable one has

$$x(t-\tau) = x(t) - \int_{t-\tau}^{t} \dot{x}(s)ds = x(t) - \int_{t-\tau}^{t} Ax(s) + \sigma A_d x(s-\tau)ds$$

Thus the original equation can be written as a transformed model

$$\dot{x}(t) = (A+\sigma A_d)x(t) - \int_{t-\tau}^{t} \sigma A_d A x(s) + \sigma^2 A_d^2 x(s-\tau)ds. \tag{19}$$

Choosing the Lyapunov–Razumikhin function as $V(x(t)) = x^\dagger(t) P x(t) > 0$ one finds its derivative to equal

$$\begin{aligned} \tfrac{d}{dt} V(x(t)) = \dot{x}^\dagger(t) P x(t) + x^\dagger(t) P \dot{x}(t) &= x^\dagger(t)\left[(A+\sigma A_d)^\dagger P + P(A+\sigma A_d)\right] x(t) \\ &- \int_{t-\tau}^{t} \overline{\sigma} x^\dagger(s) A^T A_d^T P x(t) + \sigma x^\dagger(t) P A_d A x(s) ds \\ &- \int_{t-\tau}^{t} \overline{\sigma}^2 x^\dagger(s-\tau)(A_d^2)^T P x(t) + \sigma^2 x^\dagger(t) P A_d^2 x(s-\tau) ds \end{aligned} \tag{20}$$

The integral terms in Eq. (20) are denoted as

$$\eta_1 = -\int_{-\tau}^{0} \overline{\sigma} x^{\dagger}(t+\vartheta) A^T A_d^T P x(t) + \sigma x^{\dagger}(t) P A_d A x(t+\vartheta) d\vartheta,$$

and

$$\eta_2 = -\int_{-\tau}^{0} \overline{\sigma}^2 x^{\dagger}(t-\tau+\vartheta)(A_d^2)^T P x(t) + \sigma^2 x^{\dagger}(t) P A_d^2 x(t-\tau+\vartheta) d\vartheta.$$

One finds by completing the squares with $P_1 > 0$ that

$$\begin{aligned}
&(\overline{\sigma} A^T A_d^T P x(t) + P_1^{-1} x(t+\vartheta))^{\dagger} P_1 (\overline{\sigma} A^T A_d^T P x(t) + P_1^{-1} x(t+\vartheta)) \geq 0,\\
&|\sigma|^2 x^{\dagger}(t) P A_d A P_1 A^T A_d^T P x(t) + \sigma x^{\dagger}(t) P A_d A x(t+\vartheta)\\
&\quad + \overline{\sigma} x^{\dagger}(t+\vartheta) A^T A_d^T P x(t) + x^{\dagger}(t+\vartheta) P_1^{-1} x(t+\vartheta) \geq 0,\\
&\quad - \left[\sigma x^{\dagger}(t) P A_d A x(t+\vartheta) + \overline{\sigma} x^{\dagger}(t+\vartheta) A^T A_d^T P x(t)\right]\\
&\leq x^{\dagger}(t) |\sigma|^2 P A_d A P_1 A^T A_d^T P x(t) + x^{\dagger}(t+\vartheta) P_1^{-1} x(t+\vartheta).
\end{aligned}$$

Whence one has

$$\begin{aligned}
\eta_1 &= -\int_{-\tau}^{0} \overline{\sigma} x^{\dagger}(t+\vartheta) A^T A_d^T P x(t) + \sigma x^{\dagger}(t) P A_d A x(t+\vartheta) d\vartheta\\
&\leq \int_{-\tau}^{0} |\sigma|^2 x^{\dagger}(t) P A_d A P_1 A^T A_d^T P x(t) + x^{\dagger}(t+\vartheta) P_1^{-1} x(t+\vartheta) d\vartheta\\
\eta_1 &\leq \tau |\sigma|^2 x^{\dagger}(t) P A_d A P_1 A^T A_d^T P x(t) + \int_{-\tau}^{0} x^{\dagger}(t+\vartheta) P_1^{-1} x(t+\vartheta) d\vartheta
\end{aligned}$$

In a similar manner, completing the squares with $P_2 > 0$ one finds that

$$\begin{aligned}
&(\overline{\sigma}^2 (A_d^2)^T P x(t) + P_2^{-1} x(t-\tau+\vartheta))^{\dagger} P_2 (\overline{\sigma}^2 (A_d^2)^T P x(t) + P_2^{-1} x(t-\tau+\vartheta)) \geq 0,\\
&|\sigma|^4 x^{\dagger}(t) P A_d^2 P_2 (A_d^2)^T P x(t) + \sigma^2 x^{\dagger}(t) P A_d^2 x(t-\tau+\vartheta)\\
&\quad + \overline{\sigma}^2 x^{\dagger}(t-\tau+\vartheta)(A_d^2)^T P x(t) + x^{\dagger}(t-\tau+\vartheta) P_2^{-1} x(t-\tau+\vartheta) \geq 0,\\
&\quad - \left[\sigma^2 x^{\dagger}(t) P A_d^2 x(t-\tau+\vartheta) + \overline{\sigma}^2 x^{\dagger}(t-\tau+\vartheta)(A_d^2)^T P x(t)\right]\\
&\leq x^{\dagger}(t) |\sigma|^4 P A_d^2 P_2 (A_d^2)^T P x(t) + x^{\dagger}(t-\tau+\vartheta) P_2^{-1} x(t-\tau+\vartheta).
\end{aligned}$$

Whence one has

$$\begin{aligned}
\eta_2 &= -\int_{-\tau}^{0} \overline{\sigma}^2 x^{\dagger}(t-\tau+\vartheta)(A_d^2)^T P x(t) + \sigma^2 x^{\dagger}(t) P A_d^2 x(t-\tau+\vartheta) d\vartheta\\
&\leq \int_{-\tau}^{0} x^{\dagger}(t) |\sigma|^4 P A_d^2 P_2 (A_d^2)^T P x(t) + x^{\dagger}(t-\tau+\vartheta) P_2^{-1} x(t-\tau+\vartheta) d\vartheta\\
\eta_2 &\leq \tau |\sigma|^4 x^{\dagger}(t) P A_d^2 P_2 (A_d^2)^T P x(t) + \int_{-\tau}^{0} x^{\dagger}(t-\tau+\vartheta) P_2^{-1} x(t-\tau+\vartheta) d\vartheta
\end{aligned}$$

Inserting those terms in Eq. (20) one finds the bound

$$\begin{aligned}
\tfrac{d}{dt} V(x(t)) &= x^{\dagger}(t)\left[(A+\sigma A_d)^{\dagger} P + P(A+\sigma A_d)\right] x(t) + \eta_1 + \eta_2\\
\frac{d}{dt} V(x(t)) &\leq x^{\dagger}(t)\left[(A+\sigma A_d)^{\dagger} P + P(A+\sigma A_d) + \tau |\sigma|^2 P A_d A P_1 A^T A_d^T P\right.\\
&\qquad \left. + \tau |\sigma|^4 P A_d^2 P_2 (A_d^2)^T P\right] x(t)
\end{aligned}$$

$$+\int_{-\tau}^{0} x^{\dagger}(t+\vartheta)P_1^{-1}x(t+\vartheta)d\vartheta+\int_{-\tau}^{0} x^{\dagger}(t-\tau+\vartheta)P_2^{-1}x(t-\tau+\vartheta)d\vartheta.$$

Under the condition $P_1^{-1}<P,\ \ P_2^{-1}<P$ one has

$$\begin{aligned}\tfrac{d}{dt}V(x(t)) &\le x^{\dagger}(t)\big[(A+\sigma A_d)^{\dagger}P+P(A+\sigma A_d)+\tau|\sigma|^2PA_dAP_1A^TA_d^TP\\ &\quad+\tau|\sigma|^4PA_d^2P_2(A_d^2)^TP\big]x(t)\\ &\quad+\int_{-\tau}^{0} x^{\dagger}(t+\vartheta)P_1^{-1}x(t+\vartheta)d\vartheta+\int_{-\tau}^{0} x^{\dagger}(t-\tau+\vartheta)P_2^{-1}x(t-\tau+\vartheta)d\vartheta\\ &\le x^{\dagger}(t)\big[(A+\sigma A_d)^{\dagger}P+P(A+\sigma A_d)+\tau|\sigma|^2PA_dAP_1A^TA_d^TP+\tau|\sigma|^4PA_d^2P_2(A_d^2)^T\\ &\quad\times P\big]x(t)+\int_{-\tau}^{0} x^{\dagger}(t+\vartheta)Px(t+\vartheta)d\vartheta+\int_{-\tau}^{0} x^{\dagger}(t-\tau+\vartheta)Px(t-\tau+\vartheta)d\vartheta\\ &= x^{\dagger}(t)\big[(A+\sigma A_d)^{\dagger}P+P(A+\sigma A_d)+\tau|\sigma|^2PA_dAP_1A^TA_d^TP+\tau|\sigma|^4PA_d^2P_2(A_d^2)^T\\ &\quad\times P\big]x(t)+\int_{-\tau}^{0} V(x(t+\vartheta))d\vartheta+\int_{-\tau}^{0} V(x(t-\tau+\vartheta))d\vartheta \qquad (21)\end{aligned}$$

Following Razumikhin condition, if $V(x(\vartheta))<\varepsilon V(x(t))\ \ \forall\vartheta\in[t-2\tau,t]$ for some $\varepsilon>1$, the time derivative of the Lyapunov–Razumikin function satisfies

$$\begin{aligned}\frac{d}{dt}V(x(t)) &\le x^{\dagger}(t)\big[(A+\sigma A_d)^{\dagger}P+P(A+\sigma A_d)+\tau|\sigma|^2PA_dAP_1A^TA_d^TP\\ &\quad+\tau|\sigma|^4PA_d^2P_2(A_d^2)^TP+2\tau\varepsilon P\big]x(t). \qquad (22)\end{aligned}$$

To find an appropriate $\varepsilon>1$ and $\delta>0$ such that for $V(x(\vartheta))<\varepsilon V(x(t)),\ \ \forall\vartheta\in[t-2\tau,t]$ one has $\dot V(x(t))\le-\delta V(x(t))$ let us proceed as follows. If the condition of the theorem is satisfied then there exists $\delta_1>0$ such that

$$\begin{aligned}&(A+\sigma A_d)^{\dagger}P+P(A+\sigma A_d)+\tau_0|\sigma|^2PA_dAP_1A^TA_d^TP+\tau_0|\sigma|^4PA_d^2P_2(A_d^2)^TP\\ &\quad+2\tau_0(1+2\delta_1)P<0.\end{aligned}$$

Take $\varepsilon=1+\delta_1$, then

$$\begin{aligned}&(A+\sigma A_d)^{\dagger}P+P(A+\sigma A_d)+\tau_0|\sigma|^2PA_dAP_1A^TA_d^TP+\tau_0|\sigma|^4PA_d^2P_2(A_d^2)^TP\\ &\quad+2\tau_0\varepsilon P<-2\delta_1\tau_0P\end{aligned}$$

so

$$\dot V(x(t))\le-2\delta_1\tau_0V(x(t)).$$

Given a fixed $\sigma\in C$ if stability is guaranteed for some τ_0 then it is guaranteed for $0\le\tau\le\tau_0$, since the delay τ multiplies only positive (semi)definite terms, hence the inequality (18) is satisfied for all smaller values, completing the proof.

It should be noted that stability results of this section are based on the transformed model (19), which involves additional dynamics [25], hence are only sufficient for stability of Eq. (13). The stability conditions of Theorems 2 and 3 are therefore inherently conservative, as they account also for dynamics not present in the original single-delay Eq. (13). Moreover, apart from additional dynamics stemming from Eq. (19) the use of Razumikhin stability results adds to conservatism. For retarded functional differential equations Lyapunov–Krasovskii results give

necessary and sufficient conditions for stability [25]. The necessity is afforded by a fairly general structure of Lyapunov–Krasovskii functional, as compared to relatively simple Lyapunov–Razumikhin functions. Generally, level of conservativeness and convergence rate estimates depend on the precise form of the Lyapunov–Krasovskii functional [25]. In order to establish a simple connection to delay-free results [12,13], this paper employs Lyapunov–Razumikhin functions rather than Krasovskii functionals. Gained simplicity is paid by conservative nature of results. For large delays Razumikhin sufficient conditions, however, come close to being necessary as well [36].

The following corollary presents a connection between Theorem 3 and properties of an asymptotically stable system in delay-free case.

Corollary 1. Assume asymptotic stability of system (13) in the delay-free case, $\tau = 0$, characterized by the Lyapunov inequality

$$(A + \sigma A_d)^{\dagger} P + P(A + \sigma A_d) \leq -Q, \tag{23}$$

where $Q = Q^T > 0$. Choose symmetric positive definite matrices $P_1^{-1} < P, P_2^{-1} < P$, with $P = P^T > 0$ a solution of Eq. (23). Then the condition for asymptotic stability (18) is certainly satisfied if

$$-Q + \tau_0 |\sigma|^2 P A_d A P_1 A^T A_d^T P + \tau_0 |\sigma|^4 P A_d^2 P_2 (A_d^2)^T P + 2\tau_0 P < 0. \tag{24}$$

This guarantees asymptotic stability for delays less than the delay margin

$$\tau_0 \leq \| Q^{-T/2} \left[|\sigma|^2 P A_d A P_1 A^T A_d^T P + |\sigma|^4 P A_d^2 P_2 (A_d^2)^T P + 2P \right] Q^{-1/2} \|^{-1}. \tag{25}$$

Proof. The first condition of Theorem 3 is satisfied with the choice $P_1^{-1} < P$, $P_2^{-1} < P$. Then it follows that the second condition of Theorem 3

$$(A + \sigma A_d)^{\dagger} P + P(A + \sigma A_d) + \tau_0 |\sigma|^2 P A_d A P_1 A^T A_d^T P + \tau_0 |\sigma|^4 P A_d^2 P_2 (A_d^2)^T P + 2\tau_0 P < 0$$

is satisfied if

$$-Q + \tau_0 |\sigma|^2 P A_d A P_1 A^T A_d^T P + \tau_0 |\sigma|^4 P A_d^2 P_2 (A_d^2)^T P + 2\tau_0 P < 0.$$

This is surely so if one has

$$\tau_0 Q^{-T/2} \left[|\sigma|^2 P A_d A P_1 A^T A_d^T P + |\sigma|^4 P A_d^2 P_2 (A_d^2)^T P + 2P \right] Q^{-1/2} < I,$$

meaning

$$\tau_0 \| Q^{-T/2} \left[|\sigma|^2 P A_d A P_1 A^T A_d^T P + |\sigma|^4 P A_d^2 P_2 (A_d^2)^T P + 2P \right] Q^{-1/2} \| < 1,$$

whence the condition (25) on the delay follows, completing the proof.

The stability conclusions depend both on σ and τ. Relation (23) defines a region in the complex plane, a subset of a synchronizing region, when delays are absent. In that case the stability margin given by $Q > 0$ allows for stability under delays. The delay margin bound (25) implicitly provides an estimate of the delay-dependent synchronizing region $S_c(\tau \leq \tau_0)$. Note also, that since Theorem 3 and Corollary 1 guarantee asymptotic stability for all delays τ less than the delay margin τ_0, the delay-dependent synchronizing regions estimated by those stability

results satisfy the inclusion property

$$S_c(\tau_2)\subseteq S_c(\tau_1) \text{ for } \tau_1\le\tau_2. \tag{26}$$

Taking $\tau_1=0$ gives the delay-free synchronizing region which contains all delay-dependent ones $S_c(\tau>0)$ and is in that sense the largest.

Remark 1. In Corollary 1 one needs to choose matrices $P_1^{-1}<P$, $P_2^{-1}<P$. The delay-dependent synchronizing region estimate depends on those matrices, and there is a possibility of optimizing this choice, as mentioned in [21]. However, a more straightforward choice can be made. Having matrix P as a solution to the Lyapunov inequality (23), one can choose $P_1=\beta_1P^{-1}$, $P_2=\beta_2P^{-1}$, with $\beta_{1,2}>1$. Then the delay margin bound (25) becomes

$$\tau_0\le\|Q^{-T/2}\left[\beta_1|\sigma|^2PA_dAP^{-1}A^TA_d^TP+\beta_2|\sigma|^4PA_d^2P^{-1}(A_d^2)^TP+2P\right]Q^{-1/2}\|^{-1}$$

5. Cooperative control design for synchronization under delays

This section applies results of Section 4 to the original problem of synchronization for multi-agents systems on directed communication graphs with uniform control signal delay. Conclusions presented below extend results of [3,17], to LTI agents on directed graphs, and results of [12,13] to the case of a uniform delay in controls. Design methodology for the cooperative feedback control is proposed, guaranteeing synchronization with a delay margin.

With guaranteed delay-dependent synchronizing region for a given delay margin, all the scaled graph matrix eigenvalues must be in that synchronizing region. On the other hand, knowing the scaled graph matrix eigenvalues one can find an upper bound on the delay margin in the system. Corollary 1 introduces a bound on the delay margin which is a decreasing function of the modulus of σ, whence one expects a bounded delay-dependent synchronizing region. Bounded synchronizing region restricts the graph topology in a way qualitatively similar to discrete-time synchronization case [15]. This property is also similar to a tradeoff between rate of convergence to consensus and robustness to delays found in single-integrator agents on undirected graphs, first mentioned in [3]. The distributed feedback design proceeds by choosing first the feedback gain matrix K, which determines the delay-dependent synchronizing region, then the coupling gain $c>0$ is chosen such that it scales all the graph matrix eigenvalues into it.

5.1. An estimate of the synchronizing region for local feedback gain stabilizing a single-agent system with a nonzero delay margin

The optimal Riccati feedback gain stabilizes the single agent system without delays and allows for synchronization under fairly mild conditions [12,13]. This approach is extended here to agents with delay in a sense that a single-agent system is stabilized with a delay margin τ_0, and then a guaranteed delay dependent synchronizing region $S_c(\tau)$ is found for that particular stabilizing feedback.

Theorem 4. Let (A,B) be stabilizable. Choose the local feedback gain as

$$K = R^{-1}B^TP, \tag{27}$$

with $P>0$ a real symmetric solution of the algebraic matrix equation

$$A^TP + PA + Q - PBR^{-1}B^TP + \tau_0(PA_dAP_1A^TA_d^TP + PA_d^2P_2(A_d^2)^TP + 2P) = 0 \tag{28}$$

where $A_d = -BK = -BR^{-1}B^TP$, $Q>0$ and $P_1>0$, $P_2>0$ symmetric matrices chosen to satisfy

$$P_1^{-1}<P,\ \ P_2^{-1}<P.$$

Then the single-agent closed loop system is asymptotically stable with the delay margin τ_0 and the guaranteed synchronizing region for the delay margin τ is determined by inequalities

$$\mathrm{Re}\sigma > 1/2 \tag{29}$$

$$\begin{aligned}&(1-2\mathrm{Re}\sigma)Q^{-T/2}PBR^{-1}B^TPQ^{-1/2}\\ &\quad + Q^{-T/2}((\tau|\sigma|^2-\tau_0)PA_dAP_1A^TA_d^TP + (\tau|\sigma|^4-\tau_0)PA_d^2P_2(A_d^2)^TP\\ &\quad + 2(\tau-\tau_0)P)Q^{-1/2} < I\end{aligned} \tag{30}$$

Proof. If the real positive definite symmetric solution of Eq. (28) exists, with the feedback gain (27), the closed loop system matrix $A + A_d = A - BR^{-1}B^TP$ satisfies

$$\begin{aligned}&(A-BR^{-1}B^TP)^TP + P(A-BR^{-1}B^TP)\\ &\quad + \tau_0(PA_dAP_1A^TA_d^TP + PA_d^2P_2(A_d^2)^TP + 2P) = -Q - PBR^{-1}B^TP < 0,\end{aligned}$$

guaranteeing stability of the closed loop single agent system ($\sigma = 1$) with the delay margin τ_0. The synchronizing region for the delay margin τ, generally different than τ_0, follows by Theorem 3 as

$$\begin{aligned}&(A-\sigma BR^{-1}B^TP)^{\dagger}P + P(A-\sigma BR^{-1}B^TP) + \tau(|\sigma|^2PA_dAP_1A^TA_d^TP + |\sigma|^4PA_d^2P_2(A_d^2)^TP + 2P)\\ &= A^TP + PA - 2\mathrm{Re}\sigma(PBR^{-1}B^TP) + \tau(|\sigma|^2PA_dAP_1A^TA_d^TP + |\sigma|^4PA_d^2P_2(A_d^2)^TP + 2P)\\ &= -Q + (1-2\mathrm{Re}\sigma)PBR^{-1}B^TP - \tau_0(PA_dAP_1A^TA_d^TP + PA_d^2P_2(A_d^2)^TP + 2P)\\ &\quad + \tau(|\sigma|^2PA_dAP_1A^TA_d^TP + |\sigma|^4PA_d^2P_2(A_d^2)^TP + 2P)\\ &= -Q + (1-2\mathrm{Re}\sigma)PBR^{-1}B^TP + ((\tau|\sigma|^2-\tau_0)PA_dAP_1A^TA_d^TP\\ &\quad + (\tau|\sigma|^4-\tau_0)PA_d^2P_2(A_d^2)^TP + 2(\tau-\tau_0)P)\end{aligned}$$

For stability the above matrix expression needs to be negative definite, which is equivalent to

$$\begin{aligned}&-I + (1-2\mathrm{Re}\sigma)Q^{-T/2}PBR^{-1}B^TPQ^{-1/2}\\ &+Q^{-T/2}((\tau|\sigma|^2-\tau_0)PA_dAP_1A^TA_d^TP + (\tau|\sigma|^4-\tau_0)PA_d^2P_2(A_d^2)^TP\\ &+2(\tau-\tau_0)P)Q^{-1/2} < 0.\end{aligned}$$

Condition (29) guarantees stability when delays are neglected. This concludes the proof.

Note that a real positive definite solution to Eq. (28) surely exists under the conditions of the theorem for the delay margin τ_0 sufficiently small, as it equals the solution of the ARE with the Q

matrix appropriately redefined by subtracting the resulting term multiplied by τ_0. For sufficiently small τ_0 the Q matrix thus redefined is still positive definite.

5.2. An estimate of the delay-dependent synchronizing region for Riccati local feedback gain

The following result relates stability properties of the Riccati local feedback [12,13] in the delay-free case to its delay-dependent synchronizing region. This result is a special case of Theorem 4 for a design choice $\tau_0 = 0$.

Corollary 2. Let (A, B) be stabilizable. Choose the local feedback gain as

$$K = R^{-1}B^T P, \tag{31}$$

with $P>0$ a real symmetric solution of the algebraic Riccati equation

$$A^T P + PA + Q - PBR^{-1}B^T P = 0, \tag{32}$$

where $Q = Q^T > 0$. Choose symmetric matrices $P_1 > 0$, $P_2 > 0$ satisfying $P_1^{-1} < P$, $P_2^{-1} < P$. Then the guaranteed delay-dependent synchronizing region $S_c(\tau)$ for Eq. (13) is determined by inequalities

$$\mathrm{Re}\sigma > 1/2, \tag{33}$$

$$\begin{aligned}&(1-2\mathrm{Re}\sigma)Q^{-T/2}PBR^{-1}B^T PQ^{-1/2}\\ &\quad+\tau Q^{-T/2}\left[|\sigma|^2 PBKAP_1A^T K^T B^T P + |\sigma|^4 P(BK)^2 P_2 (K^T B^T)^2 P + 2P\right]Q^{-1/2} < I.\end{aligned} \tag{34}$$

In case of matrix B not being a square matrix of full rank, which is commonly so and certainly true for SISO systems, the delay margin bound (34) simplifies as detailed in the following corollary.

Corollary 3. In case B matrix is not a nonsingular square matrix the delay-dependent synchronizing region is determined by Eq. (33) and

$$\tau \le \|Q^{-T/2}\left[|\sigma|^2 PBKAP_1A^T K^T B^T P + |\sigma|^4 P(BK)^2 P_2 (K^T B^T)^2 P + 2P\right]Q^{-1/2}\|^{-1}. \tag{35}$$

Proof.

$$\begin{aligned}&(1-2\mathrm{Re}\sigma)Q^{-T/2}PBR^{-1}B^T PQ^{-1/2}\\ &\quad+\tau Q^{-T/2}\left[|\sigma|^2 PBKAP_1A^T K^T B^T P + |\sigma|^4 P(BK)^2 P_2 (K^T B^T)^2 P + 2P\right]Q^{-1/2} < I\\ &\tau Q^{-T/2}\left[|\sigma|^2 PBKAP_1A^T K^T B^T P + |\sigma|^4 P(BK)^2 P_2 (K^T B^T)^2 P + 2P\right]Q^{-1/2}\\ &\quad< I + (2\mathrm{Re}\sigma - 1)Q^{-T/2}PBR^{-1}B^T PQ^{-1/2}\end{aligned} \tag{36}$$

is certainly satisfied if

$$\begin{aligned}&\tau\|Q^{-T/2}\left[|\sigma|^2 PBKAP_1A^T K^T B^T P + |\sigma|^4 P(BK)^2 P_2 (K^T B^T)^2 P\right.\\ &\quad\left.+2P\right]Q^{-1/2}\| < \lambda_{min}\left[I + (2\mathrm{Re}\sigma - 1)Q^{-T/2}PBR^{-1}B^T PQ^{-1/2}\right]\\ &\tau\|Q^{-T/2}\left[|\sigma|^2 PBKAP_1A^T K^T B^T P\right.\\ &\quad\left.+|\sigma|^4 P(BK)^2 P_2 (K^T B^T)^2 P + 2P\right]Q^{-1/2}\| < 1\\ &\quad+(2\mathrm{Re}\sigma - 1)\lambda_{min}(Q^{-T/2}PBR^{-1}B^T PQ^{-1/2})\end{aligned}$$

Here the assumption $2\mathrm{Re}\sigma-1>0$ was tacitly used. This furnishes a bound on the delay margin

$$\tau<\frac{1+(2\mathrm{Re}\sigma-1)\lambda_{min}(Q^{-T/2}PBR^{-1}B^{T}PQ^{-1/2})}{\|Q^{-T/2}\left[|\sigma|^{2}PBKAP_{1}A^{T}K^{T}B^{T}P+|\sigma|^{4}P(BK)^{2}P_{2}(K^{T}B^{T})^{2}P+2P\right]Q^{-1/2}\|},$$

which implicitly determines the delay-dependent synchronizing region $S_c(\tau)$. But if $\lambda_{min}(Q^{-T/2}PBR^{-1}B^{T}PQ^{-1/2})=0$, the expression (34) simplifies to Eq. (35).

Remark 2. When the quadratic form determining stability in Eq. (36) is evaluated at the nontrivial kernel of $B^{T}PQ^{-1/2}$ Eq. (34) reduces to $\tau 2\|Q^{-T/2}PQ^{-1/2}\|<1$, which is surely satisfied under Eq. (35). Therefore condition (35) guarantees stability, albeit on the complement of $\ker(B^{T}PQ^{-1/2})$ one has a less conservative condition (34), with $\lambda_{>0\ min}$ instead of λ_{min}. Hence one has the condition

$$\tau_1=(2\|Q^{-T/2}PQ^{-1/2}\|)^{-1}$$

$$\tau_2=\frac{1+(2\mathrm{Re}\sigma-1)\lambda_{>0\ min}(Q^{-T/2}PBR^{-1}B^{T}PQ^{-1/2})}{\|Q^{-T/2}\left[|\sigma|^{2}PBKAP_{1}A^{T}K^{T}B^{T}P+|\sigma|^{4}P(BK)^{2}P_{2}(K^{T}B^{T})^{2}P+2P\right]Q^{-1/2}\|}$$

$$\tau\leq\min(\tau_1,\tau_2)$$

Both in Theorem 4 and Corollary 2 one can make the choice of matrices P_1, P_2 suggested by Remark 1, thereby simplifying the expression for the delay margin bound accordingly.

Remark 3. Theorem 4 and Corollary 2 have several important consequences. First, as $|\sigma|\to\infty$ the delay margin bound (34), guaranteeing stability for Eqs. (31) and (32), implies $\tau\to 0$. Comparing this with an unbounded right half-plane synchronizing region of the delay-free Riccati feedback [12,13] shows that to recover the unbounded right half-plane guaranteed synchronizing region the delay margin must be zero. Nonzero delay margin results in a bounded guaranteed synchronizing region. This boundedness restricts the graph matrix eigenvalues so that they can be scaled into such a region [15].

It should also be noted that Eq. (32) has a unique solution whenever (A,B) is stabilizable, $(A,Q^{1/2})$ detectable, but Eq. (28) generally does not. Stabilizability of (A,B) remains a necessary condition for existence of a stabilizing solution for Eq. (28), as feedback (27) stabilizes the system (1) without delay as well. The existence of a stabilizing solution for Eq. (28) naturally depends on τ_0.

5.3. The relation between the coupling gain and the delay margin for the Riccati feedback gain

This subsection reveals the relation between the delay occurring in the system and the value of the coupling gain. The synchronizing region determines the lower bound of the coupling gain, and that value, with the largest graph matrix eigenvalue modulus, then bounds the delay margin from above.

Theorem 5. Let the graph satisfy the connectivity condition of Lemma 2. Choose the local feedback matrix as the Riccati gain of Corollary 2. Then the multi-agent system (6) synchronizes

for the choice of

$$c \geq \frac{1}{2 \min \mathrm{Re}\lambda(L+G)}, \tag{37}$$

if the delay margin τ satisfies the condition

$$(1-2\mathrm{Re}c\lambda_j)Q^{-T/2}PBR^{-1}B^TPQ^{-1/2} + \tau Q^{-T/2}\left[|c\lambda_j|^2PBKAP_1A^TK^TB^TP + |c\lambda_j|^4P(BK)^2P_2(K^TB^T)^2P + 2P\right]Q^{-1/2} < I, \tag{38}$$

for all $c\lambda_j$.

Proof. For synchronization, according to Lemma 1, all scaled eigenvalues of the graph matrix $(L+G)$, $c\lambda_j$, must be in the synchronizing region $S_c(\tau)$. The existence of a spanning tree with at least one nonzero pinning gain connecting to a root node guarantees by Lemma 2 and conditions of Theorem 4 that $\forall j$ there exists a c

$$c \geq \frac{1}{2\mathrm{Re}\lambda_j} \Rightarrow \mathrm{Re}c\lambda_j \geq \frac{1}{2}.$$

Hence the lower bound on the coupling gain value c for synchronization in a delay-free case follows, as in [13]

$$c \geq \frac{1}{2 \min \mathrm{Re}\lambda(L+G)}.$$

The delay margin τ guaranteeing stability for the multi-agent system can be found as the largest value that satisfies the inequality

$$(1-2\mathrm{Re}\sigma)Q^{-T/2}PBR^{-1}B^TPQ^{-1/2} + \tau Q^{-T/2}\left[|\sigma|^2PBKAP_1A^TK^TB^TP + |\sigma|^4P(BK)^2P_2(K^TB^T)^2P + 2P\right]Q^{-1/2} < I,$$

for scaled eigenvalues $\sigma = c\lambda_j$, $\forall j$. With such delay margin all the systems (12) are asymptotically stable to the trivial solution, guaranteeing, by Lemma 1, the cooperative stability of the entire multi-agent system.

Remark 4. For guaranteed stability the delay in the system must satisfy the delay margin. Hence a nonzero delay τ enforces a bound on the guaranteed synchronizing region $S_c(\tau)$, which shrinks with increasing values of the delay margin, Eq. (26). In delay-free case the synchronizing region for Riccati local feedback contains the unbounded right half-plane [13]. The Riccati local feedback gain of Corollary 2, Eq. (31), is thus robust with respect to delays, guaranteeing synchronization in delay-free case as well as for sufficiently small delays. Conversely, for a fixed nonzero delay margin, as the delay-dependent synchronizing region is bounded, there is an upper bound on the coupling gain $c>0$ depending on the largest graph matrix eigenvalue modulus. Given the lower bound for the coupling gain, Eq. (37), this constrains the graph topologies that are guaranteed to allow for synchronization under that particular delay margin. Qualitatively similar relation holds also for the feedback proposed in Theorem 4 where the bound on τ is determined via Eq. (30).

The synchronizing region estimate (30) points to the fact that graph matrix eigenvalues having small real and large imaginary part, stemming from high frequency weakly damped oscillatory

modes of the single-integrator consensus system without delays [1,3], are especially detrimental to stability in presence of delays. In contrast, the graphs whose graph matrix eigenvalues have relatively larger minimal real parts and smaller maximal modulus tolerate larger delay margins.

The upper bound on the coupling gain in relation to the delay margin should be compared to the result in [1,3], for one-dimensional single-integrator agents. Note that this section presents sufficient conditions only while [3] gives necessary and sufficient conditions, albeit for a simpler system. The relation between the two conditions is expounded in Section 7.

6. Synchronization with a prescribed exponential convergence

Motivated by practical considerations where convergence rates are prescribed as a design requirement, and a convergence result in [9] for delay-free systems, this section strengthens the results of Sections 4 and 5 dealing with asymptotic stability to exponential stability. Exponential stability of time-delay systems is studied in [25,36,37,38], to name just a few. Both Krasovskii [37] and Razumikhin [36,38] sufficient conditions are known. Hence, to proceed along the lines of Section 4 one starts with the following definition.

Definition 2. Given a complex retarded functional differential Eq. (13) the delay-dependent synchronizing region for exponential stability with a prescribed convergence rate, $\alpha \in R^+$, is a subset of the complex plane C depending on the delay τ

$$S_c(\tau,\gamma) = \{\sigma \in C : Ay(t) + \sigma A_d y(t-\tau) e.s.\} \tag{39}$$

with exponential stability characterized by the prescribed convergence rate.

A sufficient condition for asymptotic stability with exponential convergence rate for RFDEs based on Razumikhin stability functions is detailed in the following theorem. Proof is given in [36].

Theorem 6. (*Lyapunov–Razumikhin exponential stability result* [36]). Let the conditions of Theorem 1 be satisfied with $\lambda\|x\|^p = \alpha(\|x\|)$ for some $\lambda > 0$, $p \in R$, $p \geq 1$, $\gamma > 0$, and

$$\frac{d}{dt}V(x(t)) \leq -\gamma V(x(t)) \text{ if } V(x(\vartheta)) < V(x(t))e^{\gamma\tau}, \ \forall \vartheta \in [t-\tau, t]. \tag{40}$$

Then the trivial solution, $x(t) \equiv 0$, is exponentially stable with the convergence rate γ/p.

Linear delay differential systems, *e.g.* Eq. (8), satisfy the spectrum-determined growth assumption [26,37]. Therefore in case of exponential stability the convergence rate is determined by the spectral abscissa. Theorem 6 applied to Eq. (8) provides a Lyapunov–Razumikhin bound on the spectral abscissa. The following result guarantees exponential stability with a prescribed convergence rate in dependence of delays for the complex Eq. (13). It is considered a stricter version of Theorem 3.

Theorem 7. (*Lyapunov–Razumikhin delay dependent exponential stability result for the complex equation*). Let the conditions of Theorem 3 be satisfied with

$$\begin{aligned}&(A+\sigma A_d)^{\dagger}P + P(A+\sigma A_d) + \tau_0|\sigma|^2 P A_d A P_1 A^T A_d^T P + \tau_0|\sigma|^4 P A_d^2 P_2 (A_d^2)^T P \\ &\quad + 2\tau_0 e^{2\gamma\tau_0} P < -\gamma P\end{aligned} \tag{41}$$

where $\gamma \in R^+$. Then, for given $\sigma \in C$, the trivial solution, $x(t) \equiv 0$, of Eq. (13) is exponentially stable for $0 \leq \tau \leq \tau_0$, with convergence rate $\gamma/2$.

Proof. Follows from Theorem 6 and the proof of Theorem 3. With the quadratic Lyapunov–Razumikhin function one has $p=2$ in Theorem 6. Provisions (40) of Theorem 6 on the interval $[t-2\tau,t]$; $V(x(\vartheta))<V(x(t))e^{2\gamma\tau}\ \forall\vartheta\in[t-2\tau,t]$, applied to the integral terms in Eq. (21), yield the inequality

$$\frac{d}{dt}V(x(t))\le x^{\dagger}(t)\big[(A+\sigma A_d)^{\dagger}P+P(A+\sigma A_d)+\tau|\sigma|^2PA_dAP_1A^TA_d^TP$$
$$+\tau|\sigma|^4PA_d^2P_2(A_d^2)^TP+2\tau e^{2\gamma\tau}P\big]x(t)$$

instead of Eq. (22). By the condition (41) of the theorem, for $0\le\tau\le\tau_0$

$$\frac{d}{dt}V(x(t))\le-\gamma V(x(t)),$$

thus, according to Theorem 6, completing the proof.

Exponential stability of the transformed model (19) with prescribed convergence rate is sufficient to guarantee the same for the original system (13).

Note that Theorems 6 and 7 reduce to Theorems 1 and 3 in the limit $\gamma\to0^+$. Result similar to Corollary 1 is obtained if, following [9], one guarantees the prescribed exponential convergence

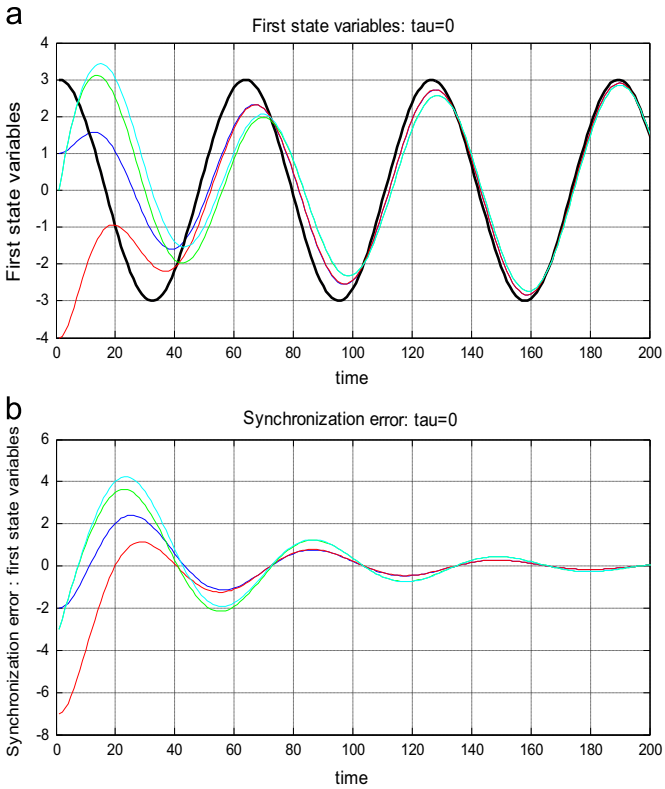

Fig. 1. (a) First state variables, $\tau=0$. (b) Synchronization error, $\tau=0$.

rate for the delay-free system

$$(A+\sigma A_d)^{\dagger}P+P(A+\sigma A_d)<-\gamma P.$$

Then $(A+\sigma A_d)^{\dagger}P+P(A+\sigma A_d)=-\gamma P-Q$, for some $Q>0$, and condition (41) of Theorem 7 is satisfied if

$$-Q+\tau_0|\sigma|^2PA_dAP_1A^TA_d^TP+\tau_0|\sigma|^4PA_d^2P_2(A_d^2)^TP+2\tau_0e^{2\gamma\tau_0}P<0, \tag{42}$$

which is certainly true given sufficiently small values of τ_0. The exact bound on the delay is not as simple as Eq. (25) due to the transcendental character of Eq. (42).

Exponential stability with a prescribed convergence rate is stronger than asymptotic stability; hence the synchronizing region satisfying the prescribed convergence rate (39) is contained in the asymptotic stability synchronizing region for the same time-delay

$$S_c(\tau,\gamma)\subseteq S_c(\tau).$$

Due to the exponential terms the exponential synchronizing region estimate (41) is strongly dependent on the values of delay τ and the prescribed convergence rate γ. As Theorem 7 shows, the inclusion property (26) with respect to decreasing delays holds naturally for the estimates of prescribed convergence rate exponential stability synchronizing region (41). Furthermore the synchronizing region for greater convergence rates γ is necessarily contained in that for smaller

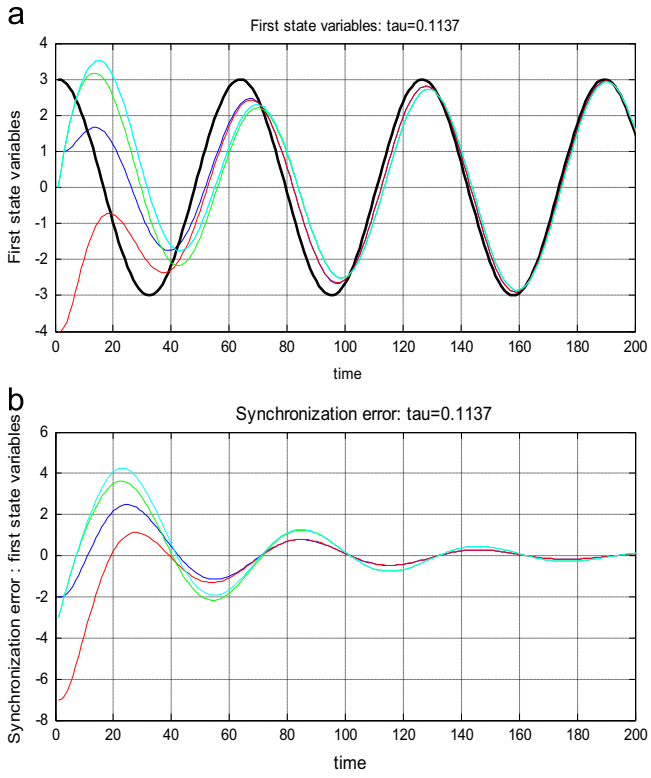

Fig. 2. (a) First state variables, $\tau=0.1137$. (b) Synchronization error, $\tau=0.1137$.

ones

$$S_c(\tau,\gamma_1)\subseteq S_c(\tau,\gamma_2) \text{ for } \gamma_1\geq\gamma_2.$$

These considerations reflect the robustness of exponential stability in dependence of delays.

Design methodology of Section 5 is applicable verbatim for synchronizing region with a prescribed exponential convergence rate, Eq. (39). One only needs to consider the algebraic matrix equation

$$A^TP+PA+Q-PBR^{-1}B^TP+\tau_0(PA_dAP_1A^TA_d^TP+PA_d^2P_2(A_d^2)^TP+2e^{2\gamma\tau_0}P)=-\gamma P$$

guaranteeing exponential stability for the single-agent system instead of asymptotic stability guaranteed by Eq. (28). Then an estimate of the synchronizing region for exponential stability with the same convergence rate γ but possibly different delays τ follows similarly as in Theorem 4 from the matrix inequality

$$-Q+(1-2\mathrm{Re}\sigma)PBR^{-1}B^TP+(\tau|\sigma|^2-\tau_0)PA_dAP_1A^TA_d^TP+(\tau|\sigma|^4-\tau_0)PA_d^2P_2(A_d^2)^TP$$
$$+2(\tau e^{2\gamma\tau}-\tau_0e^{2\gamma\tau_0})P<0$$

It should be remarked that for the delay free case, $\tau=0=\tau_0$ results of this section reduce to those reported in [9].

If all the diagonal blocks in Eq. (11), *i.e.* all the systems (12) are exponentially stable with a prescribed convergence rate, as guaranteed by the synchronizing region (39), then the original system (7) shares the same convergence property. Therefore synchronization is guaranteed with a

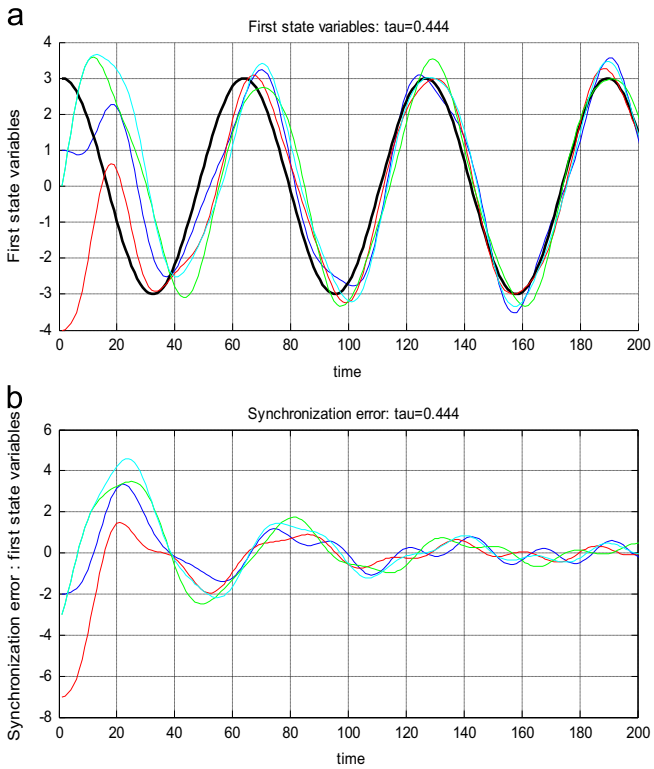

Fig. 3. (a) First state variables, $\tau=0.444$. (b) Synchronization error, $\tau=0.444$.

prescribed exponential convergence rate if all the graph matrix eigenvalues are scaled into a pertaining synchronizing region.

7. Special case of single-integrator agents on undirected graphs

General stability conditions of Section 5 are specialized here to archetypal consensus systems of one-dimensional single-integrator agents on undirected graphs [1,3,4]. For such systems necessary and sufficient conditions for stability with delays are given in [3].

Let the system be given as

$$\dot{x}_i = ax_i + bu_i,$$

with $a = 0$, $b = 1$. Furthermore, choose $Q = 1 = R$ in the Riccati Eq. (32) so that $P = 1 = K$, and $c = 1$ guarantee synchronization in the absence of delay. Then the closed loop system (5) is given as

$$\dot{x}_i(t) = -e_i(t-\tau). \tag{43}$$

This gives

$$\dot{\delta}(t) = -(L+G)\delta(t-\tau), \tag{44}$$

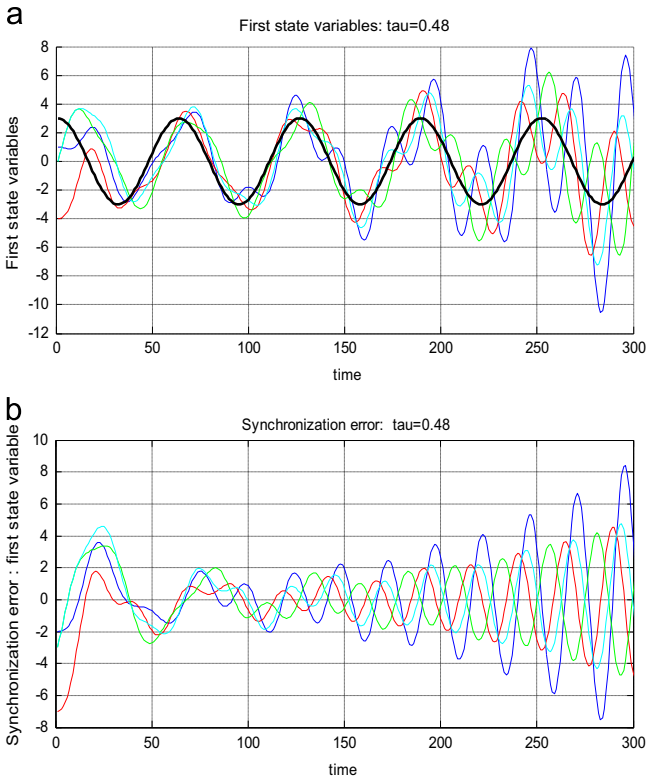

Fig. 4. (a) First state variables, $\tau = 0.48$. (b) Synchronization error, $\tau = 0.48$.

where $L+G$ is the symmetric graph matrix of the underlying undirected communication graph, which is assumed connected. For system (44) to be asymptotically stably it is necessary and sufficient that [1,3]

$$\tau < \pi/2\lambda_{max}(L+G), \tag{45}$$

The bound (34), with $P_2 = \beta_2 P^{-1}$, $\beta_2 > 1$, in this case gives

$$(1-2\lambda_j) + \tau\left[|\lambda_j|^4\beta_2 + 2\right] < 1. \tag{46}$$

It can be seen that one has

$$\tau \le \min_j \left\{2\lambda_j/(\beta_2\lambda_j^4 + 2)\right\} < \pi/2\lambda_{max}(L+G), \tag{47}$$

where one has to take $\lambda_j(L+G) > 1/2$. This can always be satisfied by considering $c(L+G)$ with an appropriate coupling gain absorbed in the graph matrix $L+G$.

The tradeoff between fast convergence to consensus and robustness to delays, alluded to in [1] by the necessary and sufficient condition (45) for single-integrator agents on undirected graphs, applies here to guaranteed synchronizing region for LTI agents on directed graph topologies by results of Sections 4 and 5.

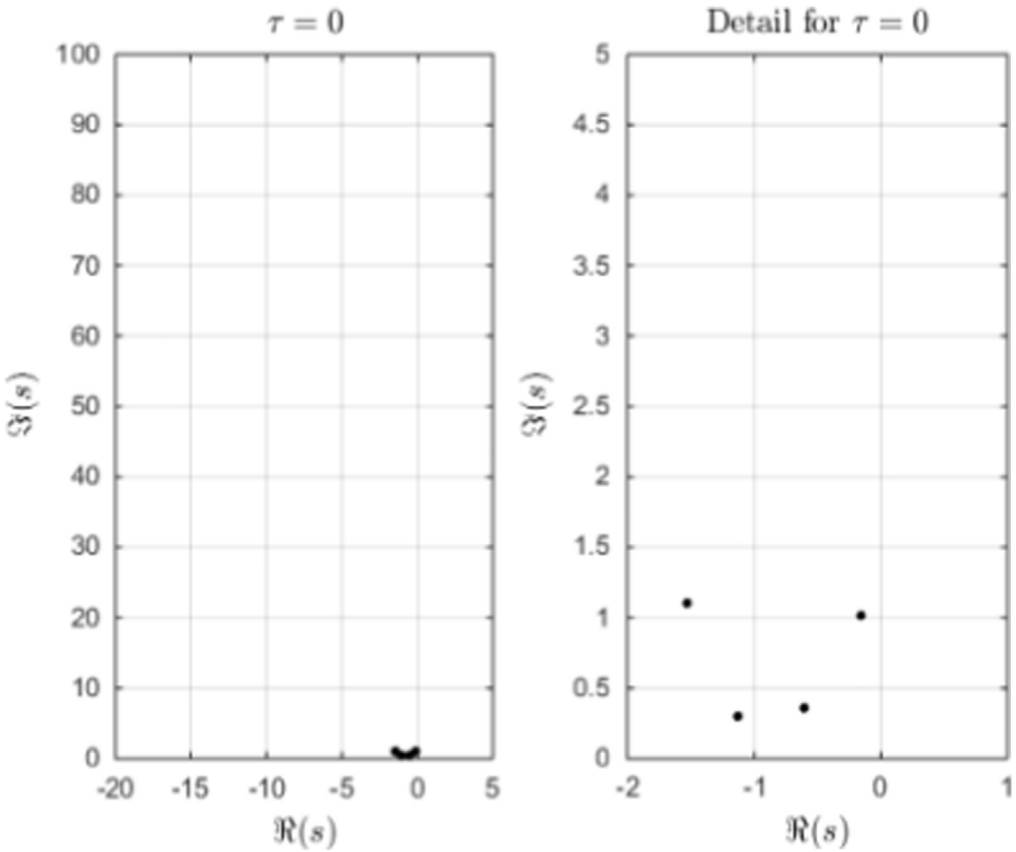

Fig. 5. Closed-loop poles, $\tau = 0$.

8. Numerical example

The considered multi-agent system consists of 4 agents having the LTI dynamics

$$\dot{x} = \begin{bmatrix} 0 & 1 \\ -1 & 0 \end{bmatrix} x + \begin{bmatrix} 0 \\ 1 \end{bmatrix} u.$$

The communication digraph topology is described by its Laplacian matrix and pinning gains

$$L = \begin{bmatrix} 2 & -1 & 0 & -1 \\ 0 & 1 & -1 & 0 \\ -1 & 0 & 1 & 0 \\ 0 & -1 & -1 & 2 \end{bmatrix}, \quad G = \mathrm{diag}(1, 1, 0, 0).$$

One has that $\lambda_{min}(L+G) = 0.3820$ and $|\lambda_{max}(L+G)| = 2.6457$. For the design choice $Q = 0.21 I_2$, $R = 1$ in the Riccati Eq. (32) the local feedback gain matrix, Eq. (31), and the coupling gain satisfying Eq. (33) follow as

$$K = \begin{bmatrix} 0.1 & 0.6403 \end{bmatrix}, c = 1.34.$$

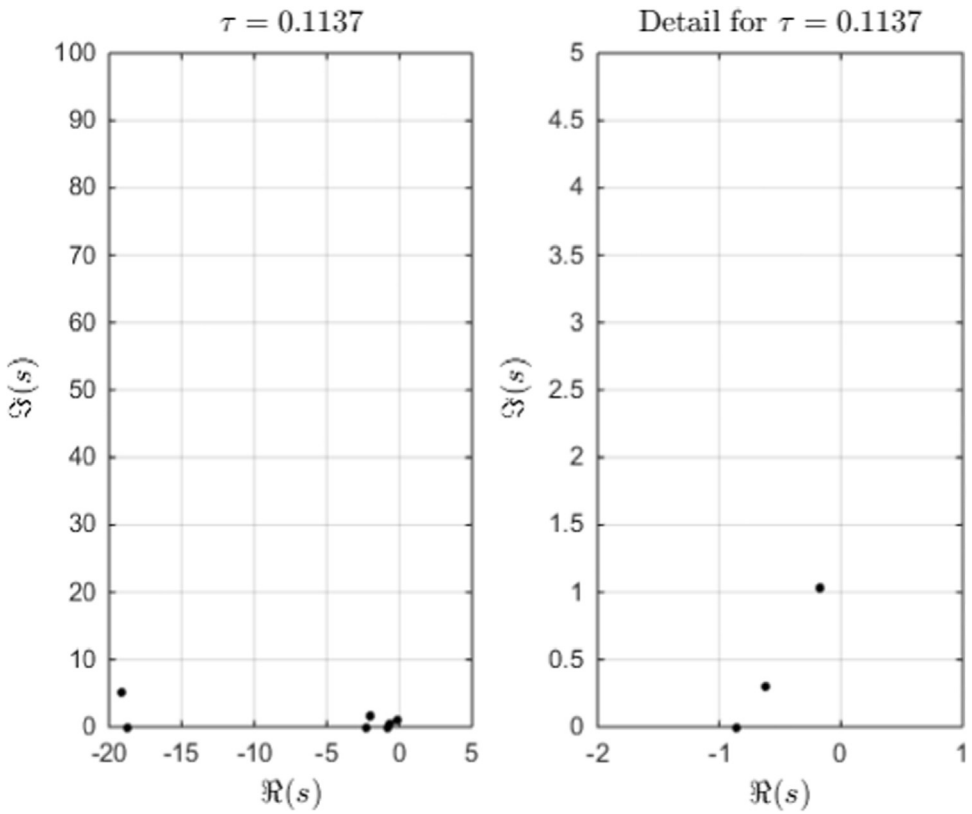

Fig. 6. Closed-loop poles, $\tau = 0.1137$.

The nonlinear matrix inequality (34) is solved for P using the standard ARE solver in Matlab applied in iterations. Given the largest scaled graph matrix eigenvalue magnitude, iterative procedure is applied for increasing delay values as long as admissible solutions are being obtained, yielding a delay margin estimate. The found solution equals

$$P = \begin{bmatrix} 0.7043 & 0.1 \\ 0.1 & 0.6403 \end{bmatrix},$$

and the choice $P_1 = P_2 = 1.01P^{-1}$ is made. The multi-agent system is then guaranteed to tolerate delays smaller than the delay margin $\tau_0 = 0.1137$. The exact delay margin for this cooperative feedback, obtained by spectral domain analysis of the entire system, using QPmR algorithm [31] is found to be $\tau = 0.4445$.

Time dependence of first state variable for 4 agents, and the leader, is depicted on the following figures for different delays. Pertinent synchronization error dynamics are also given. One should note that greater delays give slower convergence and poorer transient. Figs. 1–3a and b show stable synchronization dynamics, while Fig. 4a and b shows unstable dynamics for the delay of 0.48.

The poles of respective closed-loop synchronization error systems, Eq. (7), for above considered cases are depicted in Figs. 5–8, showing the upper half-plane only. Poles are calculated using QPmR algorithm [31].

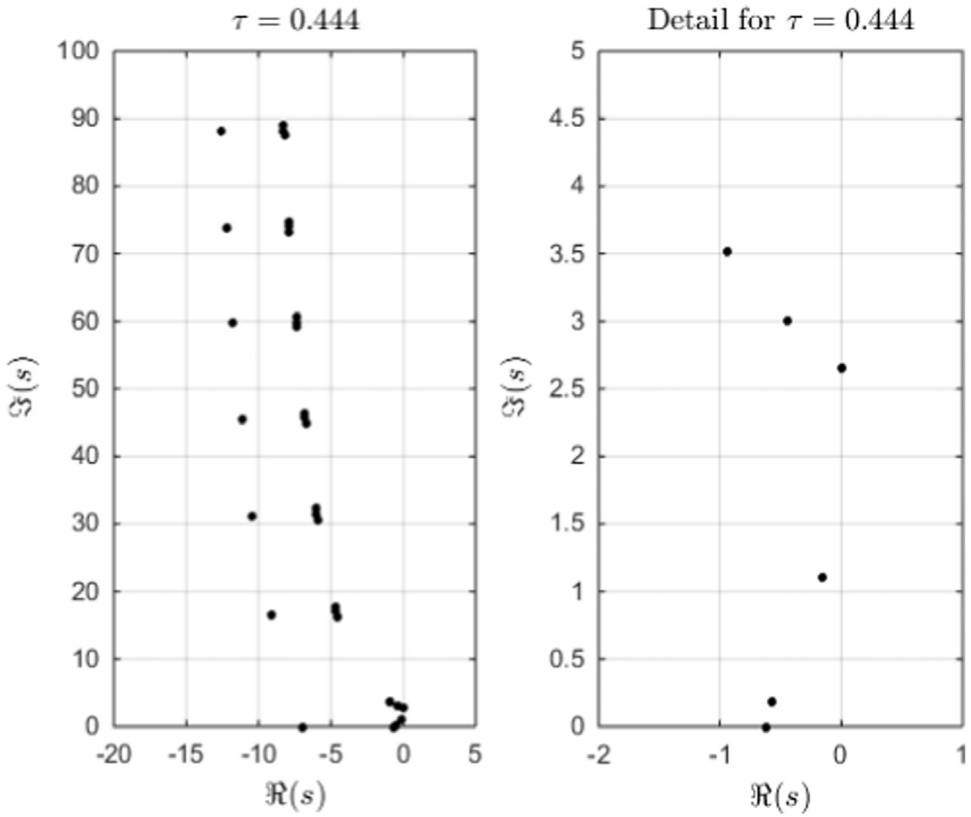

Fig. 7. Closed-loop poles, $\tau = 0.444$.

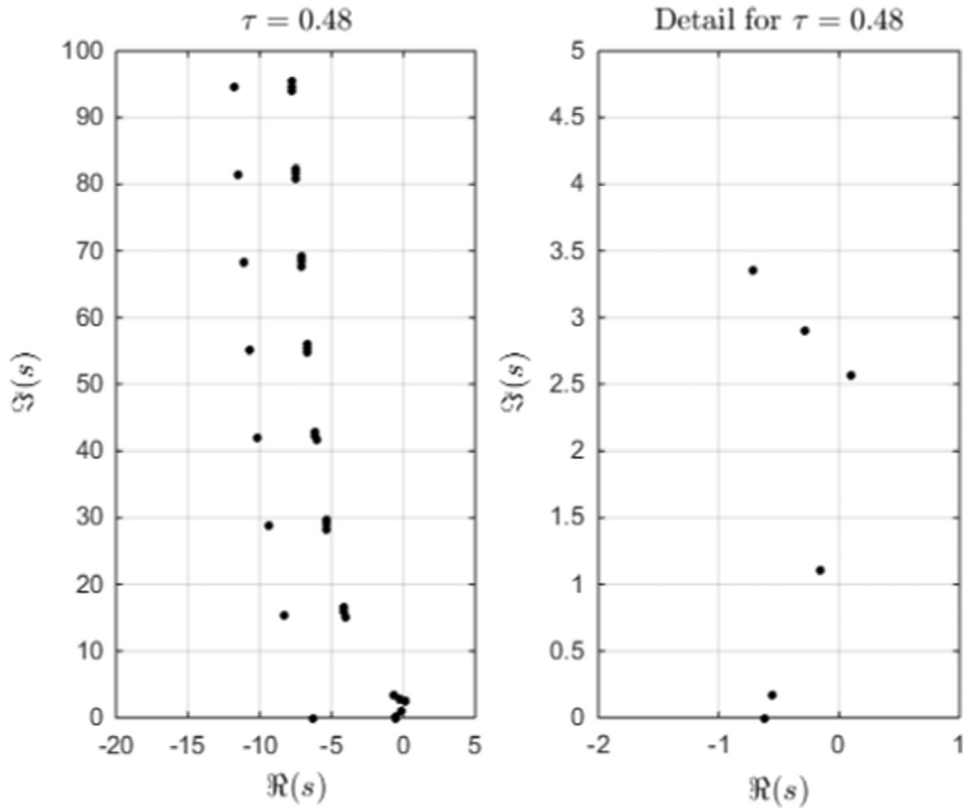

Fig. 8. Closed loop poles, $\tau = 0.48$.

9. Concluding remarks

This paper investigates synchronization of multi-agent systems with constant uniform control delays. Agents are described by general LTI dynamics with delayed controls, which constitute RFDEs. Classical stability results for RFDEs are applied with modification to complex RFDE to guarantee a delay-dependent synchronizing region. The guaranteed synchronizing region provides sufficient conditions for multi-agent system synchronization in the presence of delays. Furthermore, the synchronizing region approach decouples the single-agent properties from the underlying communication graph topology, dealing with graph effects by robust stabilization. Following those lines a design procedure is proposed based on algebraic matrix equations, guaranteeing cooperative stability. The guaranteed delay-dependent synchronizing region for local feedback gains is found to be bounded in dependence on the delay margin, restricting the values of admissible coupling gains. The bounded synchronizing region for delayed cooperative feedback is to be contrasted with an unbounded synchronizing region of the delay-free case, and compared to results known from the literature on a tradeoff between the rate of convergence to consensus and robustness to delays. Stronger results guaranteeing exponential cooperative

stability with a prescribed convergence rate are presented as a special case. Numerical example validates the proposed design.

References

[1] R. Olfati-Saber, J.A. Fax, R.M. Murray, Consensus and cooperation in networked multi-agent systems, Proc. IEEE 95 (1) (2007) 215–233, http://dx.doi.org/10.1109/JPROC.2006.887293.

[2] J. Tsitsiklis, Problems in Decentralized Decision Making and Computation, Dept. Elect. Eng. and Comput. Sci., MIT, Cambridge, MA, 1984 (Ph.D. dissertation).

[3] R. Olfati-Saber, R.M. Murray, Consensus problems in networks of agents with switching topology and time-delays, IEEE Trans. Autom. Control 49 (9) (2004) 1520–1533, http://dx.doi.org/10.1109/TAC.2004.834113.

[4] A. Jadbabaie, J. Lin, A. Morse, Coordination of groups of mobile autonomous agents using nearest neighbour rules, IEEE Trans. Autom. Control 48 (6) (2003) 988–1001, http://dx.doi.org/10.1109/TAC.2003.812781.

[5] R. Olfati-Saber, R.M. Murray, Consensus protocols for networks of dynamic agents, in: Proceedings of American Control Conference, 2003, pp. 951–956.

[6] J. Fax, R.M. Murray, Information flow and cooperative control of vehicle formations, IEEE Trans. Autom. Control 49 (9) (2004) 1465–1476, http://dx.doi.org/10.1109/TAC.2004.834433.

[7] X.F. Wang, G. Chen, Pinning control of scale free dynamical networks, Physica A 310 (2002) 521–531.

[8] Z. Li, Z. Duan, G. Chen, L. Huang, Consensus of multiagent systems and synchronization of complex networks: a unified viewpoint, IEEE Trans. Circuits Syst. I: Regul. Pap. 57 (1) (2010) 213–224, http://dx.doi.org/10.1109/TCSI.2009.2023937.

[9] Z. Li, Z. Duan, G. Chen, Dynamic consensus of linear multi-agent systems, IET Control Theory Appl. 5 (1) (2011) 19–28, http://dx.doi.org/10.1049/iet-cta.2009.0466.

[10] L.M. Pecora, T.L. Carroll, Master stability functions for synchronized coupled systems, Phys. Rev. Lett. 80 (10) (1998) 2109–2112.

[11] Z. Duan, G. Chen, L. Huang, Disconnected synchronized regions of complex dynamical networks, IEEE Trans. Autom. Control 54 (4) (2009) 845–849, http://dx.doi.org/10.1109/TAC.2008.2009690.

[12] S.E. Tuna, LQR-based coupling gain for synchronization of linear systems, arXiv:0801.3390v1 [math.OC], 2008.

[13] H. Zhang, F.L. Lewis, Optimal design for synchronization of cooperative systems: state feedback, observer and output feedback, IEEE Trans. Autom. Control 56 (8) (2011) 1948–1953, http://dx.doi.org/10.1109/TAC.2011.2139510.

[14] Y. Hong, X. Wang, Z. Jiang, Multi-agent coordination with general linear models: a distributed output regulation approach, in: 8th IEEE International Conference on Control and Automation (ICCA), 2010, pp. 137–142, 10.1109/ICCA.2010.5524157.

[15] K. Hengster-Movric, Y. Keyou, F.L. Lewis, L. Xie, Synchronization of discrete-time multi-agent systems on graphs using Riccati design, Automatica 49 (2) (2013) 414–423, http://dx.doi.org/10.1016/j.automatica.2012.11.038.

[16] C. Yong-Yan, Z. Lin, H. Tingshu, Stability analysis of linear time-delay systems subject to input saturation, IEEE Trans. Circuits Syst.—I: Fundam. Theory Appl. 49 (2) (2002) 233–240, http://dx.doi.org/10.1109/81.983870.

[17] R. Sipahi, W. Qiao, Responsible eigenvalue concept for the stability of a class of single-delay consensus dynamics with fixed topology, IET Control Theory Appl. 5 (4) (2011) 622–629, http://dx.doi.org/10.1049/iet-cta.2010.0202.

[18] E. Fridman, New Lyapunov–Krasovskii functionals for stability of linear retarded and neutral type systems, Syst. Control Lett. 43 (2001) 309–319.

[19] C.E., De Souza, L., Xi, Delay dependent stability of linear time delay systems: an LMI approach, in: Proceedings of the 3rd IEEE Mediterranean Symposium on New Directions in Control and Automation, Limassol, Cyprus, 1995.

[20] W. Kinzel, A. Englert, G. Reents, M. Zigzag, I. Kanter, Synchronization of networks of chaotic units with time-delayed couplings, Phys. Rev. E 79 (2009) 056207, http://dx.doi.org/10.1103/PhysRevE.79.056207.

[21] S.-I. Niculescu, A.T. Neto, J.-M. Dion, L. Dugard, Delay-dependent stability of linear systems with delayed state: an LMI approach, in: Proceedings of 34th Conference on Decision & Control New Orleans, LA, 1995, pp. 1495–1496.

[22] S.-I. Niculescu, C.E. de Souza, L. Dugard, J.-M. Dion, Robust exponential stability of uncertain systems with time-varying delays, IEEE Trans. Autom. Control 43 (5) (1998) 743–748, http://dx.doi.org/10.1109/9.668851.

[24] Jack K. Hale Applied Mathematical Sciences, Introduction to Functional Differential Equations, 99, Springer, 1993.

[25] Kequin Gu, Vladimir L. Kharitonov, Chen Jie, Stability of Time-Delay Systems, Birkhauser, Boston, 2002.

[26] Zhihua Qu, Cooperative Control of Dynamical Systems, Springer, 2008.

[27] J. Zhang, C.R. Knospe, P. Tsiotras, Stability of linear time-delay systems: a delay-dependent criterion with a tight conservatism bound, Proc. Am. Control Conf. 2 (2000) 1458–1462, http://dx.doi.org/10.1109/ACC.2000.876743.

[28] H.G. Tanner, D.K. Christodoulakis, State synchronization in local-interaction networks is robust with respect to time delays, in: Proceedings of the 2005 and 2005 European Control Conference; CDC-ECC '05; 44th IEEE Conference on Decision and Control, 12-15 Dec. 2005, pp. 4945–4950, 10.1109/CDC.2005.1582945.
[29] Q. Jia, W.K.S. Tang, W.A. Halang, Leader following of nonlinear agents with switching connective network and coupling delay, IEEE Trans. Circuits Syst.—I 58 (10) (2011) 2508–2519, http://dx.doi.org/10.1109/TCSI.2011.2131230.
[30] U. Münz, A. Papachristodoulou, F. Allgöwer, Delay robustness in non-identical multi-agent systems, IEEE Trans. Autom. Control 57 (6) (2012) 1597–1603, http://dx.doi.org/10.1109/TAC.2011.2178336.
[31] T. Vyhlídal, P. Zítek, QPmR—Quasi-polynomial root-finder: algorithm update and examples, Adv. Delays Dyn. 1 (2014) 299–312, http://dx.doi.org/10.1007/978-3-319-01695-5_22.
[32] Luo Yi-ping, Zhou Bi-feng, Guaranteed cost synchronization of complex network systems with delay, Asian J. Control 17 (4) (2015) 1–11, http://dx.doi.org/10.1002/asjc.992.
[33] Wenwu Yu, Jinde Cao, Jinhu Lü, Global synchronization of linearly hybrid coupled networks with time-varying delay, SIAM J. Appl. Dyn. Syst. 7 (1) (2008) 108–133, http://dx.doi.org/10.1137/070679090.
[34] H.R. Karimi, Robust delay-dependent H_inf control of uncertain time-delay systems with mixed neutral, discrete and distributed time-delays and Markovian switching parameters, IEEE Trans. Circuits Syst. I 58 (8) (2011) 1910–1923, http://dx.doi.org/10.1109/tcsi.2011.2106090.
[35] H.R. Karimi, M. Zapateiro, N. Luo, Adaptive synchronization of master-slave systems with mixed neutral and discrete time-delays and nonlinear perturbations, Asian J. Control 14 (1) (2012) 251–257.
[36] B. Xu, Stability of retarded dynamical systems: a Lyapunov function approach, J. Math. Anal. Appl. 253 (2001) 590–615.
[37] V.L. Kharitonov, D. Hinrichsen, Exponential estimates for time delay systems, Syst. Control Lett. 53 (2004) 395–405.
[38] S. Xi-Ming, G.M. Dimitrovski, J. Zhao, W. Wang, Exponential stability for switched delay systems based on average dwell time technique and Lyapunov function method, in: Proceedings of the 2006 American Control Conference, Minneapolis, Minnesota, USA, June 14–16, 2006, pp. 1539–1543.

4. H_∞-OUTPUT REGULATION OF LINEAR HETEROGENEOUS MULTIAGENT SYSTEMS OVER SWITCHING GRAPHS

Farnaz A. Yaghmaie, Kristian Hengster Movric, Frank L. Lewis, Rong Su, Michael Sebek**, H_∞-output regulation of linear heterogeneous multiagent systems over switching graphs**, *International Journal of Robust and Nonlinear Control* 28 (13), pp. 3852-3870, 2018

This paper published in the Wiley's *International Journal of Robust and Nonlinear Control* (IF: 3.856), in 2018, considers a more general class of multi-agent systems, namely those consisting of heterogeneous agents, which do not admit a treatment *via* synchronizing region methods. Furthermore, the canonical distributed control problem appropriate for such multi-agent systems is output synchronization instead of state synchronization. Following the seminal 2009 paper by Wieland, Sepulchre, Allgower, the Internal Model Principle is necessary and sufficient for achieving this goal. However, the Internal Model Principle further hints at a general geometrical structure of heterogeneous agents that may synchronize over general outputs. This insight is used in control design *via* LMIs for such generalized agents to guarantee an output-synchronization L_2 bound in case of unmodelled disturbances acting on the system. These results are perfectly applicable in case of modelled disturbances as well, combining complementary geometrical requirements on single-agent structure.

This chapter analyzes H_∞ output regulation of linear heterogeneous multi-agent systems. The agents are subject to modeled and unmodeled disturbances and communicate over a switching graph. A sufficient condition that guarantees H_∞ output regulation is derived for the mentioned setup. This sufficient condition places requirements on both the single-agent systems and the switching graph. The requirement on the single-agent systems is an H_∞ -criterion which should be satisfied by a proper design of the controller. Meanwhile, the switching graph needs to be maximally connected. Moreover, an upper bound is derived for the overall L_2-gain of the output synchronization error with respect to the unmodeled disturbances over a fixed communication graph. Technical developments are illustrated by a simulation example.

INTERNATIONAL JOURNAL OF ROBUST AND NONLINEAR CONTROL
Int. J. Robust. Nonlinear Control 2018; **00**:1–**??**
Published online in Wiley InterScience (www.interscience.wiley.com). DOI: 10.1002/rnc

H_∞ Output Regulation of Linear Heterogeneous Multi-agent Systems over Switching Graphs

Farnaz Adib Yaghmaie [1], Kristian Hengster Movric [2], Frank L. Lewis [3], Rong Su [1], Michael Sebek [2] ,

[1] *School of Electrical & Electronic Engineering, Nanyang Technological University, Singapore,*
[2] *Department of Control Engineering, Faculty of Electrical Engineering, Czech Technical University in Prague, Prague, Czech.*
[3] *University of Texas at Arlington Research Institute, The University of Texas at Arlington, Texas, USA and Qian Ren Consulting Professor, Northeastern University, Shenyang 110036, China.*

SUMMARY

In this paper we analyze H_∞ output regulation of linear heterogeneous multi-agent systems. The agents are subject to modeled and unmodeled disturbances and communicate over a switching graph. We derive a sufficient condition that guarantees H_∞ output regulation for the mentioned setup. This sufficient condition places requirements on both the single-agent systems and the switching graph. The requirement on the single-agent systems is an H_∞-criterion which should be satisfied by a proper design of the controller. Meanwhile, the switching graph needs to be maximally connected. Moreover, we derive an upper bound for the overall $\mathcal{L}_2$-gain of the output synchronization error with respect to the unmodeled disturbances over a fixed communication graph. We illustrate our technical developments by a simulation example. Copyright © 2018 John Wiley & Sons, Ltd.

Received ...

1. INTRODUCTION

Output regulation studies control design schemes for a dynamic system such that the output of the system tracks a reference trajectory while rejecting the effect of disturbances with known models [1, 2]. Usually, the dynamics of the reference trajectory and the disturbance model are combined into a single dynamic model named *exo-system* in the literature [1, 2]. Recently, output regulation problem has been studied in multi-agent systems where distributed controllers are designed such that the outputs of all agents track a common reference trajectory, while the information of the reference is directly available only to a small group of agents [3]-[4].

One can solve such output regulation problem for linear heterogeneous multi-agent systems by using the *Internal Model Principle (IMP)*. One possible solution is to incorporate a *p-copy* of the internal model of the exo-system, where p is the dimension of the output, to achieve output synchronization to the exo-system's output [5, 6, 7, 8, 9]. This idea is used in [5, 6, 7] to study output regulation of linear heterogeneous agents communicating over an acyclic graph. Also, it is used in [10] to study output regulation of linear, yet homogeneous, agents over a general graph. The limiting assumptions of the acyclic graph and the homogeneity of the agents are removed in [8, 9] which suggest an H_∞-criterion to guarantee output regulation of linear heterogeneous agents over

*Correspondence to: Farnaz Adib Yaghmaie, School of Electrical & Electronic Engineering, 50 Nanyang Avenue, Singapore 639798. Email: farnaz001@e.ntu.edu.sg. Phone: +65 6790-6042. Fax: +65 6793-3318.

a general graph. In [4], it is shown that the IMP is necessary and sufficient for output regulation of linear heterogeneous agents communicating over a uniformly connected time-varying graph. The properties of passive systems are used in [3] to prove that the IMP is necessary and sufficient for output regulation of linear heterogeneous passive agents.

In the aforementioned results, either it is assumed that the agents are not subject to any disturbances at all [4, 6, 7], or only modeled disturbances are considered [5, 8, 9]. However, in practice, the agents are subject to both modeled and *unmodeled* disturbances where the dynamics of unmodeled disturbance is unknown. Because of unmodeled disturbances, the IMP alone cannot be used for disturbance rejection and H_∞ control methods are required. A significant part of the research on H_∞ control for multi-agent systems refers to H_∞ state synchronization of homogeneous agents using state-feedback [11, 12] or output-feedback [13]. In fact, considering homogeneous agents, one can use a similarity transformation to bring the overall system of all agents into a block diagonal/triangular form which simplifies the analysis of H_∞ control [11, 12, 13]. Such a transformation is not applicable to systems of heterogeneous agents.

In this paper, we study the problem of H_∞ output regulation of linear heterogeneous agents over switching graphs, where the agents are subject to both modeled and unmodeled disturbances. This problem is challenging for two reasons. The first reason is related to the heterogeneity of the agents. Due to the heterogeneity of agents, we cannot use the similarity transformation as it is used in [11, 12, 13] to bring the overall system into a block diagonal/triangular form. We emphasize that this approach significantly simplifies the analysis of H_∞ control for homogeneous agents. The second reason is related to the switching nature of the graph. Considering switching graphs, one needs to prove $\mathcal{L}_2$-stability for a linear system with switching dynamics which is not simply equivalent to closed-loop stability. Indeed, one needs to obtain a condition to guarantee $\mathcal{L}_2$-stability. Comparing with few results on H_∞ output regulation of linear heterogeneous agents [14, 15, 16], the communication graph in [14, 15] is fixed and the switching graph in [16] can only change over a fixed set of topologies containing spanning trees.

This paper has two main contributions. Firstly, we consider a group of heterogeneous agents in contrast to the homogeneous agents considered in [11, 12, 13]. We assume that the agents are subject to both modeled and unmodeled disturbances and aim to achieve H_∞ output regulation in comparison with [4, 9, 8] which do not consider unmodeled disturbances. Secondly, we allow the agents to communicate over a general class of switching graphs. In comparison, [14, 15] do not consider switching graphs and the switching graphs in [16] can change only over a set of topologies containing spanning trees. We do not need those assumptions in our paper. We propose to achieve these two objectives using the simplest form of the controller which is a static distributed output-feedback controller in a general framework without requiring limiting assumptions like acyclic graph [5, 6, 7], homogeneity [10, 11, 12] or passivity of the agents [3].

The rest of the paper is organized as follows: Section 2 discusses notation conventions and reviews preliminaries. Section 3 defines the H_∞ output regulation problem and brings the necessary assumptions. Section 4 studies H_∞ output regulation over fixed graphs and computes an upper bound on the overall $\mathcal{L}_2$-gain of the output synchronization error with respect to unmodeled disturbances. Section 5 studies H_∞ output regulation over switching graphs. Section 6 contains a simulation example and Section 7 concludes the paper.

2. PRELIMINARIES

2.1. Notation

The following notation will be used throughout this paper. Let $\mathbb{R}^{n\times m}$ be the set of $n \times m$ real matrices. I_n denotes the identity matrix of dimension $n \times n$. We drop the subscript and denote the identity matrix with I when there is no ambiguity. $\mathbf{1}_N$ is an N column vector of 1 and $\mathbf{0}$ denotes a matrix of zeros with compatible dimensions. The Kronecker product of two matrices A and B is denoted by $A \otimes B$. The positive (semi) definiteness constraint on the matrix P is expressed as $(P \geq 0)$ $P > 0$. The matrix $A = [a_{ij}]$ is nonnegative if $a_{ij} \geq 0$, $\forall i, j$. Let $A_i \in \mathbb{R}^{n_i\times m_i}$ for

$i = 1, ..., N$, where N is a positive integer. The operator $\underset{1:N}{Diag}\{A_i\}$ is then defined as

$$\underset{1:N}{Diag}\{A_i\} = \begin{bmatrix} A_1 & \mathbf{0} & \dots & \mathbf{0} \\ \mathbf{0} & A_2 & \dots & \mathbf{0} \\ \vdots & \mathbf{0} & \ddots & \vdots \\ \mathbf{0} & \mathbf{0} & \dots & A_N \end{bmatrix}. \tag{1}$$

The maximum singular value of a matrix A is denoted by $\overline{\sigma}(A)$ and its kernel is denoted by $Ker(A)$. An eigenvalue of a square matrix A is denoted by $\lambda_i(A)$. The spectrum of matrix A is denoted by $Spec(A) = \{\lambda_i(A)\}$ and its spectral radius is denoted by $\rho(A) = \max\{|\lambda_i(A)|\}$. The determinant of a square matrix A is denoted by $Det(A)$. The a modulo n is denoted by $mod(a, n)$. The inverse Laplace transform is denoted by $\mathfrak{L}^{-1}(.)$.

2.2. $\mathcal{L}_p$-norm, $\mathcal{L}_{pe}$-norm and $\mathcal{L}_p$-gain

The following concepts and definitions are taken from [17]. For $p \in [1, +\infty)$, let $\mathcal{L}_p = \mathcal{L}_p^n[0, +\infty)$ denote the space of functions $a(t) \in \mathbb{R}^n$ such that $t \to |a(t)|^p$ is integrable over $[0, +\infty)$, where $|a(t)|$ is the instantaneous Euclidean norm of the vector $a(t)$. The $\mathcal{L}_p$-norm of $a(t) \in \mathcal{L}_p^n[0, +\infty)$ is defined as

$$\|a(t)\|_{\mathcal{L}_p} = \left(\int_0^\infty |a(\tau)|^p d\tau\right)^{1/p} < +\infty.$$

Let $\mathcal{L}_{pe} = \mathcal{L}_{pe}^n[0, T]$ denote the space of functions $b(t) \in \mathbb{R}^n$ such that $t \to |b(t)|^p$ is integrable over $[0, T]$, $\forall T < \infty$. The $\mathcal{L}_{pe}$-norm of $b(t) \in \mathcal{L}_{pe}^n[0, T]$ is defined as

$$\|b(t)\|_{\mathcal{L}_{pe}} = \left(\int_0^T |b(\tau)|^p d\tau\right)^{1/p} < +\infty.$$

Clearly, $\mathcal{L}_p^n \subset \mathcal{L}_{pe}^n$. Given the system $G : \mathcal{L}_{pe}^n \to \mathcal{L}_{pe}^m$, the $\mathcal{L}_p$-gain of G is denoted by $\beta_p(G)$ and is defined as

$$\beta_p(G) = \sup_{T \geq 0} \sup_{x \neq 0} \frac{\|G(x)\|_{\mathcal{L}_{pe}}}{\|x\|_{\mathcal{L}_{pe}}}. \tag{2}$$

The following technical results are in order.

Lemma 1 (modified version of Theorem 12 of [17])
Consider the following system

$$\begin{aligned} r_i &= \sum_{j=1}^{N} H_{ij}(e_j) \\ e_i &= f_i(r_i) + g_i(\omega_i) \end{aligned} \tag{3}$$

where $\omega_i \in \mathcal{L}_{pe}^{mi}$. Suppose all operators $f_i : \mathcal{L}_{pe}^{ni} \to \mathcal{L}_{pe}^{ni}$, $g_i : \mathcal{L}_{pe}^{mi} \to \mathcal{L}_{pe}^{ni}$ have finite $\mathcal{L}_p$-gains. Assume that $H_{ij} : \mathcal{L}_{pe}^{nj} \to \mathcal{L}_{pe}^{ni}$ is a linear operator and $\beta_p(H_{ij}f_j)$, $\beta_p(H_{ij}g_j)$ are finite for all i, j. Define the test matrix $Q_1 = [q_{1ij}]$ by

$$q_{1ij} = \beta_p(H_{ij}f_j).$$

Then the system (3) is $\mathcal{L}_p$-stable if $\rho(Q_1) < 1$.

Proof
By definition of $\beta_p(H_{ij}f_j)$ and $\beta_p(H_{ij}g_j)$, there exist finite constants b_{ij} and c_{ij} such that

$$\begin{aligned} \|H_{ij}f_j(r_j)\|_{\mathcal{L}_{pe}} &\leq \beta_p(H_{ij}f_j)\|r_j\|_{\mathcal{L}_{pe}} + b_{ij}, \\ \|H_{ij}g_j(\omega_j)\|_{\mathcal{L}_{pe}} &\leq \beta_p(H_{ij}g_j)\|\omega_j\|_{\mathcal{L}_{pe}} + c_{ij}. \end{aligned}$$

Taking norm in (3) and applying the above result

$$\begin{aligned}\|r_i\|_{\mathcal{L}_{pe}} \leq \sum_{j=1}^{N} \|H_{ij}(e_j)\|_{\mathcal{L}_{pe}} \leq \sum_{j=1}^{N} (\|H_{ij} f_j(r_j)\|_{\mathcal{L}_{pe}} + \|H_{ij} g_j(\omega_j)\|_{\mathcal{L}_{pe}}) \\ \leq \sum_{j=1}^{N} (\beta_p(H_{ij} f_j)\|r_j\|_{\mathcal{L}_{pe}} + \beta_p(H_{ij} g_j)\|\omega_j\|_{\mathcal{L}_{pe}}) + \tau_i,\end{aligned} \tag{4}$$

where $\tau_i = \sum_{j=1}^{N}(b_{ij} + c_{ij})$. Define the total vectors

$$\bar{r} = [\|r_1\|_{\mathcal{L}_{pe}}, ..., \|r_N\|_{\mathcal{L}_{pe}}]^T,\ \bar{\omega} = [\|\omega_1\|_{\mathcal{L}_{pe}}, ..., \|\omega_N\|_{\mathcal{L}_{pe}}]^T,\ \tau = [\tau_1, ..., \tau_N]^T$$

and let $Q_2 = [q_{2ij}],\ q_{2ij} = \beta_p(H_{ij} g_j)$ Then (4) reads

$$(I_N - Q_1)\bar{r} \leq Q_2\bar{\omega} + \tau.$$

Since $\rho(Q_1) < 1$, all leading principal minors of $I_N - Q_1$ are positive and we have that $(I_N - Q_1)^{-1}$ contains all nonnegative elements (Lemmas 8 and 9 of [17])

$$\bar{r} \leq (I_N - Q_1)^{-1} Q_2\bar{\omega} + (I_N - Q_1)^{-1}\tau$$

and hence, the $\mathcal{L}_p$ stability is guaranteed if $\rho(Q_1) < 1$. □

Lemma 2 ([9], Lemma 7)
Let $Q = [Q_{ij}]$ with $Q_{ij} \in \mathbb{C}^{n_i \times n_j}$ where $\mathbb{C}^{n_i \times n_j}$ is the set of $n_i \times n_j$ complex matrices. Let $\tilde{Q} = [\|Q_{ij}\|]$ be its block-norm matrix. Then, $\rho(Q) \leq \rho(\tilde{Q})$.

Lemma 3 ([9], Lemma 8)
Let Q be any nonnegative matrix and $\Theta = \underset{1:N}{Diag}\{\theta_i\}$ be a positive definite diagonal matrix. Then $\rho(\Theta Q) \leq \max_i \theta_i \rho(Q)$.

Lemma 4 ([18], Corollary 8.1.19)
Let $A = [a_{ij}]$ and $B = [b_{ij}]$ be nonnegative square matrices with compatible dimensions. If $a_{ij} \leq b_{ij},\ \forall i, j$ then, $\rho(A) \leq \rho(B)$.

Lemma 5 ([19], Lemma 4.2-Barbalat's Lemma)
If $a(t) \in \mathcal{L}_p[0, +\infty)$ for some $p = [1, +\infty)$ and $\dot{a}(t) \in \mathcal{L}_\infty$, then $\lim_{t\to+\infty} a(t) = 0$.

2.3. Graph theory

Given a piece-wise constant switching signal $\sigma : [0, +\infty) \to \mathcal{P} = \{1, ..., \varrho\}$ and a set of ϱ time-invariant graphs $\bar{\mathcal{G}}_i = (\bar{V}, \bar{\mathcal{E}}_i),\ i = 1, ..., \varrho$, we define an augmented switching graph $\bar{\mathcal{G}}_{\sigma(t)} = (\bar{V}, \bar{\mathcal{E}}_{\sigma(t)}) \in \{\bar{\mathcal{G}}_i | i = 1, ..., \varrho\}$ with a finite set of $N + 1$ nodes $\bar{V} = \{v_0, v_1, ..., v_N\}$ and $\bar{\mathcal{E}}_{\sigma(t)} \subseteq \bar{V} \times \bar{V}$. The node v_0 is associated with the leader and the nodes v_i are associated with followers $i,\ i = 1, ..., N$.

Let $\mathcal{G}_{\sigma(t)} = (V, \mathcal{E}_{\sigma(t)})$ be a subgraph of $\bar{\mathcal{G}}_{\sigma(t)}$ where $V = \{v_1, ..., v_N\}$ and $\mathcal{E}_{\sigma(t)} \subseteq V \times V$ is obtained from $\bar{\mathcal{E}}_{\sigma(t)}$ by removing all edges between node v_0 and the nodes in V. Let $E_{\sigma(t)} = [\alpha_{ij}(t)]$ be the adjacency matrix of $\mathcal{G}_{\sigma(t)}$ with $\alpha_{ij}(t) = 1$ if $(v_j, v_i) \in \mathcal{E}_{\sigma(t)},\ i, j \in \{1, ..., N\}$ and $\alpha_{ij}(t) = 0$ otherwise. Let $G_{\sigma(t)} = \underset{1:N}{Diag}\{g_i(t)\}$ be the pinning matrix with $g_i(t) = 1$ if there exists a link from v_0 to v_i at time t and $g_i(t) = 0$ otherwise. The graph is simple, *i.e.* $\alpha_{ii}(t) = 0,\ i = 1, ..., N$.

A *directed path* from node v_i to node v_j is a sequence of edges joining v_i to v_j. If there exists a directed path from node v_i to node v_j then it is said that node v_i is *reachable* from v_j. The set of *neighbors of node* v_i is $N_i(t) = \{v_j : (v_j, v_i) \in \mathcal{E}_{\sigma(t)}\}$. For graph $\mathcal{G}_{\sigma(t)}$, the *in-degree matrix* $D_{\sigma(t)}$ is a diagonal matrix $D_{\sigma(t)} = \underset{1:N}{Diag}\{d_i(t)\}$ with $d_i(t) = \sum_{j\in N_i} \alpha_{ij}(t)$. The *laplacian matrix* for graph $\mathcal{G}_{\sigma(t)}$ is defined as $L_{\sigma(t)} = D_{\sigma(t)} - E_{\sigma(t)}$. A graph $\mathcal{G}_{\sigma(t)}$ is *strongly connected* if there

exists a path from v_i to v_j for all $v_i, v_j \in V$. If the initial and the terminal nodes of a path are the same, the path is called a *cycle*. A graph without any cycle is named an *acyclic graph*. A directed graph is a *connected directed tree* if every node except one node, called *the root*, has in-degree equal to one. The root node has its in-degree equal to zero. A graph has a *spanning tree* if there exists a directed tree containing every node in V. A graph is *complete* if there exists a directed edge between any two nodes $v_i, v_j \in V,\ v_i \neq v_j$.

3. SYSTEM DESCRIPTION AND THE CONTROL PROBLEM

Consider a set of $N+1$ heterogeneous agents with N followers given as LTI systems

$$\dot{x}_i = A_i x_i + B_i u_i + Q_i d + P_i \omega_i, \tag{5}$$
$$y_i = C_i x_i + H_i d, \tag{6}$$
$$z_i = D_i x_i + J_i d, \tag{7}$$

in which $x_i \in \mathbb{R}^{n_i}$, $y_i \in \mathbb{R}^p$, $z_i \in \mathbb{R}^q$ and $u_i \in \mathbb{R}^{m_i}$ denote the state, the synchronization output, the measured output and the control signal for follower $i = 1, ..., N$. All followers are subject to disturbances, where, $d \in \mathbb{R}^{n_d}$ denotes a modeled disturbance whose model is given by

$$\dot{d} = Sd, \tag{8}$$

and $\omega_i \in \mathcal{L}_{2e}^{r_i}[0, T]$ denotes an unmodeled disturbance. The leader's dynamics is given by

$$\dot{\xi}_0 = X\xi_0, \tag{9}$$
$$y_0 = R_1\xi_0, \tag{10}$$
$$z_0 = R_2\xi_0, \tag{11}$$

The $\xi_0 \in \mathbb{R}^l$, $y_0 \in \mathbb{R}^p$ and $z_0 \in \mathbb{R}^q$ denote the state, the synchronization output and the measured output of the leader. The motivation behind introducing two outputs y_i, z_i is to achieve synchronization in outputs y_i, by communicating the measured outputs z_i where $q \leq p$ hence decreasing the communication burden.

We suggest a distributed static output-feedback controller of the following form

$$u_i = K_i e_{zi}, \tag{12}$$
$$e_{zi} = \sum_{j \in N_i(t)} \alpha_{ij}(t)(z_j - z_i) + g_i(t)(z_0 - z_i), \tag{13}$$

where e_{zi} is the local neighborhood error in z-outputs and $K_i \in \mathbb{R}^{m_i \times q}$. To reject the effect of the modeled disturbance, the output regulation controller usually contains a term $L_i d$, which would add the term $B_i L_i d$ to the agent's dynamics in (5). Here, we assume that the resulting term $B_i L_i$ is absorbed in the matrix Q_i and we only consider a pure distributed output-feedback control (13). The necessary condition for the rejection of the modeled disturbance is then given in terms of the matrix Q_i in the next subsection.

Define the y-output synchronization error and the z-output synchronization error as

$$\delta_{yi} = y_i - y_0, \tag{14}$$
$$\delta_{zi} = z_i - z_0. \tag{15}$$

Let $x = [x_1^T, ..., x_N^T]^T$, $y = [y_1^T, ..., y_N^T]^T$, $z = [z_1^T, ..., z_N^T]^T$, $\omega = [\omega_1^T, ..., \omega_N^T]^T$, $\delta_y = [\delta_{y1}^T, ..., \delta_{yN}^T]^T$ and $\delta_z = [\delta_{z1}^T, ..., \delta_{zN}^T]^T$ denote the overall vectors of x_i, y_i, z_i, ω_i, δ_{yi} and δ_{zi} respectively. Then, the overall closed-loop system of all followers, their controllers, the modeled disturbance and the

leader is given by the following

$$\begin{aligned}
\dot{x} &= A_{cl}x + B_{cl}\xi_0 + Q_{cl}d + P_{cl}\omega,\\
\dot{d} &= Sd,\\
\dot{\xi}_0 &= X\xi_0,\\
\delta_y &= C_{cl}x + H_{cl}d - \mathbf{1}_N \otimes R_1\xi_0,\\
\delta_z &= D_{cl}x + J_{cl}d - \mathbf{1}_N \otimes R_2\xi_0,
\end{aligned} \tag{16}$$

where

$$\begin{aligned}
A_{cl} &= \underset{1:N}{Diag}\{A_i\} - \underset{1:N}{Diag}\{B_iK_i\}((L_{\sigma(t)} + G_{\sigma(t)}) \otimes I_q)\underset{1:N}{Diag}\{D_i\},\\
B_{cl} &= \underset{1:N}{Diag}\{B_iK_i\}((L_{\sigma(t)} + G_{\sigma(t)}) \otimes I_q)\mathbf{1}_N \otimes R_2,\\
Q_{cl} &= [Q_1^T, ..., Q_N^T]^T - \underset{1:N}{Diag}\{B_iK_i\}((L_{\sigma(t)} + G_{\sigma(t)}) \otimes I_q)[J_1^T, ..., J_N^T]^T,\\
C_{cl} &= \underset{1:N}{Diag}\{C_i\}, \quad D_{cl} = \underset{1:N}{Diag}\{D_i\}, \quad P_{cl} = \underset{1:N}{Diag}\{P_i\},\\
H_{cl} &= [H_1^T, ..., H_N^T]^T, \quad J_{cl} = [J_1^T, ..., J_N^T]^T.
\end{aligned}$$

Usually, the dynamics of the reference trajectory (leader in this paper) and the modeled disturbance are merged together into a single *exo-system*

$$\dot{x}_0 = \begin{bmatrix} S & \mathbf{0} \\ \mathbf{0} & X \end{bmatrix} x_0, \quad x_0 = [d^T, \xi_0^T]^T. \tag{17}$$

Now, we define the H_∞ output regulation problem.

Problem 1
Consider a group of $N+1$ heterogeneous LTI systems defined by (5-11). Design the feedback gains K_i such that with (12), the closed-loop system of (5-11) achieves the following properties:

1. For $\omega \equiv 0$ and $x_0 \equiv 0$, the origin of the system $\dot{x} = A_{cl}x$ is asymptotically stable.
2. For $\omega \equiv 0$, we have $\delta_y \to 0$ as $t \to +\infty$ for all initial conditions $x_0(0)$.
3. For $\omega \in \mathcal{L}_{2e}$ and $T < +\infty$

$$\frac{\int_0^T |\delta_y|^2 dt}{\int_0^T |\omega|^2 dt} < +\infty. \tag{18}$$

Properties 1-2 define the output regulation problem [20, 1] in absence of unmodeled disturbance; i.e. $\omega \equiv 0$. Property 1 states that the origin of the overall closed-loop system (16) needs to be exponentially stable when the exo-system's state is identically zero. Property 2 means that when the exo-system is present, the multi-agent system achieves output synchronization to the output of the exo-system. Property 3 concerns with H_∞-output regulation in presence of unmodeled disturbances.

3.1. Necessary assumptions for output regulation

We make the following assumptions throughout this paper.

Assumption 1
The leader's dynamics X in (9) does not have any strictly stable poles.

Assumption 2
The triple (A_i, B_i, D_i) is output-feedback stabilizable.

Assumption 1 means that the leader generates a reference trajectory which does not converge to zero. We make Assumption 1, without loss of generality (Remark 1.3 of [1] and [4]), to exclude the trivial case of synchronization to zero. This case is trivial because the agents do not need to cooperate to achieve synchronization to zero. Note that the modes associated with the stable eigenvalues of X would decay to zero and have no permanent effect on the asymptotic behavior of the leader. Note also that a leader satisfying Assumption 1 can generate a large class of reference trajectories, such as a combination of step, ramp and parabolic functions which are of interest in applications. Assumption 2 is the standard assumption of output-feedback stabilizability of the triple (A_i, B_i, D_i). It means that it is possible to stabilize the pair (A_i, B_i) by an output feedback with D_i. This assumption is necessary for designing a stabilizing output-feedback.

According to Lemma 1.4 of [1], the closed-loop system (16) achieves y-output synchronization to the y-output of the leader in (9-11) for $\omega \equiv 0$ only if there exists an invariant subspace for the closed-loop system (16) where $y_i = y_0,\ i = 1, ..., N$

$$\begin{bmatrix} A_{cl} & Q_{cl} & B_{cl} \\ \mathbf{0} & S & \mathbf{0} \\ \mathbf{0} & \mathbf{0} & X \end{bmatrix} \begin{bmatrix} \Pi_1 & \Pi_2 \\ I_{n_d} & \mathbf{0} \\ \mathbf{0} & I_l \end{bmatrix} = \begin{bmatrix} \Pi_1 & \Pi_2 \\ I_{n_d} & \mathbf{0} \\ \mathbf{0} & I_l \end{bmatrix} \begin{bmatrix} S & \mathbf{0} \\ \mathbf{0} & X \end{bmatrix}, \tag{19}$$

$$\begin{bmatrix} C_{cl} & \mathbf{0} & \mathbf{0} \end{bmatrix} \begin{bmatrix} \Pi_1 & \Pi_2 \\ I_{n_d} & \mathbf{0} \\ \mathbf{0} & I_l \end{bmatrix} = \begin{bmatrix} -H_{cl} & \mathbf{1}_N \otimes R_1 \end{bmatrix}, \tag{20}$$

where $\Pi_1 \in \mathbb{R}^{\sum_{i=1}^N n_i \times n_d}$, $\Pi_2 \in \mathbb{R}^{\sum_{i=1}^N n_i \times l}$. If this invariant subspace also satisfies the z-output synchronization condition, then

$$\begin{bmatrix} D_{cl} & \mathbf{0} & \mathbf{0} \end{bmatrix} \begin{bmatrix} \Pi_1 & \Pi_2 \\ I_{n_d} & \mathbf{0} \\ \mathbf{0} & I_l \end{bmatrix} = \begin{bmatrix} -J_{cl} & \mathbf{1}_N \otimes R_2 \end{bmatrix}. \tag{21}$$

The above equations (19)-(21) read

$$\begin{aligned} &\begin{bmatrix} A_{cl}\Pi_1 + Q_{cl} & A_{cl}\Pi_2 + B_{cl} \end{bmatrix} = \begin{bmatrix} \Pi_1 S & \Pi_2 X \end{bmatrix}, \\ &\begin{bmatrix} C_{cl}\Pi_1 & C_{cl}\Pi_2 \end{bmatrix} = \begin{bmatrix} -H_{cl} & \mathbf{1}_N \otimes R_1 \end{bmatrix}, \\ &\begin{bmatrix} D_{cl}\Pi_1 & D_{cl}\Pi_2 \end{bmatrix} = \begin{bmatrix} -J_{cl} & \mathbf{1}_N \otimes R_2 \end{bmatrix}. \end{aligned} \tag{22}$$

Using the last equation in (22), the first equation in (22) is simplified to

$$\begin{bmatrix} \underset{1:N}{Diag\{A_i\}}\Pi_1 + [Q_1^T, ..., Q_N^T]^T & \underset{1:N}{Diag\{A_i\}}\Pi_2 \end{bmatrix} = \begin{bmatrix} \Pi_1 S & \Pi_2 X \end{bmatrix}. \tag{23}$$

Let $\Pi_1 = [\Pi_{11}^T, \Pi_{12}^T, ..., \Pi_{1N}^T]$ and $\Pi_2 = [\Pi_{21}^T, \Pi_{22}^T, ..., \Pi_{2N}^T]$, where $\Pi_{1i} \in \mathbb{R}^{n_i \times n_d}$ and $\Pi_{2i} \in \mathbb{R}^{n_i \times l}$. Hence, a set of necessary assumptions for y-output synchronization and z-output synchronization is given by Assumptions 1-2 and the following.

Assumption 3
For each $i = 1, ..., N$, there exist $\Pi_{1i} \in \mathbb{R}^{n_i \times n_d}$ and $\Pi_{2i} \in \mathbb{R}^{n_i \times l}$ such that

$$\begin{aligned} &A_i\Pi_{1i} + Q_i = \Pi_{1i}S, \quad A_i\Pi_{2i} = \Pi_{2i}X, \\ &C_i\Pi_{1i} = -H_i, \qquad\quad C_i\Pi_{2i} = R_1, \\ &D_i\Pi_{1i} = -J_i, \qquad\quad D_i\Pi_{2i} = R_2, \quad i = 1, ..., N. \end{aligned} \tag{24}$$

3.2. Coordinate transformations

In this subsection, we introduce two coordinate transformations. The first one decouples the agent's dynamics from the modeled disturbance and the second transformation reveals the shared invariant subspace of the agents which allows synchronization to the leader.

DOI: 10.1002/rnc

Let (24) hold. Introduce a new variable $\delta_{di} = x_i - \Pi_{1i} d$. Then the dynamics of δ_{di} and the output synchronization errors $\delta_{yi},\ \delta_{zi}$ read

$$\begin{aligned}
\dot{\delta}_{di} &= \dot{x}_i - \Pi_{1i}\dot{d} = A_i x_i + B_i u_i + Q_i d + P_i \omega_i - \Pi_{1i} S d \\
&= A_i x_i + B_i u_i + Q_i d + P_i \omega_i - A_i \Pi_{1i} d - Q_i d \\
&= A_i \delta_{di} + B_i u_i + P_i \omega_i, \\
\delta_{yi} &= C_i x_i + H_i d - R_1 \xi_0 = C_i (x_i - \Pi_{1i} d) + (\underbrace{H_i + C_i \Pi_{1i}}_{0}) d - R_1 \xi_0 \\
&= C_i \delta_{di} - R_1 \xi_0, \\
\delta_{zi} &= D_i x_i + J_i d - R_2 \xi_0 = D_i (x_i - \Pi_{1i} d) + (\underbrace{J_i + D_i \Pi_{1i}}_{0}) d - R_2 \xi_0 \\
&= D_i \delta_{di} - R_2 \xi_0.
\end{aligned} \tag{25}$$

The dynamics of the new variable δ_{di} is completely independent of the modeled disturbance d. Moreover, the output synchronization errors $\delta_{yi},\ \delta_{zi}$ can be completely expressed without d. It means that the agent's dynamics in the new coordinates can be considered independent of the modeled disturbance d. This is a direct result of the necessary assumptions on the left-hand side of the output regulation equations in (24).

According to the top-right equation in (24), each single-agent dynamics $A_i,\ i = 1, ..., N$ has an invariant subspace which is spanned by columns of $\Pi_{2i} \in \mathbb{R}^{n_i \times l}$. Supplement the columns of Π_{2i} by a set of linearly independent columns of $\Psi_i \in \mathbb{R}^{n_i \times (n_i - l)}$ to form a complete basis of the single-agent state space $\mathbb{R}^{n_i}$. Then in such basis, one has the transformed state $[\xi_i^T, \nu_i^T]^T \in \mathbb{R}^{n_i}$.

$$\delta_{di} = \begin{bmatrix} \Pi_{2i} & \Psi_i \end{bmatrix} \begin{bmatrix} \xi_i \\ \nu_i \end{bmatrix} = T_i \begin{bmatrix} \xi_i \\ \nu_i \end{bmatrix}, \tag{26}$$

with (24) generally leading to

$$T_i^{-1} A_i T_i = \begin{bmatrix} X & F_i \\ \mathbf{0} & M_i \end{bmatrix}. \tag{27}$$

Define $\bar{x}_i = [\delta_{\xi i}^T, \nu_i^T]^T$, where $\delta_{\xi i} = \xi_i - \xi_0$. Then the closed-loop dynamics of system (5) in the transformed coordinates equals

$$\begin{aligned}
\dot{\bar{x}}_i &= \hat{A}_i \bar{x}_i + \hat{B}_i u_i + \hat{P}_i \omega_i, \\
\delta_{yi} &= y_i - y_0 = \hat{C}_i \bar{x}_i, \\
\delta_{zi} &= z_i - z_0 = \hat{D}_i \bar{x}_i, \\
u_i &= K_i \left(\sum_{j \in N_i(t)} \alpha_{ij}(t) (\hat{D}_j \bar{x}_j - \hat{D}_i \bar{x}_i) - g_i(t) \hat{D}_i \bar{x}_i \right),
\end{aligned} \tag{28}$$

where

$$\begin{aligned}
&\hat{A}_i := T_i^{-1} A_i T_i = \begin{bmatrix} X & F_i \\ \mathbf{0} & M_i \end{bmatrix},\ \hat{B}_i := T_i^{-1} B_i,\ \hat{P}_i := T_i^{-1} P_i, \\
&\hat{C}_i := C_i T_i = \begin{bmatrix} R_1 & C_i \Psi_i \end{bmatrix},\ \hat{D}_i := D_i T_i = \begin{bmatrix} R_2 & D_i \Psi_i \end{bmatrix}.
\end{aligned} \tag{29}$$

The description of the system in the new coordinates will be useful in designing the controller as detailed in the following section.

Remark 1

In this paper, we use the coordinate transformation to transform the agent's dynamics into the part which is shared between the agents and the leader, (denoted by X in this paper), and the unshared

part. We use this transformation to study H_∞ output regulation of linear heterogeneous agents where the agents are subject to both modeled and unmodeled disturbances and they communicate over a switching graph. Such a transformation is also used in [21, 22] to study output regulation; however, [21, 22] do not consider modeled and unmodeled disturbances and the communication graph in [22] is static.

4. H_∞ OUTPUT REGULATION OVER A STATIC GRAPH

In this section we analyze H_∞ output regulation over a static graph $\bar{\mathcal{G}} = (\bar{V}, \bar{\mathcal{E}})$ and as such, we drop the time variable t from all expressions in this section. We obtain a single-agent sufficient condition that guarantees H_∞ output regulation and derive an upper bound for the overall $\mathcal{L}_2$-gain of y-output synchronization error with respect to the disturbance ω. At the end of this section, we show how to design the controller gains such that the sufficient condition is indeed satisfied.

4.1. Single-agent sufficient condition for output regulation in absence of ω-disturbances

This subsection gives a single-agent sufficient condition for output regulation in the absence of $\omega-$disturbances. We show how to satisfy this sufficient condition by either specifying the structure of matrix A_i as detailed in this subsection, or a proper design of the controller gain K_i, as detailed in subsection 4.3. The interest in the specific structure of A_i is motivated by existing results in distributed output regulation [7, 8, 9, 23, 5], which incorporate a p-copy model of X by some hierarchical structure and suggest a state-feedback or an output-feedback. In contrast, we do not incorporate a p-copy of the leader but instead, we find a structure of the drift dynamics A_i; namely F_i and M_i in (27).

For the developments of this section, we use a simple redefinition of the feedback gain. For a graph $\bar{\mathcal{G}} = (\bar{V}, \bar{\mathcal{E}})$, define *the normalized adjacency matrix* as $Z_g = [\frac{\alpha_{ij}}{d_i+g_i}]$ where $(d_i + g_i)$ is *the normalizing factor* of node i. Redefine the control gain as $\hat{K}_i := (d_i + g_i)K_i$. Hence the control (12) can be written as

$$\begin{aligned} u_i &= K_i \left(\sum_{j\in N_i} \alpha_{ij}(z_j - z_i) + g_i(z_0 - z_i) \right) \\ &= K_i(d_i + g_i) \left(\sum_{j\in N_i} \frac{\alpha_{ij}}{d_i + g_i}(z_j - z_i) + \frac{g_i}{d_i + g_i}(z_0 - z_i) \right) \\ &= \hat{K}_i \left(\sum_{j\in N_i} \frac{\alpha_{ij}}{d_i + g_i}(z_j - z_i) + \frac{g_i}{d_i + g_i}(z_0 - z_i) \right) \end{aligned}$$

Hence, we design $\hat{K}_i$ and assume that the agents communicate over a graph with normalized edge weights. Note that one can always compute the matrix K_i from $K_i = \frac{1}{d_i+g_i}\hat{K}_i$ locally. Define

$$A_i^c := \hat{A}_i - \hat{B}_i\hat{K}_i\hat{D}_i,\ A_i^n := \begin{bmatrix} X & \mathbf{0} \\ \mathbf{0} & \mathbf{0} \end{bmatrix} - \hat{B}_i\hat{K}_i\hat{D}_i,\ C_i^n := \begin{bmatrix} \mathbf{0} & I_{n_i-l} \end{bmatrix},\ L_i^n := \begin{bmatrix} F_i \\ M_i \end{bmatrix}. \tag{30}$$

Theorem 1
Consider a group of linear heterogeneous systems defined in (5-11). Let the static augmented communication graph $\bar{\mathcal{G}} = (\bar{V}, \bar{\mathcal{E}})$ contain a spanning tree with the leader as its root node. Let Assumptions 1-3 hold. If the controller gains $\hat{K}_i$ are selected such that

$$\|\hat{D}_i(sI - A_i^c)^{-1}\hat{B}_i\hat{K}_i\|_\infty < \frac{1}{\rho(Z_g)} = \gamma_z, \tag{31}$$

for $i = 1, ..., N$, then the $\omega-$disturbance-free system (5-11) achieves y-output regulation and there exists a $0 < \gamma_i < +\infty$ such that

$$\|\hat{C}_i(sI - A_i^c)^{-1}\hat{P}_i\|_\infty < \gamma_i, \quad i = 1, ..., N. \tag{32}$$

Prepared using rncauth.cls
DOI: 10.1002/rnc

Proof
First note that by output-feedback stabilizability of (A_i, B_i, D_i) in Assumption 2, the transformed triple $(\hat{A}_i, \hat{B}_i, \hat{D}_i)$ is output-feedback stabilizable and the pairs $(\hat{A}_i, \hat{B}_i)$ and $(\hat{A}_i, \hat{D}_i)$ are stabilizable and detectable respectively. As a result, one can show that $(A_i^c, \hat{B}_i)$ and $(A_i^c, \hat{D}_i)$ are stabilizable and detectable. Set $\omega_i \equiv 0,\ i = 1, ..., N$. Then, the overall closed-loop system of (28) reads

$$\begin{aligned}\dot{\bar{x}} &= (\bar{A} - \bar{B}\underset{1:N}{Diag}\{K_i\}((L+G)\otimes I_q)\bar{D})\bar{x} = \left(\bar{A} - \bar{B}\bar{K}((I_N - Z_g)\otimes I_q)\bar{D}\right)\bar{x} = A_{ov}\bar{x},\\ \delta_y &= \bar{C}\bar{x},\end{aligned} \tag{33}$$

where $\bar{x} = [\bar{x}_1^T, ..., \bar{x}_N^T]^T$ and

$$\bar{A} := \underset{1:N}{Diag}\{\hat{A}_i\},\ \bar{B} := \underset{1:N}{Diag}\{\hat{B}_i\},\ \bar{C} := \underset{1:N}{Diag}\{\hat{C}_i\},\ \bar{D} := \underset{1:N}{Diag}\{\hat{D}_i\},\ \bar{K} := \underset{1:N}{Diag}\{\hat{K}_i\}.$$

Now we prove that if (31) holds, the $\omega-$disturbance-free system achieves y-output regulation. That is: 1. A_{cl} is strictly stable and 2. $\delta_y \to 0$ as $t \to \infty$ according to properties 1-2 in Problem 1.

1. $A_{ov} = T^{-1}A_{cl}T$, where $T = \underset{1:N}{Diag}\{T_i\}$, with T_i from (26), is the similarity transformation. The characteristic equation of A_{cl} denoted by Δ reads

$$\begin{aligned}\Delta &= Det(sI - A_{cl}) = Det(sI - T^{-1}A_{cl}T) = Det(sI - A_{ov})\\ &= Det(sI - \bar{A} + \bar{B}\bar{K}\bar{D} - \bar{B}\bar{K}(Z_g\otimes I_q)\bar{D})\\ &= Det(sI - (\bar{A} - \bar{B}\bar{K}\bar{D}))Det(I - \bar{D}(sI - \bar{A} + \bar{B}\bar{K}\bar{D})^{-1}\bar{B}\bar{K}(Z_g\otimes I_q))\\ &= Det(\underset{1:N}{Diag}\{sI - A_i^c\})Det\mathcal{F}(s),\end{aligned}$$

   where $\mathcal{F}(s) = I - F_{22}(s)(Z_g\otimes I_q),\ F_{22}(s) = \underset{1:N}{Diag}\{F_{i22}(s)\}$ and $F_{i22}(s) = \hat{D}_i(sI - A_i^c)^{-1}\hat{B}_i\hat{K}_i$.
   The stability of $\mathcal{F}(s) = I - F_{22}(s)(Z_g\otimes I_q)$ in a small gain sense implies that all poles of $F_{i22}(s)$ are stable. Because of stabilizability and detectability of $(A_i^c, \hat{B}_i)$ and $(A_i^c, \hat{D}_i)$, we can then also conclude that all $\lambda(A_i^c)$ have negative real parts. Hence, if we can prove the stability of $\mathcal{F}(S)$ in the small gain sense, then we can conclude that A_{ov} is stable; i.e. A_{cl} is stable. By the small gain theorem, $\mathcal{F}(s)$ is asymptotically stable if $\rho(F_{22}(s)(Z_g\otimes I_q)) < 1$. Using Lemmas 2-3, $\rho(F_{22}(s)(Z_g\otimes I_q)) \le \max_i \|F_{i22}\|_\infty \rho(Z_g)$. Hence, if (31) holds for $i = 1, ..., N$, then A_{cl} is stable.
2. Since A_{ov} in (33) is strictly stable, then $\delta_y \to 0$ as $t \to \infty$ and the $\omega-$disturbance-free system (5-11) achieves y-output regulation.

Next, we prove that (32) holds. According to Theorem 6.4 of [24], an LTI system with a Hurwitz system matrix, is finite-gain $\mathcal{L}_2$-stable. The condition (31) guarantees asymptotic stability of A_i^c for $i = 1, ..., N$ and as a result, there exists a $0 < \gamma_i < \infty$ for $i = 1, ..., N$ such that (32) holds. □

The next theorem suggests a structure of the drift dynamics $\hat{A}_i$ that guarantees (31).

Theorem 2
Consider a group of linear heterogeneous systems defined in (5-11). Let the static augmented communication graph $\bar{\mathcal{G}} = (\bar{V}, \bar{\mathcal{E}})$ contain a spanning tree with the leader as its root node. Let Assumptions 1-3 hold. Given $\hat{K}_i$ for $i = 1, ..., N$, assume that $P_i^L > 0$ and $\sigma_i > 0$ form a feasible solution to the following LMI

$$\begin{bmatrix}(A_i^n)^T P_i^L + P_i^L A_i^n - \sigma_i (C_i^n)^T C_i^n + \hat{D}_i^T\hat{D}_i & P_i^L\hat{B}_i\hat{K}_i\\ \hat{K}_i^T\hat{B}_i^T P_i^L & -\gamma_z^2 I_q\end{bmatrix} < 0. \tag{34}$$

Then, the $\omega-$disturbance-free system (5-11) achieves y-output regulation if the following structure is imposed on the drift dynamics of each agent

$$L_i^n = \begin{bmatrix} F_i \\ M_i \end{bmatrix} = -\frac{\sigma_i}{2}(P_i^L)^{-1}(C_i^n)^T. \tag{35}$$

Proof
According to Theorem 1, the $\omega-$disturbance-free system (5-11) achieves y-output regulation if (31) is satisfied. According to [25], the norm condition (31) is equivalent to

$$\begin{bmatrix} (\hat{A}_i - \hat{B}_i\hat{K}_i\hat{D}_i)^T P_i^L + P_i^L(\hat{A}_i - \hat{B}_i\hat{K}_i\hat{D}_i) + \hat{D}_i^T\hat{D}_i & P_i^L\hat{B}_i\hat{K}_i \\ \hat{K}_i^T\hat{B}_i^T P_i^L & -\gamma_z^2 I_q \end{bmatrix} < 0$$

or

$$\begin{bmatrix} (A_i^n + L_i^n C_i^n)^T P_i^L + P_i^L(A_i^n + L_i^n C_i^n) + \hat{D}_i^T\hat{D}_i & P_i^L\hat{B}_i\hat{K}_i \\ \hat{K}_i^T\hat{B}_i^T P_i^L & -\gamma_z^2 I_q \end{bmatrix} < 0.$$

Introducing $Y^i = P_i^L L_i^n$, the above inequality reads

$$\begin{bmatrix} (A_i^n)^T P_i^L + P_i^L(A_i^n) + Y^i C_i^n + (Y^i C_i^n)^T + \hat{D}_i^T\hat{D}_i & P_i^L\hat{B}_i\hat{K}_i \\ \hat{K}_i^T\hat{B}_i^T P_i^L & -\gamma_z^2 I_q \end{bmatrix} < 0.$$

Considering $\sigma_i > 0$ the above inequality is equivalent to (34) if L_i^n is selected as in (35). □

Remark 2
One can easily see that M_i resulting from (35) is negative definite. Let

$$Q_i^L = (P_i^L)^{-1} = \begin{bmatrix} Q_{i11}^L & Q_{i12}^L \\ (Q_{i12}^L)^T & Q_{i22}^L \end{bmatrix}.$$

Based on (35), $M_i = -\frac{\sigma_i}{2}Q_{i22}^L$. Since Q_{i22}^L is positive definite, the resulting M_i is necessarily negative definite and strictly stable. This explains that the unshared dynamics of the agents which is parameterized by ν_i should be strictly stable for a possible y-output regulation.

Remark 3
In contrast to [7, 5, 6], which assume an acyclic graph in order to transform the resulting system matrix A_{ov} to an upper block triangular form, here we drop that limiting assumption by using the small gain theorem to prove the asymptotic stability of the overall system matrix A_{ov}. Our general result in Theorem 1 (the norm condition (31)) contains the special case of acyclic graphs reported in [7, 5, 6]. Corollary 1 shows that for acyclic graphs, the norm condition in (31) reduces to the asymptotic stability of the single-agent system's matrix A_i^c.

Corollary 1
Consider a group of linear heterogeneous systems defined in (5-11). Let the static augmented communication graph $\bar{\mathcal{G}} = (\bar{V}, \bar{\mathcal{E}})$ be acyclic and contain a spanning tree with the leader as its root node. Let Assumptions 1-3 hold. Assume that the controller gains $\hat{K}_i$ are selected such that the matrices A_i^c are Hurwitz for $i = 1, ..., N$. Then, the $\omega-$disturbance-free system (5-11) achieves y-output regulation.

Proof
For an acyclic graph $\rho(Z_g) = 0$ ([9]) and the condition (31) in Theorem 1 reduces to the boundedness of $\|\hat{D}_i(sI - A_i^c)^{-1}\hat{B}_i\hat{K}_i\|$ which is guaranteed by asymptotic stability of A_i^c. Note that we can always select $\hat{K}_i$ to make A_i^c stable by Assumption 2. □

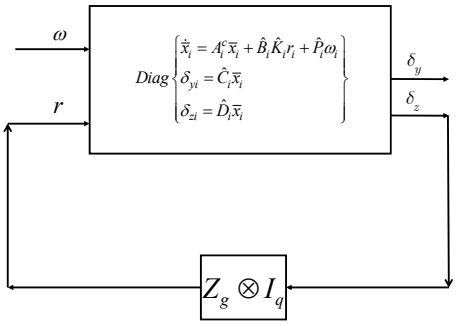

Figure 1. The representation of the overall closed-loop system of (28)

4.2. Calculation of the overall $\mathcal{L}_2$-gain

In this subsection we prove that the sufficient condition (31) is also sufficient for H_∞ y-output regulation when $\omega-$disturbances are present and we calculate an upper bound for the overall $\mathcal{L}_2$-gain. Figure 1 schematically represents the overall closed-loop system of (28). Let

$$F_{11}(s) = \underset{1:N}{Diag}\{\hat{C}_i(sI - A_i^c)^{-1}\hat{P}_i\},\ F_{12}(s) = \underset{1:N}{Diag}\{\hat{C}_i(sI - A_i^c)^{-1}\hat{B}_i\hat{K}_i\},$$
$$F_{21}(s) = \underset{1:N}{Diag}\{\hat{D}_i(sI - A_i^c)^{-1}\hat{P}_i\},\ F_{22}(s) = \underset{1:N}{Diag}\{\hat{D}_i(sI - A_i^c)^{-1}\hat{B}_i\hat{K}_i\}.$$

Then the transfer function from input ω to δ_y, denoted by $F_{tot}(s)$, is

$$F_{tot}(s) = F_{11}(s) + F_{12}(s)(Z_g \otimes I_q)(I - F_{22}(s)(Z_g \otimes I_q))^{-1}F_{21}(s).$$

Let $F_{tot}(s)(i,:)$ denote the transfer function from input ω to δ_{yi} which is given by the ith block row of dimension p of $F_{tot}(s)$.

Theorem 3
Consider a group of linear heterogeneous systems defined in (5-11). Let the static augmented communication graph $\bar{\mathcal{G}} = (\bar{V}, \bar{\mathcal{E}})$ contain a spanning tree with the leader as its root node. Let Assumptions 1-3 hold. Assume that the controller gains $\hat{K}_i$ are selected such that (31) holds for $i = 1, ..., N$. Then,

1. The system of (5-11) achieves H_∞ y-output regulation.
2. An upper bound for the $\mathcal{L}_2$-gain of δ_y with respect to ω is given by

$$\mathbf{L} = \gamma_{11} + \gamma_{12}\bar{\sigma}(Z_g)\gamma_{22}\gamma_{21}, \tag{36}$$
$$\gamma_{11} = \max_i \gamma_i,\ \gamma_{12} = \max_i \|\hat{C}_i(sI - A_i^c)^{-1}\hat{B}_i\hat{K}_i\|_\infty, \tag{37}$$
$$\gamma_{21} = \max_i \|\hat{D}_i(sI - A_i^c)^{-1}\hat{P}_i\|_\infty,\ \gamma_{22} = \|(I - F_{22}(s)(Z_g \otimes I_q))^{-1}\|_\infty.$$

3. An upper bound for the $\mathcal{L}_2$-gain of δ_{yi} with respect to ω is given by

$$\mathbf{L}_i = \|F_{tot}(s)(i,:)\|_\infty. \tag{38}$$

Proof
The proof contains three parts.

1. According to small gain-theorem, a sufficient condition for the $\mathcal{L}_2$ stability of the $F_{tot}(s)$ is $\rho(F_{22}(s)(Z_g \otimes I_q)) < 1$. Using Lemmas 2-3, $\rho(F_{22}(s)(Z_g \otimes I_q)) \leq \max_i \|\hat{D}_i(sI - A_i^c)^{-1}\hat{B}_i\hat{K}_i\|_\infty \rho(Z_g)$. Hence, if (31) is satisfied, then $F_{tot}(s)$ is $\mathcal{L}_2$-gain stable.
2. Next, we obtain an upper bound for the $\mathcal{L}_2$-gain of the y-output synchronization error δ_y with respect to ω

$$\begin{aligned}\|F_{tot}(s)\|_\infty \leq & \|F_{11}(s)\|_\infty + \|F_{12}(s)\|_\infty \overline{\sigma}(Z_g)\|(I - F_{22}(s)(Z_g \otimes I_q))^{-1}\|_\infty \|F_{21}(s)\|_\infty \\ \leq & \max_i \|\hat{C}_i(sI - A_i^c)^{-1}\hat{P}_i\|_\infty + \max_i \|\hat{C}_i(sI - A_i^c)^{-1}\hat{B}_i\hat{K}_i\|_\infty \overline{\sigma}(Z_g) \times \\ & \|(I - F_{22}(s)(Z_g \otimes I_q))^{-1}\|_\infty \max_i \|\hat{D}_i(sI - A_i^c)^{-1}\hat{P}_i\|_\infty.\end{aligned}$$

   According to (32), $\|\hat{C}_i(sI - A_i^c)^{-1}\hat{P}_i\|_\infty < \gamma_i$. By Theorem 1 and Theorem 5.4 of [24], γ_{12}, γ_{21} and γ_{22} exist and (36) follows.
3. The $\mathcal{L}_2$-gain of δ_{yi} with respect to ω is given by the H_∞-norm of the transfer function from input ω to δ_{yi} which is $\|F_{tot}(s)(i,:)\|_\infty$.

□

4.3. Controller design

According to Theorem 3, (31) is a single-agent sufficient condition that guarantees H_∞-output regulation. In this section we will show how to design the matrix $\hat{K}_i$ such that (31) indeed holds. Define

$$\Xi_i = \begin{bmatrix} \hat{A}_i^T P_i^L + P_i^L \hat{A}_i & \mathbf{0} & \hat{D}_i^T \\ \mathbf{0} & -\gamma_z^2 I_q & \mathbf{0} \\ \hat{D}_i & \mathbf{0} & -I_q \end{bmatrix}, \Xi_i^y = \begin{bmatrix} \hat{A}_i Q_i^L + Q_i^L \hat{A}_i & \mathbf{0} & Q_i^L \hat{D}_i^T \\ \mathbf{0} & -\gamma_z^2 I_q & \mathbf{0} \\ \hat{D}_i Q_i^L & \mathbf{0} & -I_q \end{bmatrix}, \tag{39}$$

$$U_i = \begin{bmatrix} -\hat{D}_i & I_q & \mathbf{0} \end{bmatrix}, V_i = \begin{bmatrix} \hat{B}_i^T P_i^L & \mathbf{0} & \mathbf{0} \end{bmatrix} = Y_i E_i, Y_i = \begin{bmatrix} \hat{B}_i^T & \mathbf{0} & \mathbf{0} \end{bmatrix}, \tag{40}$$

$$E_i = \begin{bmatrix} P_i^L & \mathbf{0} & \mathbf{0} \\ \mathbf{0} & I_q & \mathbf{0} \\ \mathbf{0} & \mathbf{0} & I_q \end{bmatrix}. \tag{41}$$

Theorem 4
Let W_{U_i}, W_{V_i} and W_{Y_i} be the orthogonal complements of U_i, V_i and Y_i respectively. The single-agent condition (31) is satisfied if and only if there exist matrices $Q_i^L, P_i^L > 0 \in \mathbb{R}^{n_i \times n_i}$ such that

$$W_{Y_i}^T \Xi_i^y W_{Y_i} < 0, \tag{42}$$

$$W_{U_i}^T \Xi_i W_{U_i} < 0, \tag{43}$$

$$Q_i^L P_i^L = I_{n_i}. \tag{44}$$

The controller gain $\hat{K}_i$ is then obtained as a feasible solution to the inequality

$$\Xi_i + V_i^T \hat{K}_i U_i + U_i^T \hat{K}_i^T V_i < 0. \tag{45}$$

Proof
According to [25], the norm condition in (31) is satisfied if and only if there exists a $P_i^L > 0$ such that

$$\begin{bmatrix} (\hat{A}_i - \hat{B}_i\hat{K}_i\hat{D}_i)^T P_i^L + P_i^L(\hat{A}_i - \hat{B}_i\hat{K}_i\hat{D}_i) & P_i^L \hat{B}_i \hat{K}_i & \hat{D}_i^T \\ \hat{K}_i^T \hat{B}_i^T P_i^L & -\gamma_z^2 I_q & \mathbf{0} \\ \hat{D}_i & \mathbf{0} & -I_q \end{bmatrix} < 0. \tag{46}$$

According to the definitions in (39-41), the above LMI reads

$$\Xi_i + V_i^T \hat{K}_i U_i + U_i \hat{K}_i^T V_i < 0. \tag{47}$$

Using the Elimination of Matrix Variable Lemma [25], the above inequality is feasible if and only if

$$\begin{aligned} W_{V_i}^T \Xi_i W_{V_i} < 0, \\ W_{U_i}^T \Xi_i W_{U_i} < 0. \end{aligned} \tag{48}$$

As the columns of W_{Y_i} span $Ker(Y_i)$, one has that $Y_i W_{Y_i} = 0$. Similarly, as the columns of $E_i^{-1} W_{Y_i}$ span $Ker(V_i) = Ker(Y_i E_i)$, it follows that $Y_i E_i E_i^{-1} W_{Y_i} = 0$ and we can conclude that $W_{V_i} = E_i^{-1} W_{Y_i}$. Then (48) reads

$$\begin{aligned} W_{Y_i}^T E_i^{-1} \Xi_i E_i^{-1} W_{Y_i} < 0, \\ W_{U_i}^T \Xi_i W_{U_i} < 0. \end{aligned}$$

Introducing $\Xi_i^y = E_i^{-1} \Xi_i E_i^{-1}$

$$\Xi_i^y = \begin{bmatrix} \hat{A}_i (P_i^L)^{-1} + (P_i^L)^{-1} \hat{A}_i^T & \mathbf{0} & (P_i^L)^{-1} \hat{D}_i^T \\ \mathbf{0} & -\gamma_z^2 I_q & \mathbf{0} \\ \hat{D}_i (P_i^L)^{-1} & \mathbf{0} & -I_q \end{bmatrix}.$$

Let $Q_i^L = (P_i^L)^{-1}$, then (44) follows. □

According to Theorem 4, the single-agent sufficient condition (31) is satisfied if and only if there exists a feasible solution to the set of two LMIs and one non-convex algebraic constraint in (42-44). The following algorithm is suggested in [8] to find a feasible solution to (42-44).

Algorithm 1 Iterative solution to (42-44)

1: **Initialization:** Set k=0. Find a feasible solution $Q_i^{L(0)}, P_i^{L(0)}$ to

$$\begin{cases} W_{Y_i}^T \Xi_i^{y(0)} W_{Y_i} < 0, \\ W_{U_i}^T \Xi_i^{(0)} W_{U_i} < 0, \\ \begin{bmatrix} Q_i^{L(0)} & I_{n_i} \\ I_{n_i} & P_i^{L(0)} \end{bmatrix} \geq 0. \end{cases} \tag{49}$$

2: **repeat**

3: Set $\Phi_i^{(k)} = Q_i^{L(k)}$ and $\Upsilon_i^{(k)} = P_i^{L(k)}$. Find $Q_i^{L(k+1)}$ and $P_i^{L(k+1)}$ that solve

$$\min \quad \mathbf{Tr}(Q_i^{L(k+1)} \Upsilon_i^{(k)} + \Phi_i^{L(k)} P_i^{(k+1)}) \tag{50}$$

$$\mathbf{w.r.t} \quad \begin{cases} W_{Y_i}^T \Xi_i^{y(k+1)} W_{Y_i} < 0 \\ W_{U_i}^T \Xi_i^{(k+1)} W_{U_i} < 0 \\ \begin{bmatrix} Q_i^{L(k+1)} & I_{n_i} \\ I_{n_i} & P_i^{L(k+1)} \end{bmatrix} \geq 0 \end{cases}. \tag{51}$$

4: **until** $|\mathbf{Tr}(Q_i^{L(k+1)} \Upsilon_i^{(k)} + \Phi_i^{(k)} P_i^{L(k+1)} - Q_i^{L(k)} \Upsilon_i^{(k-1)} - \Phi_i^{(k-1)} P_i^{L(k)})| < \varepsilon_{thre}$

In the above, ε_{thre} is a convergence threshold. Algorithm 1 iterates over a linear programming problem and it is proved in [8] that there exists a feasible solution to (42-44) if and only if the global solution to the optimization problem in Algorithm 1 is $2n_i$. Hence, the solution $2n_i$ for the cost

function (50) in Algorithm 1 is both necessary and sufficient for the solvability of (42-44) and the existence of a gain matrix $\hat{K}_i$. Once this condition is satisfied, the algorithm gives the converged values of Q_i^L and P_i^L and those are used in (45) to find the controller gain $\hat{K}_i$. Note that to implement Algorithm 1 and to calculate $\hat{K}_i$, one only needs to solve linear programming problems and for those, many standard solvers like MATLAB are readily available. For the proof of convergence see [26].

5. H_∞ OUTPUT REGULATION OVER A SWITCHING GRAPH

In practice, the communication graph might not be connected at all times. The communication links can be created or lost due to several reasons like packet loss, state-dependent networks, etc. In this section, we consider switching graphs where the graph structure can change over a set of topologies [27], and we study H_∞ output regulation over such graphs. In the sequel, we define the new concept of maximally connected switching graph.

Definition 1
A switching augmented graph $\bar{\mathcal{G}}_{\sigma(t)} = (\bar{V}, \bar{\mathcal{E}}_{\sigma(t)})$ with the adjacency matrix $E_{\sigma(t)} = [\alpha_{ij}(t)]$ and the pinning matrix $G_{\sigma(t)} = \underset{1:N}{Diag}\{g_i(t)\}$ is *maximally connected* if there exists an $0 < h < +\infty$ such that

$$\begin{aligned} E^k &= [\max_{t\in[t_k,t_k+h]} \alpha_{ij}(t)], \\ G^k &= \underset{1:N}{Diag}\{\max_{t\in[t_k,t_k+h]} g_i(t)\},\ \forall t_k,\ 0 \le t_k < +\infty \end{aligned} \tag{52}$$

are the adjacency matrix and the pinning matrix corresponding to some rooted graph $\bar{\mathcal{G}}^k = (\bar{V}, \bar{\mathcal{E}}^k)$ with node v_0 as its root node. The rooted graph $\bar{\mathcal{G}}^k$ is called the maximal graph of $\bar{\mathcal{G}}(t) = (\bar{V}, \bar{\mathcal{E}}(t))$ over $[t_k, t_k + h]$.

Conceptually speaking, for a maximally connected graph, there exists a sufficiently long time interval $[t, t + h]$ such that each agent receives information from the leader either directly or indirectly through other agents during its duration h.

Remark 4
There are different categories of time-varying graphs present in the literature:

1. Frequently connected graph with period T: if $\forall t$, $\exists t^* \in [t, t + T)$, such that the graph is strongly connected at t^* [28, 29].
2. Jointly (Uniformly) connected graph: if the union of the switching graphs over a time interval forms a strongly connected graph [4, 30].
3. Periodically switching graph: if the graph switches among a set of topologies periodically [31].

It is instructive to compare now maximally connected graphs with the above-defined types. 1. Frequently connected graph is completely different from maximally connected graph in the sense that the frequently connected graph needs to be strongly connected at some time in each interval while the maximally connected graph does not. 2. On the other hand, the maximally and jointly connected graphs are indeed similar in topology but differ in their edge weights. The edge weights in the maximal graph are obtained as the maximum of the weights of the switching graph while in the jointly connected graph those are obtained by averaging of the weights. 3. Periodically switching graph switches between elements of a fixed set of graph topologies periodically while in the maximally connected graph, the set of switching topologies might be different from one period to another. We emphasize that here we define the edge weights by the maximum operation instead of averaging which is commonly used in the jointly connected and periodically switching graphs [4, 30, 31]. Finally, note that the above definitions are given for the graph of followers and they can be easily extended to the augmented graph by replacing the condition of "strongly connected" with the condition of "existence of a spanning tree with the leader as the root node".

DOI: 10.1002/rnc

Theorem 5
Consider a group of linear heterogeneous systems defined in (5-11) communicating over the augmented graph $\bar{\mathcal{G}}_{\sigma(t)} = (\bar{V}, \bar{\mathcal{E}}_{\sigma(t)})$. Let Assumptions 1-3 hold and A_i be marginally stable. Let $\bar{\mathcal{G}}_{\sigma(t)}$ be maximally connected over $[t_k, t_k + h]$ for $k = 0, 1, ..., +\infty$ where $t_0 = 0$, $t_{k+1} = t_k + h$ and $0 < h < +\infty$. Let $\bar{Z}_k$ be the normalized adjacency matrix of the maximal graph of $\bar{\mathcal{G}}_{\sigma(t)}$ over $[t_k, t_k + h]$ and $\underline{\gamma_z} = {}^1/_{\max_k \rho(\bar{Z}_k)}$. If the controller gains $\hat{K}_i$ are designed such that

$$\|\hat{D}_i(sI - A_i^c)^{-1}\hat{B}_i\hat{K}_i\|_\infty < \underline{\gamma_z}, \tag{53}$$

for $i = 1, ..., N$, then the multi-agent system (5-11) achieves H_∞ y-output regulation.

Proof
We first prove the $\mathcal{L}_2$-stability and then, the y-output regulation for the $\omega-$disturbance-free system.

The proof of $\mathcal{L}_2$-stability: We prove the $\mathcal{L}_2$-stability of the overall closed-loop system (5-11) over $[t_k, t_k + h]$ for $k = 0, 1, ..., +\infty$. Let Ω_i^k denote the normalizing factor of node i in the maximal graph $\bar{\mathcal{G}}^k = (\bar{V}, \bar{\mathcal{E}}^k)$. Let $\alpha_{ij}^k = \max_{t_k \le t \le t_k+h} \alpha_{ij}(t)$, $g_i^k = \max_{t_k \le t \le t_k+h} g_i(t)$, $\Omega_i^k = \sum_{j=1}^N \alpha_{ij}^k + g_i^k$ and $\bar{Z}_k = [\frac{\bar{\alpha}_{ij}^k}{\Omega_i^k}]$. Let $K_i^k = \frac{1}{\Omega_i^k}\hat{K}_i$. The overall closed-loop system (28) is written as

$$\begin{aligned}
r_i &= \frac{1}{\Omega_i^k} \sum_{j \in N_i(t)} \alpha_{ij}(t)\delta_{z_j}, \\
\dot{\bar{x}}_i &= A_i^c\bar{x}_i + \hat{B}_i\hat{K}_i r_i + \hat{P}_i\omega_i, \\
\delta_{zi} &= z_i - z_0 = \hat{D}_i\bar{x}_i, \\
\delta_{yi} &= y_i - y_0 = \hat{C}_i\bar{x}_i.
\end{aligned} \tag{54}$$

Let $F_{i22}(s) = \hat{D}_i(sI - A_i^c)^{-1}\hat{B}_i\hat{K}_i$ and $f_{i22}(t) = \mathfrak{L}^{-1}(F_{i22}(s))$ be a system with input r_i and output δ_{zi} and $f_{22}(t) = \underset{1:N}{Diag}\{f_{i22}(t)\}$. Let $Q_1(t) = (Z_g(t) \otimes I_q)f_{22}(t) = [q_{1ij}(t)]$, where $q_{1ij}(t) = \frac{\alpha_{ij}(t)}{\Omega_i^k} f_{j22}(t)$.

Set $k = 0$. According to Lemma 1, the $\mathcal{L}_2$-stability of the closed-loop system (54) is guaranteed by $\rho([\beta_2(q_{1ij})]) < 1$. Now, we use (2) to calculate $\beta_2(q_{1ij})$

$$\begin{aligned}
\beta_2(q_{1ij}) &= \sup_{T \ge 0} \sup_{r_j \ne 0} \frac{\|\frac{\alpha_{ij}(t)}{\Omega_i^0}\delta_{zj}(t)\|_{\mathcal{L}_{2e}}}{\|r_j(t)\|_{\mathcal{L}_{2e}}}, \\
\|\delta_{zj}(t)\frac{\alpha_{ij}(t)}{\Omega_i^0}\|_{\mathcal{L}_{2e}} &= \frac{1}{\Omega_i^0}\Big(\int_0^T \delta_{zj}(\tau)^2\alpha_{ij}^2(\tau)d\tau\Big)^{0.5}.
\end{aligned}$$

To show the $\mathcal{L}_2$-stability of the overall closed-loop system (54) over $[0, h]$, we assume $\alpha_{ij}(t) = 0$, $t > h$. Then,

$$\begin{aligned}
\beta_2(q_{1ij}) &= \frac{1}{\Omega_i^0} \sup_{T \ge 0} \sup_{r_j \ne 0} \frac{(\int_0^T \delta_{zj}^2(\tau)\alpha_{ij}^2(\tau)d\tau)^{0.5}}{\|r_j(t)\|_{\mathcal{L}_{2e}}} \le \frac{1}{\Omega_i^0} \sup_{T \ge 0} \sup_{r_j \ne 0} \frac{(\int_0^T \delta_{zj}^2(\tau)(\alpha_{ij}^0)^2d\tau)^{0.5}}{\|r_j(t)\|_{\mathcal{L}_{2e}}} \\
&= \frac{1}{\Omega_i^0}\alpha_{ij}^0 \sup_{T \ge 0} \sup_{r_j \ne 0} \frac{\|\delta_{zj}(t)\|_{\mathcal{L}_{2e}}}{\|r_j(t)\|_{\mathcal{L}_{2e}}} = \frac{1}{\Omega_i^0}\alpha_{ij}^0\beta_2(f_{j22}).
\end{aligned}$$

Hence we have $\beta_2(q_{1ij}) \le \frac{1}{\Omega_i^0}\alpha_{ij}^0\beta_2(f_{j22}) = \frac{1}{\Omega_i^0}\alpha_{ij}^0\|F_{j22}(s)\|_\infty$ where the last equality is due to the fact that the $\mathcal{L}_2$-gain of a stable linear system is equivalent to its H_∞ norm [24]. According to Lemmas 1-4, a sufficient condition for $\mathcal{L}_2$-stability is

$$\rho([\beta_2(q_{1ij})]) \le \rho([\|F_{j22}\|_\infty \frac{\alpha_{ij}^0}{\Omega_i^0}]) \le \max_j \|F_{j22}\|_\infty \rho(\bar{Z}_0) < 1, \Rightarrow \|F_{j22}\|_\infty < \frac{1}{\rho(\bar{Z}_0)}.$$

DOI: 10.1002/rnc

One can repeat the above procedure for $t \in [t_k, t_k + h],\ k = 1, ..., +\infty$. The $\mathcal{L}_2$-stability condition for the kth time interval is given by $\|F_{j22}\|_\infty < {}^1/_{\rho(\bar{Z}_k)}$. As a result, the system is $\mathcal{L}_2$-stable if (53) holds.

The proof of y-output regulation: Next, we prove that the $\omega-$disturbance-free system, $\omega \equiv 0$, achieves y-output regulation. For this purpose, we prove properties 1-2 in Problem 1 by showing that $\bar{x}_j \to 0$ and $\delta_{yi} \to 0$ as $t \to +\infty$ for a generally nonzero exo-system's state. The requirement $\delta_{yi} \to 0$ is exactly property 2 in Problem 1 and $\bar{x}_j \to 0$ implies property 1 when $\xi_0 \equiv 0,\ d \equiv 0$. To see the latter, if $\xi_0 \equiv 0,\ d \equiv 0$, by the definition of the coordinate transformations in Subsection 3.2, we have $\bar{x}_j = T_j^{-1} x_j$ for T_j in (26). In other words, when $\xi_0 \equiv 0,\ d \equiv 0$, $\bar{x}_j \to 0$ implies $x_j \to 0$ which is property 1.

The $\mathcal{L}_2$-stability of the overall closed-loop system (28) generally implies that $\bar{x}_j,\ \delta_{yj} \in \mathcal{L}_2$. To show $\bar{x}_j(t),\ \delta_{yj}(t) \to 0$ as $t \to +\infty$, we use Lemma 5 (Barbalat's Lemma) and we only need to prove that $\dot{\bar{x}}_j,\ \dot{\delta}_{yj} = \hat{C}_j \dot{\bar{x}}_j = \hat{C}_j \hat{A}_j \bar{x}_j + \hat{C}_j \hat{B}_j u_j, j = 1, ..., N$ are bounded. In an interval $0 < \triangle t \leq h < +\infty$ where the communication graph is fixed, we divide the nodes into two subgroups: the first subgroup, denoted by V_1, containing the nodes that do not have any incoming edge from the neighbors and the second subgroup containing the remaining nodes $V_2 = V \setminus V_1$. For $j \in V_1$, we have $u_j = 0$ and $\dot{\bar{x}}_j = \hat{A}_j \bar{x}_j,\ \dot{\delta}_{yj} = \hat{C}_j \hat{A}_j \bar{x}_j$ remain bounded because A_j is marginally stable. The remaining nodes, $j \in V_2$, are interconnected and the closed-loop system of them in (54) is strictly stable by means of (53). This guarantees boundedness of $\bar{x}_j,\ r_j$ for $j \in V_2$ and subsequently $\dot{\bar{x}}_j = A_j^c \bar{x}_j + \hat{B}_j \hat{K}_j r_j,\ \dot{\delta}_{yj} = \hat{C}_j \dot{\bar{x}}_j$. This means that $\dot{\bar{x}}_j,\ \dot{\delta}_{yj}$ are bounded for all intervals where the communication graph is fixed. Hence by Lemma 5, $\lim_{t\to+\infty} \bar{x}_j(t) = 0,\ \lim_{t\to+\infty} \delta_{yj}(t) = 0,\ j = 1, ..., N$ and the $\omega-$disturbance-free multi-agent system achieves y-output regulation. □

Remark 5

The topology of the maximal graph might not be completely known in practice. In this case, one can consider the maximal graph as an augmented complete graph where the subgraph of the followers is complete and the leader pins to all the follower nodes. The reason for this is that any possible rooted topology over a finite set of N follower nodes and one leader can be considered as a subgraph of an augmented complete graph. Select the normalizing factor for each node i as $\Omega_i^k = N$. Then, the normalized adjacency matrix of the maximal graph is given by $\bar{Z}_k = \frac{1}{N}(\mathbf{1}_N \mathbf{1}_N^T - I_N)$. Since all entries of $\bar{Z}_k$ are nonnegative, $\rho(\bar{Z}_k) \in Spec(\bar{Z}_k)$ (Theorem 8.3.1 of [18]). One has

$$\lambda_i \left(\frac{1}{N}(\mathbf{1}_N \mathbf{1}_N^T - I_N) \right) = \frac{1}{N}\{\underbrace{-1, ..., -1}_{N-1}, N-1\}, \tag{55}$$

and hence, the spectral radius of an augmented complete graph is given by $\rho(\bar{Z}_k) = \frac{N-1}{N}$. In short, one can use the conservative bound in (55) to guarantee the sufficient condition for H_∞ output regulation over switching graphs when the topology of the maximal graph is completely unknown.

Remark 6

The sufficient condition for H_∞ output regulation over switching graph (53) is more stringent than the one over a static graph (31). According to Theorem 5, the H_∞-norm of the single-agent system in (53) should be bounded by $\underline{\gamma_z} = {}^1/_{\max_k \rho(\bar{Z}_k)}$. This condition is harder to satisfy than (31) when the topology of the maximal graph is not perfectly known in advance, because one then needs to resort to a conservative estimate of $\underline{\gamma_z}$, like the one we bring for the completely unknown switching graph in Remark 5. Moreover, similar to [4], the agent's dynamics in the case of switching graphs needs to be marginally stable to ensure that the agent's trajectory remains bounded when there is no distributed control acting on the agent (see the definition of V_1 in the proof of Theorem 5).

Remark 7

Similarly as for sufficient condition (31), one can satisfy the H_∞ criterion for switching graphs (53) by designing the controller gains $\hat{K}_i$, as detailed in Theorem 4, or by specifying the structure of the drift dynamics A_i, as detailed in Theorem 2, by using the upper bound ${}^1/_{\max_k \rho(\bar{Z}_k)}$ instead of ${}^1/_{\rho(Z_g)}$.

6. SIMULATION RESULTS

Consider a set of five followers and one leader. The leader's dynamics and the modeled disturbance's dynamics are described by the following

$$\text{Leader :} \qquad X=\begin{bmatrix}0 & 1\\ -1 & 0\end{bmatrix},\ R_1=\begin{bmatrix}1 & 0\\ 0 & 1\end{bmatrix},\ R_2=\begin{bmatrix}1 & 1\end{bmatrix},$$

$$\text{Modeled disturbance :} \qquad S=\begin{bmatrix}0 & 1\\ -10 & 0\end{bmatrix},$$

The followers' dynamics are given as

$$f_{1,3,5}: \quad A_1=\begin{bmatrix}0 & 1 & 2\\ -1 & 0 & 3\\ 0 & 0 & -7\end{bmatrix},\ B_1=\begin{bmatrix}0\\ 1\\ 0\end{bmatrix},\ P_1=\begin{bmatrix}0\\ 1\\ 0\end{bmatrix},\ Q_1=\begin{bmatrix}-4 & 2\\ -15 & 3\\ 24 & -5\end{bmatrix},$$

$$C_1=\begin{bmatrix}1 & 0 & 1\\ 0 & 1 & 1\end{bmatrix},\ D_1=\begin{bmatrix}1 & 1 & 1\end{bmatrix},\ H_1=\begin{bmatrix}-3 & 1-2 & 0\end{bmatrix},\ J_1=\begin{bmatrix}-3 & 0\end{bmatrix},$$

$$f_{2,4}: \quad A_2=\begin{bmatrix}0 & 1 & 1 & 1\\ -1 & 0 & 0 & 2\\ 0 & 0 & 0 & 1\\ 0 & 0 & -1 & -1\end{bmatrix},\ B_2=\begin{bmatrix}2\\ 1\\ 0.1\\ 1\end{bmatrix},\ P_2=\begin{bmatrix}1\\ 0\\ 0\\ -1\end{bmatrix},\ Q_2=\begin{bmatrix}-3 & 0\\ -11 & -2\\ 9 & 1\\ -7 & 1\end{bmatrix},$$

$$C_2=\begin{bmatrix}1 & 0 & 0 & 2\\ 0 & 1 & -1 & 1\end{bmatrix},\ D_2=\begin{bmatrix}1 & 1 & 1 & 0\end{bmatrix},\ H_2=\begin{bmatrix}-3 & -21 & -3\end{bmatrix},\ J_2=\begin{bmatrix}-3 & 0\end{bmatrix}.$$

Our aim is to design the controller gain in (12) such that the agents achieve H_∞ output synchronization to the output of the leader in (9)-(11) in presence of umodeled disturbances $\omega_i,\ i=1,...,N$, while the effect of the modeled disturbance d in (8) is rejected. Simple calculations reveal that

$$\Pi_{1i}=\begin{bmatrix}1 & 0\\ 0 & 1\\ 2 & -1\end{bmatrix},\ \Pi_{2i}=\begin{bmatrix}1 & 0\\ 0 & 1\\ 0 & 0\end{bmatrix},\ \Psi_i=\begin{bmatrix}0\\ 0\\ 1\end{bmatrix},\ i=1,3,5,$$

$$\Pi_{1j}=\begin{bmatrix}1 & 0\\ 0 & 1\\ 2 & -1\\ 1 & 1\end{bmatrix},\ \Pi_{2j}=\begin{bmatrix}1 & 0\\ 0 & 1\\ 0 & 0\\ 0 & 0\end{bmatrix},\ \Psi_j=\begin{bmatrix}0 & 0\\ 0 & 0\\ 1 & 0\\ 0 & 1\end{bmatrix},\ j=2,4.$$

The switching communication graph for $\mod(t,2)<1$ and $1\leq \mod(t,2)<2$ is depicted in Fig. 2a and 2b respectively. According to Definition 1, the switching graph is maximally connected and for $h=2$

$$\bar{Z}_k=\begin{bmatrix}0 & \frac{1}{3} & 0 & 0 & \frac{1}{3}\\ 1 & 0 & 0 & 0 & 0\\ \frac{1}{3} & \frac{1}{3} & 0 & \frac{1}{3} & 0\\ 0 & 0 & 0 & 0 & 1\\ 0 & 0 & 1 & 0 & 0\end{bmatrix},$$

and $\rho(\bar{Z}_k)=0.9009$. Feasible solutions to (42-44) for each follower are

$$P^L_{1,3,5}=\begin{bmatrix}0.590 & 0.165 & 0.048\\ 0.165 & 0.343 & -0.032\\ 0.048 & -0.032 & 0.542\end{bmatrix},\qquad Q^L_{1,3,5}=\begin{bmatrix}1.986 & -0.977 & -0.235\\ -0.977 & 3.412 & 0.288\\ -0.235 & 0.288 & 1.885\end{bmatrix},$$

$$P^L_{2,4}=\begin{bmatrix}0.918 & -0.140 & 0.813 & 0.589\\ -0.140 & 0.754 & 0.035 & 0.457\\ 0.813 & 0.035 & 3.576 & 0.661\\ 0.589 & 0.457 & 0.661 & 4.114\end{bmatrix},\quad Q^L_{2,4}=\begin{bmatrix}1.931 & 0.457 & -0.629 & -0.173\\ 0.457 & 1.562 & -0.093 & -0.272\\ -0.629 & -0.093 & 0.632 & -0.016\\ -0.173 & -0.272 & -0.016 & 0.505\end{bmatrix}.$$

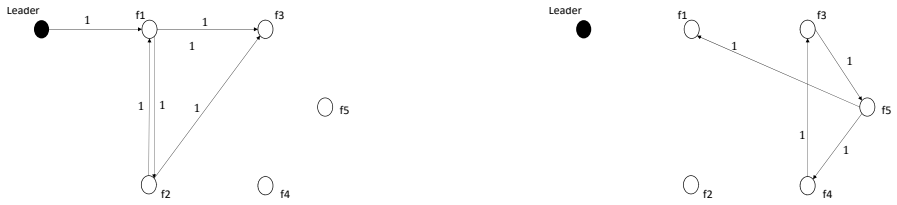

(a) when $\mod(t,2) < 1$ (b) when $1 \leq \mod(t,2) < 2$

Figure 2. The switching communication graph

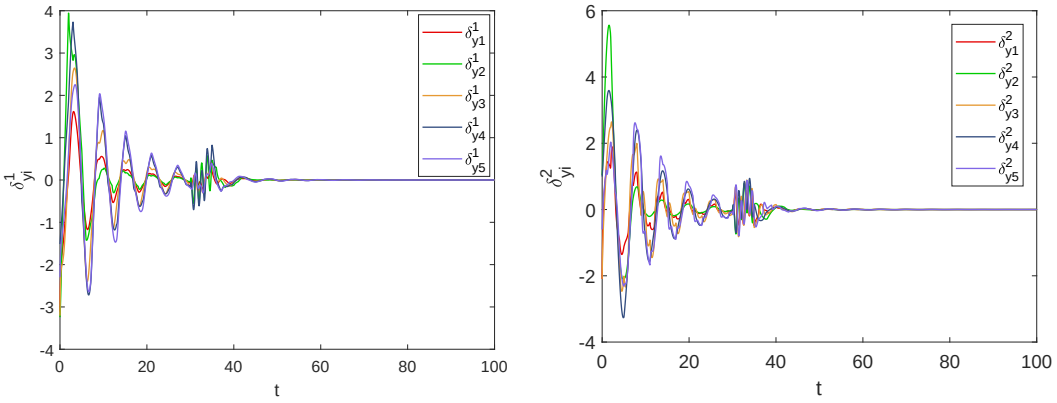

(a) The first component of δ_{yi}, i.e., δ^1_{yi} (b) The second component of δ_{yi}, i.e., δ^2_{yi}

Figure 3. The output regulation error δ_{yi} over the switching graph in Fig. 2 for $i = 1, ..., N$

After finding Q_i^L and P_i^L, the gains $\hat{K}_i$ are obtained as feasible solutions to (45) which are $\hat{K}_{1,3,5} = 4.5409$ and $\hat{K}_{2,4} = 0.3630$. Each controller gain K_i is obtained from $K_i = \frac{1}{\Omega_i}\hat{K}_i$, which are $K_{1,3} = 1.5136,\ K_{2,4} = 0.3630,\ K_5 = 4.5409$. For the simulation, we assume that all followers are subject to the following unmodeled disturbance

$$\omega_i = \begin{cases} 2\sin(5t), & 30 \leq t \leq 35 \\ 0, & \text{otherwise.} \end{cases}$$

Figure 3 depicts the H_∞ output regulation of the multi-agent system in the mentioned setup. The initial conditions for all followers and the leader are selected randomly.

7. CONCLUSION

In this paper, we have analyzed H_∞ output regulation of linear heterogeneous multi-agent systems subject to modeled and unmodeled disturbances over switching graphs. We have defined the concept of maximally connected graphs and proved that the multi-agent system achieves H_∞ output regulation if the switching graph is maximally connected. We have derived a single-agent sufficient condition that guarantees H_∞ output regulation and obtained an upper bound for the overall $\mathcal{L}_2$-gain of the output synchronization error with respect to unmodeled disturbances when the communication graph is fixed. In all aforementioned results, we have used the simplest form of the controller (a static distributed output-feedback controller) in a general framework; namely, the communication graph might be switching and cyclic, no p-copy of the leader is incorporated as a part of the controller and no observer is designed to estimate the trajectory of the leader.

ACKNOWLEDGMENT

This paper is supported by the GACR grant 16-25493Y, ONR grant N00014-17-1-2239, China NSFC grant 61633007, the ATMRI-CAAS Project on Air Traffic Flow Management with the project reference number ATMRI:2014-R7-SU and the European Regional Development Fund under the project Rob4Ind4.0 (reg. no. CZ.02.1.01/0.0/0.0/15_003/0000470).

REFERENCES

1. J. Huang, *Nonlinear output regulation: Theory and applications*. SIAM, 2004, vol. 8.
2. A. Saberi, A. A. Stoorvogel, and Z. Lin, "Generalized output regulation for linear systems," in *American Control Conference, 1997. Proceedings of the 1997*, vol. 6. IEEE, 1997, pp. 3909–3914.
3. S.-J. Lee, K.-K. Oh, and H.-S. Ahn, "Non-trivial output synchronization of heterogeneous passive systems," *Automatic Control, IEEE Transactions on*, vol. 60, no. 12, pp. 3322–3327, 2015.
4. P. Wieland, R. Sepulchre, and F. Allgöwer, "An internal model principle is necessary and sufficient for linear output synchronization," *Automatica*, vol. 47, no. 5, pp. 1068–1074, 2011.
5. X. Wang, Y. Hong, J. Huang, and Z.-P. Jiang, "A distributed control approach to a robust output regulation problem for multi-agent linear systems," *Automatic Control, IEEE Transactions on*, vol. 55, no. 12, pp. 2891–2895, 2010.
6. J. Lunze, "Synchronization of heterogeneous agents," *IEEE transactions on automatic control*, vol. 57, no. 11, pp. 2885–2890, 2012.
7. F. Adib Yaghmaie, F. L. Lewis, and R. Su, "Output regulation of heterogeneous linear multi-agent systems with differential graphical game," *International Journal of Robust and Nonlinear Control*, vol. 26, pp. 2256–2278, 2016.
8. ——, "Output regulation of linear heterogeneous multi-agent systems via output and state feedback," *Automatica*, vol. 67, pp. 157–164, 2016.
9. C. Huang and X. Ye, "Cooperative output regulation of heterogeneous multi-agent systems: An H_∞ criterion," *Automatic Control, IEEE Transactions on*, vol. 59, pp. 267–273, 2014.
10. Y. Su, Y. Hong, and J. Huang, "A general result on the robust cooperative output regulation for linear uncertain multi-agent systems," *Automatic Control, IEEE Transactions on*, vol. 58, no. 5, pp. 1275–1279, 2013.
11. Y. Liu and Y. Jia, "Robust H_∞ consensus control of uncertain multi-agent systems with time delays," *International Journal of Control, Automation and Systems*, vol. 9, no. 6, pp. 1086–1094, 2011.
12. X. Yang and J. Wang, "Finite-gain $\mathcal{L}_p$ consensus of multi-agent systems," *International Journal of Control, Automation and Systems*, vol. 11, no. 4, pp. 666–674, 2013.
13. Y. Liu and Y. Jia, "H_∞ consensus control of multi-agent systems with switching topology: a dynamic output feedback protocol," *International Journal of Control*, vol. 83, no. 3, pp. 527–537, 2010.
14. F. Adib Yaghmaie, K. Henster Movric, F. L. Lewis, R. Su, and M. Sebek, "Output H_∞ synchronization of heterogeneous linear multi-agent systems via a distributed output feedback," in *Decision and Control (CDC), 2016 IEEE 55th Conference on*, 2016, pp. 2677–2682.
15. Q. Jiao, H. Modares, F. L. Lewis, S. Xu, and L. Xie, "Distributed L_2-gain output-feedback control of homogeneous and heterogeneous systems," *Automatica*, vol. 71, pp. 361–368, 2016.
16. M. Zhang, A. Saberi, and A. A. Grip, Havard F.and Stoorvogel, "H_∞ almost output synchronization for heterogeneous networks without exchange of controller states," *IEEE transactions on control of network systems*, vol. 2, no. 4, pp. 348–357, 2015.
17. Vidyasagar, *Input-Output Analysis of Large-Scale Interconnected Systems*, Vidyasagar, Ed. Springer Berlin Heidelberg, 1981.
18. R. A. Horn and C. R. Johnson, *Matrix analysis*. Cambridge university press, 2012.
19. J.-J. E. Slotine, W. Li *et al.*, *Applied nonlinear control*. prentice-Hall Englewood Cliffs, NJ, 1991, vol. 199, no. 1.
20. A. Isidori, *Nonlinear control systems*. Springer Science & Business Media, 2013.
21. Z. Meng, T. Yang, D. V. Dimarogonas, and K. H. Johansson, "Coordinated output regulation of heterogeneous linear systems under switching topologies," *Automatica*, vol. 53, pp. 362–368, 2015.
22. H. F. Grip, T. Yang, A. Saberi, and A. A. Stoorvogel, "Output synchronization for heterogeneous networks of non-introspective agents," *Automatica*, vol. 48, no. 10, pp. 2444–2453, 2012.
23. Y. Su and J. Huang, "Cooperative output regulation of linear multi-agent systems," *Automatic Control, IEEE Transactions on*, vol. 57, no. 4, pp. 1062–1066, 2012.
24. H. K. Khalil, *Noninear Systems*. Prentice-Hall, New Jersey, 1996, vol. 2, no. 5.
25. S. P. Boyd, L. El Ghaoui, E. Feron, and V. Balakrishnan, *Linear matrix inequalities in system and control theory*. SIAM, 1994, vol. 15.
26. L. El Ghaoui, F. Oustry, and M. AitRami, "A cone complementarity linearization algorithm for static output-feedback and related problems," *Automatic Control, IEEE Transactions on*, vol. 42, no. 8, pp. 1171–1176, 1997.
27. R. Olfati-Saber, J. A. Fax, and R. M. Murray, "Consensus and cooperation in networked multi-agent systems," *Proceedings of the IEEE*, vol. 95, no. 1, pp. 215–233, 2007.
28. Z. Lin, M. Broucke, and B. Francis, "Local control strategies for groups of mobile autonomous agents," *IEEE Transactions on automatic control*, vol. 49, no. 4, pp. 622–629, 2004.
29. J. Wang, D. Cheng, and X. Hu, "Consensus of multi-agent linear dynamic systems," *Asian Journal of Control*, vol. 10, no. 2, pp. 144–155, 2008.
30. A. Jadbabaie, J. Lin, and A. S. Morse, "Coordination of groups of mobile autonomous agents using nearest neighbor rules," *IEEE Transactions on automatic control*, vol. 48, no. 6, pp. 988–1001, 2003.
31. M. Porfiri, D. G. Roberson, and D. J. Stilwell, "Tracking and formation control of multiple autonomous agents: A two-level consensus approach," *Automatica*, vol. 43, no. 8, pp. 1318–1328, 2007.

5. DIFFERENTIAL GRAPHICAL GAMES FOR H_∞ CONTROL OF LINEAR HETEROGENEOUS MULTI-AGENT SYSTEMS

Farnaz Adib Yaghmaie, Kristian Hengster Movric, Frank L. Lewis, Rong Su, **Differential Graphical Games for H_∞ Control of Linear Heterogeneous Multi-agent Systems,** *submitted to IJRNC, 2018, pp.1-20.*

Building further on the revealed necessary and sufficient geometrical structure of general heterogeneous single-agents required for output-synchronization over general outputs, this chapter shows how their synchronization and disturbance suppression problems can be cast in the form of a $N/2N$ player graphical games. Graphical games were introduced in the literature, starting in 2010, to deal with homogeneous agent state synchronization and the corresponding L_2-bound, but as these novel results show, they are equally applicable in this more general context.

Differential graphical games have been introduced in the literature to solve state synchronization problem for linear homogeneous agents. When the agents are heterogeneous, the previous notion of graphical games cannot be used anymore and a new definition is required. In this chapter, a novel concept of differential graphical games is defined for linear heterogeneous agents subject to external unmodelled disturbances, which contain the previously introduced graphical games for homogeneous agents as a special case. Using the new formulation, one can solve both the output regulation and H_∞ output regulation problems. Proposed graphical game framework yields coupled Hamilton-Jacobi-Bellman equations which are, in general, impossible to solve analytically. Therefore, a new actor-critic algorithm is proposed to solve these coupled equations numerically in real-time. Moreover, an explicit upper bound is found for the overall L_2-gain of the output synchronization error with respect to disturbance. These developments are demonstrated by a simulation example.

INTERNATIONAL JOURNAL OF ROBUST AND NONLINEAR CONTROL
Int. J. Robust. Nonlinear Control 2018; **00**:1–20
Published online in Wiley InterScience (www.interscience.wiley.com). DOI: 10.1002/rnc

Differential Graphical Games for H_∞ Control of Linear Heterogeneous Multi-agent Systems

Farnaz Adib Yaghmaie [1], Kristian Hengster Movric [2], Frank L. Lewis[3], Rong Su [1]

[1]*School of Electrical & Electronic Engineering, Nanyang Technological University, Singapore,*
[2]*Department of Control Engineering, Faculty of Electrical Engineering, Czech Technical University in Prague, Prague, Czech,*
[3]*University of Texas at Arlington Research Institute, The University of Texas at Arlington, Texas, USA and Qian Ren Consulting Professor, Northeastern University, Shenyang 110036, China.*

SUMMARY

Differential graphical games have been introduced in the literature to solve state synchronization problem for linear homogeneous agents. When the agents are heterogeneous, the previous notion of graphical games cannot be used anymore and a new definition is required. In this paper, we define a novel concept of differential graphical games for linear heterogeneous agents subject to external unmodelled disturbances which contain the previously introduced graphical game for homogeneous agents as a special case. Using our new formulation, we can solve both the output regulation and H_∞ output regulation problems. Our graphical game framework yields coupled Hamilton-Jacobi-Bellman equations which are, in general, impossible to solve analytically. Therefore, we propose a new actor-critic algorithm to solve these coupled equations numerically in real time. Moreover, we find an explicit upper bound for the overall $\mathcal{L}_2$-gain of the output synchronization error with respect to disturbance. We demonstrate our developments by a simulation example. Copyright © 2018 John Wiley & Sons, Ltd.

Received . . .

1. INTRODUCTION

The next generation of networked systems is currently emerging from a number of different engineering domains. We already have examples of Internet of Things (IoT), Industry 4.0, smart cities and various other cyber-physical systems characterized by the requirement to coordinate efforts across large networks of different agents. In the near future, these systems are expected to increase in importance, with an ever-widening range of applications. Main design goals there are versatility, flexibility, easy real time reconfigurability, low communication burden, along with robustness to component failures and resilience to disturbances. These complex interconnected multi-agent systems create the need for novel team decision, distributed control, optimization and online computation methodologies.

A multi-agent system is defined as a group of interconnected dynamical systems interacting to achieve a desired collective behavior like state synchronization [1, 2, 3], output regulation [4, 5, 6], formation control [7], etc. The canonical distributed control problem of state synchronization is usually defined for homogeneous agents where it is possible to use the local state synchronization error [1, 2, 3]. If the agents are *heterogeneous*, meaning that they have different internal dynamics,

*Correspondence to: Farnaz Adib Yaghmaie, School of Electrical & Electronic Engineering, 50 Nanyang Avenue, Singapore 639798. Email: farnaz001@e.ntu.edu.sg. Phone: +46-762909978.

it is not generally meaningful to achieve state synchronization; instead, one may consider an output regulation problem where a distributed controller is designed such that the outputs of all agents synchronize to a reference trajectory while the effect of *modeled disturbances*, i.e. disturbance with known dynamic model, is rejected. In these cases, the dynamics of the reference trajectory and the disturbance model are usually combined into a single dynamic model named *exo-system* in the literature [8, 4]. One possible solution to such output regulation problems is by the means of *Internal Model Principle (IMP)* where the idea is to incorporate an internal model of the exo-system in the dynamic controller of each agent [8, 9, 10, 4, 6]. If the agents are additionally subject to *unmodeled disturbances* then the IMP alone cannot be used for disturbance rejection and H_∞ control methods are required. A significant part of the research on H_∞ control of multi-agent systems is on H_∞ state synchronization of homogeneous agents [11, 12] and more recently H_∞ output regulation of heterogeneous agents [13, 14, 15].

In the context of multi-agent systems, various optimization methods are utilized to achieve the required design characteristics. One has the conventional centralized optimization [16, 17] as well as more recent distributed approaches [18, 19] aiming at flexibility, reconfigurability, and robustness. The optimal control of a single dynamic system, also called a *single-player game* [20, 21], is the simplest dynamic optimization problem. However, this approach is usually found lacking in robustness to external disturbances acting on the system and possibly subsystem failures. The optimal control of a dynamic system subject to unmodelled disturbance is termed *two-player zero-sum game* where dynamic system player tries to minimize a cost function while the disturbance player maximizes it [22, 23]. More recently, the idea of *graphical game* is introduced to capture and exploit the locality and influences of dynamic systems on each other. In graphical games, the dynamics and the objective function of each player are influenced by other players in the neighborhood. A graphical game for *homogeneous agents* i.e. agents with the identical internal dynamics is suggested in [18] to achieve state synchronization using local state synchronization error. This concept is extended to H_∞ graphical game where the agents are subject to external disturbances [19]. These graphical games provide a suitable platform for distributed optimal controller designs for the identical agents. The choice of individual player objective function, as discussed above, ensures that the multi-agent system achieves the desired collective behavior e.g. state or H_∞-state synchronization [18, 19].

Reinforcement Learning (RL) is concerned with learning optimal policies from interaction with an environment [24]. In RL, a decision-making system modifies its control policy based on the stimuli received in response to its previous policies to optimize the cost. In this sense, RL implies a cause and effect relationship between policies and costs [25], and as such, RL based frameworks enjoy optimality and adaptivity. Over the past few years, dynamic programming is utilized to develop RL techniques for adaptive-optimal control of dynamic systems, see [20, 22, 23, 17, 18, 19] to name a few. Hence, RL is by now fairly standard in solving the single-player optimal and robust control problems [20, 21]. However, as of recently, RL can also be used to tackle even more complicated optimization structures like multiple interconnected dynamics system, namely a multi-player game, where a single centralized dynamics contains the dynamics of all players [16, 17]. Likewise, RL methods have also been successfully applied in graphical games [18, 19]. Moreover, faced with complicated coupled design equations arising from such problems, RL remains the only viable method applicable in real time. Such recent approaches are particularly appropriate for problems arising from the domain of multi-agent systems.

In this paper, we aim to develop a novel graphical game framework for linear heterogeneous multi-agent systems. For this purpose, we bring together distributed control of heterogeneous multi-agent systems, graphical games, and reinforcement learning techniques. There are four main contributions in this paper. (1) We define the novel concept of graphical games for heterogeneous agents as opposed to homogeneous agents considered in [18, 19]. This allows us to achieve output regulation among heterogeneous agents. Graphical game for heterogeneous agents is also considered in [10], however, the communication graph in [10] is required to be acyclic (i.e. there is no-loop in the graph). This restrictive assumption significantly simplifies the formulation and decouples the controller design of each agent from the others. (2) We assume that the agents are

subject to unmodeled disturbances and define an H_∞ graphical game for heterogeneous agents. The only reference pertaining to H_∞ control of multi-agent systems in the graphical game framework [19] considers only homogeneous agents. (3) H_∞ graphical game for heterogeneous agents results in coupled Hamilton-Jacobi-Bellman equations that are difficult to solve analytically. We use RL and develop new actor-critic networks to obtain solutions to these equations. In contrast, the actor-critic networks in [18, 19] can be used only for homogeneous agents. (4) We obtain an upper bound for the $\mathcal{L}_2$-gain of output synchronization error with respect to unmodeled disturbances; in contrast to [19], which does not calculate the upper bound but only contends its existence.

The rest of the paper is organized as follows. In Section 2, we discuss notation conventions and review preliminaries. In Section 3, we define the H_∞ output regulation problem. In Section 4, we define the novel graphical games for linear heterogeneous agents. In Section 5, we present our results regarding H_∞ output regulation using graphical games and derive the resulting overall $\mathcal{L}_2$ gain of output synchronization error with respect to disturbances. In Section 6, we suggest a distributed online procedure for solving the H_∞ output regulation graphical game. We demonstrate the validity of theoretical developments with a simulation example in Section 7. We conclude the paper in Section 8.

2. PRELIMINARIES

2.1. Notation

The following notation will be used throughout this paper. Let $\mathbb{R}^{n\times m}$ be the set of $n \times m$ real matrices. I_n denotes the identity matrix of dimension $n \times n$ and $\mathbf{1}_N$ is an N column vector of 1. $\mathbf{0}$ denotes a matrix of zeros with compatible dimensions. The Kronecker product of two matrices A and B is denoted by $A \otimes B$. The positive (semi) definiteness constraint on the matrix P is expressed as $P > 0$ ($P \geq 0$). Let $A_i \in \mathbb{R}^{n_i\times m_i}$ for $i = 1, ..., N$, where N is a positive integer. The operator $\underset{1:N}{Diag}\{A_i\}$ is defined as

$$\underset{1:N}{Diag}\{A_i\} = \begin{bmatrix} A_1 & \mathbf{0} & \dots & \mathbf{0} \\ \mathbf{0} & A_2 & \dots & \mathbf{0} \\ \vdots & \mathbf{0} & \ddots & \vdots \\ \mathbf{0} & \mathbf{0} & \dots & A_N \end{bmatrix}. \tag{1}$$

The maximum singular value of a matrix A is denoted by $\overline{\sigma}(A)$ and its kernel is denoted by $Ker(A)$. An eigenvalue of a square matrix A is denoted by $\lambda_i(A)$.

2.2. $\mathcal{L}_p$-norm

For $p \in [1, +\infty)$, let $\mathcal{L}_p = \mathcal{L}_p^n[0, +\infty)$ denote the space of functions $a(t) \in \mathbb{R}^n$ such that $t \to |a(t)|^p$ is integrable over $[0, +\infty)$, where $|a(t)|$ is the instantaneous Euclidean norm of the vector $a(t)$. The $\mathcal{L}_p$-norm of $a(t) \in \mathcal{L}_p^n[0, \infty)$ is defined as

$$\|a(t)\|_{\mathcal{L}_p} = \left(\int_0^\infty |a(\tau)|^p d\tau\right)^{1/p} < +\infty.$$

2.3. Graph theory

Suppose that the interaction among the followers is represented by an undirected graph $\mathcal{G} = (V, \mathcal{E})$ with a finite set of N nodes $V = \{v_1, ..., v_N\}$ and a set of undirected edges $\mathcal{E} \subseteq V \times V$. $E = [\alpha_{ij}]$ is the *adjacency matrix* with $\alpha_{ij} = 1$ if $(v_j, v_i) \in \mathcal{E}$ and $\alpha_{ij} = 0$ otherwise. Since the graph is undirected, the adjacency matrix is symmetric. The graph is simple, *i.e.* $\alpha_{ii} = 0$, $i = 1, ..., N$. A *path* from node v_i to node v_j is a sequence of edges joining v_i to v_j. If there exists a path from node v_i to node v_j then it is said that node v_i is *reachable* from v_j. The set of *neighbors of node* v_i is

DOI: 10.1002/rnc

$N_i = \{v_j : (v_j, v_i) \in \mathcal{E}\}$. For graph $\mathcal{G}$, the *in-degree matrix* D is a diagonal matrix $D = \underset{1:N}{Diag}\{d_i\}$ with $d_i = \sum_{j \in N_i} \alpha_{ij}$. The *laplacian matrix* for graph $\mathcal{G}$ is defined as $L = D - E$. Suppose that matrix $G = \underset{1:N}{Diag}\{g_i\}$ shows the pinning from the leader (v_0) to the followers ($v_1, ..., v_N$). Then, $g_i = 1$ if there is a link between the leader and follower i and $g_i = 0$ otherwise. Denote the augmented graph by $\bar{\mathcal{G}} = (\bar{V}, \bar{\mathcal{E}})$ which is obtained by attaching node v_0 and its outgoing edges to $\mathcal{G}$. Graph $\bar{\mathcal{G}}$ shows the interaction among the followers and the leader.

A graph $\mathcal{G} = (V, \mathcal{E})$ is *connected* if there exists a path from v_i to v_j for all $v_i, v_j \in V$. If the initial and the terminal nodes of a path are the same, the path is called a *cycle*. A graph without any cycle is named an *acyclic graph*. A graph is a *connected tree* if every node except one node, called *the root*, has in-degree equal to one. The root node has its in-degree equal to zero. A graph has a *spanning tree* if there exists a tree containing every node in V.

3. H_∞ OUTPUT REGULATION PROBLEM

Consider a set of $N + 1$ heterogeneous agents with N followers given as LTI systems

$$\dot{x}_i = A_i x_i + B_i u_i + P_i \omega_i, \tag{2}$$
$$y_i = C_i x_i, \tag{3}$$
$$z_i = D_i x_i, \tag{4}$$

and a leader given by

$$\dot{\xi}_0 = X \xi_0, \tag{5}$$
$$y_0 = R_1 \xi_0, \tag{6}$$
$$z_0 = R_2 \xi_0, \tag{7}$$

in which $x_i \in \mathbb{R}^{n_i},\ y_i \in \mathbb{R}^p, z_i \in \mathbb{R}^q$ and $u_i \in \mathbb{R}^{m_i}$ denote the state, the synchronization output, the measured output and the control signal for follower $i = 1, ..., N$. The $\xi_0 \in \mathbb{R}^l,\ y_0 \in \mathbb{R}^p$ and $z_0 \in \mathbb{R}^q$ denote the state, the synchronization output and the measured output of the leader. All followers are subject to external unmodeled disturbances $\omega_i \in \mathcal{L}_2$. The motivation behind introducing two outputs $y_i,\ z_i$ is to achieve synchronization in outputs y_i, by communicating the measured outputs z_i.

We suggest a distributed static output-feedback controller of the following form

$$u_i = K_i e_{zi}, \tag{8}$$
$$e_{zi} = \sum_{j \in N_i} \alpha_{ij}(z_i - z_j) + g_i(z_i - z_0), \tag{9}$$

where e_{zi} is the local neighborhood error in z-outputs and $K_i \in \mathbb{R}^{m_i \times q}$. Define the y-output synchronization error and the z-output synchronization error as

$$\delta_{yi} = y_i - y_0, \tag{10}$$
$$\delta_{zi} = z_i - z_0. \tag{11}$$

Let $x = [x_1^T, ..., x_N^T]^T, y = [y_1^T, ..., y_N^T]^T, z = [z_1^T, ..., z_N^T]^T, \omega = [\omega_1^T, ..., \omega_N^T]^T, \delta_y = [\delta_{y1}^T, ..., \delta_{yN}^T]^T$ and $\delta_z = [\delta_{z1}^T, ..., \delta_{zN}^T]^T$ denote the overall vectors of $x_i, y_i, z_i, \omega_i, \delta_{yi}$ and δ_{zi} respectively. Then, the overall closed-loop system of all followers, their controllers and the leader is given by the following

$$\begin{aligned} \dot{x} &= A_{cl} x + B_{cl} \xi_0 + P_{cl} \omega, \\ \dot{\xi}_0 &= X \xi_0, \\ \delta_y &= C_{cl} x - \mathbf{1}_N \otimes R_1 \xi_0, \\ \delta_z &= D_{cl} x - \mathbf{1}_N \otimes R_2 \xi_0, \end{aligned} \tag{12}$$

DOI: 10.1002/rnc

where

$$A_{cl} = \underset{1:N}{Diag}\{A_i\} + \underset{1:N}{Diag}\{B_i K_i\}((L+G)\otimes I_q)\underset{1:N}{Diag}\{D_i\},$$
$$B_{cl} = -\underset{1:N}{Diag}\{B_i K_i\}((L+G)\otimes I_q)\mathbf{1}_N \otimes R_2,$$
$$C_{cl} = \underset{1:N}{Diag}\{C_i\},\ D_{cl} = \underset{1:N}{Diag}\{D_i\},\ P_{cl} = \underset{1:N}{Diag}\{P_i\}.$$

Now, we define the H_∞ output regulation problem.

Problem 1 (H_∞ output regulation problem for linear heterogeneous multi-agent systems)
Consider a group of $N+1$ heterogeneous LTI systems defined by (2-7). Design the feedback gains K_i such that for $\forall x_i(0),\ i = 1, ..., N$, the closed-loop system of (2)-(7) using (8) achieves the following properties:

a. For $\omega \equiv \mathbf{0}$ and $\xi_0 \equiv \mathbf{0}$, the origin of the system $\dot{x} = A_{cl}x$ is asymptotically stable.
b. For $\omega \equiv \mathbf{0}$, we have $\delta_y \to \mathbf{0}$ and $\delta_z \to \mathbf{0}$ as $t \to +\infty$ for all initial conditions $\xi_0(0)$.
c. For $\omega \in \mathcal{L}_2$ and $T > 0$

$$L^2_{\delta_y \omega} = \frac{\int_0^T \|\delta_y\|_2^2 d\tau}{\int_0^T \|\omega\|_2^2 d\tau} < +\infty. \tag{13}$$

Properties a.-b. define the output regulation problem [26, 27] in absence of unmodeled disturbance; i.e. $\omega \equiv \mathbf{0}$. Property c. concerns H_∞ control in presence of unmodeled disturbances [30]. According to [13] the set of necessary assumptions for y-output and z-output regulation in absence of disturbances ω is given by the following.

Assumption 1
The augmented graph $\bar{\mathcal{G}} = (\bar{V}, \bar{\mathcal{E}})$ contains a spanning tree with the leader as its root node.

Assumption 2
The leader's dynamics X in (5) does not have any strictly stable pole.

Assumption 3
The triple (A_i, B_i, D_i) is output-feedback stabilizable.

Assumption 4
For each $i = 1, ..., N$, there exists a matrix $\Pi_i \in \mathbb{R}^{n_i \times l}$ such that

$$\begin{aligned} A_i\Pi_i &= \Pi_i X, \\ C_i\Pi_i &= R_1, \\ D_i\Pi_i &= R_2. \end{aligned} \tag{14}$$

3.1. Coordinate Transformations

In this subsection, we introduce a coordinate transformation which is useful in formulating the output regulation problem and the graphical game in Section 4. Building on Assumption 4, supplement the columns of Π_i in (14) by a set of linearly independent columns of $\Psi_i \in \mathbb{R}^{n_i \times (n_i - l)}$ to form a complete basis $T_i = [\Pi_i\ \Psi_i] \in \mathbb{R}^{n_i \times n_i}$ of the single-agent state space $\mathbb{R}^{n_i}$. Then in such basis, one has the transformed state $[\xi_i^T, \nu_i^T]^T$

$$x_i = \begin{bmatrix} \Pi_i & \Psi_i \end{bmatrix} \begin{bmatrix} \xi_i \\ \nu_i \end{bmatrix} = T_i \begin{bmatrix} \xi_i \\ \nu_i \end{bmatrix}. \tag{15}$$

Define the following matrices

$$\hat{A}_i := T_i^{-1} A_i T_i = \begin{bmatrix} X & F_i \\ \mathbf{0} & M_i \end{bmatrix}, \quad \hat{B}_i := T_i^{-1} B_i = \begin{bmatrix} \hat{B}_{1i} \\ \hat{B}_{2i} \end{bmatrix}, \quad \hat{P}_i := T_i^{-1} P_i = \begin{bmatrix} \hat{P}_{1i} \\ \hat{P}_{2i} \end{bmatrix}. \tag{16}$$

Define the local neighborhood error in ξ_is

$$e_{\xi_i} = \sum_{j=1}^{N} \alpha_{ij}(\xi_i - \xi_j) + g_i(\xi_i - \xi_0). \tag{17}$$

Let $\epsilon_i = [e_{\xi_i}^T, \nu_i^T]^T$. Then, the dynamics of system (2) and the control (8) in the transformed coordinates ϵ_i read

$$\dot{\epsilon}_i = \bar{A}_i\epsilon_i + \bar{B}_i u_i + \bar{P}_i\omega_i - \sum_{j=1}^{N} \alpha_{ij}(\underline{B}_j u_j + \underline{P}_j\omega_j + \underline{F}_j\nu_j), \tag{18}$$

$$u_i = K_i R_2 e_{\xi_i} + (d_i + g_i)K_i D_i \Psi_i \nu_i - K_i \sum_{j=1}^{N} \alpha_{ij} D_j \Psi_j \nu_j, \tag{19}$$

where

$$\begin{aligned} &\bar{A}_i := \begin{bmatrix} X & (d_i+g_i)F_i \\ \mathbf{0} & M_i \end{bmatrix}, \quad \bar{B}_i := \begin{bmatrix} (d_i+g_i)\hat{B}_{1i} \\ \hat{B}_{2i} \end{bmatrix}, \quad \bar{P}_i := \begin{bmatrix} (d_i+g_i)\hat{P}_{1i} \\ \hat{P}_{2i} \end{bmatrix}, \\ &\underline{B}_j := \begin{bmatrix} \hat{B}_{1j} \\ \mathbf{0} \end{bmatrix}, \quad \underline{P}_j := \begin{bmatrix} \hat{P}_{1j} \\ \mathbf{0} \end{bmatrix}, \quad \underline{F}_j := \begin{bmatrix} F_j \\ \mathbf{0} \end{bmatrix}. \end{aligned} \tag{20}$$

Equation (18) describes agent i dynamics in the new $\epsilon_i^T = [e_{\xi_i}^T, \nu_i^T]$-coordinates. The following technical lemma can be used to simplify the dynamics in (19).

Lemma 1
One can always select Ψ_i in (15) such that $F_i = \mathbf{0}$ in (16).

Proof
From the definition of $\hat{A}_i$ in (16)

$$A_i \begin{bmatrix} \Pi_i & \Psi_i \end{bmatrix} = \begin{bmatrix} \Pi_i & \Psi_i \end{bmatrix} \begin{bmatrix} X & F \\ \mathbf{0} & M_i \end{bmatrix}.$$

Hence, one has $A_i\Psi_i - \Psi_i M_i = \Pi_i F_i$, which is a Sylvester equation. Using the Kronecker product's property, this is equivalent to $(I_{\tilde{n}_i} \otimes A_i - M_i^T \otimes I_{n_i})vec(\Psi_i) = vec(\Pi_i F_i)$, where $\tilde{n}_i = n_i - l$. If one wants $F_i = \mathbf{0}$, then one should select

$$vec(\Psi_i) \in null(I_{\tilde{n}_i} \otimes A_i - M_i^T \otimes I_{n_i}). \tag{21}$$

Let $\lambda_k \in spec(A_i)$, $\tilde{\lambda}_k \in spec(M_i)$. Then, $(\lambda_k - \tilde{\lambda}_k) \in spec(I_{\tilde{n}_i} \otimes A_i - M_i^T \otimes I_{n_i})$. Since $spec(M_i) \subset spec(A_i)$, we have $0 \in spec(I_{\tilde{n}_i} \otimes A_i - M_i^T \otimes I_{n_i})$ and it is always possible to satisfy (21). For a more general result, please see Theorem 4.4.14 of [28]. □

Using Lemma 1, we hereafter assume that we have selected Ψ_i such that $F_i = \mathbf{0}$ for $i = 1, ..., N$.

3.2. Closed-loop system and node error dynamics for graphical game

In this subsection, we define the node error dynamics which are suitable for graphical games formulation for heterogeneous agents fully developed in Section 4. To do so, we express the closed-loop system of (18) using the control (19)

$$\begin{aligned}\dot{e}_{\xi_i} =& Xe_{\xi_i} + (d_i+g_i)\tilde{B}_{1i}K_iR_2e_{\xi_i} + (d_i+g_i)^2\tilde{B}_{1i}K_iD_i\Psi_i\nu_i + (d_i+g_i)\tilde{P}_{1i}\omega_i \\ &- (d_i+g_i)\tilde{B}_{1i}K_i\sum_{j=1}^{N}\alpha_{ij}D_j\Psi_j\nu_j - \sum_{j=1}^{N}\alpha_{ij}\tilde{B}_{1j}K_jR_2e_{\xi_j} \\ &- \sum_{j=1}^{N}\alpha_{ij}(d_j+g_j)\tilde{B}_{1j}K_jD_j\Psi_j\nu_j + \sum_{j=1}^{N}\alpha_{ij}\tilde{B}_{1j}K_j\sum_{l=1}^{N}\alpha_{jl}D_l\Psi_l\nu_l - \sum_{j=1}^{N}\alpha_{ij}\tilde{P}_{1j}\omega_j, \\ \dot{\nu}_i =& \tilde{A}_i\nu_i + \tilde{B}_{2i}K_iR_2e_{\xi_i} + (d_i+g_i)\tilde{B}_{2i}K_iD_i\Psi_i\nu_i + \tilde{P}_{2i}\omega_i - \tilde{B}_{2i}K_i\sum_{j=1}^{N}\alpha_{ij}D_j\Psi_j\nu_j\end{aligned} \tag{22}$$

Define

$$\beta_i := -K_i\sum_{j=1}^{N}\alpha_{ij}D_j\Psi_j\nu_j + (d_i+g_i)(K_iD_i\Psi_i - \bar{K}_i)\nu_i,\ \beta = \left[\beta_1^T,\quad ...,\quad \beta_N^T\right]^T, \tag{23}$$

$$u_{op_i} := K_iR_2e_{\xi_i} + (d_i+g_i)\bar{K}_i\nu_i, \tag{24}$$

so that $u_i = u_{op_i} + \beta_i$. In (23)-(24), $\bar{K}_i \in \mathbb{R}^{m_i\times(n_i-l)}$ is a gain matrix which has no effect on the design of the controller but we introduce it to facilitate the following theoretical developments of the optimal design. The signal β_i in (23) contains the term $-(d_i+g_i)\bar{K}_i\nu_i$ and u_{op_i} in (24) contains $(d_i+g_i)\bar{K}_i\nu_i$. Clearly, this term has no effect on the design of the controller because u_{op_i} and β_i always appear added together.

By definitions in (23)-(24), the closed-loop system (22) can be represented as

$$\dot{\epsilon}_i = \bar{A}_i\epsilon_i + \bar{B}_iu_{op_i} + \bar{P}_i\omega_i + \bar{B}_i\beta_i - \sum_{j=1}^{N}\alpha_{ij}(\underline{B}_ju_{op_j} + \underline{P}_j\omega_j + \underline{B}_j\beta_j). \tag{25}$$

We call (25) *the node error dynamics for graphical games for heterogeneous agents*. It is important to point out that (25) is in a standard form of the dynamics usually considered in the graphical game framework [19, 18], *i.e.* it depends on the states, policies and disturbances of other agents in the neighborhood. Note however that while the agents in [19, 18] are homogeneous, the dynamics in (25) are heterogeneous.

Remark 1

Note that ν_is and the related β_is stem from agents heterogeneity and they pose additional complications for control design that do not arise in identical agents. In this more general setup with heterogeneous agents, we develop the graphical game in Section 4 in the sequel, whereas the existing results along similar lines consider only identical agents. For a special case of identical agents, our formulation indeed reduces to the familiar one in [19, 18].

In Section 4, we use (25) to develop the graphical game and devise the appropriate controls. In Section 5 then, we bring additional conditions guaranteeing that the results of Section 4 solve the original Problem 1.

4. GRAPHICAL GAME FOR LINEAR HETEROGENEOUS AGENTS

In this section, we use the machinery of graphical games and define an H_∞ graphical game for linear heterogeneous agents. Using this graphical game framework, we ultimately solve our H_∞ output regulation problem of Section 3.

Prepared using rncauth.cls
DOI: 10.1002/rnc

4.1. H_∞ graphical game formulation

As it can be seen from (25), the dynamics of each agent depends on the neighboring agents. In a similar way, we define the $\mathcal{L}_2$ condition for agent i such that it contains the policies and disturbances of other agents in its neighborhood. Let $u_{op_{-i}} = \{u_{op_j},\ j \in N_i\}$, $\omega_{-i} = \{\omega_j,\ j \in N_i\}$ and $\beta_{-i} = \{\beta_j,\ j \in N_i\}$. Define the $\mathcal{L}_2$-condition for the dynamics (25) as

$$\begin{aligned}\int_0^T \{\epsilon_i^T Q_i \epsilon_i + u_{op_i}^T R_{ii} u_{op_i} + \sum_{j=1}^N \alpha_{ij} u_{op_j}^T R_{ij} u_{op_j}\} d\tau \leq \\ \gamma_{\xi\nu_i}^2 \int_0^T \{\omega_i^T S_{1ii} \omega_i + \sum_{j=1}^N \alpha_{ij} \omega_j^T S_{1ij} \omega_j\} d\tau + \gamma_{\beta_i}^2 \int_0^T \{\beta_i^T S_{2ii} \beta_i + \sum_{j=1}^N \alpha_{ij} \beta_j^T S_{2ij} \beta_j\} d\tau,\end{aligned} \tag{26}$$

where $Q_i > 0,\ R_{ii} > 0,\ R_{ij} \geq 0,\ S_{1ii} > 0,\ S_{1ij} \geq 0,\ S_{2ii} > 0,\ S_{2ij} \geq 0,\ \gamma_{\xi\nu_i} > 0,\ \gamma_{\beta_i} > 0$ and $T > 0$. The $\mathcal{L}_2$-condition in (26) is equivalent to the optimization of the following quadratic performance index

$$\begin{aligned}J_i(\epsilon_i(0), u_{op_i}, u_{op_{-i}}, \omega_i, \omega_{-i}, \beta_i, \beta_{-i}) = \int_0^{+\infty} L_i(\epsilon_i, u_{op_i}, u_{op_{-i}}, \omega_i, \omega_{-i}, \beta_i, \beta_{-i}) d\tau \\ = \int_0^{+\infty} \{\epsilon_i^T Q_i \epsilon_i + u_{op_i}^T R_{ii} u_{op_i} + \sum_{j=1}^N \alpha_{ij} u_{op_j}^T R_{ij} u_{op_j} - \gamma_{\xi\nu_i}^2 [\omega_i^T S_{1ii} \omega_i \\ + \sum_{j=1}^N \alpha_{ij} \omega_j^T S_{1ij} \omega_j] - \gamma_{\beta_i}^2 [\beta_i^T S_{2ii} \beta_i + \sum_{j=1}^N \alpha_{ij} \beta_j^T S_{2ij} \beta_j]\} d\tau.\end{aligned} \tag{27}$$

In (27), we have two players: the control player u_{op_i} which tries to minimize the performance index and the disturbance player $\{\omega_i, \beta_i\}$ which tries to maximize it. The optimal value of this zero-sum graphical game is defined as

$$\begin{aligned}V_i^*(\epsilon_i(0)) &= \min_{u_{op_i}} \max_{\omega_i, \beta_i} J_i(\epsilon_i(0), u_{op_i}, u_{op_{-i}}^*, \omega_i, \omega_{-i}^*, \beta_i, \beta_{-i}^*) \\ &= \max_{\omega_i, \beta_i} \min_{u_{op_i}} J_i(\epsilon_i(0), u_{op_i}, u_{op_{-i}}^*, \omega_i, \omega_{-i}^*, \beta_i, \beta_{-i}^*)\end{aligned} \tag{28}$$

where, $u_{op_{-i}}^*$ and $\{\omega_{-i}^*, \beta_{-i}^*\}$ are the optimal control and disturbance policies of the players in the neighborhood of player i. For the fixed control and disturbance policies u_{op_i} and ω_i, β_i, the quadratic value function is defined as

$$\begin{aligned}V_i(\epsilon_i(t), u_{op_i}, u_{op_{-i}}, \omega_i, \omega_{-i}, \beta_i, \beta_{-i}) = \int_t^{+\infty} \{\epsilon_i^T Q_i \epsilon_i + u_{op_i}^T R_{ii} u_{op_i} + \sum_{j=1}^N \alpha_{ij} u_{op_j}^T R_{ij} u_{op_j} \\ - \gamma_{\xi\nu_i}^2 [\omega_i^T S_{1ii} \omega_i + \sum_{j=1}^N \alpha_{ij} \omega_j^T S_{1ij} \omega_j] - \gamma_{\beta_i}^2 [\beta_i^T S_{2ii} \beta_i + \sum_{j=1}^N \alpha_{ij} \beta_j^T S_{2ij} \beta_j]\} d\tau.\end{aligned} \tag{29}$$

We make the following assumption regarding the performance index.

Assumption 5
The performance index (27) is zero-state observable.

Assumption 5 guarantees that no solution can identically stay in zero cost other than the zero solution [29]. It is a necessary assumption to prove stability of disturbance-free system under optimal control [30]. Now, we are ready to define the H_∞ graphical game for linear heterogeneous multi-agent systems.

Problem 2 (H_∞ graphical game for linear heterogeneous multi-agent systems)
Consider a group of $N+1$ heterogeneous LTI systems defined by (2-7). Design u_{op_i} to solve optimization problem (28) with respect to dynamics (25).

In the sequel we solve the H_∞ graphical game problem.

4.2. Solution of the H_∞ graphical game

When the value function (29) is finite, using the Leibniz's formula, a differential equivalent to the value function is given in terms of the Hamiltonian

$$H_i = L_i(\epsilon_i, u_{op_i}, u_{op_{-i}}, \omega_i, \omega_{-i}, \beta_i, \beta_{-i}) + \nabla V_i^T \dot{\epsilon}_i = 0 \tag{30}$$

where $\nabla V_i = \frac{\partial V_i}{\partial \epsilon_i}$. At the equilibrium, one has the stationarity conditions

$$\frac{\partial H_i}{\partial u_{op_i}} = \mathbf{0}, \rightarrow u^*_{op_i} = -\frac{1}{2} R_{ii}^{-1} \bar{B}_i^T \nabla V_i, \tag{31}$$

$$\frac{\partial H_i}{\partial \omega_i} = \mathbf{0}, \rightarrow \omega^*_i = \frac{1}{2} \gamma_{\xi\nu_i}^{-2} S_{1ii}^{-1} \bar{P}_i^T \nabla V_i, \tag{32}$$

$$\frac{\partial H_i}{\partial \beta_i} = \mathbf{0}, \rightarrow \beta^*_i = \frac{1}{2} \gamma_{\beta_i}^{-2} S_{2ii}^{-1} \bar{B}_i^T \nabla V_i. \tag{33}$$

Substituting the optimal policy (31) and the worst-case disturbances (32)-(33) into (30) yields coupled Hamilton-Jacobi-Bellman (HJB) equations

$$\begin{aligned}
&\epsilon_i^T Q_i \epsilon_i + \frac{1}{4} \nabla V_i^T \bar{B}_i R_{ii}^{-1} \bar{B}_i^T \nabla V_i + \frac{1}{4} \sum_{j=1}^{N} \alpha_{ij} \nabla V_j^T \bar{B}_j R_{jj}^{-1} R_{ij} R_{jj}^{-1} \bar{B}_j^T \nabla V_j \\
&- \gamma_{\xi\nu_i}^2 \frac{1}{4} [\gamma_{\xi\nu_i}^{-4} \nabla V_i^T \bar{P}_i S_{1ii}^{-1} \bar{P}_i^T \nabla V_i + \sum_{j=1}^{N} \alpha_{ij} \gamma_{\xi\nu_j}^{-4} \nabla V_j^T \bar{P}_j S_{1jj}^{-1} S_{1ij} S_{1jj}^{-1} \bar{P}_j^T \nabla V_j] \\
&- \gamma_{\beta_i}^2 \frac{1}{4} [\gamma_{\beta_i}^{-4} \nabla V_i^T \bar{B}_i S_{2ii}^{-1} \bar{B}_i^T \nabla V_i + \sum_{j=1}^{N} \alpha_{ij} \gamma_{\beta_j}^{-4} \nabla V_j^T \bar{B}_j S_{2jj}^{-1} S_{2ij} S_{2jj}^{-1} \bar{B}_j^T \nabla V_j] \\
&+ \nabla V_i^T [\bar{A}_i \epsilon_i - \frac{1}{2} \bar{B}_i R_{ii}^{-1} \bar{B}_i^T \nabla V_i + \frac{1}{2} \gamma_{\xi\nu_i}^{-2} \bar{P}_i S_{1ii}^{-1} \bar{P}_i^T \nabla V_i + \frac{1}{2} \gamma_{\beta_i}^{-2} \bar{B}_i S_{2ii}^{-1} \bar{B}_i^T \nabla V_i] \\
&- \nabla V_i^T [\sum_{j=1}^{N} \alpha_{ij} \{ -\frac{1}{2} \underline{B}_j R_{jj}^{-1} \bar{B}_j^T \nabla V_j + \frac{1}{2} \gamma_{\xi\nu_j}^{-2} \underline{P}_j S_{1jj}^{-1} \bar{P}_j^T \nabla V_j + \frac{1}{2} \gamma_{\beta_j}^{-2} \underline{B}_j S_{2jj}^{-1} \bar{B}_j^T \nabla V_j \}] = 0.
\end{aligned} \tag{34}$$

Based on (34), the HJB equation of player i depends on the HJB equations of other players in its neighborhood. It is in general impossible to solve the coupled HJB equations (34) analytically [30]. Later in Section 6, we use RL techniques and develop a numerical procedure to bring the solutions in real time. For further developments in this section however, we assume the solutions are available.

Let V_i^* be the quadratic optimal solution to (34) and $u^*_{op_i}(V_i^*)$, $\omega_i^*(V_i^*)$ and $\beta_i^*(V_i^*)$ in (31)-(32) be the optimal policy and the worst-case disturbances in terms of V_i^*. In the next theorem, we prove that such V_i^* satisfies the $\mathcal{L}_2$-condition (26).

Theorem 1
Suppose V_i^* is a quadratic positive semi-definite solution to (34) for $i = 1, ..., N$. Let Assumption 5 hold. Using the optimal policy $u^*_{op_i}(V_i^*)$ in (31),

1. The disturbance-free system (25) ($\omega_i \equiv \mathbf{0},\ \beta_i \equiv \mathbf{0},\ i = 1, ..., N$) is asymptotically stable.
2. For all disturbances $\omega_i,\ \omega_{-i},\ \beta_i, \beta_{-i} \in \mathcal{L}_2$, the $\mathcal{L}_2$-condition (26) is satisfied.

Proof
The proof contains two parts. In the first part, we prove the stability of the disturbance-free system (25) and in the second part, we prove the $\mathcal{L}_2$-condition (26).

1. For any smooth value function V_i, the Hamiltonian is defined as

$$\begin{aligned} &H_i(\epsilon_i, \nabla V_i, u_{op_i}, u_{op_{-i}}, \omega_i, \omega_{-i}, \beta_i, \beta_{-i}) = \\ &\epsilon_i^T Q_i \epsilon_i + u_{op_i}^T R_{ii} u_{op_i} + \sum_{j=1}^{N} \alpha_{ij} u_{op_j}^T R_{ij} u_{op_j} - \gamma_{\xi\nu_i}^2 [\omega_i^T S_{1ii} \omega_i \\ &+ \sum_{j=1}^{N} \alpha_{ij} \omega_j^T S_{1ij} \omega_j] - \gamma_{\beta_i}^2 [\beta_i^T S_{2ii} \beta_i + \sum_{j=1}^{N} \alpha_{ij} \beta_j^T S_{2ij} \beta_j] + \frac{dV_i}{dt}. \end{aligned} \tag{35}$$

Let V_i^* be a smooth positive semi-definite solution to (34). Completing the squares leads to

$$\begin{aligned} &H_i(\epsilon_i, \nabla V_i^*, u_{op_i}, u_{op_{-i}}^*, \omega_i, \omega_{-i}^*, \beta_i, \beta_{-i}^*) = \\ &H_i(\epsilon_i, \nabla V_i^*, u_{op_i}^*, u_{op_{-i}}^*, \omega_i^*, \omega_{-i}^*, \beta_i^*, \beta_{-i}^*) + (u_{op_i} - u_{op_i}^*)^T R_{ii} (u_{op_i} - u_{op_i}^*) \\ &- \gamma_{\xi\nu_i}^2 (\omega_i - \omega_i^*)^T S_{1ii} (\omega_i - \omega_i^*) - \gamma_{\beta_i}^2 (\beta_i - \beta_i^*)^T S_{2ii} (\beta_i - \beta_i^*). \end{aligned}$$

Selecting $u_{op_i} = u_{op_i}^*(V_i^*)$, one has

$$\begin{aligned} &\epsilon_i^T Q_i \epsilon_i + u_{op_i}^{*T} R_{ii} u_{op_i}^* + \sum_{j=1}^{N} \alpha_{ij} u_{op_j}^{*T} R_{ij} u_{op_j}^* - \gamma_{\xi\nu_i}^2 [\omega_i^T S_{1ii} \omega_i \\ &+ \sum_{j=1}^{N} \alpha_{ij} \omega_j^T S_{1ij} \omega_j] - \gamma_{\beta_i}^2 [\beta_i^T S_{2ii} \beta_i + \sum_{j=1}^{N} \alpha_{ij} \beta_j^T S_{2ij} \beta_j] + \frac{dV_i^*}{dt} \leq 0. \end{aligned} \tag{36}$$

Set $\omega_i \equiv \mathbf{0},\ \omega_{-i} \equiv \mathbf{0},\ \beta_i = \mathbf{0},\ \beta_{-i} \equiv \mathbf{0}$. According to (36)

$$\frac{dV_i^*}{dt} \leq -(\epsilon_i^T Q_i \epsilon_i + u_{op_i}^{*T} R_{ii} u_{op_i}^* + \sum_{j=1}^{N} \alpha_{ij} u_{op_j}^{*T} R_{ij} u_{op_j}^*) \leq 0.$$

Because of Assumption 5, one can conclude from the above inequality that the disturbance-free system (25) is asymptotically stable.

2. Integrate (36)

$$\begin{aligned} &V_i^*(\epsilon_i(T)) - V_i^*(\epsilon_i(0)) + \int_0^T \{\epsilon_i^T Q_i \epsilon_i + u_{op_i}^{*T} R_{ii} u_{op_i}^* + \sum_{j=1}^{N} \alpha_{ij} u_{op_j}^{*T} R_{ij} u_{op_j}^* - \gamma_{\xi\nu_i}^2 [\omega_i^T S_{1ii} \omega_i \\ &+ \sum_{j=1}^{N} \alpha_{ij} \omega_j^T S_{1ij} \omega_j] - \gamma_{\beta_i}^2 [\beta_i^T S_{2ii} \beta_i + \sum_{j=1}^{N} \alpha_{ij} \beta_j^T S_{2ij} \beta_j]\} d\tau \leq 0. \end{aligned}$$

Select $\epsilon_i(0) = \mathbf{0}$. Since $V_i^*(\epsilon_i(0)) = 0$ and $V_i^*(\epsilon_i(T)) > 0$, (26) is satisfied.

□

Remark 2

Assuming a quadratic structure for the value function $V_i^* = 0.5\epsilon_i^T P_i^g \epsilon_i$, the control signal (31) reads

$$u_{op_i} = -R_{ii}^{-1} \bar{B}_i^T P_i^g \epsilon_i = -R_{ii}^{-1} \bar{B}_i^T P_i^g \begin{bmatrix} e_{\xi_i} \\ \nu_i \end{bmatrix} = K_{i1} e_{\xi_i} + K_{i2} \nu_i.$$

The above equation is useful in finding the controller gain K_i. Recall the definition of policy u_{op_i} in (24)

$$u_{op_i} = K_i R_2 e_{\xi_i} + (d_i + g_i) \bar{K}_i \nu_i.$$

In order to calculate K_i from $K_{i1} = K_i R_2$, the following standard condition is required

$$Rank(R_2) = Rank\left(\begin{bmatrix} R_2 \\ K_{i1} \end{bmatrix}\right). \tag{37}$$

One can satisfy (37) by e.g. selecting any invertible R_2 similar to [2, 3]. Then, $K_i = K_{i1} R_2^{-1}$ and $\bar{K}_i = \frac{1}{(d_i+g_i)} K_{i2}$. For convenience we assume,

Assumption 6
R_2 is invertible.

4.3. Nash equilibrium solution

In an H_∞ graphical game, we are interested in convergence to a Nash equilibrium (NE). The game has a well-defined NE if

$$\begin{aligned} J_i(u^*_{op_i}, u^*_{op_{-i}}, \omega_i, \omega^*_{-i}, \beta_i, \beta^*_{-i}) &\leq J_i(u^*_{op_i}, u^*_{op_{-i}}, \omega^*_i, \omega^*_{-i}, \beta^*_i, \beta^*_{-i}) \\ &\leq J_i(u_{op_i}, u^*_{op_{-i}}, \omega^*_i, \omega^*_{-i}, \beta^*_i, \beta^*_{-i}). \end{aligned} \tag{38}$$

The following theorem shows that a positive solution to (34) also guarantees convergence to an NE.

Theorem 2
Let V_i^* be a quadratic positive semi-definite solution to (34) for $i = 1, ..., N$ such that the closed-loop system of

$$\dot{\epsilon}_i = \bar{A}_i \epsilon_i + \bar{B}_i u^*_{op_i} + \bar{P}_i \omega^*_i + \bar{B}_i \beta^*_i - \sum_{j=1}^{N} \alpha_{ij} (\underline{B}_j u^*_{op_j} + \underline{P}_j \omega^*_{op_j} + \underline{B}_j \beta^*_j) \tag{39}$$

is asymptotically stable. Let Assumption 5 hold. Then,

1. The control signal and disturbances (31)-(33) form an NE.
2. The optimal value of the game is then $V_i^*(\epsilon_i(0))$.
3. The optimal control (31) solves Problem 2.

Proof

1. First, we show that (31)-(33) form an NE. Rewriting (27) and adding zero

$$\begin{aligned} J_i &= \int_0^{+\infty} L_i d\tau + \int_0^{+\infty} \dot{V}_i d\tau + V_i(\epsilon_i(0)) - V_i(\epsilon_i(+\infty)) \\ &= \int_0^{+\infty} H_i(\epsilon_i, \nabla V_i, u_{op_i}, u_{op_{-i}}, \omega_i, \omega_{-i}, \beta_i, \beta_{-i}) d\tau + V_i(\epsilon_i(0)) - V_i(\epsilon_i(+\infty)). \end{aligned}$$

Let V_i^* be a smooth positive semi-definite solution to (34). By completing the squares one has

$$\begin{aligned}
J_i =& V_i(\epsilon_i(0)) - V_i(\epsilon_i(+\infty)) + \int_0^{+\infty} \{H_i(\epsilon_i, \nabla V_i^*, u_{op_i}^*, u_{op_{-i}}^*, \omega_i^*, \omega_{-i}^*, \beta_i^*, \beta_{-i}^*) \\
&+ (u_{op_i} - u_{op_i}^*)^T R_{ii}(u_{op_i} - u_{op_i}^*) + \sum_{j=1}^{N} \alpha_{ij}(u_{op_j} - u_{op_j}^*)^T R_{ij}(u_{op_j} - u_{op_j}^*) \\
&+ 2\sum_{j=1}^{N} \alpha_{ij} u_{op_j}^{*T} R_{ij}(u_{op_j} - u_{op_j}^*) - \sum_{j=1}^{N} \alpha_{ij} \nabla V_i^T \underline{B}_j (u_{op_j} - u_{op_j}^*) \\
&- \gamma_{\xi\nu_i}^2 (\omega_i - \omega_i^*)^T S_{1ii}(\omega_i - \omega_i^*) - \gamma_{\xi\nu_i}^2 \sum_{j=1}^{N} \alpha_{ij}(\omega_j - \omega_j^*)^T S_{1ij}(\omega_j - \omega_j^*) \\
&- 2\gamma_{\xi\nu_i}^2 \sum_{j=1}^{N} \alpha_{ij} \omega_j^{*T} S_{1ij}(\omega_j - \omega_j^*) - \sum_{j=1}^{N} \alpha_{ij} \nabla V_i^T \underline{P}_j (\omega_j - \omega_j^*) \\
&- \gamma_{\beta_i}^2 (\beta_i - \beta_i^*)^T S_{2ii}(\beta_i - \beta_i^*) - \gamma_{\beta_i}^2 \sum_{j=1}^{N} \alpha_{ij}(\beta_j - \beta_j^*)^T S_{2ij}(\beta_j - \beta_j^*) \\
&- \gamma_{\beta_i}^2 \sum_{j=1}^{N} \alpha_{ij} \beta_j^{*T} S_{2ij}(\beta_j - \beta_j^*) - \sum_{j=1}^{N} \alpha_{ij} \nabla V_i^T \underline{B}_j (\beta_j - \beta_j^*)\} d\tau.
\end{aligned}$$

Since (39) is asymptotically stable, $V_i^*(\epsilon_i(+\infty)) = 0$. Set $u_{op_j} = u_{op_j}^*$, $\omega_j = \omega_j^*$, $\beta_j = \beta_j^*$, $\forall j \in N_i$ in the above equation. Then (38) follows easily.

2. Next, we obtain the optimal value of the game. Set $u_{op_i} = u_{op_i}^*$, $\omega_i = \omega_i^*$, $\beta_i = \beta_i^*$; then, $J_i^* = V_i^*(\epsilon_i(0))$.
3. It is concluded from part 2.

□

Remark 3

Theorem 2 shows that the controls $u_{op_i}^*$ in (31) lead to the desired NE satisfying the $\mathcal{L}_2$ condition (26) and thus solve Problem 2. Note however that Problem 2, and indeed all the developments of this section, consider u_{op_i} and β_i as independent signals, whereas those are in fact inseparably linked in the actual control signal (19). This fact requires additional conditions, elaborated further in Section 5, guaranteeing that the control design proposed here solves the original Problem 1 of Section 3.

5. H_∞ OUTPUT REGULATION USING GRAPHICAL GAME

In Section 4, we shown that V_i^* in (34) solves Problem 2, (see Theorem 2). Building on developments of Section 4, in this section, we give conditions guaranteeing that the graphical game solution V_i^* and the control designed from it can indeed be used to solve the H_∞ output regulation problem (Problem 1). Moreover, we give an upper bound for the overall $\mathcal{L}_2$-gain of output synchronization error with respect to disturbances; *i.e.* $L_{\delta_y \omega}$.

The overall system of (23)-(25) can be represented as in Fig. 1. There, we have two interconnected subsystems. We name the upper block subsystem *the nominal system*, whose description is given in (24)-(25) and we call the lower block subsystem *the interconnected system* whose description is given in (23). This representation is useful as we can use a version of small-gain theorem (given below) to prove $\mathcal{L}_2$-stability.

Theorem 3

Let H_1 and H_2 be two subsystems, whose inputs are u_1, ω and u_2, ω and outputs are y_1, y_2, respectively. Let $\omega_1,\ \omega_2 \in \mathcal{L}_2$, and assume that H_1 and H_2 are interconnected as depicted in Fig. 2

Prepared using rncauth.cls
DOI: 10.1002/rnc

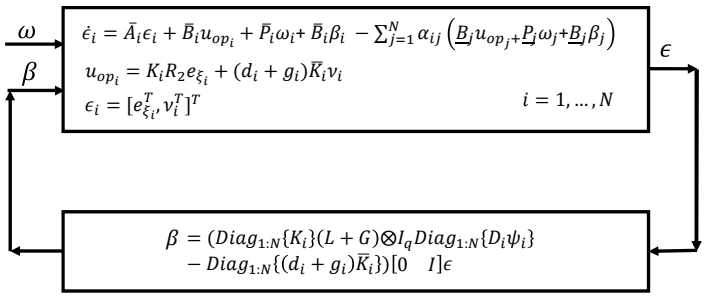

Figure 1. The representation of the nominal and the interconnected systems

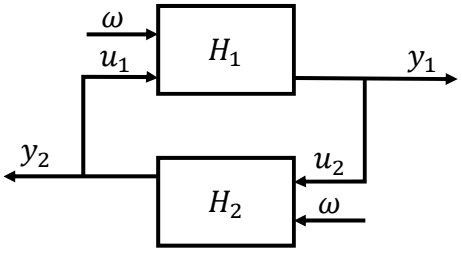

Figure 2. The interconnected system

and

$$\|y_1\|_{\mathcal{L}_2} \leq L_{11}\|\omega\|_{\mathcal{L}_2} + L_{12}\|u_1\|_{\mathcal{L}_2}, \quad \|y_2\|_{\mathcal{L}_2} \leq L_{22}\|\omega\|_{\mathcal{L}_2} + L_{21}\|u_2\|_{\mathcal{L}_2}. \tag{40}$$

If $L_{12}L_{21} < 1$, then $y_1 \in \mathcal{L}_2$ and

$$\|y_1\|_{\mathcal{L}_2} \leq (1 - L_{12}L_{21})^{-1}(L_{11} + L_{12}L_{22})\|\omega\|_{\mathcal{L}_2}. \tag{41}$$

Proof
According to (40)

$$\begin{aligned}\|y_1\|_{\mathcal{L}_2} &\leq L_{11}\|\omega\|_{\mathcal{L}_2} + L_{12}\|u_1\|_{\mathcal{L}_2} \leq L_{11}\|\omega\|_{\mathcal{L}_2} + L_{12}\|y_2\|_{\mathcal{L}_2} \\ &\leq L_{11}\|\omega\|_{\mathcal{L}_2} + L_{12}(L_{22}\|\omega\|_{\mathcal{L}_2} + L_{21}\|y_1\|_{\mathcal{L}_2}).\end{aligned}$$

Hence

$$(1 - L_{12}L_{21})\|y_1\|_{\mathcal{L}_2} \leq (L_{11} + L_{12}L_{22}\|\omega\|_{\mathcal{L}_2}).$$

By the small gain theorem, the $\mathcal{L}_2$-gain stability is guaranteed if $L_{12}L_{21} < 1$ and (41) follows. □

The following theorem presents one of the main results of this paper; it specifies the set of conditions such that V_i^* in (34) and the control based on it solve the H_∞ output regulation problem (Problem 1). Define

$$
\begin{aligned}
&S_{m_i} := \max_{i,j\in N_i}\{\overline{\sigma}(\sqrt{\alpha_{ij}S_{1ij}}),\overline{\sigma}(\sqrt{S_{1ii}})\},\quad \beta_{m_i} := \max_{i,j\in N_i}\{\overline{\sigma}(\sqrt{\alpha_{ij}S_{2ij}}),\overline{\sigma}(\sqrt{S_{2ii}})\},\\
&L_y = \max_i\{\bar{\sigma}(C_iT_i)\}\frac{1}{\underline{\sigma}(T_g)},\quad L_{21} = \max_i \bar{\sigma}(K_i)\bar{\sigma}(L+G)\max_i\bar{\sigma}(D_i\Psi_i) + \max_i\bar{\sigma}((d_i+g_i)\bar{K}_i)\\
&L_{11} = \sqrt{\sum_{i=1}^{N}\underline{\sigma}(\sqrt{Q_i})^{-2}\gamma_{\xi\nu_i}^2 S_{m_i}^2},\quad L_{12} = \sqrt{\sum_{i=1}^{N}\underline{\sigma}(\sqrt{Q_i})^{-2}\gamma_{\beta_i}^2\beta_{m_i}^2},\\
&T_g = \begin{bmatrix}(L+G)\otimes I_l & \mathbf{0}\\ \mathbf{0} & I_{\sum_{i=1}^{N}n_i - Nl}\end{bmatrix}.
\end{aligned}
\tag{42}
$$

Theorem 4
Let Assumptions 1-5 hold. Let V_i^* be a quadratic positive semi-definite solution to (34) and $u_{op_i}^*(V_i^*)$ in (31) be the optimal policy. Assume that the controller gain K_i is obtained according to Remark 2. If either (i) $\bar{\sigma}(K_i)\bar{\sigma}(D_i\Psi_i)$ and $\bar{\sigma}(\bar{K}_i)$ are sufficiently small or (ii) γ_{β_i} is sufficiently small for $i = 1, ..., N$, then,

1. An upper bound for the $\mathcal{L}_2$-gain of output synchronization error δ_y with respect to ω is given by
$$L_{\delta_y\omega} = L_y(1 - L_{12}L_{21})^{-1}L_{11}. \tag{43}$$
2. Distributed control (8) solves the H_∞ output regulation problem (Problem 1).

Proof

1. Consider subsystem H_1 from Theorem 3 as the overall system of (25). This subsystem has two inputs ω and β, where ω is the disturbance input and β is related to the subsystem H_2, and one output ϵ. First note that we always have
$$\int_0^T \underline{\sigma}(\sqrt{Q_i})^2\|\epsilon_i\|_2^2 d\tau \le \int_0^T \epsilon_i^T Q_i\epsilon_i + u_{op_i}^T R_{ii}u_{op_i} + \sum_{j=1}^{N}\alpha_{ij}u_{op_j}^T R_{ij}u_{op_j}d\tau.$$
Using the above inequality in accordance with (26),
$$
\begin{aligned}
\int_0^T \|\epsilon\|_2^2 d\tau &= \int_0^T \sum_{i=1}^{N}\|\epsilon_i\|_2^2 d\tau\\
&\le \sum_{i=1}^{N}\underline{\sigma}(\sqrt{Q_i})^{-2}\gamma_{\xi\nu_i}^2 S_{m_i}^2\int_0^T\|\omega\|_2^2 d\tau + \sum_{i=1}^{N}\underline{\sigma}(\sqrt{Q_i})^{-2}\gamma_{\beta_i}^2\beta_{m_i}^2\int_0^T\|\beta\|_2^2 d\tau.
\end{aligned}
$$
Hence, the $\mathcal{L}_2$ gain of ϵ with respect to ω and β reads
$$\|\epsilon\|_{\mathcal{L}_2} \le \sqrt{\sum_{i=1}^{N}\underline{\sigma}(\sqrt{Q_i})^{-2}\gamma_{\xi\nu_i}^2 S_{m_i}^2}\|\omega\|_{\mathcal{L}_2} + \sqrt{\sum_{i=1}^{N}\underline{\sigma}(\sqrt{Q_i})^{-2}\gamma_{\beta_i}^2\beta_{m_i}^2}\|\beta\|_{\mathcal{L}_2}. \tag{44}$$
Next, we consider the subsystem H_2 from Theorem 3 as (23) with input ϵ and output β. According to the definition of β in (23), the $\mathcal{L}_2$ gain of β with respect to ϵ reads
$$\|\beta\|_{\mathcal{L}_2} \le (\max_i\bar{\sigma}((d_i+g_i)\bar{K}_i) + \max_i\bar{\sigma}(K_i)\bar{\sigma}(L+G)\max_i\bar{\sigma}(D_i\Psi_i))\|\omega\|_{\mathcal{L}_2}. \tag{45}$$

By substituting (45) in (44)

$$\|\epsilon\|_{\mathcal{L}_2} \leq (1 - L_{12}L_{21})^{-1} L_{11} \|\omega\|_{\mathcal{L}_2}. \tag{46}$$

By Theorem 3, $\epsilon \in \mathcal{L}_2$ if $L_{12}L_{21} < 1$ which is satisfied by either of the conditions (i)-(ii) in the body of the theorem. Let $\bar{x}_i = [\delta_{\xi_i}^T, \nu_i^T]$ where $\delta_{\xi_i} = \xi_i - \xi_0$. Let ϵ and $\bar{x}$ be the overall vectors of ϵ_i and $\bar{x}_i$ respectively. Then,

$$\epsilon = T_g \bar{x}, \tag{47}$$

where T_g is given in (42). Using (46)-(47), the $\mathcal{L}_2$-gain of the output synchronization error $\delta_{y_i} = C_i x_i - R_1 \xi_0 = C_i T_i \bar{x}_i$ in (12) with respect to ω reads

$$\|\delta_y\|_{\mathcal{L}_2} \leq L_y (1 - L_{12}L_{21})^{-1} L_{11} \|\omega\|_{\mathcal{L}_2}, \tag{48}$$

which gives the upper bound in (43).

2. To prove that (8) solves the H_∞ output regulation problem, we need to show that the three properties in Problem 1 hold.
   a. By (46)-(47), $\bar{x} \in \mathcal{L}_2$. Because of the linearity of the system and by setting $\omega \equiv \mathbf{0}$, one can conclude that $\bar{x} \to \mathbf{0}$. Using the definition of $\bar{x}_i^T = [\xi_i - \xi_0, \nu_i]$, by setting $\xi_0 \equiv \mathbf{0}$, we have $x_i \to \mathbf{0}$.
   b. By (48), $\delta_y \in \mathcal{L}_2$. By linearity of the system and $\omega \equiv \mathbf{0}$, we conclude that $\delta_y \to \mathbf{0}$. Similarly, we can show that $\delta_z \to \mathbf{0}$.
   c. The $\mathcal{L}_2$-gain of δ_y with respect to ω is given in (48) and its finiteness is guaranteed by the conditions (i) or (ii) in the body of the theorem.

□

Remark 4
In Section 4, the designed control u_{op_i} and the signal β_i were considered separate while they are linked in the actual control signal (19) owing to heterogeneity of the agents. Theorem 4 reconciles development of graphical games in Section 4 with the original problem and takes the linkage of u_{op_i} and β_i in the actual control signal (19) into consideration. This requires additional conditions (given in the body of Theorem 4) that do not appear for homogeneous agents. Note that conclusions of Theorem 4 indeed reduce for identical agents to the cases familiar from the literature [18, 19]. Note also that the graph in our result is not required to be acyclic [31].

6. ONLINE SOLUTION TO H_∞ GRAPHICAL GAME

As we dicussed in Section 4, one needs to obtain solutions to the coupled partial differential HJB equations (34) to solve the graphical game problem. It is in general impossible to solve these equations analytically. However, RL has shown promising results in solving such complicated coupled equations numerically and is the only viable method applicable in real time. In this section, we propose a numerical RL procedure to design the controller gain K_i and to obtain solutions to the coupled HJB equations (34) in real time. Note that because of the heterogeneity of the agents in our paper, the RL frameworks in [18, 19] cannot be used.

Our online learning structure uses four adaptive networks. The first network approximates the value function and is named the critic network. The second one approximates the control policy and is named the actor network. The third and fourth networks approximate the disturbances ω_i and β_i.

Assume that the value function $V_i(\epsilon_i(t))$ is smooth. Then, according to Weierstrass higher-order approximation theorem, one can approximate $V_i(\epsilon_i(t))$ by

$$V_i(\epsilon_i) = W_i^T \Phi_i(\epsilon_i) + \varepsilon_i,$$

in which, Φ_i is a basis function vector with μ_{n_i} neurons, W_i is the optimal weight and ε_i is the approximation error. The weights of the critic network, which provide the best approximation to (34), are unknown. Let $\hat{W}_i$ denote the current estimate of the critic weights. Then, the approximated value function is given by

$$\hat{V}_i(\epsilon_i) = \hat{W}_i^T \Phi_i(\epsilon_i), \tag{49}$$

and the approximated error of the Bellman equation is

$$H_i = L_i + \hat{W}_i^T \nabla\Phi_i \dot{\epsilon}_i = \varepsilon_{H_i}. \tag{50}$$

Next, we define an actor network to approximate the optimal policy

$$\hat{u}_{op_i} = -\frac{1}{2} R_{ii}^{-1} \bar{B}_i^T \nabla\Phi_i^T \hat{W}_{i+N}, \tag{51}$$

where $\hat{W}_{i+N}$ denotes the current estimate of the actor weights. Also, we use two additional networks to approximate the worst-case disturbances (32)-(33)

$$\hat{\omega}_i = \frac{1}{2} \gamma_{\xi\nu_i}^{-2} S_{1ii}^{-1} \bar{P}_i^T \nabla\Phi_i^T \hat{W}_{i+2N}, \tag{52}$$

$$\hat{\beta}_i = \frac{1}{2} \gamma_{\beta_i}^{-2} S_{2ii}^{-1} \bar{B}_i^T \nabla\Phi_i^T \hat{W}_{i+3N}, \tag{53}$$

where $\hat{W}_{i+2N}$ and $\hat{W}_{i+3N}$ denote the current estimates of the weights of disturbances ω_i and β_i respectively.

The following theorem presents another main result of this paper; it gives the tuning laws for the adaptive network weights such that the HJB equation (34) is solved numerically, and closed-loop system of (25), the weight estimation errors $\tilde{W}_i = W_i - \hat{W}_i$, $\tilde{W}_{i+N} = W_i - \hat{W}_{i+N}$, $\tilde{W}_{i+2N} = W_i - \hat{W}_{i+2N}$, $\tilde{W}_{i+3N} = W_i - \hat{W}_{i+3N}$ are Uniformly Ultimately Bounded (UUB) [18].

Theorem 5
Consider Problem 2 and let the conditions in Theorem 4 hold. Assume that the value function, the policy and the disturbances are estimated by (49) and (51)-(53) respectively. Assume that

$$\sigma_{i+N} = \nabla\Phi_i \{ \bar{A}_i \epsilon_i + \bar{B}_i \hat{u}_{op_i} + \bar{P}_i \hat{\omega}_i + \bar{B}_i \hat{\beta}_i - \sum_{j=1}^{N} \alpha_{ij} (\underline{B}_j \hat{u}_{op_j} + \underline{P}_j \hat{\omega}_j + \underline{B}_j \hat{\beta}_j) \}, \tag{54}$$

is Persistently Exciting (PE). Tune the weights of the critic network as

$$\dot{\hat{W}}_i = -a_i \frac{\sigma_{i+N}}{(1 + \sigma_{i+N}^T \sigma_{i+N})^2} \varepsilon_{H_i}^{op} \tag{55}$$

Prepared using rncauth.cls
DOI: 10.1002/rnc

where $\varepsilon_{H_i}^{op}$ is obtained by inserting (51)-(53) in (50). Tune the weights of the actor and disturbance networks as

$$\begin{aligned}\dot{\hat{W}}_{i+N} =& -a_{i+N}\{(\bar{S}_{1i}\hat{W}_{i+N} - \bar{T}_{1i}\bar{\sigma}_{i+N}^T\hat{W}_i) - \frac{1}{4}\bar{D}_i\hat{W}_{i+N}\frac{\bar{\sigma}_{i+N}^T}{m_{s_i}}\hat{W}_i \\ &- \frac{1}{4}\sum_{j=1}^{N}\alpha_{ji}\nabla\Phi_i\bar{B}_iR_{ii}^{-1}R_{ji}R_{ii}^{-1}\bar{B}_i^T\nabla\Phi_i^T\hat{W}_{i+N}\frac{\bar{\sigma}_{j+N}^T}{m_{s_j}}\hat{W}_j\},\end{aligned} \tag{56}$$

$$\begin{aligned}\dot{\hat{W}}_{i+2N} =& -a_{i+2N}\{(\bar{S}_{2i}\hat{W}_{i+2N} - \bar{T}_{2i}\bar{\sigma}_{i+N}^T\hat{W}_i) + \frac{1}{4}\gamma_{\xi\nu_i}^{-2}\bar{E}_{2i}\hat{W}_{i+2N}\frac{\bar{\sigma}_{i+N}^T}{m_{s_i}}\hat{W}_i \\ &+ \frac{1}{4}\gamma_{\xi\nu_i}^{-2}\sum_{j=1}^{N}\alpha_{ji}\nabla\Phi_i\bar{P}_iS_{1ii}^{-1}S_{1ji}S_{1ii}^{-1}\bar{P}_i^T\nabla\Phi_i^T\hat{W}_{i+2N}\frac{\bar{\sigma}_{j+N}^T}{m_{s_j}}\hat{W}_j\},\end{aligned} \tag{57}$$

$$\begin{aligned}\dot{\hat{W}}_{i+3N} =& -a_{i+3N}\{(\bar{S}_{3i}\hat{W}_{i+3N} - \bar{T}_{3i}\bar{\sigma}_{i+N}^T\hat{W}_i) + \frac{1}{4}\gamma_{\beta_i}^{-2}\bar{E}_{3i}\hat{W}_{i+3N}\frac{\bar{\sigma}_{i+N}^T}{m_{s_i}}\hat{W}_i \\ &+ \frac{1}{4}\gamma_{\beta_i}^{-2}\sum_{j=1}^{N}\alpha_{ji}\nabla\Phi_i\bar{B}_iS_{2ii}^{-1}S_{2ji}S_{2ii}^{-1}\bar{B}_i^T\nabla\Phi_i^T\hat{W}_{i+3N}\frac{\bar{\sigma}_{j+N}^T}{m_{s_j}}\hat{W}_j\},\end{aligned} \tag{58}$$

where,

$$\begin{aligned}&\bar{\sigma}_{i+N} = \frac{\sigma_{i+N}}{1+\sigma_{i+N}^T\sigma_{i+N}}, \quad m_{s_i} = 1+\sigma_{i+N}^T\sigma_{i+N}, \\ &\bar{D}_i = \nabla\Phi_i\bar{B}_iR_{ii}^{-1}\bar{B}_i^T\nabla\Phi_i^T, \quad \bar{E}_{2i} = \nabla\Phi_i\bar{P}_iS_{1ii}^{-1}\bar{P}_i^T\nabla\Phi_i^T, \quad \bar{E}_{3i} = \nabla\Phi_i\bar{B}_iS_{2ii}^{-1}\bar{B}_i^T\nabla\Phi_i^T,\end{aligned} \tag{59}$$

and $a_i > 0$, $a_{i+N} > 0$, $a_{i+2N} > 0$, $\bar{T}_{1i} > 0$, $\bar{S}_{1i} > 0$, $\bar{T}_{2i} > 0$, $\bar{S}_{2i} > 0$, $\bar{T}_{3i} > 0$, $\bar{S}_{3i} > 0$, $i = 1, ..., N$ are the tuning parameters. Then,

1. The closed-loop system of (25), the weight estimation errors $\tilde{W}_i$, $\tilde{W}_{i+N}$, $\tilde{W}_{i+2N}$ and $\tilde{W}_{i+3N}$ are UUB.
2. ε_{H_i} is UUB and $\hat{W}_i$ converges to the approximated solution of the HJB equation (34) for $i = 1, ..., N$.
3. $\hat{u}_{op_i}$, $\hat{\omega}_i$, $\hat{\beta}_i$ converge to the approximated NE.

Proof
The proof is similar as in [17]. □

Remark 5
The tuning laws (55)-(58) in Theorem 5 are fully distributed and they depend only on local information available to each single-agent. Hence those are indeed applicable on undirected graphs, satisfying Assumption 1. The tuning laws (55)-(56) bring solutions to coupled HJB equations (34) and the applicable controls (19) in real time for heterogeneous agents. Additional adaptive networks (53) are used to estimate the β_i signals stemming from agent heterogeneity. These networks are absent for homogeneous agents, see [18, 19].

7. SIMULATION RESULTS

Consider a group of five followers and one leader communicating with each other according to the graph shown in Fig. 3. The edge weights in the communication graph are all set to one. Consider the followers' dynamics as

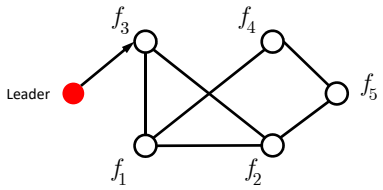

Figure 3. The communication graph

$$\begin{cases} \dot{x}_i = \begin{bmatrix} 0 & 1 & 0 & 0 \\ -1 & 0 & 0 & 0 \\ 0 & 0 & -7 & 2 \\ 0 & 0 & 0 & -4 \end{bmatrix} x_i + \begin{bmatrix} 0 \\ 1 \\ -0.2 \\ 0 \end{bmatrix} u_i + \begin{bmatrix} 0 \\ 1 \\ 0 \\ 0 \end{bmatrix} \omega_i \\ y_i = \begin{bmatrix} 1 & 1 & 1 & 1 \end{bmatrix} x_i, \quad z_i = \begin{bmatrix} 1 & 0 & 0 & 0 \\ 0 & 1 & 0.005 & 0 \end{bmatrix} x_i, \quad \text{for} \quad i = 1, 3, 5, \end{cases}$$

$$\begin{cases} \dot{x}_2 = \begin{bmatrix} 0 & 1 & 0 \\ -1 & 0 & 0 \\ 0 & 0 & -2 \end{bmatrix} x_i + \begin{bmatrix} 0.1 \\ 1 \\ 0.2 \end{bmatrix} u_i + \begin{bmatrix} 0 \\ 1 \\ 1 \end{bmatrix} \omega_i, \\ y_i = \begin{bmatrix} 1 & 1 & -1 \end{bmatrix} x_i, \quad z_i = \begin{bmatrix} 1 & 0 & 0.001 \\ 0 & 1 & -0.003 \end{bmatrix} x_i, \quad \text{for} \quad i = 2, 4. \end{cases}$$

Consider the leader's dynamics as

$$\dot{\xi}_0 = \begin{bmatrix} 0 & 1 \\ -1 & 0 \end{bmatrix} \xi_0, \quad y_0 = \begin{bmatrix} 1 & 1 \end{bmatrix} \xi_0, \quad z_0 = \begin{bmatrix} 1 & 0 \\ 0 & 1 \end{bmatrix} \xi_0.$$

According to the followers' and the leader's dynamics one can find that

$$\Pi_i = \begin{bmatrix} 1 & 0 \\ 0 & 1 \\ 0 & 0 \\ 0 & 0 \end{bmatrix}, \ \Psi_i = \begin{bmatrix} 0 & 0 \\ 0 & 0 \\ 1 & 0 \\ 0 & 1 \end{bmatrix}, \quad \text{for } i = 1, 3, 5, \text{ and } \quad \Pi_i = \begin{bmatrix} 1 & 0 \\ 0 & 1 \\ 0 & 0 \end{bmatrix}, \ \Psi_i = \begin{bmatrix} 0 \\ 0 \\ 1 \end{bmatrix}, \quad \text{for } i = 2, 4.$$

We use four adaptive networks as detailed in Section 6 to solve the differential graphical game for H_∞ output regulation in real time. The weights in the $\mathcal{L}_2$-condition (26) are selected as

$$\begin{aligned} &Q_i = 10I, \quad S_{1ii} = 1I, \quad S_{2ii} = 1I, \quad R_{ii} = 0.5, \quad S_{1ij} = 0.05I, \quad S_{2ij} = 0.05I \\ &R_{ij} = 0.05, \quad \gamma_{\xi\nu_i} = 1.5, \quad \gamma_{\beta_i} = 0.8, \quad i = 1, ..., 5, \quad j \in N_i. \end{aligned}$$

We select the tuning parameters as

$$a_i = 1,\ a_{i+N} = a_{i+2N} = a_{i+3N} = 0.1,\ \bar{S}_{1i} = \bar{S}_{2i} = \bar{S}_{3i} = 1I,\ \bar{T}_{1i} = \bar{T}_{2i} = \bar{T}_{3i} = 1I,\ i = 1, ..., 5.$$

The graphical game is implemented according to Theorem 5 and the gain K_i is obtained as shown in Remark 2. The worst-case disturbances in (52) are applied to the agents and are shown in Fig. 4a. The y-output synchronization errors for followers 1-5 are shown in Fig. 4b. Our simulation example illustrates feasibility and efficiency of adaptive networks for solving coupled HJB equations (34)-those networks perform sufficiently fast to be run online for reasonably large systems.

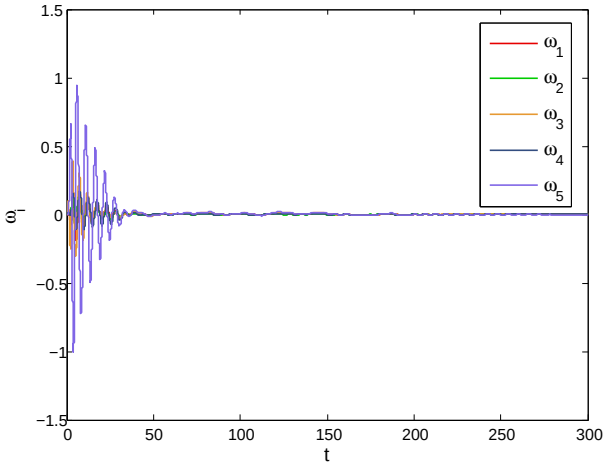

(a) The worst-case disturbances $\omega_i,\ i = 1, ..., 5$

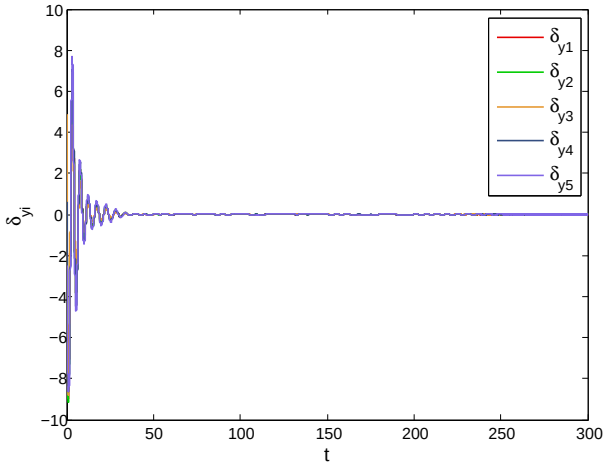

(b) y-output synchronization error $\delta_{yi},\ i = 1, ..., 5$

Figure 4. H_∞ output regulation results

8. CONCLUSION

In this paper, we have defined H_∞ graphical games for linear heterogeneous agents. Because of heterogeneity of the agents, we have used the output regulation theory to define the node error dynamics properly. Our graphical games formulation has two important properties: firstly, the agents are heterogeneous and secondly, unmodelled disturbances are present. This allows us to solve output regulation and H_∞ output regulation problems. We have obtained an upper bound for the $\mathcal{L}_2$-gain of the output synchronization error with respect to disturbances which has not been hitherto derived in the graphical game framework. We believe that the current developments shed some light on the problem of graphical games with heterogeneous agents.

ACKNOWLEDGEMENT

This paper is supported by the GACR grant 16-25493Y and NRF BCA GBIC grant on Scalable and Smart Building Energy Management (NRF2015ENC-GBICRD001-057).

REFERENCES

1. K. Hengster-Movric, F. L. Lewis, and M. Sebek, "Distributed static output-feedback control for state synchronization in networks of identical LTI systems," *Automatica*, vol. 53, pp. 282–290, 2015.
2. C.-Q. Ma and J.-F. Zhang, "Necessary and sufficient conditions for consensusability of linear multi-agent systems," *IEEE Transactions on Automatic Control*, vol. 55, no. 5, pp. 1263–1268, 2010.
3. L. Scardovi and R. Sepulchre, "Synchronization in networks of identical linear systems," *Automatica*, vol. 45, no. 11, pp. 2557–2562, 2009.
4. F. Adib Yaghmaie, F. L. Lewis, and R. Su, "Output regulation of linear heterogeneous multi-agent systems via output and state feedback," *Automatica*, vol. 67, pp. 157–164, 2016.
5. P. Wieland, R. Sepulchre, and F. Allgöwer, "An internal model principle is necessary and sufficient for linear output synchronization," *Automatica*, vol. 47, no. 5, pp. 1068–1074, 2011.
6. C. Huang and X. Ye, "Cooperative output regulation of heterogeneous multi-agent systems: An H_∞ criterion," *Automatic Control, IEEE Transactions on*, vol. 59, pp. 267–273, 2014.
7. F. Adib Yaghmaie, R. Su, F. L. Lewis, and L. Xie, "Multi-party consensus of linear heterogeneous multi-agent systems," *IEEE Transactions on Automatic Control*, vol. 62(11), pp. 5578 – 5589, 2017.
8. X. Wang, Y. Hong, J. Huang, and Z.-P. Jiang, "A distributed control approach to a robust output regulation problem for multi-agent linear systems," *Automatic Control, IEEE Transactions on*, vol. 55, no. 12, pp. 2891–2895, 2010.
9. J. Lunze, "Synchronization of heterogeneous agents," *IEEE transactions on automatic control*, vol. 57, no. 11, pp. 2885–2890, 2012.
10. F. Adib Yaghmaie, F. L. Lewis, and R. Su, "Output regulation of heterogeneous linear multi-agent systems with differential graphical game," *International Journal of Robust and Nonlinear Control*, vol. 26, pp. 2256–2278, 2016.
11. Y. Liu and Y. Jia, "Robust H_∞ consensus control of uncertain multi-agent systems with time delays," *International Journal of Control, Automation and Systems*, vol. 9, no. 6, pp. 1086–1094, 2011.
12. X. Yang and J. Wang, "Finite-gain $\mathcal{L}_p$ consensus of multi-agent systems," *International Journal of Control, Automation and Systems*, vol. 11, no. 4, pp. 666–674, 2013.
13. F. Adib Yaghmaie, K. Henster Movric, F. L. Lewis, R. Su, and M. Sebek, "H_∞ output regulation of linear heterogeneous multi-agent systems over switching graphs," *International Journal of Robust and Nonlinear Control*, vol. Accepted, 2018.
14. Q. Jiao, H. Modares, F. L. Lewis, S. Xu, and L. Xie, "Distributed l2-gain output-feedback control of homogeneous and heterogeneous systems," *Automatica*, vol. 71, pp. 361–368, 2016.
15. M. Zhang, A. Saberi, and A. A. Grip, Havard F.and Stoorvogel, "H_∞ almost output synchronization for heterogeneous networks without exchange of controller states," *IEEE transactions on control of network systems*, vol. 2, no. 4, pp. 348–357, 2015.
16. D. Liu, H. Li, and D. Wang, "Online synchronous approximate optimal learning algorithm for multi-player non-zero-sum games with unknown dynamics," *IEEE Transactions on Systems, Man, and Cybernetics: Systems*, vol. 44, no. 8, pp. 1015–1027, 2014.
17. K. G. Vamvoudakis and F. L. Lewis, "Multi-player non-zero-sum games: Online adaptive learning solution of coupled hamilton–jacobi equations," *Automatica*, vol. 47, no. 8, pp. 1556–1569, 2011.
18. K. G. Vamvoudakis, F. L. Lewis, and G. R. Hudas, "Multi-agent differential graphical games: Online adaptive learning solution for synchronization with optimality," *Automatica*, vol. 48, no. 8, pp. 1598–1611, 2012.
19. Q. Jiao, H. Modares, S. Xu, F. L. Lewis, and K. G. Vamvoudakis, "Multi-agent zero-sum differential graphical games for disturbance rejection in distributed control," *Automatica*, vol. 69, pp. 24–34, 2016.
20. T. Bian and Z.-P. Jiang, "Value iteration and adaptive dynamic programming for data-driven adaptive optimal control design," *Automatica*, vol. 71, pp. 348–360, 2016.
21. D. Vrabie, O. Pastravanu, M. Abu-Khalaf, and F. L. Lewis, "Adaptive optimal control for continuous-time linear systems based on policy iteration," *Automatica*, vol. 45, no. 2, pp. 477–484, 2009.
22. D. Liu, H. Li, and D. Wang, "Neural-network-based zero-sum game for discrete-time nonlinear systems via iterative adaptive dynamic programming algorithm," *Neurocomputing*, vol. 110, pp. 92–100, 2013.
23. D. Vrabie and F. Lewis, "Adaptive dynamic programming for online solution of a zero-sum differential game," *Journal of Control Theory and Applications*, vol. 9, no. 3, pp. 353–360, 2011.
24. F. L. Lewis and D. Vrabie, "Reinforcement learning and adaptive dynamic programming for feedback control," *IEEE circuits and systems magazine*, vol. 9, no. 3, 2009.
25. R. S. Sutton and A. G. Barto, *Reinforcement learning: An introduction*. MIT press Cambridge, 1998, vol. 1, no. 1.
26. A. Isidori, *Nonlinear control systems*. Springer Science & Business Media, 2013.
27. J. Huang, *Nonlinear output regulation: Theory and applications*. SIAM, 2004, vol. 8.
28. R. A. Hom and C. R. Johnson, *Topics in matrix analysis*, 1991.
29. H. K. Khalil, *Noninear Systems*. Prentice-Hall, New Jersey, 1996, vol. 2, no. 5.
30. F. L. Lewis, D. Vrabie, and V. L. Syrmos, *Optimal control*. John Wiley & Sons, 2012.
31. F. Adib Yaghmaie, F. L. Lewis, and R. Su, "Output regulation of heterogeneous multi-agent systems: A graphical game approach," in *American Control Conference (ACC), 2015*, 2015, pp. 2272–2277.

6. DISTRIBUTED OBSERVER AND CONTROLLER DESIGN FOR SPATIALLY DISTRIBUTED SYSTEMS

Xueji Zhang, Kristian Hengster-Movric, Michael Sebek, Wim Desmet, Cassio Faria, **Distributed observer and controller design for spatially distributed systems**, *IEEE Transactions on Control Systems Technology*, pp. 1-13, 2017

This chapter appears originally published in the IEEE *Transactions on Control Systems Technology,* (IF: 4.883), in 2017. Its main motivation is to address the pressing industrial concerns over vibration suppression in emerging smart materials and structures. In order to satisfy the ever stricter environmental criteria the manufacturers are looking into light-weight constructions that usually have decreased inherent vibration damping; hence the need for smart materials or piezo-composites that are able to do the job. Results presented in this paper show a successful application of distributed estimation *via* cooperative consensus for each actuating agent to gain an estimate of the overall environment, which is then used for its control. Measurements from different sensing agents are fused by the network to achieve this. Separation principle is found not to hold for this dynamic regulator architecture so some care must be exercised in specifying the observers' and controllers' parameters to guarantee overall observer convergence and system stability. The measurements considered here are only partial, but otherwise assumed to be of perfect accuracy.

This chapter tackles networked distributed observer and controller design problems over directed graph topology for spatially interconnected systems. Traditional centralized design methods suffer from a lack of adaptability to graph variations incurred by network reconfiguration, communication failures, and redundant sensors integration. In this paper, to handle the foregoing limitations imposed by centralized design, state observers are designed in a distributed manner facilitated by pinning control precepts. On the one hand, this novel approach adds fault tolerance with respect to communication link failures. On the other hand, the proposed approach brings flexibility of integrating additional sensors into the network. In addition, this approach affords a reduction of computational cost. A sufficient condition to guarantee stability of the closed-loop system is derived. The controllers, though in the end implemented in a distributed way, are designed in a centralized framework, where linear-quadratic-regulator theory is adopted to handle the fact that separation principle fails to hold in the networked observer and controller design. Numerical simulation results of a piezoelectric actuated smart flexible system are presented, and the effectiveness of the proposed design is thereby verified.

Distributed Observer and Controller Design for Spatially Interconnected Systems

Xueji Zhang, *Student Member, IEEE*, Kristian Hengster-Movrić, Michael Šebek, *Senior Member, IEEE*, Wim Desmet, and Cassio Faria

***Abstract*— This paper tackles networked distributed observer and controller design problem over directed graph topology for spatially interconnected systems. Traditional centralized design methods suffer from a lack of adaptability to graph variations incurred by network reconfiguration, communication failures, and redundant sensors integration. In this paper, to handle the foregoing limitations imposed by centralized design, state observers are designed in a distributed manner facilitated by pinning control precepts. On the one hand, this novel approach adds fault tolerance with respect to communication link failures. On the other hand, the proposed approach brings flexibility of integrating additional sensors into the network. In addition, this approach affords a reduction of computational cost. A sufficient condition to guarantee stability of the closed-loop system is derived. The controllers, though in the end implemented in a distributed way, are designed in a centralized framework, where linear-quadratic-regulator theory is adopted to handle the fact that separation principle fails to hold in the networked observer and controller design. Numerical simulation results of a piezoelectric actuated smart flexible system are presented, and the effectiveness of the proposed design is thereby verified.**

***Index Terms*— Consensus, distributed control, flexible structures, large-scale systems, networked control, pinning control, vibration damping.**

I. Introduction

TODAY is witnessing a more and more automated and networked world, and the concepts of smart factory, smart cities, automated highway, and Internet of Things have paved the way for a more intelligent future world. With rapid advances and integration of computing, communication, and smart sensing technologies, small-size and low-cost sensing devices empowered with embedded processing and communication capabilities have been deployed in a wide range of environments [1]–[4]. These technical achievements have attracted researchers from a variety of disciplines to the emerging field of networked control systems [5]–[7], and their synonymous cyber-physical systems in which cyber networks interact with humans and physical plants intensively [8]–[10].

The nascent networked/distributed control systems exhibit many advantages. First, communication *via* a network provides the potential to improve the overall system performance compared to purely decentralized control architectures, since fusion of global information enables the distributed control stations (decision makers) to gain deeper insights into the considered plant and thereafter make more intelligent decisions. Second, it reduces the implementation costs and complexity: for large-scale plants—a large number of system states and inputs/outputs or a geographically distributed plant—it might be costly to have a complete network with all-to-all links [11] or send all sensory information to a centralized controller, which would require a high communication bandwidth. Peer-to-peer networks, instead, can mitigate the communication overhead since each *node* or *agent* in the network communicates (transmits and/or receives information) only with its neighborhood. Physical wires are further eliminated in wireless actuator and sensor networks [12], [13]. Furthermore, with redundant communication links, networked/distributed control architecture can add the fault-tolerance property or retain graceful degradation in the case of single components (like sensors, actuators, and control stations) failures [5]. In contrast, a centralized controller might suffer a potential catastrophic failure. Additionally, the networked system benefits from *scalability* or *flexibility* if extra components such as actuators, sensors, or even control stations are integrated into the network in a plug-and-play fashion.

Versatile as it is, networked control paradigm induces many challenges as well [5], [6], of which distributed estimation/observation of system states is a fundamental problem, especially when observer-based control strategies are exploited to improve the system performance. In the past decade, a variety of related results have been reported [14]–[17]. In particular, with the theoretical framework of consensus protocols introduced in [18] and [19], consensus-based estimation has been extensively reported for linear systems (see [20]–[29]).

Manuscript received July 10, 2017; accepted October 3, 2017. Manuscript received in final form October 29, 2017. This work was supported in part by the European Commission under Marie Skłodowska-Curie Actions Grant 605087 and in part by the Czech Science Foundation GACR junior under Grant 16-25493Y. Recommended by Associate Editor C. Prieur. *(Corresponding author: Xueji Zhang.)*

X. Zhang is with the Department of Control Engineering, Faculty of Electrical Engineering, Czech Technical University, 166 36 Prague, Czech Republic, and also with the Production Engineering, Machine Design and Automation Division, Department of Mechanical Engineering, KU Leuven, 3001 Leuven, Belgium, and also with the LMS Engineering Service Division, Siemens Industry Software NV, 3001 Leuven, Belgium (e-mail: jay.xzhang2012@gmail.com).

K. Hengster-Movrić and M. Šebek are with the Department of Control Engineering, Faculty of Electrical Engineering, Czech Technical University, 166 36 Prague, Czech Republic (e-mail: kristian.hengster@gmail.com; michael.sebek@fel.cvut.cz).

W. Desmet is with the Production Engineering, Machine Design and Automation Division, Department of Mechanical Engineering, KU Leuven, 3001 Leuven, Belgium, and also with Flanders Make, 3001 Leuven, Belgium (e-mail: wim.desmet@kuleuven.be).

C. Faria is with the LMS Engineering Service Division, Siemens Industry Software NV, 3001 Leuven, Belgium (e-mail: cassio.faria@siemens.com).

Color versions of one or more of the figures in this paper are available online at http://ieeexplore.ieee.org.

Digital Object Identifier 10.1109/TCST.2017.2769019

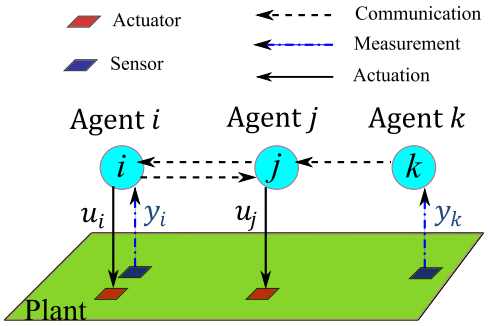

Fig. 1. Networked architecture equipped with distributed actuators and sensors over a large-scale plant.

Effort has also been devoted to tackling multiagent systems with nonlinear dynamics for consensus reaching and tracking [30]–[34].

In this paper, we design networked observers that fuse state estimates and controllers for linear-time-invariant spatially interconnected plants. Examples of such plants are furnished by large-scale flexible structures such as aircraft fuselage, truss bridges, and lattice towers. Mechanical and structural vibrations could be detrimental to the functioning and safety of these plants, hence effective vibration suppression is desired in many occasions. A schematic of the architecture in the networked control context is depicted in Fig. 1. Each *agent* possesses all or some of the following functions: sensing, actuation, communication, and information processing. Design of state observers and controllers for all the *agents* is a crucial problem for the considered networked architecture. As is widely known, observability is a measure for how well internal states of a system can be inferred from the knowledge of external system outputs [35]. In the networked system shown in Fig. 1, each measurement can have a different contribution from different system internal states. For example, a sensor placed at a given location on a flexible structure can detect some vibration modes more easily than others [36]. Hence, in this paper, each observer builds part of state estimates based on its local measurements, and the remaining part based on the consensus algorithm. Specifically, each observer has a communication matrix with a predefined structure depending on its local observability. Facilitated by the concept of synchronizing region in pinning control theory [37], [38], a distributed design procedure for the observers is proposed. The controllers, though in the end implemented in a distributed way, are designed in a centralized framework, where linear-quadratic-regulator theory is adopted to handle the fact that the *separation principle* fails to hold in the networked observer and controller design.

This paper differs from the spirit of many prior results. Our scheme allows the sensors in each agent to observe only some portions of the total plant states and requires only *global observability*, i.e., observability from all outputs taken together. This should be contrasted with [15], where each agent necessarily observes all the unstable states of the system. However, unlike [15], we do not consider the process and measurement noises, as this paper mainly focuses on the convergence and stability of designed distributed observers and controllers. Since we want all the observers' states to reach consensus asymptotically and to track the plant states, in consequence, each observer needs to estimate the total plant states, which is different from [25] where heterogeneous subspaces of the plant state are estimated among the distributed observers. On the one hand, we do not need to consider the projection matrices to match the heterogeneous subspaces of states of neighboring observers. On the other hand, however, we do require *global observability* of the network of distributed observers. Compared to [29], we do not guarantee optimality in any sense, but our proposed approach is distributed since the observer design equations are single-agent based. This leads to *scalability* or *flexibility* in terms of integrating additional sensors to the existent network and *robustness* to communication link failures as long as the connectivity requirements are satisfied. An additional merit of our distributed approach, in contrast with [29], is reduction of computational effort, as the total computational complexity grows linearly with the number of agents, while for each single agent, the effort depends only on the order of the plant. An early-stage work along these lines has been reported in [39], which relies on an assumption [39, Assumption 1] adopted for mathematical simplicity. This assumption presumes that the internal states of the considered plant can be decomposed into disjoint groups according to the measured outputs, and it is found to be at odds with some important realistic cases, in particular flexible structures. This paper therefore attempts to relax this assumption, so that the design procedure can be more successfully applied to vibration damping for flexible structures. The main contributions of this paper are as follows.

1) The communication graph topology is separated from the observer/controller design. And the requirements on graph topology are relaxed from (connected) undirected graphs to more general directed graphs, compared with [15], [28], and [34].
2) Since the observer design is single-agent based, it leads to *flexibility* in terms of integrating additional sensors to the existent network and graceful degradation in case of communication link failures as long as connectivity requirements remain satisfied. These properties are not expected in [29].

This paper is organized as follows. Necessary mathematical preliminaries and problem formulation are given in Section II. Distributed observer design without considering controls is elaborated in Section III. Distributed controller design is analyzed in Section IV. Numerical simulations of vibration reduction for a representative smart flexible structure are presented in Section V. Finally, Section VI concludes this paper.

II. Preliminaries and Problem Formulation

A. Preliminaries on Graph Theory and Notation

The communication topology for state estimates is represented by a directed graph [40]. A directed graph $\mathcal{G} = (\mathcal{V}, \mathcal{E}, \mathcal{A})$ consists of a set of *nodes* $\mathcal{V} \triangleq \{1, 2, \ldots, p\}$,

a set of edges $\mathcal{E} \subset \mathcal{V} \times \mathcal{V}$, and an associated adjacency matrix $\mathcal{A} = [a_{ij}]$. An edge (i, j) is graphically depicted by an arrow with the head *node i* and the tail *node j*, indicating that the information flows from *node j* to *node i*. Each entry a_{ij} of $\mathcal{A}$ is the weight associated with the pair (i, j), and in this paper, it is taken that $a_{ij} = 1$ if $(i, j) \in \mathcal{E}$; $a_{ij} = 0$, otherwise. We consider simple graphs with no self-edges, namely, $a_{ii} = 0$ and $\forall i \in \mathcal{V}$. The set of neighbors of *node i* is denoted as $\mathcal{N}_i \triangleq \{j | (i, j) \in \mathcal{E}\}$. Define the in-degree of *node i* as $d_i \triangleq \sum_{j=1}^{p} a_{ij}$ and in-degree matrix as $\mathcal{D}_{\text{in}} \triangleq \text{diag}\{d_i\}$. The graph Laplacian matrix is then defined as $\mathcal{L} \triangleq \mathcal{D}_{\text{in}} - \mathcal{A}$.

A sequence of successive edges in the form of $\{(i, k), (k, l), \ldots, (m, j)\}$ is a directed path from *node j* to *node i*. A directed tree is an acyclic directed graph with a root node such that there is a unique directed path from that root node to every other *node* in the directed tree. A spanning tree of $\mathcal{G}$ is a directed tree that contains all the *nodes* of $\mathcal{G}$ [40]. A directed forest is a disjoint union of directed trees. A spanning forest of $\mathcal{G}$ is a directed forest that contains all the *nodes* of $\mathcal{G}$. A graph $\mathcal{H}$ is a subgraph of $\mathcal{G}$ if $\mathcal{V}(\mathcal{H}) \subseteq \mathcal{V}(\mathcal{G})$, $\mathcal{E}(\mathcal{H}) \subseteq \mathcal{E}(\mathcal{G})$ and $\mathcal{A}(\mathcal{H})$ is a restriction of $\mathcal{A}(\mathcal{G})$ [40]. A square matrix is an *M-matrix* if all its off-diagonal elements are nonpositive and all its eigenvalues have positive real parts [41], [42].

Throughout this paper, $\otimes$ is used to denote the Kronecker product [43]. $\mathbf{1}_p$ denotes a vector of dimension of p with all entries equal *1*. I_p denotes an identity matrix of dimension $p \times p$. $\mathbf{0}$ stands for a zero matrix with a compatible dimension in context. $\mathbf{0}_{m\times n}$ denotes a zero matrix with dimension $m \times n$. $\lambda(A)$ denotes the eigenvalue of the matrix A. $Re(\lambda)$ represents the real part of λ. $\lambda_{\min}(A)$ and $\lambda_{\max}(A)$ are adopted to denote the minimum and maximum eigenvalue of a real symmetric matrix A, respectively. $|\mathcal{V}|$ denotes the cardinality of the set $\mathcal{V}$.

B. Problem Formulation

The considered dynamics of the plant is in the form of

$$\begin{cases} \dot{x}(t) = Ax(t) + \sum_{i=1}^{p} B_i u_i(t) = Ax(t) + Bu(t) \\ y_i(t) = C_i x(t), i = 1, 2, \ldots, p \end{cases} \tag{1}$$

where $x \in \mathbb{R}^n$ is the state of the plant, $u_i \in \mathbb{R}^{m_i}$ and $i \in \mathcal{V}$, are the control inputs of agent i, $y_i \in \mathbb{R}^{p_i}$ and $i \in \mathcal{V}$ are the system outputs which are measurements by different agents, and

$$B = \begin{bmatrix} B_1 & B_2 & \ldots & B_p \end{bmatrix} \in \mathbb{R}^{n\times m}$$
$$u = \begin{bmatrix} u_1^T & u_2^T & \ldots & u_p^T \end{bmatrix}^T \in \mathbb{R}^m.$$

To allow for a distributed design in Section III, we need to transform $A \in \mathbb{R}^{n\times n}$ to a block diagonal matrix. For example, one widely used technique is Jordan decomposition [44]. In fact there always exists a nonsingular real matrix $\Pi = \begin{bmatrix} \Pi_1 & \Pi_2 & \ldots & \Pi_l \end{bmatrix} \in \mathbb{R}^{n\times n}$ such that $A\Pi_i = \Pi_i A_i$ and $A\Pi = \Pi\tilde{A}$, where

$$\tilde{A} = \begin{bmatrix} A_1 & & & \\ & A_2 & & \\ & & \ddots & \\ & & & A_l \end{bmatrix} \in \mathbb{R}^{n\times n}, \quad \Pi_i \in \mathbb{R}^{n\times n_i}.$$

$A_i \in \mathbb{R}^{n_i\times n_i}$ is the Jordan block which has one of two forms [45]. However, it should be pointed out that the Jordan decomposition here serves only as an example for the block-diagonalization of the real matrix A; it is by no means the unique approach. The main motivation for focusing on block-diagonal system matrices here is our consideration of the eigenmodes in flexible structures. For the problem considered in this paper, we suppose that Π is given or can be found without difficulty such that $\tilde{A} = \Pi^{-1}A\Pi$ is block diagonal. With the linear transformation $x = \Pi z = \sum_{i=1}^{l} \Pi_i z_i$, where $z = [z_1^T \; z_2^T \; \ldots \; z_l^T]^T \in \mathbb{R}^n$, $z_i \in \mathbb{R}^{n_i}$, and $\sum_{i=1}^{l} n_i = n$, the dynamics of the plant becomes

$$\begin{cases} \dot{z}(t) = \tilde{A}z(t) + \sum_{i=1}^{p} \tilde{B}_i u_i(t) \\ y_i(t) = C_i \Pi z(t) \end{cases} \quad i \in \mathcal{V}. \tag{2}$$

Herein, $\tilde{B}_i = \Pi^{-1}B_i$. Furthermore, for conciseness and clarity of notation, throughout the rest of the paper, we define the set $\mathcal{S} \triangleq \{1, 2, \ldots, l\}$. In addition, we make the following assumption.

Assumption 1: $C_{ij} \triangleq C_i\Pi_j \neq \mathbf{0}$, where $i \in \mathcal{V}$ and $j \in \mathcal{S}$, if and only if the state group z_j is observable from the measurement y_i.

Remark 1: In general, *Assumption 1* is a strong assumption: if z_j is observable from y_i, certainly $C_{ij} \neq \mathbf{0}$, but not necessarily *vice versa*. *Assumption 1* is equivalent to saying that a state-group permutation alone can bring the system to a Kalman decomposed form [46]. This is trivially satisfied if all A_j blocks are distinct and have the dimension of 1: $n_j = 1$ and $\forall j \in \mathcal{S}$. For A_j blocks of dimension larger than 1, this assumption is reasonable in this paper due to two facts; the first one is that *Assumption 1* is approximately satisfied by flexible structure dynamics, as we consider the eigenmodes which are dynamically independent, and this induces a partition of each output C_i into C_{ij} matrices; the second fact is that even if *Assumption 1* is only approximately satisfied, in the sense that if $C_{ij} \neq \mathbf{0}$ but small in magnitude, such C_{ij} can be neglected completely for design, and hence the pertaining z_j is classified as unobservable from output y_i. Our proposed design in Section III is robust enough to withstand putting such z_j simply in the set of unobservable state groups (see the discussion in Section III-B).

Definition 1: The *observable set* of *agent i*, $i \in \mathcal{V}$, is defined as $\mathcal{O}_i \triangleq \{j \in \mathcal{S} | C_{ij} \neq \mathbf{0}\}$; the *unobservable set* of *agent* $i \in \mathcal{V}$ is defined as $\overline{\mathcal{O}}_i \triangleq \{j \in \mathcal{S} | j \notin \mathcal{O}_i\}$.

Definition 2: The *converse observable set* of z_j, $j \in \mathcal{S}$, is defined as $\mathcal{D}_j \triangleq \{i \in \mathcal{V} | C_{ij} \neq \mathbf{0}\}$; the *converse unobservable set* of z_j is defined as $\overline{\mathcal{D}}_j \triangleq \{i \in \mathcal{V} | i \notin \mathcal{D}_j\}$.

Note that *Definition 1* and *Definition 2* are conjugate: $j \in \mathcal{O}_i \Longleftrightarrow i \in \mathcal{D}_j$; $j \in \overline{\mathcal{O}}_i \Longleftrightarrow i \in \overline{\mathcal{D}}_j$.

Assumption 2: The system is globally observable

$$\mathcal{O}_1 \cup \mathcal{O}_2 \cup \ldots \cup \mathcal{O}_p = \mathcal{S}.$$

This simply means that the entire system is observable from all outputs taken together.

As introduced in Section I, *p agents* are assigned to the plant. The structure of *agent* i, $i \in \mathcal{V}$, is in the form of

$$\begin{cases} \dot{\hat{z}}_i(t) = \tilde{A}\hat{z}_i(t) + L_i(y_i(t) - \hat{y}_i(t)) \\ \qquad\qquad +\mathcal{F}_i \cdot \left(\sum_{k\in\mathcal{N}_i} a_{ik}(\hat{z}_k(t) - \hat{z}_i(t)) \right) + \tilde{B}\hat{U}_i(t) \\ \hat{y}_i(t) = C_i \Pi \hat{z}_i(t) \\ \hat{U}_i(t) = K\hat{z}_i(t) \\ u_i(t) = K_i\hat{z}_i(t) \end{cases} \tag{3}$$

where $\hat{z}_i \in \mathbb{R}^n$ is the state estimate vector of observer i, $L_i \in \mathbb{R}^{n\times p_i}$ is the Luenberger-like observer gain [47], $\mathcal{F}_i \in \mathbb{R}^{n\times n}$ is the communication matrix, and $\tilde{B} = \Pi^{-1}B$. Note that $\hat{z}_i$ has a different dimension from $z_i \in \mathbb{R}^{n_i}$, since $\hat{z}_i$ is the state estimate of the total system; while z_i is a subset of the system states. Note also that all the observers share the same drift dynamics $\tilde{A}$ which equals that of the plant. This way, each observer replicates the dynamics of the entire plant and if synchronized to the plant state, they would all continue to track it with no need for further communication. The agent i estimates the system states *via* two information sources: one is the local measurement y_i, accounted by the term $L_i(y_i - \hat{y}_i)$, and the other is the state estimate from neighboring agents, appearing in the term $\mathcal{F}_i \cdot [\sum_{k\in\mathcal{N}_i} a_{ik}(\hat{z}_k(t) - \hat{z}_i(t)]$. It is considered that the controller in each *agent* generates an estimate-based local control action to the plant, $u_i(t)$, as shown in (3). Herein, $K_i \in \mathbb{R}^{m_i\times n}$ is the local feedback matrix to be designed for *agent* i. $\hat{U}_i \in \mathbb{R}^m$ is the estimation, by *agent* i, of the overall control action applied to the plant, and it is constructed based on the local state estimate: $\hat{U}_i = K\hat{z}_i$, where $K \in \mathbb{R}^{m\times n}$ is the global feedback matrix

$$K = \begin{bmatrix} K_1^T & K_2^T & \ldots & K_p^T \end{bmatrix}^T. \tag{4}$$

Remark 2: Different possibilities for $\hat{U}_i$ exist, for example, neighboring estimates could be used. However, in all such distributed cases, unless all the local state estimates $\hat{z}_i$, $\forall i \in \mathcal{V}$, reach consensus, each control estimation $\hat{U}_i$ is different from the actual control action u applied to the system. This mismatch leads to a feature not appearing in the conventional centralized observer and feedback design. Specifically speaking, the controller design is not completely separated from the observer design, making the problem complex as elaborated later in Section IV.

Note that even though in (3) the local control action u_i appears for each *agent*, in practice depending on matrix B or $\tilde{B}$, it is allowed that some *agents* apply no control actions, as long as the following *global controllability* holds.

Assumption 3: The pair (A, B) (or equivalently the pair $(\tilde{A}, \tilde{B})$) is controllable.

Assumption 4: The communication graph $\mathcal{G}$, given *a priori*, satisfies the following condition: for any $j \in \mathcal{S}$, the subgraph $\mathcal{G}_j$, formed by the *nodes* belonging to $\mathcal{D}_j$, has outgoing edges pinning into all the roots of a spanning forest of the subgraph $\overline{\mathcal{G}}_j$, formed by the *nodes* belonging to $\overline{\mathcal{D}}_j$.

Remark 3: Note that we consider general directed graph, whereas many existing results [15], [28], [34] focus only on undirected graphs.

In summary, the problem addressed in this paper is to design distributed observers (parameters: $\{L_i\}, \{\mathcal{F}_i\}$ in (3)) and controllers (parameters: $\{K_i\}$ in (3)) to achieve asymptotic state *omniscience* [48] and stabilization, namely

$$\begin{cases} \lim_{t\to\infty} (\hat{z}_i(t) - z(t)) = 0, \forall i \in \mathcal{V} \\ \lim_{t\to\infty} z(t) = 0. \end{cases} \tag{5}$$

III. Distributed Observer Design

This section proposes a distributed design for the distributed observers. Observers are designed here without applying any control actions u_is and also without control signal estimates $\hat{U}_i$s, namely, in (3) let $K_i = \mathbf{0}$ and $\forall i \in \mathcal{V}$.

A. Main Results

The dynamics of the autonomous plant becomes

$$\begin{cases} \dot{z}(t) = \tilde{A}z(t) \\ y_i(t) = C_i\Pi z(t) = \sum_{j\in\mathcal{O}_i} C_{ij} z_j(t), i \in \mathcal{V}. \end{cases} \tag{6}$$

Accordingly, the dynamics of the observers then reads

$$\begin{cases} \dot{\hat{z}}_i(t) = \tilde{A}\hat{z}_i(t) + L_i(y_i(t) - \hat{y}_i(t)) \\ \qquad\qquad +\mathcal{F}_i \cdot \left(\sum_{k\in\mathcal{N}_i} a_{ik}(\hat{z}_k(t) - \hat{z}_i(t)) \right) \quad i \in \mathcal{V}. \\ \hat{y}_i(t) = C_i\Pi\hat{z}_i(t) \end{cases} \tag{7}$$

Similar to the internal states of the plant, states of each observer are divided accordingly into l groups

$$\hat{z}_i \triangleq \begin{bmatrix} \hat{z}_{i1} \\ \hat{z}_{i2} \\ \vdots \\ \hat{z}_{il} \end{bmatrix} \in \mathbb{R}^n, \quad \forall i \in \mathcal{V},\ \hat{z}_{ij} \in \mathbb{R}^{n_j},\ \forall j \in \mathcal{S}. \tag{8}$$

We rearrange the states of each observer i, $i \in \mathcal{V}$, such that the new state vector $\hat{z}_i^{\text{new}}$ is a tandem of observable state vector $\hat{z}_{io} \in \mathbb{R}^{n_{io}}$, containing z_{ij}s, for $j \in \mathcal{O}_i$ and unobservable state vector $\hat{z}_{i\bar{o}} \in \mathbb{R}^{n_{i\bar{o}}}$, containing z_{ij}s, for $j \in \overline{\mathcal{O}}_i$. Specifically, for each $\hat{z}_i$, there is a permutation matrix T_i such that $\hat{z}_i^{\text{new}} = [\hat{z}_{io}\ \hat{z}_{i\bar{o}}] = T_i\hat{z}_i$. Correspondingly, in the new coordinates, the dynamical and output matrices are

$$\begin{cases} T_i\tilde{A}T_i^{-1} = T_i\tilde{A}T_i^T = \begin{bmatrix} A_{io} & \\ & A_{i\bar{o}} \end{bmatrix} \\ C_i\Pi T_i^T = \begin{bmatrix} C_{io} & \mathbf{0}_{p_i\times n_{i\bar{o}}} \end{bmatrix}. \end{cases} \tag{9}$$

Remark 4: After this permutation of state groups, the plant is in Kalman decomposed form, as made possible by *Assumption 1*. It can be concluded that for $\hat{z}_{io}$, a Luenberger-like

observer can be designed relying only on the local measurements y_i to estimate the corresponding part of the plant states.

However, to make the state $\hat{z}_{i\bar{o}}$ converge to the corresponding part of system state which is unobservable for agent i, the local measurements are to no avail, so the observer i needs information from the communication network. The dynamics of each component of $\hat{z}_{i\bar{o}}$, $\hat{z}_{ij}$, is considered separately. Hence, we propose to decompose the dynamics of each observer i, $i \in \mathcal{V}$, in

$$\begin{cases} \dot{\hat{z}}_{io}(t) = A_{io}\hat{z}_{io}(t) + L_{io}(y_i(t) - \hat{y}_i(t)) \\ \dot{\hat{z}}_{ij}(t) = A_j\hat{z}_{ij}(t) \\ \qquad\qquad + c_j F_j \left(\sum_{k\in\mathcal{N}_i} a_{ik}(\hat{z}_{kj}(t) - \hat{z}_{ij}(t)) \right), j \in \overline{\mathcal{O}}_i \\ \hat{y}_i(t) = \sum_{j\in\mathcal{O}_i} C_{ij}\hat{z}_{ij}(t) = C_{io}\hat{z}_{io}(t). \end{cases} \quad (10)$$

Herein L_{io} is the observer gain matrix, $c_j > 0$ is the scalar coupling gain, and $F_j \in \mathbb{R}^{n_j \times n_j}$ is the communication matrix. For the observer i, L_{io}, $\{c_j\}$ and $\{F_j\}$, $j \in \overline{\mathcal{O}}_i$ are the parameters to be designed. The rationale of decomposing the dynamics of each observer as shown in (10) is to allow for a distributed design later.

Remark 5: In (10), c_j and F_j can take a more general form, reflected by notation c_{ij} and F_{ij}. However, with the first subscript omitted here, different observers share some of the design parameters. For example, if $\overline{\mathcal{O}}_i \cap \overline{\mathcal{O}}_k \neq \emptyset$, then for $j \in \overline{\mathcal{O}}_i \cap \overline{\mathcal{O}}_k$, observer i and k will share the same parameters c_j, F_j. The motivation for omitting the first subscript is to adopt the synchronizing region theory for distributed design as illustrated later in this section.

For system integration, it is worth to explicitly relate (7) with (10) *via* the following equations:

$$L_i = T_i^T \begin{bmatrix} L_{io} \\ \mathbf{0}_{n_{i\bar{o}} \times p_i} \end{bmatrix} \quad (11)$$

$$\mathcal{F}_i = T_i^T \begin{bmatrix} \mathbf{0}_{n_{io}\times n_{io}} & \mathbf{0}_{n_{io}\times n_{i\bar{o}}} \\ \mathbf{0}_{n_{i\bar{o}}\times n_{io}} & \mathrm{diag}\{c_j F_j\} \end{bmatrix} T_i. \quad (12)$$

For convergence analysis, define the observation error of observer i for the state z_j as

$$\delta_{ij} \triangleq \hat{z}_{ij} - z_j. \quad (13)$$

For observer i, stack all the δ_{ij} values with $j \in \mathcal{O}_i$ together, and denote them as δ_{io}. These are the observation errors of observer i for state groups z_js which observer i estimates locally.

Proposition 1: The dynamics of $\delta_{io}, i \in \mathcal{V}$ is

$$\dot{\delta}_{io} = (A_{io} - L_{io}C_{io})\delta_{io}. \quad (14)$$

The proof is immediate from (6) and (10).

Proposition 2: For $j \in \overline{\mathcal{O}}_i$, the dynamics of δ_{ij} is

$$\begin{aligned} \dot{\delta}_{ij} &= A_j\delta_{ij} + c_j F_j \left[\sum_{k\in\mathcal{N}_i} a_{ik}(\delta_{kj} - \delta_{ij}) \right] = A_j\delta_{ij} \\ &\quad + c_j F_j \left[\sum_{\substack{k\in\mathcal{N}_i, \\ k\in\overline{\mathcal{D}}_j}} a_{ik}(\delta_{kj} - \delta_{ij}) + \sum_{\substack{k\in\mathcal{N}_i, \\ k\in\mathcal{D}_j}} a_{ik}(\delta_{kj} - \delta_{ij}) \right] \\ &= A_j\delta_{ij} + c_j F_j \left[\sum_{k\in\overline{\mathcal{D}}_j} a_{ik}\delta_{kj} - \sum_{k\in\mathcal{N}_i} a_{ik}\delta_{ij} \right] \\ &\quad + c_j F_j \sum_{k\in\mathcal{D}_j} a_{ik}\delta_{kj}. \end{aligned} \quad (15)$$

The proof is immediate from (6) and (10). We denote the last term in (15) as $\upsilon_{ij} = c_j F_j \sum_{k\in\mathcal{D}_j} a_{ik}\delta_{kj}$.

Fixing j, stack all the δ_{ij}s with $i \in \overline{\mathcal{D}}_j$, denoted as $\delta_{\bar{o}j} \in \mathbb{R}^{n_j|\overline{\mathcal{D}}_j|}$. These are the observation errors with respect to state z_j for all those observers that do not estimate z_j directly, relying not on the local measurements but rather on the information from the network.

Proposition 3: The dynamics of $\delta_{\bar{o}j}$, $j \in \mathcal{S}$, is

$$\dot{\delta}_{\bar{o}j} = (I_{|\overline{\mathcal{D}}_j|} \otimes A_j - c_j\mathcal{L}_j \otimes F_j)\delta_{\bar{o}j} + \upsilon_j \quad (16)$$

where υ_j is a stack of υ_{ij}s with all $i \in \overline{\mathcal{D}}_j$. $\mathcal{L}_j$ is obtained *via* deleting the kth row and column from the original Laplacian matrix $\mathcal{L}$ of graph $\mathcal{G}$, for all $k \in \mathcal{D}_j$.

Proof: From (15), we know for $i \in \overline{\mathcal{D}}_j$ (or equivalently $j \in \overline{\mathcal{O}}_i$)

$$\begin{aligned} \dot{\delta}_{ij} &= A_j\delta_{ij} + c_j F_j \left[\sum_{k\in\overline{\mathcal{D}}_j} a_{ik}\delta_{kj} - \sum_{k\in\mathcal{N}_i} a_{ik}\delta_{ij} \right] \\ &\quad + c_j F_j \sum_{k\in\mathcal{D}_j} a_{ik}\delta_{kj} \\ &= A_j\delta_{ij} - c_j F_j \left[d_i\delta_{ij} + \sum_{k\in\overline{\mathcal{D}}_j} (-a_{ik})\delta_{kj} \right] + \upsilon_{ij}. \end{aligned} \quad (17)$$

The coefficients appearing in the term $[d_i\delta_{ij} + \sum_{k\in\overline{\mathcal{D}}_j}(-a_{ik})\delta_{kj}]$, d_i, and $-a_{ik}$s, form the ith row of $\mathcal{L}$ with the i_xth columns removed for $i_x \in \mathcal{D}_j$. Fixing j, stacking δ_{ij}s for all $i \in \overline{\mathcal{D}}_j$ to construct $\delta_{\bar{o}j}$, one immediately gets (16) from (17). ■

Remark 6: Note that for construction of $\delta_{\bar{o}j}$, we only select δ_{ij}s with $i \in \overline{\mathcal{D}}_j$. However, the dynamics of $\delta_{\bar{o}j}$ is also influenced by δ_{ij}s with $i \in \mathcal{D}_j$, and all such δ_{ij} values are included in υ_j in (16), hence the constructed $\mathcal{L}_j$ is a square matrix.

Lemma: Under *Assumption 4*, $\mathcal{L}_j$ constructed in (16) is a nonsingular *M-matrix*. □

Proof: From the original graph, a group of *nodes* ($i \in \mathcal{V}$ and $i \in \mathcal{D}_j$) is excluded. The effect of these excluded *nodes* on the remaining ones, as reflected by $\mathcal{L}_j$, is the same as if the

remaining *nodes* were pinned by a single leader, with appropriately summed pinning gains.[1] In the latter instance, the pertaining pinned Laplacian matrix is a nonsingular *M-matrix* if the single leader pins into all the *roots* of a *spanning forest* [49]. In the former, original, instance, this condition is equivalent to the excluded group of *nodes* pinning with their outgoing edges into all *roots* of the *spanning forest* of the subgraph $\overline{\mathcal{G}}_j$, formed by the *nodes* belonging to $\overline{\mathcal{D}}_j$. According to *Assumption 4*, $\mathcal{L}_j$ is a nonsingular *M-matrix*. ■

Then, define the total observation error for observer i as $\delta_i = \hat{z}_i - z$. Put these observation errors for all observers together in a compact form $\delta = [\delta_1^T \ \delta_2^T \ \dots \ \delta_p^T]^T$.

Proposition 4: The dynamics of δ is given by

$$\dot{\delta} = A_\epsilon \delta \tag{18}$$

where $A_\epsilon = \text{diag}\{\tilde{A} - L_i C_i \Pi\} - \mathcal{F} \cdot (\mathcal{L} \otimes I_n)$, and $\mathcal{F} = \text{diag}\{\mathcal{F}_i\}$.

Proof: From (6) and (7), the dynamics of δ_i can be derived as

$$\dot{\delta}_i = (\tilde{A} - L_i C_i \Pi)\delta_i + \mathcal{F}_i \cdot \sum_{k \in \mathcal{N}_i} a_{ik}(\delta_k - \delta_i). \tag{19}$$

The proof of *Proposition 4* is immediately completed by stacking the dynamics of all the δ_i values together. ■

Propositon 5: A_ϵ is Hurwitz iff the dynamics of $\delta_{io}, \forall i \in \mathcal{V}$, and $\delta_{\overline{o}j}, \forall j \in \mathcal{S}$ are asymptotically stable.

This result can be easily proved by noticing that the components of δ include all the components of $\delta_{io}, \forall i \in \mathcal{V}$, and $\delta_{\overline{o}j}, \forall j \in \mathcal{S}$, and *vice versa*.

The following theorem proposes a distributed design of the parameters for all the observers to estimate the plant states when no controls or their estimates are present.

Theorem 1: Under *Assumptions 1*, 2, and 4 the following hold.

1) Let each L_{io}, $i \in \mathcal{V}$, be selected such that the matrix $A_{io} - L_{io}C_{io}$ is Hurwitz.

2) Let $F_j = \hat{R}_j^{-1}\hat{P}_j$, $j \in \mathcal{S}$, where $\hat{P}_j = \hat{P}_j^T \succ 0 \in \mathbb{R}^{n_j \times n_j}$ is the unique positive definite solution of the following control algebraic Riccati equation:

$$A_j^T \hat{P}_j + \hat{P}_j A_j - \hat{P}_j \hat{R}_j^{-1} \hat{P}_j + \hat{Q}_j = 0 \tag{20}$$

where $\hat{Q}_j \succeq 0 \in \mathbb{R}^{n_j \times n_j}$ and $\hat{R}_j \succ 0 \in \mathbb{R}^{n_j \times n_j}$ are given.

3) Let c_j, $j \in \mathcal{S}$, satisfy the condition

$$c_j \geq \frac{1}{2\underline{\lambda}_{R_j}}, \quad j \in \mathcal{S} \tag{21}$$

with $\underline{\lambda}_{R_j} = \min_k Re(\lambda_{jk})$, and $\lambda_{j\bullet}$ are the eigenvalues of $\mathcal{L}_j$. Then with the dynamics of (6) and (7), $\lim_{t\to\infty}(\hat{z}_i(t) - z(t)) = 0$, $\forall i \in \mathcal{V}$. □

Proof: Since each matrix $A_{io} - L_{io}C_{io}$ is Hurwitz, the dynamics (14) of all the $\delta_{io}, \forall i \in \mathcal{V}$ is asymptotically stable.

Under *Assumption 2*, all δ_{io}s $\forall i \in \mathcal{V}$ consist of all δ_{kj}s, where $\forall j \in \mathcal{S}$ and $\forall k \in \mathcal{D}_j$. Therefore, $v_{ij} = c_j F_j \sum_{k \in \mathcal{D}_j} a_{ik}\delta_{kj}$ in (15) vanishes asymptotically in time. Hence the stability of $\delta_{\bar{o}j}$ is determined by the matrix $I_{|\overline{\mathcal{D}}_j|} \otimes A_j - c_j\mathcal{L}_j \otimes F_j$ in (16).

Based on the *Lemma*, $\mathcal{L}_j$ is a nonsingular *M-matrix*, hence satisfying preconditions on pinned Laplacians for synchronization [38, Assumption 1]. According to [38, Th. 1], the matrix $I_{|\overline{\mathcal{D}}_j|} \otimes A_j - c_j\mathcal{L}_j \otimes F_j$ for all $j \in \mathcal{S}$ is Hurwitz, if all F_js are designed based on (20) and all c_j values satisfy (21). Therefore the dynamics of $\delta_{\bar{o}j}$ for all $j \in \mathcal{V}$ is asymptotically stable.

Given that the dynamics of both $\delta_{io}, \forall i \in \mathcal{V}$ and $\delta_{\overline{o}j}, \forall j \in \mathcal{S}$ is asymptotically stable, according to *Proposition 5*, A_ϵ is Hurwitz. This completes the proof. ■

Remark 7: Theorem 1 is one of the main results of this paper. It provides a distributed observer design for A_ϵ to be Hurwitz. One specific way of selecting L_{io} to obtain a Hurwitz matrix $A_{io} - L_{io}C_{io}$ is by using LQR theory: let $L_{io} = P_i C_{io}^T R_i^{-1}$, $i \in \mathcal{V}$, where $P_i = P_i^T \succ 0 \in \mathbb{R}^{n_{io} \times n_{io}}$ is the unique solution of the observer algebraic Riccati equation

$$A_{io}P_i + P_i A_{io}^T + Q_i - P_i C_{io}^T R_i^{-1} C_{io} P_i = 0, \tag{22}$$

where $Q_i \succeq 0 \in \mathbb{R}^{n_{io} \times n_{io}}$ and $R_i \succ 0 \in \mathbb{R}^{p_i \times p_i}$ are properly chosen. Any other design of a stabilizing L_{io}, pole-placement for example, is equally applicable.

Remark 8: In *Theorem 1*, (20) and (21) are chosen with an eye toward the synchronizing region results familiar from cooperative control theory. The aim in cooperative control is to render matrices like A_ϵ Hurwitz. However, that cannot be generally achieved by straightforward classical pole-placement if the graph is allowed to vary or is imperfectly known. Synchronizing region approach achieves asymptotic stability while providing a certain level of robustness to varying graphs. Namely, the subsystems, in our case A_j values, are considered separately from the detailed graph topology. In particular, the distributed gain designed as in (20) and (21) yields an unbounded synchronizing region, allowing for a wide class of communication graphs. Hence this design can handle less-than-perfectly reliable graphs, with possible agent or link failures. Conventional pole placement would generally not result in these specific properties.

Remark 9: Furthermore, the additional merit of this distributed approach is to reduce the computational effort needed for design. The total computational complexity grows linearly in the number of agents, while for each single agent, the effort depends only on the order of the plant. This should be contrasted with centralized designs existing in the literature (see [29] and *Remark 16* in Section V-A).

Remark 10: Nevertheless, other approaches to yield a Hurwitz A_ϵ do exist; for example, as proposed in [28], let $M = [M_1^T, M_2^T, \dots, M_p^T]^T \in \mathbb{R}^{n \times n}$ such that the matrix $\tilde{A} - M\tilde{C}$ is Hurwitz, where $\tilde{C} = [C_1^T, C_2^T, \dots, C_p^T]^T \Pi$, then in (7) with $L_i = pM_i$ and $\mathcal{F}_i = \gamma I_n$ with a sufficiently large positive scalar γ, the matrix A_ϵ defined in *Proposition 4* is Hurwitz. However, note that the approach in [28] is restricted to undirected graphs.

B. Discussion

In the practical design, one may encounter several issues with the developed distributed method, and some of them are thereby discussed more clearly in the following.

[1] All incoming edges a_{ik}, $k \in \mathcal{D}_j$ of a pinned node i, are summed as if originating from a single pinning leader, namely, $\sum_{k \in \mathcal{D}_j} a_{ik}$.

1) *Assumption 1* may be only approximately satisfied in the sense that for *agent* i, the magnitude of some C_{ij} is nonzero but quite small, hence the corresponding state group z_j is costly to estimate. One realistic approach to tackle this is to neglect small C_{ij} values, considering those states corresponding to small C_{ij} values as being in the *unobservable set* $\overline{\mathcal{O}}_i$. Such terms would only introduce a small vanishing disturbance which a properly designed asymptotically converging observer is robust to (see [50]). In such a case, after the design of distributed observers, it needs to be checked if the resulting matrix $\tilde{A} - L_i C_i \Pi$ is still Hurwitz. If it is not Hurwitz, then Q_i and R_i in (22) should be tuned to make L_{io} smaller in magnitude.
2) The instance of an observer i with all $C_{ij}s$, $j \in \mathcal{S}$, relatively large does not cause problems for our approach. This only means that the observer i can reconstruct all the plant states based on its local measurements y_i. It sends its state estimates to the network, but does not receive any state estimates from the network.
3) *Theorem* 1 also allows for some *agent* i to have $C_{ij} = \mathbf{0}$, $\forall j \in \mathcal{S}$. In this case that *agent* does not have a local sensing device and reconstructs all the states based only on the information from the network. It would serve as a linking node or a router in the network, and possibly as an actuator as well.

Remark 11: The systems we focus on in this paper are flexible structures which can be described to a high degree of accuracy by linear models. However, in principle, the design philosophy proposed in *Theorem 1* is applicable to a class of nonlinear systems along the lines of [32]–[34], if it is assumed, similar to *Assumption 1*, that by pure permutation of state groups, for every $i \in \mathcal{V}$, the plant dynamics can be cast into the corresponding decomposed form. Particularly, one would then have, similar to (10), for observer i

$$\begin{cases} \dot{\hat{z}}_{io} = f_{io}(\hat{z}_{io}, t) + O_i^{-1}(z_{io}) M_i [y_i(t) - h_{io}(\hat{z}_{io}(t))] \\ \dot{\hat{z}}_{ij} = f_j(\hat{z}_{ij}, t) + c_j F_j \left[\sum_{k \in \mathcal{N}_i} a_{ik} (\hat{z}_{kj}(t) - \hat{z}_{ij}(t)) \right], \; j \in \overline{\mathcal{O}}_i \end{cases} \tag{23}$$

where $O_i(z_{io})$ has full rank and is Lipschitz continuous [51], $M_i \in \mathbb{R}^{n_{io}}$ is some finite gain vector. If conditions of [51, Th. 1] are fulfilled, $\hat{z}_{io}$ would converge to z_{io}. And if each f_j satisfies special Quadratic condition [33] for $\hat{z}_{ij}, z_j \in ker(\hat{P}_j \hat{R}_j^{-1} \hat{P}_j)$

$$(\hat{z}_{ij} - z_j)^T \hat{P}_j (f_j(\hat{z}_{ij}, t) - f_j(z_j, t)) \leq -(\hat{z}_{ij} - z_j)^T \hat{Q}_j (\hat{z}_{ij} - z_j) \tag{24}$$

where $\hat{Q}_j = \hat{Q}_j^T \succ 0$, then with sufficiently large c_j and $F_j = \hat{R}_j^{-1} \hat{P}_j$, each $\hat{z}_{ij}$ would converge to the corresponding plant state z_j.

IV. Distributed Controller Design

Section III proposes a distributed design for observers without any controls acting, resulting in a Hurwitz matrix A_ϵ. In this section, we return to the original problem of (2) and (3) building on results of Section III and considering controls and their estimates. Here we propose a design of feedback matrix K which stabilizes the original system while the distributed observers maintain estimates' convergence.

Proposition 6: When controls and their estimates are applied, the dynamics of the global observation error δ for all *agents* is given by

$$\dot{\delta} = A_\epsilon \delta + B_\epsilon(K) \delta \tag{25}$$

where $B_\epsilon(K) = I_p \otimes \tilde{B} K + \mathbf{1}_p \otimes \Upsilon(K)$ and

$$\Upsilon(K) = \left[-\tilde{B}_1 K_1 \; -\tilde{B}_2 K_2 \; \ldots \; -\tilde{B}_p K_p \right].$$

Proof: From (2) and (3), the dynamics of $\delta_i = \hat{z}_i - z$ can be derived as

$$\dot{\delta}_i = (\tilde{A} - L_i C_i \Pi)\delta_i + \mathcal{F}_i \sum_{k \in \mathcal{N}_i} a_{ik} (\delta_k - \delta_i) + \tilde{B} K \delta_i - \sum_{j=1}^{p} \tilde{B}_j K_j \delta_j. \tag{26}$$

The proof of *Proposition* 6 is immediately completed by stacking the dynamics of all the δ_i values together. ■

Remark 12: When there are no control actions, the error dynamics is given by (18), which is here considered as the *nominal case*. Note that if $K = \mathbf{0}$, $B_\epsilon(K) = I_p \otimes \tilde{B} K + \mathbf{1}_p \otimes \Upsilon(K) = \mathbf{0}$. As shown in (25), the mismatch between the real control actions u and the estimated control actions $\hat{U}_i, i \in \mathcal{V}$ generates a vanishing perturbation [50], for the dynamics of observation error δ.

The following theorem gives a sufficient condition to solve the problem (5) posed in Section II.

Theorem 2: Under *Assumption 1–4*, with the plant dynamics described by (2) and the *agent* dynamics described by (3), let the conditions in *Theorem 1* be satisfied. If the matrix K is designed such that $\tilde{A} + \tilde{B} K$ is Hurwitz and $\|K\|_\infty < (\lambda_{\min}(Q)/2\sqrt{np}(1+p)\|\tilde{B}\|_\infty \lambda_{\max}(P))$, where $P = P^T \succ 0$ is the unique solution for the Lyapunov equation $A_\epsilon^T P + P A_\epsilon = -Q$ with a given $Q = Q^T \succ 0$, then the dynamics of plant (2) is asymptotically stable, and all the observers reach consensus converging to the true plant states. □

Proof: From (2) and (3), expressing $\hat{z}_i$ as $(z + \delta_i)$, the dynamics of z is

$$\dot{z} = \tilde{A} z + \sum_{i=1}^{p} \tilde{B}_i K_i (z + \delta_i) = (\tilde{A} + \tilde{B} K) z - \Upsilon(K) \delta. \tag{27}$$

Define the augmented state vector $\xi = [z^T, \delta^T]^T$. Based on (27) and *Proposition 6*, the closed-loop dynamics of ξ is

$$\dot{\xi} = \begin{bmatrix} \tilde{A} + \tilde{B} K & -\Upsilon(K) \\ \mathbf{0} & A_\epsilon + B_\epsilon(K) \end{bmatrix} \xi. \tag{28}$$

This is a hierarchical system; if $\tilde{A} + \tilde{B} K$ is Hurwitz, the stability of the closed-loop dynamics is determined by the matrix $A_\epsilon + B_\epsilon(K)$, i.e., the dynamics of (25).

A_ϵ is guaranteed to be Hurwitz by *Theorem 1*. Based on [50, Lemma 9.1, p. 341], the dynamics of (25) is asymptoti-

cally stable if

$$\begin{cases} \|B_\epsilon(K)\delta\|_2 \le \gamma \|\delta\|_2 \\ \gamma = \dfrac{\lambda_{\min}(Q)}{2\lambda_{\max}(P)}. \end{cases} \tag{29}$$

Since

$$\begin{aligned} \|B_\epsilon(K)\|_\infty &= \|I_p \otimes \tilde{B}K + \mathbf{1}_p \otimes \Upsilon(K)\|_\infty \\ &\le \|I_p \otimes \tilde{B}K\|_\infty + \|\mathbf{1}_p \otimes \Upsilon(K)\|_\infty \\ &= \|\tilde{B}K\|_\infty + \|\Upsilon(K)\|_\infty, \end{aligned}$$

and $\|\Upsilon(K)\|_\infty \le \sum_{i=1}^{p} \|\tilde{B}_i K_i\|_\infty \le p\|\tilde{B}\|_\infty \|K\|_\infty$, one has $\|B_\epsilon(K)\|_\infty \le (1+p)\|\tilde{B}\|_\infty \|K\|_\infty$. Based on matrix analysis, $\|B_\epsilon(K)\|_2 \le \sqrt{np}\|B_\epsilon(K)\|_\infty \le \sqrt{np}(1+p)\|\tilde{B}\|_\infty \|K\|_\infty$. Hence if $\sqrt{np}(1+p)\|\tilde{B}\|_\infty \|K\|_\infty < (\lambda_{\min}(Q)/2/\lambda_{\max}(P))$, that is

$$\|K\|_\infty < \frac{\lambda_{\min}(Q)}{2\sqrt{np}(1+p)\|\tilde{B}\|_\infty \lambda_{\max}(P)} \tag{30}$$

is satisfied, then (29) holds and the dynamics of (28) is asymptotically stable, which means $z \to 0$ and $\delta \to 0$. ■

Remark 13: Condition (30) reveals the fact that if the magnitude of K is bounded under a certain level, the observation error dynamics (25) remains asymptotically stable. However, it should be noted that this condition is conservative.

To ensure the matrix $\tilde{A}+\tilde{B}K$ is Hurwitz, while not yielding an unstable matrix $A_\epsilon + B_\epsilon(K)$, K can be designed using, e.g., the LQR framework for the system

$$\begin{cases} \dot{z}(t) = \tilde{A}z(t) + \tilde{B}u(t) \\ u(t) = Kz(t) \end{cases} \tag{31}$$

where $K = -\mathcal{R}^{-1}\tilde{B}^T\mathcal{P}$, and $\mathcal{P} = \mathcal{P}^T \succ 0 \in \mathbb{R}^{n\times n}$ is the unique solution of the following algebraic Riccati equation:

$$\tilde{A}^T\mathcal{P} + \mathcal{P}\tilde{A} + \mathcal{Q} - \mathcal{P}\tilde{B}\mathcal{R}^{-1}\tilde{B}^T\mathcal{P} = 0 \tag{32}$$

and $\mathcal{Q} \succeq 0 \in \mathbb{R}^{n\times n}$ and $\mathcal{R} \succ 0 \in \mathbb{R}^{m\times m}$ are given matrices.

Remark 14: Any design of stabilizing K for the dynamics (28) is, in principle, applicable. However, the LQR approach is adopted here mainly because of its neat parameterization with $\mathcal{Q}$ and $\mathcal{R}$ matrices. Through imposing a large $\mathcal{R}$, the control action would be limited to a safe range which could not deteriorate the convergence of observation errors. Note that eigenvalues of $A_\epsilon + B_\epsilon(K)$ are continuous functions of K, i.e., $\lambda(A_\epsilon + B_\epsilon(K))$. When $K = \mathbf{0}$, which is the *nominal case*, the real part of the eigenvalues $Re(\lambda(A_\epsilon + B_\epsilon(K))) = Re(\lambda(A_\epsilon)) < 0$, if A_ϵ is designed based on *Theorem 1*. Hence by imposing large $\mathcal{R}$ in (32), $A_\epsilon + B_\epsilon(K)$ is guaranteed to be Hurwitz, due to the resulting small $\|K\|_\infty$.

Remark 15: Note that in (28), K relates both observer $[A_\epsilon + B_\epsilon(K)]$ and controller $(\tilde{A} + \tilde{B}K)$ design, imposing their interdependence. The main results of this section reveal a partial separation principle of sorts. LQR approach is proposed to partially separate the observer and controller design. Observers are designed without considering controls in Section III, while controls are designed here as with perfect state information (31). This differs from the spirit of [29] where observer and controller design are inseparable.

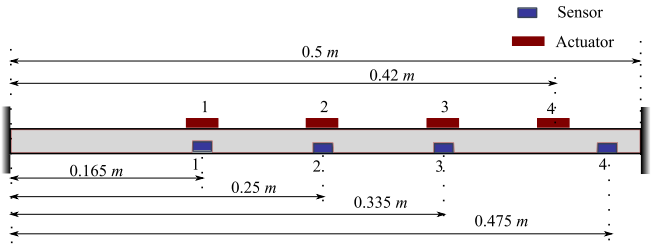

Fig. 2. Piezoelectric actuated beam clamped at both ends; four piezo actuators are distributed along the beam.

TABLE I
PARAMETER TABLE

Parameter	Value
beam length	$0.5\ m$
beam width	$0.03\ m$
Poisson ratio	0.33
beam thickness	$0.003\ m$
beam density	$2700\ kg/m^3$
Young's Modulus	$69 \times 10^9 Pa$
Piezo type	PZT 5H
actuator size	$0.03 \times 0.03 m^2$
actuator thickness	$0.001m$
1st resonance frequency	$18.5\ Hz$
2nd resonance frequency	$52.0\ Hz$
3rd resonance frequency	$104.2\ Hz$
4th resonance frequency	$176.2\ Hz$
5th resonance frequency	$270.5\ Hz$
6th resonance frequency	$380.9\ Hz$
η	0.112
ζ	2.769×10^{-7}

V. APPLICATION EXAMPLE

Active control of smart flexible structures has received extensive attention in recent years. Exemplary applications lie in the aeronautic, aerospace (satellites, telescopes, and so on), and civil engineering (earthquake-resistant buildings, lattice towers, and so on). This section gives numerical simulations to demonstrate the efficacy of the proposed distributed design of observers and centralized design of controllers applied to vibration reduction of a flexible structure. Section V-A describes a representative flexible structure and simulation results are given in Section V-B.

A. System Modeling

We consider an example of a clamped aluminum beam with four surface-bonded piezoelectric actuators as the representative smart flexible structure. The distribution of the piezoelectric actuators and sensors on the beam is depicted in Fig. 2. The parameters of the smart structure are shown in Table I. A detailed finite element (FE) model of the smart flexible structure is built using a procedure similar to the one in [53]. The beam is divided into 100 elements equidistantly. The dynamics of the sensors is neglected. The piezoelectric actuators are polarized in the thickness direction, and the electric field is assumed to be constant along the thickness of the actuator. The equation of motion of the smart flexible structure is derived using the Hamilton principle, yielding

$$[M]\ddot{q}(t) + [D]\dot{q}(t)\big([K_s] - \Theta_{q\phi}\Theta_{\phi\phi}^{-1}\Theta_{q\phi}^T\big)q(t) = -\Theta_{q\phi}u(t) \tag{33}$$

where q denotes the nodal displacement vector, consisting of transverse displacement and rotation of cross section of all the

nodes [54], $[D]$, $[M]$, and $[K_s]$ are the damping matrix, mass matrix and stiffness matrix, respectively. $\Theta_{q\phi}$ and $\Theta_{\phi\phi}$ are the piezoelectric coupling matrix and the piezoelectric capacity matrix respectively, and u is the input vector of voltages driving the piezoelectric actuators. The *Rayleigh damping* is adopted in the model [55]

$$[D] = \eta[M] + \zeta[K_s] \tag{34}$$

where the values of η and ζ are listed in Table I.

The FE model constructed has been cross-validated by LMS Samcef Field, a commercial finite element modeling solver suite from Siemens PLM Software. Velocities are considered as the measured outputs

$$y(t) = H_o\dot{q}(t) \tag{35}$$

where H_o is the location matrix for measurement channels. In practice, velocity information can be obtained either by noncontact laser Doppler vibrometers or by numerical integration of bandpass filtered outputs of accelerometers.

The first six vibration modes are extracted via mode displacement method [56]. Specifically, consider the following coordinates transformation:

$$q = \Phi_r q_m \tag{36}$$

herein Φ_r stands for the first six columns of Φ, where Φ is the matrix of the ordered natural mode shapes. Let $x = [q_m \ \dot{q}_m]$. The dynamics of the piezoelectric actuated beam expressed by (33) and (35) can be written into state-space representation

$$\begin{cases} \dot{x} = Ax + Bu \\ y = Cx \end{cases} \tag{37}$$

where

$$A = \begin{bmatrix} \mathbf{0}_{6\times 6} & I_6 \\ -\left(\Phi_r^T[M]\Phi_r\right)^{-1}\Phi_r^T[K_{aug}]\Phi_r & -\left(\Phi_r^T[M]\Phi_r\right)^{-1}[D] \end{bmatrix}$$

$$B = \begin{bmatrix} \mathbf{0}_{6\times 4} \\ -\left(\Phi_r^T[M]\Phi_r\right)^{-1}\Theta_{q\phi} \end{bmatrix}$$

$$C = L_o\Phi_r\begin{bmatrix}\mathbf{0}_{6\times 6} & I_6\end{bmatrix}$$

and

$$[K_{\text{aug}}] = [K_s] - \Theta_{q\phi}\Theta_{\phi\phi}^{-1}\Theta_{q\phi}^T.$$

Obviously, A is not block diagonal, we block-diagonalize it mode-wisely, by putting $z = \Pi^{-1}x$ in the form [36]

$$z = \left[(q_{m1},\ \dot{q}_{m1}), \quad \ldots, \quad (q_{m6}, \quad \dot{q}_{m6})\right]^T = \left[z_1, \ldots, z_6\right]^T. \tag{38}$$

Then $\tilde{A} = \text{diag}\{A_1, A_2, \ldots, A_6\}$ with $A_i = [0\ 1\ -\omega_i^2\ -2\xi_i\omega_i]$, ω_i and ξ_i are the ith modal frequency in radian per second and modal damping ratio, respectively.

The 2-norms of C_{ij} for $i = 1, 2, 3, 4$ and $j = 1, 2, 3, 4, 5, 6$ are depicted in Fig. 3. The observability of modes compared to the 2-norms of C_{ij}s is found to satisfy *Assumption 1*. In particular, the second sensor is placed in the middle of the clamped beam, hence it can observe only the first, third, and fifth mode groups, which is consistent with the $\|C_{2j}\|_2$ profile in Fig. 3. Also, as discussed in Section III-B, when the

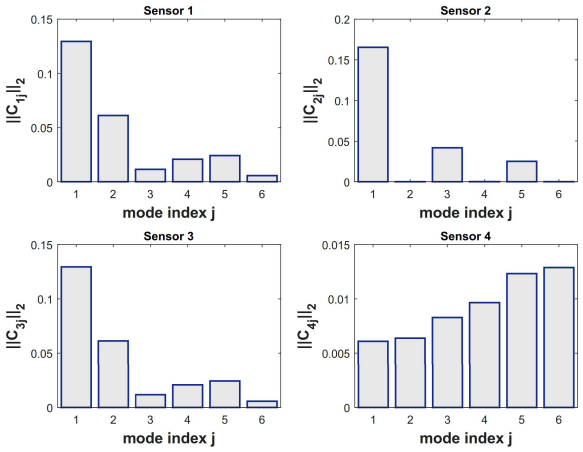

Fig. 3. $\|C_{ij}\|_2$, $i = 1, 2, 3, 4$ and $j = 1, 2, 3, 4, 5, 6$.

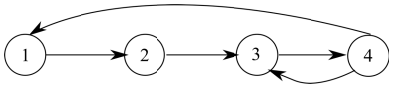

Fig. 4. Communication topology.

magnitude of some C_{ij} is relatively small, for the distributed design, one can treat that corresponding state group as being in the unobservable set $\overline{\mathcal{O}_i}$ as long as *Assumption 2* still holds, because this will only introduce small vanishing disturbances to Luenberger-like observers. Hence the *observable set* for each *agent* is allocated as follows: $\mathcal{O}_1 = \{1, 2\}$, $\mathcal{O}_2 = \{1, 3\}$, $\mathcal{O}_3 = \{1, 2\}$, and $\mathcal{O}_4 = \{4, 5, 6\}$.

The communication topology of the four *agents* is shown in Fig. 4. It can be verified that the given graph satisfies *Assumption 4*. The corresponding Laplacian matrix is

$$\mathcal{L} = \begin{bmatrix} 1 & 0 & 0 & -1 \\ -1 & 1 & 0 & 0 \\ 0 & -1 & 2 & -1 \\ 0 & 0 & -1 & 1 \end{bmatrix}.$$

Obtaining $\mathcal{L}_i, i \in \mathcal{S}$ is straightforward; for example, for $i = 3$, $\mathcal{D}_3 = \{2\}$, by eliminating the second row and column from $\mathcal{L}$, we get

$$\mathcal{L}_3 = \begin{bmatrix} 1 & 0 & -1 \\ 0 & 2 & -1 \\ 0 & -1 & 1 \end{bmatrix}.$$

L_{1o}, L_{2o}, L_{3o}, and L_{4o} are here designed based on (22): for $i = 1, 2, 3$, $Q_i = I_{n_{io}}$, $R_i = 1 \times 10^{-3}$; for $i = 4$, $Q_4 = I_6$, $R_4 = 1 \times 10^{-2}$. F_1, F_2, F_3, F_4, F_5, and F_6 are designed based on (20): for $i = 1, 2, 3, 4, 5, 6$, $\hat{Q}_i = \hat{R}_i = I_2$. In (21), $\underline{\lambda}_{R_1} = \underline{\lambda}_{R_2} = \underline{\lambda}_{R_4} = \underline{\lambda}_{R_5} = \underline{\lambda}_{R_6} = 1$; $\underline{\lambda}_{R_3} = 0.3820$. For $j = 1, 2, 3, 4, 5, 6$, $\{c_j\}$ values are chosen as $c_j = 10$ to reach the estimates' consensus fast enough. L_i values and $\mathcal{F}_i$ values are constructed based on (11) and (12), respectively. A_ϵ is checked if it is Hurwitz following the observer design. The controllers are designed based on (32), and $\mathcal{Q}$ and $\mathcal{R}$ are assigned as $\mathcal{Q} = I_{12}$ and $\mathcal{R} = 3 \times 10^{-5} I_4$.

Remark 16: Note that as mentioned in *Remark 9*, the complexity of our design procedure depends linearly on the

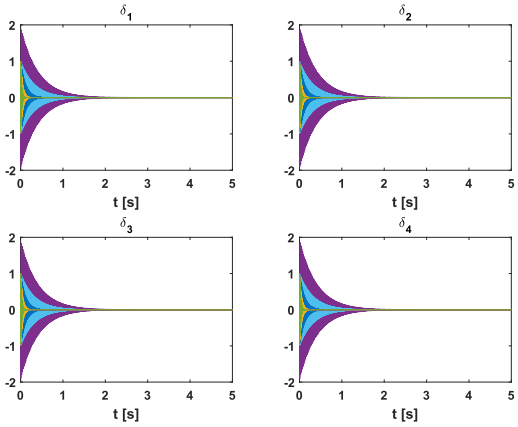

Fig. 5. State observation error of *agents* in time-domain.

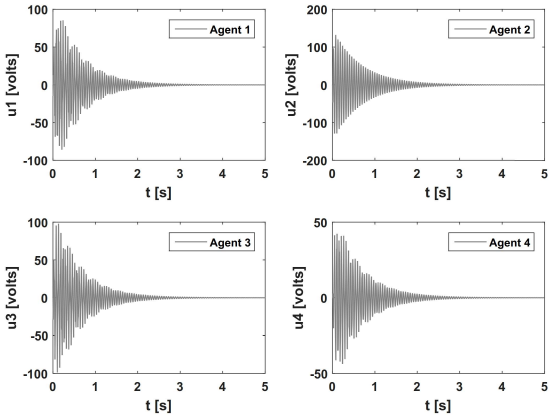

Fig. 6. Piezoelectric transducer actuation voltages.

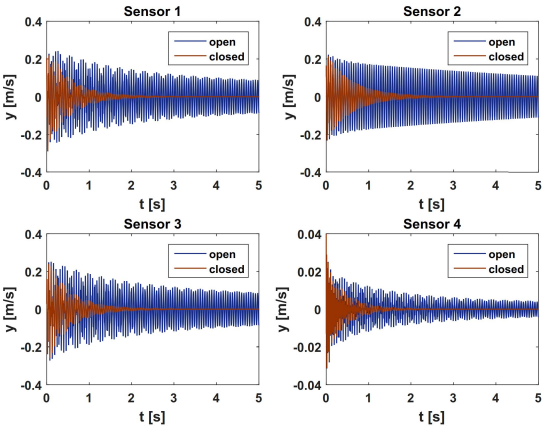

Fig. 7. Comparison of measurement signals in time-domain between open- and closed-loop.

number of agents, while for each single agent, the complexity depends only on the order of the plant. To carry out a fair comparison with [29], we have resorted to linear matrix inequality method to solve algebraic Riccati equations involved in the above design (see [57]). The computational complexity for agent i, $i \in \mathcal{V}$, and the total system is

$$J_i = O\left(n_{io}^2\right) + \frac{n_{i\bar{o}}}{2} O(2^2) \leq O(n^2) \tag{39}$$

$$J_{\text{total}} = \sum_{i=1}^{p} J_i + O(n^2) \leq (1+p) O(n^2). \tag{40}$$

Note, in practice, the design of c_j values in (21) is to choose a sufficiently large number, and hence its computational cost is negligible. Whereas the computational complexity for the centralized design in [29] is

$$J' = O\left(\frac{n^*(n^*+1)}{2}\right) + O\left(n \sum_{i=1}^{p} p_i\right) + O\left(n \sum_{i=1}^{p} m_i\right) + O\left(n^2 \sum_{i=1}^{p} d_i\right) \tag{41}$$

where $n^* = n(p+1)$. Apparently, in our distributed design, the computational complexity scales better with a growing number of agents. In fact, the computational complexity for each agent does not depend on the total agent number p.

B. Simulations

Numerical simulations are run in MATLAB/Simulink environment. The initial condition for the plant states is arbitrarily chosen as $z(0) = [0.005, 1, 0.005, 1, 0, 1, 0, 1, 0, 1]^T$. All initial states for the observers are set to zero. As depicted in Fig. 5, the local observation error $\delta_i = \hat{z}_i - z, i = 1, 2, 3, 4$ converges to zero within *2* s. The voltage transient to drive the piezoelectric actuators is shown in Fig. 6. To demonstrate the damping performance, an open-loop measurement and closed-loop measurement are compared in Fig. 7. The slow decay of the measurement signals for the open-loop case is due to the inherent low damping of the flexible beam.

1) Failure of Communication Link ④ ⟶ ③: To demonstrate that our distributed approach is *robust* against varying graphs to a certain degree, we consider a communication failure from agent *4* to agent 3. From Fig. 4, we know that the remaining graph still satisfies *Assumption 4*. The local observation error $\delta_i = \hat{z}_i - z, i = 1, 2, 3, 4$ is given in Fig. 8. Compared with Fig. 5, no critical degradation in terms of convergence time is observed, indicating the *robustness* property of the design approach. It is natural to deduce that the more redundant communication links are, the more *robust* the NCS will be.

2) Integrating an Extra Agent to the Network: This simulation scenario is to present how to integrate extra sensors to the network with only a small number of additional parameters to design. We consider adding an additional *agent* 5 with sensing capability into the well-established network. The sensor is added to measure the location 0.20 m from the left clamped end in Fig. 2. The augmented graph is depicted in Fig. 9.

We only need to design parameters for *agent* 5. The 2-norms of C_{ij} for $j = 1, 2, 3, 4, 5, 6$ are depicted in Fig. 10. The *observable set* for *agent 5* is allocated as $\mathcal{O}_5 = \{1\}$. L_{5o} is designed based on (22) with $Q_5 = I_2$, $R_5 = 1 \times 10^{-3}$. Note that even though the graph topology has changed, c_j values for $j = 1, 2, 3, 4, 5, 6$ still satisfy the condition (21),

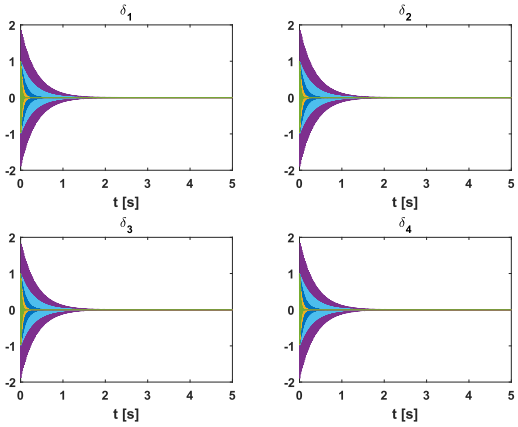

Fig. 8. State observation error of *agents* in time-domain, after a communication link failure.

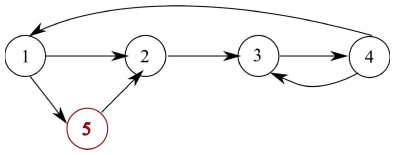

Fig. 9. Communication topology, after adding *agent 5*.

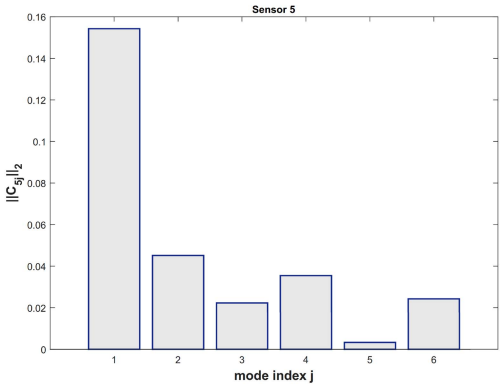

Fig. 10. Profile of $\|C_{5j}\|_2$, $j = 1, 2, 3, 4, 5, 6$.

since their values are initially chosen large enough. L_5 and $\mathcal{F}_5$ are constructed based on (11) and (12), respectively. The new A_ϵ is checked if it is Hurwitz after this additional observer design. Note that the *flexibility* demonstrated in this example stems from inherent robustness of the synchronizing region design.

3) Distributed Estimation on a More Complex Graph: This simulation scenario is to verify the proposed distributed estimation scheme on a more complex directed graph, specifically one comprising 11 agents. The sensors are distributed on the beam with the nodal index 5, 15, 25, 35, 45, 50, 60, 70, 80, 90, 95, respectively. The *observable sets* are allocated as: $\mathcal{O}_1 = \{5, 6\}$, $\mathcal{O}_2 = \{1, 2, 3, 4\}$, $\mathcal{O}_3 = \{1, 2\}$, $\mathcal{O}_4 \sim \mathcal{O}_7 = \{1\}$, $\mathcal{O}_8 = \{1, 2\}$, $\mathcal{O}_9 = \{1, 2, 3\}$, $\mathcal{O}_{10} = \{1, 2, 3, 4, 5, 6\}$, $\mathcal{O}_{11} = \{5, 6\}$. The graph topology is shown in Fig. 11, and it can be easily verified that it satisfies *Assumption 4*. As shown in Fig. 12,

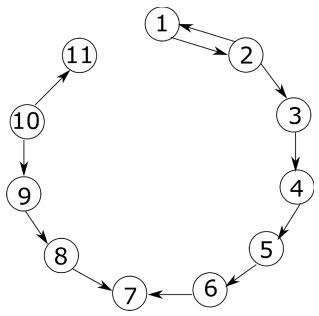

Fig. 11. Generalized communication topology with 11 agents.

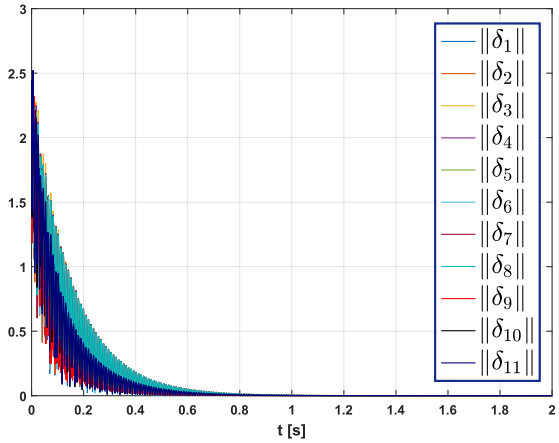

Fig. 12. Convergence of $\|\delta_i\|_2$, where $\delta_i = \hat{z}_i - z$, $i = 1, 2, \ldots, 11$.

convergence of estimates of all the 11 agents to the true states verifies the efficacy of our distributed observers on this more complex graph topology. Note that this graph is more general, or less restrictive, than strongly connected graphs, therefore adding redundant edges on this graph would strengthen its connectivity and facilitate convergence of states of distributed observers.

VI. Conclusion

In this paper, distributed observers and controllers are designed for a class of spatially interconnected systems. Each observer estimates the system states *via* two information sources: one is the local measurement and the other is the shared state estimate from the neighboring nodes. By virtue of synchronizing region methods in pinning control theory, the observers are designed in a distributed fashion. This leads to *flexibility* in integrating additional sensors to the existent network and graceful degradation in case of communication link failures as long as the connectivity requirements remain satisfied. The observer-based feedback laws are designed in a centralized fashion, though in the end they are implemented locally. LQR approach is adopted due to its neat parameterization to partially separate the interdependent design of distributed observers and controllers. Numerical simulation of a piezoelectric actuated smart flexible system verifies the efficacy of the proposed approach. A reduction of the computational cost is given as an additional merit of our distributed approach, compared with existing centralized design. Moreover, the *robustness* of our proposed approach is demonstrated

by a simulated communication link failure. By adding an extra sensor to the simulated network, we also present the *flexibility* of integrating additional sensors into the existing architecture, which only requires to design a small number of additional parameters. To demonstrate the effectiveness of our proposed distributed observer design on more complex graphs, distributed estimation performance with 11 agents on a generalized directed graph is examined.

ACKNOWLEDGMENT

The authors would like to thank anonymous reviewers for their comments.

REFERENCES

[1] R. Ferrari *et al.*, "Fusion of wireless and non-contact technologies for the dynamic testing of a historic RC bridge," *Meas. Sci. Technol.*, vol. 27, no. 12, pp. 1–15, 2016.

[2] V. Gupta, "Distributed estimation and control in networked systems," Ph.D. dissertation, Dept. Elect. Eng., California Inst. Technol., Pasadena, CA, USA, 2006.

[3] B. F. Spencer, Jr., M. E. Ruiz-Sandoval, and N. Kurata, "Smart sensing technology: Opportunities and challenges," *Struct. Control Health Monitor.*, vol. 11, no. 4, pp. 349–368, Oct./Dec. 2004.

[4] D. Estrin, R. Govindan, J. Heidemann, and S. Kumar, "Next century challenges: Scalable coordination in sensor networks," in *Proc. 5th Annu. ACM/IEEE Int. Conf. Mobile Comput. Netw.*, Aug. 1999, pp. 263–270.

[5] J. Lunze, Ed., *Control Theory of Digitally Networked Dynamic Systems*. Heidelberg, Germany: Springer, 2014.

[6] A. Bemporad, M. Heemels, and M. Vejdemo-Johansson, *Networked Control Systems* (Lecture Notes in Control and Information Sciences). London, U.K.: Springer, 2010.

[7] F.-Y. Wang and D. Liu, Eds., *Networked Control Systems: Theory and Applications*. London, U.K.: Springer, 2008.

[8] J. Lee, B. Bagheri, and H.-A. Kao, "A cyber-physical systems architecture for industry 4.0-based manufacturing systems," *Manuf. Lett.*, vol. 3, pp. 18–23, Jan. 2015.

[9] S. K. Khaitan and J. D. McCalley, "Design techniques and applications of cyberphysical systems: A survey," *IEEE Syst. J.*, vol. 9, no. 2, pp. 350–365, Jun. 2015.

[10] R. Baheti and H. Gill, "Cyber-physical systems," in *The Impact of Control Technology*, T. Samad and A. M. Annaswamy, Eds. New York, NY, USA: IEEE Control Systems Society, 2011. [Online]. Available: http://www.ieeecss.org

[11] B. S. Y. Rao, H. F. Durrant-Whyte, and J. A. Sheen, "A fully decentralized multi-sensor system for tracking and surveillance," *Int. J. Robot. Res.*, vol. 12, no. 1, pp. 22–44, 1993.

[12] F. Xia, X. Kong, and Z. Xu, "Cyber-physical control over wireless sensor and actuator networks with packet loss," in *Wireless Networking Based Control*. New York, NY, USA: Springer, 2011, pp. 85–102.

[13] F.-J. Wu, Y.-F. Kao, and Y.-C. Tseng, "From wireless sensor networks towards cyber physical systems," *Pervasive Mobile Comput.*, vol. 7, no. 4, pp. 397–413, 2011.

[14] L. Xiao, S. Boyd, and S. Lall, "A scheme for robust distributed sensor fusion based on average consensus," in *Proc. Int. Conf. Inf. Process. Sensor Netw.*, 2005, pp. 63–70.

[15] R. Olfati-Saber, "Distributed Kalman filtering for sensor networks," in *Proc. 46th IEEE Conf. Decision Control*, Dec. 2007, pp. 5492–5498.

[16] R. Olfati-Saber and P. Jalalkamali, "Coupled distributed estimation and control for mobile sensor networks," *IEEE Trans. Autom. Control*, vol. 57, no. 10, pp. 2609–2614, Oct. 2012.

[17] M. Farina, G. Ferrari-Trecate, and R. Scattolini, "Distributed moving horizon estimation for linear constrained systems," *IEEE Trans. Autom. Control*, vol. 55, no. 11, pp. 2462–2475, Nov. 2010.

[18] R. O. Saber and R. M. Murray, "Consensus protocols for networks of dynamic agents," in *Proc. Amer. Control Conf.*, 2003, pp. 951–956.

[19] R. Olfati-Saber and R. M. Murray, "Consensus problems in networks of agents with switching topology and time-delays," *IEEE Trans. Autom. Control*, vol. 49, no. 9, pp. 1520–1533, Sep. 2004.

[20] R. Olfati-Saber and J. S. Shamma, "Consensus filters for sensor networks and distributed sensor fusion," in *Proc. 44th IEEE Conf. Decision Control*, Dec. 2005, pp. 6698–6703.

[21] D. P. Spanos and R. M. Murray, "Distributed sensor fusion using dynamic consensus," in *Proc. 16th IFAC World Congr.*, 2005, pp. 1–6.

[22] R. Olfati-Saber, "Distributed Kalman filter with embedded consensus filters," in *Proc. 44th IEEE Conf. Decision Control*, Dec. 2005, pp. 8179–8184.

[23] R. Olfati-Saber, "Kalman-consensus filter: Optimality, stability, and performance," in *Proc. Joint 48th IEEE Conf. Decision Control 28th Chin. Control Conf.*, Dec. 2009, pp. 7036–7042.

[24] R. Carli, A. Chiuso, L. Schenato, and S. Zampieri, "Distributed Kalman filtering based on consensus strategies," *IEEE J. Sel. Areas Commun.*, vol. 26, no. 4, pp. 622–633, May 2008.

[25] L. Orihuela, P. Millán, C. Vivas, and F. R. Rubio, "Reduced-order H_2/H_∞ distributed observer for sensor networks," *Int. J. Control*, vol. 86, no. 10, pp. 1870–1879, 2013.

[26] P. Millán, L. Orihuela, C. Vivas, and F. R. Rubio, "Distributed consensus-based estimation considering network induced delays and dropouts," *Automatica*, vol. 48, pp. 2726–2729, Oct. 2012.

[27] I. Matei and J. S. Baras, "Consensus-based linear distributed filtering," *Automatica*, vol. 48, pp. 1776–1782, Aug. 2012.

[28] H. Zhu, K. Liu, J. Lü, Z. Lin, and Y. Chen, "On the cooperative observability of a continuous-time linear system on an undirected network," in *Proc. Int. Joint Conf. Neural Netw.*, 2014, pp. 2940–2944.

[29] L. Orihuela, P. Millán, C. Vivas, and F. R. Rubio, "Distributed control and estimation scheme with applications to process control," *IEEE Trans. Control Syst. Technol.*, vol. 23, no. 4, pp. 1563–1570, Jul. 2015.

[30] C. L. P. Chen, G.-X. Wen, Y.-J. Liu, and Z. Liu, "Observer-based adaptive backstepping consensus tracking control for high-order nonlinear semi-strict-feedback multiagent systems," *IEEE Trans. Cybern.*, vol. 46, no. 7, pp. 1591–1601, Jul. 2016.

[31] W. Meng, Q. Yang, J. Si, and Y. Sun, "Consensus control of nonlinear multiagent systems with time-varying state constraints," *IEEE Trans. Cybern.*, vol. 47, no. 8, pp. 2110–2120, Aug. 2017.

[32] P. DeLellis, M. di Bernardo, and G. Russo, "On QUAD, Lipschitz, and contracting vector fields for consensus and synchronization of networks," *IEEE Trans. Circuits Syst. I, Reg. Papers*, vol. 58, no. 3, pp. 576–583, Mar. 2011.

[33] K. Hengster-Movric, M. Sebek, and S. Celikovsky, "Structured Lyapunov functions for synchronization of identical affine-in-control agents—Unified approach," *J. Franklin Inst.*, vol. 353, no. 14, pp. 3457–3486, 2016.

[34] H. Zhu, K. Liu, and J. Lü, "Cooperative pinning synchronization of a class of undirected complex networks," in *Proc. 34th Chin. Control Conf. (CCC)*, 2015, pp. 6861–6865.

[35] R. E. Kalman, "On the general theory of control systems," *IRE Trans. Autom. Control*, vol. 4, no. 3, p. 110, Dec. 1959.

[36] W. K. Gawronski, *Advanced Structural Dynamics and Active Control of Structures* (Mechanical Engineering Series). New York, NY, USA: Springer, 2004.

[37] Z. Li, Z. Duan, G. Chen, and L. Huang, "Consensus of multiagent systems and synchronization of complex networks: A unified viewpoint," *IEEE Trans. Circuits Syst. I, Reg. Papers*, vol. 57, no. 1, pp. 213–224, Jan. 2010.

[38] H. Zhang, F. L. Lewis, and A. Das, "Optimal design for synchronization of cooperative systems: State feedback, observer and output feedback," *IEEE Trans. Autom. Control*, vol. 56, no. 8, pp. 1948–1952, Aug. 2011.

[39] X. Zhang, K. Hengster-Movrić, and M.Šebek, "Distributed observer and controller design for state-output decomposed systems," in *Proc. IEEE Conf. Control Appl. (CCA)*, Sep. 2016, pp. 450–455.

[40] J. A. Bondy and U. S. R. Murty, *Graph Theory* (Graduate Texts in Mathematics). New York, NY, USA: Springer, 2008.

[41] F. L. Lewis, H. Zhang, K. Hengster-Movric, and A. Das, *Cooperative Control of Multi-Agent Systems: Optimal and Adaptive Design Approaches*. London, U.K.: Springer, 2014.

[42] Z. Qu, *Cooperative Control of Dynamical Systems: Applications to Autonomous Vehicles*. London, U.K.: Springer-Verlag, 2009.

[43] J. W. Brewer, "Kronecker products and matrix calculus in system theory," *IEEE Trans. Circuits Syst.*, vol. CAS-25, no. 9, pp. 772–781, Sep. 1978.

[44] J. P. Hespanha, *Linear System Theory*. Princeton, U.K.: Princeton Univ. Press, 2009.

[45] R. Abraham, *Linear and Multilinear Algebra*. New York, NY, USA: W. A. Benjamin, 1966.

[46] C.-T. Chen, *Linear System Theory and Design*. New York, NY, USA: Oxford Univ. Press, 2013.

[47] D. G. Luenberger, "Observing the state of a linear system," *IEEE Trans. Military Electron.*, vol. 8, no. 2, pp. 74–80, Apr. 1964.
[48] S. Park and N. C. Martins, "Necessary and sufficient conditions for the stabilizability of a class of LTI distributed observers," in *Proc. 51st IEEE Conf. Decision Control*, Dec. 2012, pp. 7431–7436.
[49] C. W. Wu, "Localization of effective pinning control in complex networks of dynamical systems," in *Proc. IEEE Int. Symp. Circuits Syst.*, May 2008, pp. 2530–2533.
[50] H. K. Khalil, *Nonlinear Systems*, 3rd ed. Upper Saddle River, NJ, USA: Prentice-Hall, 2002.
[51] G. Ciccarella, M. Dalla Mora, and A. Germani, "A Luenberger-like observer for nonlinear systems," *Int. J. Control*, vol. 57, no. 3, pp. 537–556, 1993.
[52] M. Vidyasagar, *Nonlinear Systems Analysis*, 2nd ed. Englewood Cliffs, NJ, USA: Prentice-Hall, 1993.
[53] X. Zhang *et al.*, "Reduced-order robust controller design for vibration reduction," SAE Tech. Paper 2016-01-1845, 2016, doi: 10.4271/2016-01-1845.
[54] M. Petyt, *Introduction to Finite Element Vibration Analysis*, 2nd ed. Cambridge, U.K.: Cambridge Univ. Press, 2010.
[55] A. Preumont, *Vibration Control of Active Structures*, 2nd ed. New York, NY, USA: Kluwer, 2002.
[56] B. Besselink *et al.*, "A comparison of model reduction techniques from structural dynamics, numerical mathematics and systems and control," *J. Sound Vibrat.*, vol. 332, no. 19, pp. 4403–4422, 2013.
[57] D.-W. Gu, P. Petkov, and M. M. Konstantinov, *Robust Control Design With MATLAB* (Advanced Textbooks in Control and Signal Processing), 2nd ed. London, U.K.: Springer, 2013.

Xueji Zhang (S'16) received the B.Eng. degree in mechatronic engineering from Zhejiang University, Hangzhou, China, in 2011, and the M.Sc. degree in mechanical engineering from the Eindhoven University of Technology, Eindhoven, The Netherlands, in 2013. He is currently pursuing dual Ph.D. degrees with KU Leuven, Leuven, Belgium, and Czech Technical University in Prague, Prague, Czech Republic.

He performed his master graduation project at Océ Technologies, B.V., Venlo, The Netherlands, applying real-time iterative learning control for visual servoing on a wide-format printer. He is currently a Research Engineer with Siemens Industry Software NV, Leuven. His current research interests include networked filtering, distributed estimation, and control with applications to vibration damping of flexible structures.

Mr. Zhang is currently a Marie Curie European-Industrial-Doctorates Fellow.

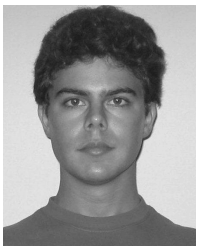

Kristian Hengster-Movrić was born in Zagreb, Croatia, in 1986. He received the M.S. degree in automatics from the College of Electrical Engineering and Computing, The University of Zagreb, Zagreb, in 2009, and the Ph.D. degree from The University of Texas at Arlington, Arlington, TX, USA, in 2013.

He joined the Department of Control Engineering, Faculty of Electrical Engineering, Czech Technical University in Prague, Prague, Czech Republic, in 2013, as a Post-Doctoral Fellow, where he has been an Assistant Professor since 2016. His current research interests include dynamical systems and control theory applied to complex, multiagent systems, and distributed systems control.

Dr. Hengster-Movrić was a recipient of Rector's Prize for 2009, the N. M. Stelmakh Outstanding Student Research Award (second place), and the Deans Fellowship in 2009.

Michael Šebek (SM'91) was born in 1954. He received the electrical engineering degree (with distinction) from CzechTech, Prague, Czech Republic, and the Ph.D. and Dr.Sc. degrees in control theory from the Czech Academy of Sciences, Prague, Czech Republic.

He held several visiting positions at ETH Zürich, Zürich, Switzerland, and Twente University, Enschede, The Netherlands. He is currently a CzechTech Professor, the Head of the Control Engineering Department, and the Head of the Cyber-Physical Systems Department with the Czech Institute for Informatics, Robotics and Cybernetics, Prague. He is also the CEO with PolyX Ltd., Prague, producer of the Polynomial Toolbox for MATLAB. He has authored over 300 research papers, developed several commercial software packages, led numerous research projects, and coordinated contract research for Honeywell, Porsche, Volkswagen, and Siemens, Leuven, Belgium. His current research interests include linear systems and control, networked systems, and vehicle formations.

Dr. Šebek was a Council Member and the General Chair of the 16th World Congress in IFAC. He served on the Conference Editorial Board in the IEEE CSS. He was a recipient of the Werner von Siemens Best Educator Prize.

Wim Desmet received the M.Sc. and Ph.D. degrees in mechanical engineering from KU Leuven, Leuven, Belgium, in 1992 and 1998, respectively.

He is currently a Full Professor in dynamics and mechatronics with the Department of Mechanical Engineering, KU Leuven, where he is currently the Head of the Noise and Vibration Research Group. He has authored or co-authored over 220 papers in international peer-reviewed journals and over 600 conference papers. His current research interests include virtual prototyping techniques in vibro-acoustics, structural dynamics, aero-acoustics and (flexible) multibody dynamics, experimental approaches for advanced dynamic testing and identification, model based virtual sensing, mechatronic system simulation, vehicle mechatronics, noise control engineering, dynamics of lightweight systems, and structural health monitoring.

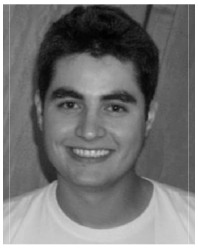

Cassio Faria received the Ph.D. degree in mechanical engineering from the Virginia Polytech Institute and State University, Blacksburg, VA, USA, in 2013.

He is currently a Senior Project Engineer with the Simulation and Test Solution Division, Siemens Digital Factory, Leuven, Belgium, where he is involved in multiattribute simulation and testing of electric drives and vehicles, design of smart structures (actuator integration and controller design), linear and nonlinear state estimator design for virtual sensing applications, and vehicle dynamics modelling and testing. The projects are sponsored by The European Commission and Innovatie door Wetenschap en Technologie.

7. DISTRIBUTED ESTIMATION ON SENSOR NETWORKS WITH MEASUREMENT UNCERTAINTIES

Štefan Knotek, Kristian Hengster-Movric, Michael Šebek, **Distributed Estimation on Sensor Networks with Measurement Uncertainties,** *submitted 2018*, pp. 1-13

Previous chapter brought compelling results on distributed estimation and control of distributed parameter systems, assuming partial measurements of perfect accuracy. Naturally this is too strong a condition, albeit one that is satisfied in practical cases to a fairly sufficient level, as indeed attested by physical experiments. Still, if several measurements of differing reliability are available one can attempt sensor fusion taking into account the varying precisions of individual measurements. This then ideally improves even on the most precise measurements. Results show appreciable disturbance suppression. The considered distributed observers can be used for control purposes along the lines of the previous section.

This chapter brings an innovative estimation scheme for large-scale distributed systems. The plant is considered affected by process disturbance and measurements are corrupted by measurement noise. The proposed approach fuses measurements of differing reliability so that all nodes reach consensus on the plant's state estimate. This architecture is flexible to addition of new nodes and to a certain extent robust to node or communication link failures. This follows from a protocol which allows existence of nodes that do not measure anything, but nevertheless contribute to the data fusion in the sensor network. Hence, in spite of limited observability of individual nodes, data fusion over sensor network allows each node to obtain the full estimate on the plant's state. Structured Lyapunov functions are used to prove the convergence of the estimator. The proposed distributed observer design is validated by numerical simulations.

Distributed Estimation on Sensor Networks with Measurement Uncertainties

Štefan Knotek, Kristian Hengster-Movric, and Michael Šebek

***Abstract*—This paper brings an innovative estimation scheme for large-scale distributed systems. The plant is considered affected by process disturbance and measurements are corrupted by measurement noise. The proposed approach fuses measurements of differing reliability so that all nodes reach consensus on the plant state estimate. This architecture is flexible to addition of new nodes and to a certain extent robust to node or communication link failures. This follows from a protocol which allows existence of nodes that do not measure anything, but contribute to the data fusion in the sensor network. Hence, in spite of limited observability of nodes, data fusion over sensor network allows each node to obtain the full estimate on the plant's state. Structured Lyapunov functions are used to prove the convergence of the estimator. The proposed distributed observer design is validated by numerical simulations.**

***Index Terms*—distributed estimation, networked systems, sensor networks, sensor fusion, large-scale systems**

I. Introduction

A recent boost in computational power paved the way to decentralization, distribution and development of networked systems. Networking allowed creation of the Internet, which laid the foundation to a new phenomenon of smart networks called Internet of Things, interconnecting smart devices all over the world and building up smart ecosystems in public and private sphere, e.g. intelligent buildings, smart cities, smart power grids, etc.

Networked systems hence also attract considerable research attention in control theory, where they give rise to Networked Control Systems (NCS) [1]–[3] and their synonymous Cyber-Physical Systems, in which cyber-networks intensely interact with physical plants and humans [4]–[6]. This integrates two complementary fields; the control theory and the algebraic graph theory [7], into an emerging field of distributed systems. These systems are composed of agents networked by a communication topology. Every agent uses its own information and information from its neighbors in the network to reach an agreement on states with all other agents, called *consensus*. Distributed consensus and synchronization are introduced in [8]–[11]. These protocols ensure synchronization of states of all agents to one common value. Other, more advanced, distributed protocols for controllers and observers using state or output-feedback in continuous and discrete-time can be found in [12]–[14]. Distributed NCS have a wide range of application in formation control of mobile robots, satellites, and vehicles [15], energy generation in micro-grids [16], estimation with the use of sensor networks [17], synchronization of coupled oscillators [18], reaching the agreement in human social networks [19], to name only a few. See the books [20], [21] for a comprehensive treatment.

The design of distributed observers is motivated by previous developments in centralized estimation. Very early results in this direction bring the Wiener filter in continuous [22] and discrete-time [23], for estimating the target of a stochastic process. To extend the Wiener filter to non-stationary processes a Kalman filter was developed [24]. A simplified version of the Kalman filter, without the statistical framework incorporating models for measurement and process noise, gave rise to the Luenberger observer [25].

Limitations of the centralized approach prompted a demand for data fusion over sensor networks. This led to the birth of first decentralized Kalman filters presented in [26]–[28], offering fast parallel processing and increased robustness to failures. A drawback of these approaches is that they require an all-to-all coupling of nodes, i.e. their network topology is a complete graph, which leads to increased communication load, computational complexity and thereby to scaling problems on large-scale networks. For example, in [26] every agent works as a sensor and an actuator, and for control purposes it uses pure measurements of all nodes in the network, without any sensor fusion. This approach is not robust to changes of the network topology due to agent failures, because the controller design is centralized; requiring recalculation of the controller following any network change. In contrast to [26], each node in [27] computes its own local estimate of an unknown state vector and then assimilates all the local estimates into a single final estimate of the plant state to accomplish globally optimal performance.

The computational complexity and scaling issues of the decentralized Kalman filter are improved upon by the distributed Kalman filter (DKF). DKF relaxes the requirements on communication topology such that each node exchanges information only with its neighbors and it also offers possible redundancy in case of node failures. One of the first scalable DKF providing data fusion over a sensor network is introduced in [29]. It is based on consensus filters [30], and dynamic average consensus [31], which solve the distributed estimation of a dynamic signal with and without measurement noise, respectively. Both approaches presented in [30], [31] use averaging consensus to estimate value of a time-varying signal. A distributed filtering algorithm presented in [30] consists of a network of micro-Kalman filters, each

Š. K., K. H. and M. Š. are with Department of Control Engineering, Faculty of Electrical Engineering, Czech Technical University in Prague. E-mail: {stefan.knotek, kristian.hengster.movric, michael.sebek}@fel.cvut.cz.

This work was supported by the Grant Agency of the Czech Technical University in Prague, grant No. SGS16/232/OHK3/3T/13 (Š. K.) and by the Czech Science Foundation, GACR, junior grant No. 16-25493Y (K. H.).

embedded with a low-pass and band-pass consensus filter. A recent work on distributed filtering of noisy measurements [32] proposes three algorithms based on Bayesian sensor fusion. It consider two types of nodes: sensing node which perform the measuring task and non-sensing nodes which mediate between sensing nodes. Extension of the DKF algorithm from [29] for application to heterogeneous sensor models with different outputs can be found in [33], which offers a popular and efficient consensus-based framework for distributed state estimation. Stability and performance of this DKF algorithm are thoroughly investigated and new optimal solution of DKF are developed in [34]. All the above mentioned approaches consider undirected network topologies, except [32] which considers directed networks. The most recent work in this field, [35], presents an optimal information-weighted DKF, which implements a novel measurement model considering noise in communication channels. The network topology in [35] is assumed directed having a spanning tree with a target node observable by at least one root node.

Different from DKF, a distributed Luenberger observer for directed sensor networks is introduced in [36]. In contrast to [29], [33], [34], this approach allows for a completely distributed observer design. Moreover, it also allows insertion of redundant sensor nodes into the network to increase robustness of the distributed observer. The recent work [37] addresses distributed estimation and control of large-scale flexible structures. It proposes a distributed Luenberger observer similar to [36], however, in contrast to [36], it allows existence of two types of nodes: sensing and non-sensing ones, similarly as in [32].

In this paper, we present a novel distributed design for sensor networks that uses sensor fusion to estimate states of a plant. The introduced distributed observer addresses primarily state-estimation of large-scale flexible structures such as aircraft fuselages, truss bridges, lattice towers, etc, under process disturbance and measurement uncertainties. Structural vibration suppression is indispensable for proper longterm functioning and safety of such plants. For the design of active dampers for flexible structures, the state of the plant first has to be know, which is the task of an observer. However, implementations of centralized solutions are often expensive and prohibitively complex on the larger scale. A solution is offered by the nascent networked/distributed systems. First of all, they reduce the implementation costs and complexity of the entire design and application. Secondly, communication via network provides a potential for improvement of overall system performance, in contrast to centralized solutions. Moreover, node redundancy provides additional fault tolerance or allows graceful degradation in the case of node failures. Thus, the networked/distributed architectures handle the drawbacks of (de)centralized approaches and enjoy many advantages, such as robustness, flexibility and scalability.

In particular, this paper brings a judicious distributed Luenberger observer design which takes into account the precision of the available measurements, similar to general Kalman filter [38] and DKF in [33]. The proposed approach extends the distributed Luenberger observer design [37] by considering process disturbance and measurement noises to achieve reasonable sensor fusion while retaining a relatively simple distributed design. Thereby it inherits flexibility, scalability on large-scale sensor networks and robustness to node or communication link failures. Moreover, it relaxes the requirements on the network topology in [37] to a graph having a spanning tree with all sensing nodes in one strongly connected component, similarly as in [35]. In comparison to DKF it is important to point out, that we do not aim here for a design of an optimal Kalman filter but rather a generally suboptimal, albeit easier to implement, consensus-based distributed estimator that nevertheless shares some desirable properties of the Kalman filter. We do not assume communication channel noise as in [35], but rather rely on digital communication channels with data validation. The convergence of the presented distributed observer is rigorously proven by structured Lyapunov functions introduced in [39], [40].

The main contributions of this paper are:

- We consider a more general communication topology than the previously proposed distributed observers.
- Nodes implement a local micro-Kalman filter to estimate the observable fraction of the plant state.
- Nodes use information on process and measurement noises and apply information-weighted fusion to reach an agreement on the estimate of a plant state.
- The design and implementation of the proposed observer is fully distributed, in the sense that each node designs its local observer based on its own information and information from its neighbors.
- Proposed design offers incorporation of redundant nodes or insertion of new communication links to the network to improve robustness to node or communication link failures.

Our distributed estimators lend themselves to control applications along the lines of [37], though this development is not pursued in this paper.

The paper is structured as follows. Section II introduces preliminaries used throughout the paper. Section III states the main problem. Section IV presents the dynamics of the distributed observer and proves its convergences. Final distributed observer design is summarized and its similarity with the Kalman filter is discussed in Section V. Numerical simulations are given in Section VI. Section VII concludes the paper.

II. Preliminaries

In general, we denote matrices with capital letters and vectors with lower case letters. An element of a matrix A is denoted as a_{ij} while an element of a column or row vector v is denoted as v_i.

The set of $m \times n$ real matrices is denoted as $\mathbb{R}^{m\times n}$. A matrix $V = \text{diag}(v_i), i = 1, \ldots, k$ is a diagonal matrix with elements of vector $v \in \mathbb{R}^k$ on the diagonal. A matrix $M = \text{diag}(M_i)$ for $M_i \in \mathbb{R}^{n_i \times n_i}$, $i = 1, 2, \ldots, k$, denotes a block-diagonal matrix with k blocks $M_1, \ldots, M_k$ on the block-diagonal. $I_N \in \mathbb{R}^{N\times N}$ is the identity matrix. Operation $A \otimes B$ denotes the Kronecker product of matrices A and B, [41]. The smallest and the largest singular value of a matrix M are denoted by $\sigma_{\min}(M)$ and $\sigma_{\max}(M)$, respectively. The same notation holds

for eigenvalues denoted by $\lambda_{\min}(M)$ and $\lambda_{\max}(M)$. Positive (semi)-definite symmetric matrix is denoted by $M \succ (\succeq) 0$. If not explicitly stated, the sum over all agents $\sum_{i=1}^{p}$ is denoted by $\sum_i$ for $i = 1, \ldots, p$. An expectation of a stochastic process $v(t)$ is denoted by $E[v]$. Variance of a stochastic process is $E[vv^T]$.

A. Graph theory

Network topology is described by a directed graph $\mathcal{G} = (\mathcal{V}, \mathcal{E})$, where $\mathcal{V} = \{1, 2, \ldots, p\}$ is a nonempty finite set of nodes and $\mathcal{E} \subseteq \mathcal{V} \times \mathcal{V}$ is a set of arcs. An arc is an ordered pair of nodes (i, j), $i \neq j$, where i is the parent node and j is the child node, i.e. the information flows from node i to node j. The graph $\mathcal{G}$ is undirected if $(i, j) \in \mathcal{E}$ implies $(j, i) \in \mathcal{E}$, otherwise the graph is directed. It is assumed that the graph $\mathcal{G}$ is simple, i.e. it has no repeated edges nor self-loops $(i, i) \notin \mathcal{E}, \forall i$. The adjacency matrix $E = [e_{ij}] \in \mathbb{R}^{p \times p}$ associated with the graph $\mathcal{G}$ is defined by $e_{ij} = 1$ if and only if $(j, i) \in \mathcal{E}$, otherwise $e_{ij} = 0$. Note that the diagonal elements satisfy $e_{ii} = 0$. Denote $\mathcal{V}_i = \{i \in \mathcal{V} : e_{ij} \neq 0\}$ as the set of neighbors of node i. Let the in-degree matrix $D = [d_{ij}] \in \mathbb{R}^{p \times p}$ be a diagonal matrix given by $d_{ii} = \sum_j e_{ij}$. Then the graph Laplacian matrix is defined by $L = D - E$.

In the sequel, directed graphs are considered. A directed path of length p from node 1 to node p is an ordered set of distinct nodes $\{1, 2, \ldots, p\}$ such that $(l, l+1) \in \mathcal{E}$ for all $l \in [1, p-1]$. A directed graph is strongly connected if there exists a directed path between any two nodes. A node is termed isolated if it has no parent node. Hence, in strongly connected graphs there are no isolated nodes. Directed tree is a directed graph with every node having only one parent except one isolated node called a *root*. A directed graph contains a spanning tree if there exists a subgraph which is a directed tree containing all nodes in $\mathcal{V}$.

The Laplacian matrix L has a simple zero eigenvalue iff its directed graph contains a spanning tree. Denote by $w \in \mathbb{R}^p$ the left eigenvector associated with the simple zero eigenvalue of L, i.e. $w^T L = 0$. The pinning matrix $G = \text{diag}(g_i) \in \mathbb{R}^{N \times N}$ associated with the graph $\mathcal{G}$ is a diagonal matrix given by $g_i = 1$ if the ith node is pinned, otherwise $g_i = 0$, [21].

A graph is reducible if there exists a permutation matrix T, that transforms its Laplacian L to a block triangular form

$$T^T L T = \begin{bmatrix} L_{11} & L_{12} \\ 0 & L_{22} \end{bmatrix}. \quad (1)$$

If the graph is not reducible it is said to be irreducible. A directed graph is irreducible iff it is strongly connected. A spanning forest is a set of directed trees such that a set of all nodes of these trees equals $\mathcal{V}$. Let the directed graph be reducible and let it contain a spanning forest. Then the Laplacian of the graph can be reduced by a node permutation to the Frobenius normal form [21]. If the graph contains a single spanning tree then its Frobenius normal form equals

$$T^T L T = \left[\begin{array}{ccc|c} \overbrace{L_{11} & \ldots & L_{1m}}^{\tilde{L}+\tilde{G}} & L_{1m+1} \\ & \ddots & \vdots & \vdots \\ 0 & & L_{mm} & L_{mm+1} \\ \hline & 0 & & L_{m+1m+1} \end{array}\right], \quad (2)$$

where all L_{ii} blocks are irreducible. This paper addresses graphs having a single spanning tree. Such graphs are either irreducible (strongly connected) or reducible and contain at most one irreducible leader group L_{m+1m+1}. A special case of the irreducible leader group is a single isolated leader. The results presented for irreducible graphs naturally specialize to connected undirected graphs.

The following two lemmas are useful in constructing Lyapunov functions for cooperative control [13].

Lemma 1. *Let L be the Laplacian matrix associated with a directed, strongly connected graph $\mathcal{G}$. Then L has a simple zero eigenvalue and its left eigenvector has all positive entries, i.e. $w_i \succ 0, \forall i$.*

Lemma 2. *For every strongly connected, irreducible graph $\mathcal{G}$ there exists a positive diagonal matrix $W = diag(w_i) \succ 0$ such that its graph Laplacian matrix L satisfies*

$$L^T W + W L \succeq 0. \quad (3)$$

If the graph contains a spanning forest with $g_i > 0$ for root nodes of all trees, then there exists a positive diagonal matrix $\Theta = diag(\theta_i) > 0$ such that

$$(L + G)^T \Theta + \Theta (L + G) \succ 0. \quad (4)$$

Proofs of Lemma 1 and the first part of Lemma 2 can be found in [20]. The proof of the second part of Lemma 2 is sketched in [40].

III. Problem statement and motivation

Consider a plant with a continuous linear time-invariant (LTI) dynamics

$$\dot{x}(t) = Ax(t) + \Gamma \omega(t), \quad (5)$$

where $x(t) \in \mathbb{R}^n$ is the plant state, $\omega(t) \in \mathbb{R}^m$ is the process noise acting on states, $A \in \mathbb{R}^{n \times n}$ is the system matrix and $\Gamma \in \mathbb{R}^{n \times m}$ is the process noise input matrix. Each node in a sensor network has a linear sensing model

$$y_i(t) = C_i x(t) + \xi_i(t), \quad i \in \mathcal{V}, \quad (6)$$

where $y_i(t) \in \mathbb{R}^{p_i}$ is the ith node measurement corrupted by the measurement noise $\xi_i(t) \in \mathbb{R}^{p_i}$ and $C_i \in \mathbb{R}^{p_i \times n}$ is the ith node observation matrix. Both $\omega(t)$ and $\xi_i(t)$ are zero-mean white Gaussian noises (WGN), uncorrelated in the sense that $E[\xi_i \omega^T] = 0, \forall i$ and $E[\xi_i \xi_j^T] = 0, \forall (i, j), i \neq j$. Note that unlike [36] some nodes in the network may be allowed not to measure anything, for such node i, y_i is not considered. Note also that [36] does not consider noises while we do.

To implement estimation of the plant's state vector x in a distributed fashion, it is convenient to transform the system

matrix A to a block diagonal form, $\tilde{A} = \text{diag}(A_j) \in \mathbb{R}^{n\times n}, A_j \in \mathbb{R}^{n_j\times n_j}, j = \{1, 2, \ldots, l\}$, where l represents the number of dynamically independent state-groups. There are two generally known representations offering block diagonal system matrix. They are the Jordan Canonical Form (JCF) and the Modal Canonical Form (MCF). A transformation to MCF is more common for models describing flexible structures [42], while JCF is used for other general systems [43]. In case of MCF for flexible structures, each block A_j corresponds to one eigenmode of a flexible structure and the blocks are of the same dimension, i.e. $n_i = n_j, \forall(i, j)$. On the other hand, blocks of the system matrix in JCF correspond to eigenvalues of the system and the dimension of each block is given by the algebraic multiplicity of the pertaining eigenvalue.

Hence, define a linear transformation $x = \Pi z = \sum_{j=1}^{l} \Pi_j z_j$ with a new state vector $z = [z_1^T, z_2^T, \ldots, z_l^T]^T \in \mathbb{R}^n$ composed of state-groups, $z_j \in \mathbb{R}^{n_j}$, and a nonsingular transformation matrix $\Pi = [\Pi_1, \Pi_2, \ldots, \Pi_l] \in \mathbb{R}^{n\times n}$, such that Π transforms the system matrix A to a block diagonal form. This transformation leads to a block-diagonal representation of the plant dynamics and the transformed sensing model

$$\dot{z}(t) = \tilde{A}z(t) + \tilde{\omega}(t), \tag{7}$$

$$y_i(t) = \tilde{C}_i z(t) + \xi_i(t), \quad i \in \mathcal{V}, \tag{8}$$

where $\tilde{A} = \Pi^{-1}A\Pi$, $\tilde{C}_i = C_i\Pi$ and $\tilde{\omega}(t) = \Pi^{-1}\Gamma\omega(t)$. Note, that there always exists a matrix Π, such that $\tilde{A} = \Pi^{-1}A\Pi$ and $\Pi_j A_j = A\Pi_j$, [44]. Let $E[\tilde{\omega}\tilde{\omega}^T] = \Omega$ and $E[\xi_i\xi_i^T] = \Xi_i$ denote covariance matrices of process noise $\tilde{\omega}(t)$ and measurement noise $\xi_i(t)$, where Ω and Ξ_i are assumed real, symmetric and positive definite.

Before proceeding further, we introduce several important definitions and assumptions adopted from [37].

Definition 1. $\mathcal{S} = \{1, 2, \ldots, l\}$ defines a set of state-groups.

Assumption 1. $C_{ij} = C_i\Pi_j \neq \mathbf{0}$, where $i \in \mathcal{V}$ and $j \in \mathcal{S}$, iff the state-group z_j is observable from measurement y_i.

This assumption tells that pairs $(\tilde{A}, \tilde{C}_i), i \in \mathcal{V}$ can be transformed to a Kalman Decomposed Form, [43], by a permutation of state-groups. In general it holds that if the state-group z_j is observable from the output y_i then $C_{ij} \neq 0$ but the converse is not necessarily true. However, the systems we address in this paper satisfy Assumption 1 either completely or approximately, [37].

Remark 1. Note, that Assumption 1 is trivially satisfied if blocks A_j are of dimension 1. For blocks A_j of dimension greater than one, $n_j > 1, j \in \mathcal{S}$, it can be approximately satisfied under both following conditions:

- if the plant is a flexible structure with independent eigenmodes corresponding to blocks A_j, it naturally leads to a decomposition of C_i into C_{ij};
- if $C_{ij} \neq 0$ but is small in magnitude, then the jth state-group can be considered as unobservable from ith node output y_i and C_{ij} can be set to zero $C_{ij} = 0$ for the purposes of the design. The distributed observer design proposed in Section V is robust to such a change as long as Assumption 2 below remains satisfied.

Definition 2. The observable and unobservable sets of state-groups from ith node's perspective, $i \in \mathcal{V}$, are defined as $\mathcal{O}_i = \{j \in \mathcal{S} | C_{ij} \neq 0\}$ and $\bar{\mathcal{O}}_i = \mathcal{S}\backslash\mathcal{O}_i$, respectively.

Definition 3. The converse observable and unobservable sets of nodes for jth state-group, $j \in \mathcal{S}$, are defined as $\mathcal{D}_j = \{i \in \mathcal{V} | C_{ij} \neq 0\}$ and $\bar{\mathcal{D}}_j = \mathcal{V}\backslash\mathcal{D}_j$, respectively.

Note, that Definition 2 and Definition 3 are complementary, i.e. $j \in \mathcal{O}_i \iff i \in \mathcal{D}_j$ and $j \in \bar{\mathcal{O}}_i \iff i \in \bar{\mathcal{D}}_j$.

Assumption 2. The plant state z is globally observable, i.e.

$$\mathcal{O}_1 \cup \mathcal{O}_2 \cup \cdots \cup \mathcal{O}_p = \mathcal{S}. \tag{9}$$

This means that the LTI dynamics of the plant (5) is observable from measurements of all nodes (6) taken together. In other words, every state-group z_j is observable at least by one node, (from one output y_i), in the network. Ideally, however we want each state-group to be observable by several nodes so to affect sensor fusion. Let us point out that all this still allows existence of nodes that do not measure anything. The main contribution of such nodes is in maintaining network connectivity. These nodes can be also used for actuation purposes, along the lines of the distributed controller design in [37]. We refer to them as to non-sensing nodes. To all the other nodes in the network we refer to as the sensing nodes.

Assumption 3. The communication topology is given by a directed graph having a spanning tree with all the sensing nodes contained in the irreducible leader group.

Remark 2. The irreducible leader group is a strongly connected component of the graph given by its Laplacian L_{m+1m+1} in the Frobenius normal form (2). It is important to point out, that the irreducible leader group can additionally contain also some non-sensing nodes.

Let each node in the network be endowed with the following LTI dynamics

$$\dot{\hat{z}}_i = \tilde{A}\hat{z}_i + G_i(y_i - \hat{y}_i) + F_i \textstyle\sum_{j\in\mathcal{V}} e_{ij}(\hat{z}_j - \hat{z}_i), \tag{10}$$

where $G_i \in \mathbb{R}^{n\times p_i}$ is the *local observer gain* and $F_i \in \mathbb{R}^{n\times n}$ is the *distributed observer gain*. The ith observer state vector, $\hat{z}_i = [\hat{z}_{i1}^T, \hat{z}_{i2}^T, \ldots, \hat{z}_{il}^T]^T \in \mathbb{R}^n$, is, similarly as the plant's state vector z, partitioned into state-groups $\hat{z}_{ij}$. Note that all nodes (10) share the same drift dynamics $\tilde{A}$, which equals the dynamics of the plant.

The node estimation dynamics (10) has a well known structure, as those presented in [33], [34], [36], and [37]. It uses two information sources necessary for the proper estimation of the plant state. The first is the measurement y_i, contained in the estimation term $G_i(y_i - \hat{y}_i)$, originating from the Luenberger observer design [25]. It ensures estimation of observable state-groups $j \in \mathcal{O}_i$ by the ith node from its local measurements. The second information source is given by the state estimates of neighboring nodes contained in the local neighborhood error term $F_i \sum_{j\in\mathcal{V}} e_{ij}(\hat{z}_j - \hat{z}_i)$. Its purpose is to synchronize the unobservable state-groups $j \in \bar{\mathcal{O}}_i$ of the ith node with those of its neighboring nodes and effect sensor fusion for the observable state-groups using information from the network.

Define an observation error as a difference between the estimated state (10) and the true state of the plant (7)

$$\eta_i(t) = \hat{z}_i(t) - z(t). \tag{11}$$

The goal of this paper is to design matrices G_i and F_i so that the observation errors (11) are uniformly ultimately bounded in the sense that the estimated states of all nodes converge to the plant's state within a bounded region whose size depends on the noises, appropriately taking into account the reliability of individual measurements.

IV. Observer convergence

For the convergence analysis of proposed estimation dynamics (10), in this section we first consider the plant dynamics (7) and sensor model (8) without noises, i.e. $\tilde{\omega} = 0$ and $\xi_i = 0, \forall i$. Our goal is then to design the local observer gains G_i and the distributed observer gains F_i so that the observation error (11) in noise-free settings, having the dynamics

$$\dot{\eta}_i = (\tilde{A} - G_i\tilde{C}_i)\eta_i + F_i \textstyle\sum_{j\in\mathcal{V}} e_{ij}(\eta_j - \eta_i), \tag{12}$$

asymptotically converges to zero

$$\lim_{t\to\infty} \eta_i(t) = 0, \quad \forall i \in \mathcal{V}. \tag{13}$$

For each node i we can reorder the state-groups $\hat{z}_{ij}$ in the state vector $\hat{z}_i$, such that the new state vector $\hat{z}_i^{\text{new}}$ is a tandem of observable $\hat{z}_{io} \in \mathbb{R}^{n_{io}}$, containing observable state-groups $\hat{z}_{ij}$ for $j \in \mathcal{O}_i$, and unobservable $\hat{z}_{i\bar{o}} \in \mathbb{R}^{n_{i\bar{o}}}$, containing unobservable state-groups $\hat{z}_{ij}$ for $j \in \bar{\mathcal{O}}_i$. Hence, for every node i there exists a permutation matrix T_i, $T_i^{-1} = T_i^T$, such that

$$\hat{z}_i^{\text{new}} = \begin{bmatrix} \hat{z}_{io} \\ \hat{z}_{i\bar{o}} \end{bmatrix} = T_i\hat{z}_i. \tag{14}$$

Correspondingly, in the new coordinates, the system and observation matrices are in the Kalman decomposed form

$$\begin{aligned} \hat{A}_i = T_i\tilde{A}T_i^T &= \begin{bmatrix} A_{io} & \mathbf{0} \\ \mathbf{0} & A_{i\bar{o}} \end{bmatrix}, \\ \hat{C}_i = \tilde{C}_iT_i^T &= \begin{bmatrix} C_{io} & \mathbf{0} \end{bmatrix}. \end{aligned} \tag{15}$$

Remark 3. The state vector of a non-sensing node is composed completely of unobservable state-groups, $\hat{z}_i^{\text{new}} = \hat{z}_i = \hat{z}_{i\bar{o}}$, hence no permutation of state-groups is needed. The matrices ($\hat{A}_i \equiv A_{i\bar{o}} \equiv \tilde{A}$, $\hat{C}_i \equiv \tilde{C}_i \equiv 0$) are then already in Kalman decomposed form. The same would hold for a sensing node observing all the state-groups, except that ($\hat{C}_i \equiv C_{io} \equiv \tilde{C}_i$), because its state vector would be composed completely of observable state-groups, $\hat{z}_i^{\text{new}} = \hat{z}_i = \hat{z}_{io}$.

Remark 4. The permutation of state-groups achieving (15) is made possible by Assumption 1. It allows each node to transform the drift dynamics $\tilde{A}$ to the Kalman decomposed form with respect to its sensing model $\tilde{C}_i$. Each node can then in principle estimate its observable state vector $\hat{z}_{io}$ using just its local measurements y_i, by designing a Luenberger-like local observer. For those states, the distributed gain is used to improve the nodes' local estimates for the observable state vector $\hat{z}_{io}$. To estimate the unobservable state vector $\hat{z}_{i\bar{o}}$, local measurements are to no avail. Therefore a node uses communication with its neighbors to gather estimates on $\hat{z}_{i\bar{o}}$. For this purpose every node designs its distributed observer for unobservable state vector.

In order to show observer convergence on the considered network topology, as detailed in Assumption 3, we proceed first by proving the convergence for strongly connected graphs representing, in general, the irreducible leader group. Then we show convergence of the remainder of the network, considered as pinned. Ultimately using those two results we conclude convergence on the entire graph satisfying Assumption 3.

The following theorem brings the design of local observer gains G_i and distributed observer gains F_i together with conclusion on convergence of the observer dynamics (10) in the noise-free case on strongly connected graphs.

Theorem 1. *Consider a network of nodes given by a directed strongly-connected graph $\mathcal{G}$. Let each node with the sensor model (8) implement the estimation dynamics (10) to estimate states of the plant dynamics (7) in the noise-free settings $\tilde{\omega} = 0$ and $\xi_i = 0, \forall i$. Suppose that Assumptions 1 and 2 hold.*

Let Q_i and U_i be symmetric positive definite matrices. Choose the local observer gain as

$$G_i = T_i^T \begin{bmatrix} \bar{M}_i^{-1}C_{io}^TU_i^{-1} \\ \mathbf{0} \end{bmatrix}, \tag{16}$$

where $T_i \in \mathbb{R}^{n\times n}$ is the permutation matrix bringing the pair $(\tilde{A}, \tilde{C}_i)$ to the Kalman decomposed form (15) and $\bar{M}_i^{-1}$ is the solution of the observer algebraic Riccati equation (ARE)

$$\bar{M}_i^{-1}A_{io}^T + A_{io}\bar{M}_i^{-1} + Q_i - \bar{M}_i^{-1}C_{io}^TU_i^{-1}C_{io}\bar{M}_i^{-1} = 0. \tag{17}$$

Furthermore, define $\bar{N}_j = \alpha_j I_{n_j}$ such that

$$0 < \alpha_j < \frac{w_{min}\sum_{i\in\mathcal{D}_j}\lambda_{\min}(\bar{M}_iQ_i\bar{M}_i)}{w_{max}(p - |\mathcal{D}_j|)\lambda_{max}\left(A_j + A_j^T\right)}, \tag{18}$$

and choose the distributed observer gain as

$$F_i = \gamma T_i^T \begin{bmatrix} \bar{M}_i^{-1} & \mathbf{0} \\ \mathbf{0} & diag(\bar{N}_j^{-1}) \end{bmatrix} T_i, \quad j \in \bar{\mathcal{O}}_i, \tag{19}$$

with $\gamma > 0$. Then each observer state $\hat{z}_i(t)$ asymptotically converges to the plant state $z(t)$, in the sense of (13) for γ sufficiently large.

The proof of Theorem 1 is relegated to Appendix A due to its length. Theorem 1 brings general methodology for the design of local observer gains G_i and distributed observer gains F_i for the strongly connected leader group.

Remark 5. From Theorem 1 it follows that both sensing and non-sensing nodes, in the irreducible leader group at least, share the same design of G_i and F_i. Moreover, all the non-sensing nodes have the same distributed observer gain $F_i = F_{\bar{o}} := \text{diag}(N_j^{-1})$ and also, trivially, the local observer gain, as it is identically zero, i.e. $G_i = G_{\bar{o}} := 0$.

Now consider the remainder of the network. It is given by a graph generally having a spanning forest with root nodes of all trees pinned by the outgoing edges of the irreducible leader group from Theorem 1, (due to the assumed existence of a spanning tree). According to Assumption 3, the nodes

in the remainder of the graph are all necessarily non-sensing. The node dynamics (10), for such nodes, can be written in the form containing two local neighborhood error terms

$$\dot{\hat{z}}_k = \tilde{A}\hat{z}_k + F_{\bar{o}} \sum_r e_{kr}(\hat{z}_r - \hat{z}_k) + F_{\bar{o}} \sum_i e_{ki}(\hat{z}_i - \hat{z}_k), \quad (20)$$

The first term $F_{\bar{o}} \sum_r e_{kr}(\hat{z}_r - \hat{z}_k)$ serves to synchronize the non-sensing nodes with their peers from the remainder of the network and the second term $F_{\bar{o}} \sum_i e_{ki}(\hat{z}_i - \hat{z}_k)$ serves to synchronize these nodes with the irreducible leader group. Because the remainder of the network contains only non-sensing nodes, the dynamics (20) has no estimation term. Let $g_k = \sum_i e_{ki}$ represent the overall pinning gain from the irreducible leader group to the kth node in the remainder of the graph. In terms of the observation error dynamics (11), the node dynamics (20) is then given by

$$\dot{\eta}_k = \tilde{A}\eta_k + F_{\bar{o}} \left(\sum_r e_{kr}(\eta_r - \eta_k) - g_k\eta_k \right) + F_{\bar{o}} \sum_i e_{ki}\eta_i, \quad (21)$$

which is considered as composed of the nominal dynamics

$$\dot{\eta}_k = \tilde{A}\eta_k + F_{\bar{o}} \left(\sum_r e_{kr}(\eta_r - \eta_k) - g_k\eta_k \right), \quad (22)$$

and the interconnection term $F_{\bar{o}} \sum_i e_{ki}\hat{z}_i$. Note that the nominal dynamics (22) is a special case of conventional leader following consensus, also known as the *cooperative tracking problem*, [21], with a static leader node representing a zero reference.

The following result proves convergence of the nominal dynamics (22) for nodes in the remainder of the network.

Proposition 1. *Consider a graph with a spanning forest having root nodes of all trees pinned. Let each node in this graph implement the nominal dynamics (22) with $F_{\bar{o}} = diag(N_j^{-1})$ with N_j as in Theorem 1. Then the nominal dynamics (22) is asymptotically stable, i.e. the observation error $\eta_k(t)$ converges to 0 as $t \to \infty$, for γ sufficiently large.*

Proof: By use of the Kronecker product, the nominal dynamics (22) can be written in the form

$$\dot{\eta} = (I_n \otimes \tilde{A})\eta - ((\tilde{L} + \tilde{G}) \otimes F_{\bar{o}})\eta, \quad (23)$$

where $\tilde{L}$ is the Laplacian matrix of the spanning forest and $\tilde{G} = \text{diag}(\tilde{g}_k)$ is the pinning matrix.

Define a Lyapunov function candidate in the quadratic form

$$V = \eta^T(\Theta \otimes M)\eta > 0, \quad (24)$$

where $\Theta = \text{diag}(\theta_i) > 0$ is selected based on Lemma 2 for $\tilde{L} + \tilde{G}$ and M is positive definite symmetric such that $MF_{\bar{o}} = \gamma I_n$. Then the time-derivative of the Lyapunov function candidate (24) equals

$$\dot{V} = \eta^T \Big(\Theta \otimes (M\tilde{A} + \tilde{A}^T M) - \gamma \Big(\Theta(\tilde{L} + \tilde{G}) + (\tilde{L} + \tilde{G})^T \Theta \Big) \otimes I_n \Big) \eta, \quad (25)$$

with $M = \text{diag}(N_j) = \text{diag}(\alpha_j I_{n_j})$.

An upper bound on the time-derivative of the Lyapunov function (25) is

$$\dot{V} < \alpha_{\max}\theta_{\max}\lambda_{\max} \left(\tilde{A} + \tilde{A}^T \right) \|\eta\|^2 - \gamma\lambda_{\min} \left(\Theta(\tilde{L} + \tilde{G})^T + (\tilde{L} + \tilde{G})\Theta \right) \|\eta\|^2, \quad (26)$$

which is negative if

$$\gamma > \frac{\alpha_{\max}\theta_{\max}\lambda_{\max} \left(\tilde{A} + \tilde{A}^T \right)}{\lambda_{\min} \left(\Theta(\tilde{L} + \tilde{G}) + (\tilde{L} + \tilde{G})^T\Theta \right)}. \quad (27)$$

As the time-derivative of the Lyapunov function (25) is negative for γ sufficiently large, this implies asymptotic stability of the nominal dynamics (22), and concludes the proof. ■

Remark 6. Design details for G_i and F_i coincide in Theorem 1 and Proposition 1 as they should for a practical design. Namely, a node need not know if it is in the irreducible leader group or in the remainder of the graph.

The entire network is thus a hierarchically coupled system given by the observation error dynamics for the irreducible leader group and the remainder of the network

$$\dot{\eta}_i = (\tilde{A} - G_i\tilde{C}_i)\eta_i + F_i \sum_j e_{ij}(\eta_j - \eta_i), \quad (28)$$

$$\dot{\eta}_k = \tilde{A}\eta_k + F_{\bar{o}} \left(\sum_r e_{kr}(\eta_l - \eta_k) - g_k\eta_k \right) + F_{\bar{o}} \sum_i e_{ki}\eta_i, \quad (29)$$

which are coupled through the interconnection term $F_{\bar{o}} \sum_i e_{ki}\eta_i$. We use results of Theorem 1, Proposition 1, and the well known results on hierarchically interconnected systems to show the convergence of the entire network satisfying Assumption 3. The following theorem constitutes the main result of this section.

Theorem 2. *Consider a network of nodes with the sensor model (8) implementing the estimation dynamics (10) to estimate states of the plant dynamics (7) under the noise-free settings $\tilde{\omega} = 0$ and $\xi_i = 0, \forall i$. Suppose that Assumptions 1, 2 and 3 hold. Let conditions of both Theorem* 1 *and Proposition* 1 *apply to the irreducible leader group and the remainder of the graph, considered as pinned. Then each node state $\hat{z}_i(t)$ asymptotically converges to the plant state $z(t)$, in the sense of (13) for γ sufficiently large.*

Proof: The entire network is a hierarchically coupled LTI system of the irreducible leader group (28) and the remainder of the graph (29). The eigenvalues of hierarchically interconnected LTI systems are given by the eigenvalues of their autonomous subsystem blocks on the system matrix block-diagonal, (which is a generally known result in linear systems). Theorem 1 shows the asymptotic stability of (28) and Proposition 1 shows the asymptotic stability of the autonomous subsystem (nominal dynamics) in (29), hence implying stability of the hierarchically coupled system. ■

Alternatively, to show the convergence of the entire network, a composite Lyapunov function could be constructed as in [40].

If the process and measurement noises are not zero, it can be shown based on Theorem 1 that the observation error (11) is indeed uniformly ultimately bounded, [21], so that the estimated state $\hat{z}_i$ converges to the plant's state z within a bounded region whose size depends on the noises.

Remark 7. Results of this section extend [32] by considering a general plant dynamics, while considering process and measurement noises, unlike [37], that assumes perfect

measurements. Moreover, different from [37], all nodes in the irreducible leader group and the remainder of the network implement the same observer dynamics (10) and design their local observer gains G_i and distributed observer gains F_i in the same way, independently of each other. In particular, a given non-sensing node need not know if it is in the irreducible leader group or the remainder of the network. Theorem 1 and Proposition 1 imply different lower bounds on γ hence, for the purposes of design, a more conservative one should be chosen by all nodes to guarantee the stability of the entire network.

The general conclusions of this section provide a basis for the specific design detailed in the following section. Theorem 1, Proposition 1 and Theorem 2 require several design parameters, Q_i, U_i, α_j, and γ, which are not specified yet. Their choice influences the performance of the proposed distributed observer dynamics. In the following section, we detail the design procedure and address the specific choice of these design parameters. Those pertain to distributed observers, nevertheless they will be chosen, in fact, to emulate certain desirable properties of the Kalman filter.

V. Design procedure

This section proposes the distributed observer design, satisfying conditions of Theorem 2, for an individual node under the original plant dynamics with process noise (7) and sensor model with measurement noise (8).

Preliminary steps:

i) Choose $\gamma > 0$ satisfying both following bounds

$$\gamma > w_{max}\frac{\lambda_{max}\left(\tilde{A}+\tilde{A}^T\right)}{\lambda_{min>0}(WL_{m+1m+1}+L_{m+1m+1}^TW)}, \quad (30)$$

and

$$\gamma > \theta_{\max}\frac{\lambda_{\max}\left(\tilde{A}+\tilde{A}^T\right)}{\lambda_{\min}\left(\Theta(\tilde{L}+\tilde{G})+(\tilde{L}+\tilde{G})^T\Theta\right)}. \quad (31)$$

ii) Choose β, such that $0 < \beta \leq 1$.

iii) Let every node i know the values of Ω, γ, and β.

Design steps:

1) Every node $i, \mathcal{O}_i \neq \emptyset$, chooses its $U_i = \Xi_i$ and $Q_i = \Omega_{io}$, where Ω_{io} is found from

$$T_i\Omega T_i^T = \begin{bmatrix} \Omega_{io} & \Omega_{i12} \\ \Omega_{i21} & \Omega_{i\bar{o}} \end{bmatrix}. \quad (32)$$

2) Every node $i, \mathcal{O}_i \neq \emptyset$, then calculates M_i^{-1} as the solution of the ARE (17).

3) Every node $i, \mathcal{O}_i \neq \emptyset$, also calculates

$$\alpha_{ij_{\max}} = \frac{w_{\min}\lambda_{\min}\left(\bar{M}_iQ_i\bar{M}_i\right)}{w_{\max}(p-1)\lambda_{\max}\left(A_j+A_j^T\right)}, j \in \mathcal{O}_i, \quad (33)$$

and communicates the value of $\alpha_{ij_{\max}}$ to all other nodes in the network.

4) Every node $k \in \bar{\mathcal{D}}_j, \forall j$, chooses its α_j as

$$\alpha_j = \min\{1, \beta\alpha_{*j_{\max}}\} \quad (34)$$

where $\alpha_{*j_{\max}} = \min\{\alpha_{ij_{max}} | i \in \mathcal{D}_j\}$.

5) All nodes design their G_i and F_i according to Theorem 1.

The preliminary steps are the only centralized elements of the design. Note that, in contrast to [33], [34], our communication scheme does not require communicating the covariances. Neither we consider channel noise as is done in [35]. This reduces the communication burden and improves stability.

Remark 8. The design procedure outlined above relies on having $Q_i \succ 0$ as this is needed in Theorem 1. If, however, there is no disturbance acting on the plant, $\Omega = 0$, we propose a slight modification of the design by choosing the design parameter Q_i as $Q_i = \epsilon I_{n_{io}}$, where ϵ is a small positive scalar chosen considering magnitudes of the noise covariances Ξ_i.

Furthermore, for purposes of the design, the assigned covariance matrices Q_i and U_i can be scaled equally by an arbitrary constant, at least for asymptotically stable plants or unstable plants with $\alpha_{*j_{\max}} > 1, \forall j \in \bigcup_{i=1}^{p}\bar{\mathcal{O}}_i$. This scaling brings an additional degree of freedom offered by the design to possibly improve the estimator performance.

Note, that the choice of α_j in (34) is conservative to satisfy the upper bound on α_j in (18). This conservativeness comes from the choice of $\alpha_{ij_{\max}}$ in (33). If $|\mathcal{D}_j| = 1$, i.e. only one node observes the jth state-group, then (33) is the same as (18). On the other hand, if $|\mathcal{D}_j| > 1$, i.e. more than one node observers the jth state-group, then (33) is more conservative that (18).

According to (34), if the upper bound on α_j is greater than 1, i.e. $\alpha_{*j_{max}} > 1$, then $\alpha_j = 1$. Otherwise α_j is chosen such that $0 < \alpha_j \leq 1$. There is no reason for α_j to be chosen greater than 1, since the greater the α_j the smaller the stability margin guaranteed by the Lyapunov function in the proof of Theorem 1. The exact value of α_j is in this case determined by the auxiliary design parameter β.

The lower bounds on γ in (30) and (31) imply (71) and (27). The lower bound (71), following from Proof of Theorem 1, is primarily determined by the indefinite term $\lambda_{max}(H+H^T)$. The block diagonal matrix $(H+H^T)$ is composed of two types of blocks $(H_{io}+H_{io}^T)$ and $(H_{i\bar{o}}+H_{i\bar{o}}^T)$. The first type, given by $H_{io} = \bar{M}_{io}(A_{io} - G_{io}C_{io}), i \in \mathcal{V}, j \in \mathcal{O}_i$, corresponds to the observable state-groups of the ith node and the eigenvalues of such a block are negative. Hence those do not affect the lower bound on γ in (71) and can be disregarded. The second type $(H_{i\bar{o}}+H_{i\bar{o}}^T)$ is also a block diagonal matrix but with indefinite blocks $(H_{ij}+H_{ij}^T) = \alpha_{\max}(A_j^T + A_j), i \in \mathcal{V}, j \in \mathcal{O}_i$, where $\alpha_{\max}$ is an upper bound on all α_j. It yields a new numerator of the lower bound (71) in the form

$$\lambda_{max}(H+H^T) \leq \alpha_{\max}\lambda_{max}(A_j+A_j^T). \quad (35)$$

Taking into consideration an upper bound on α_j, (34), one can put $\alpha_{\max} = 1$. Then the new numerator (35) of (71) and also the second lower bound (31), yield simplified lower bounds (30) and (31).

Hereby we showed that the outlined design indeed satisfies conditions of Theorem 1 and Proposition 1, guaranteeing observer convergence as per Theorem 2.

Remark 9. The conservative choice of α_js brings robustness to a sensor failure. If one node stops measuring and its previ-

ously measured state-groups are still measured by other nodes in the network, the observation error dynamics remains stable according to Theorem 2. This property allows incorporation of redundant nodes to the network to increase robustness of the distributed observer. Moreover, fixing of the upper bound on α_j, (34), brings an additional benefit; it establishes definite lower bounds on γ, which are independent of α_j.

A. Theoretical analysis

This subsection provides further discussion on the properties of the presented distributed observer design, in particular reflecting on the similarities with the celebrated Kalman filter.

Remark 10. Design parameters Q_i and U_i are chosen as covariance matrices of the process and measurement noise to emulate the Kalman filter design. Hence every sensing node implements its local Kalman filter to estimate observable state-groups of the plant given its local measurements and noises. This brings local sensor fusion.

To elucidate this further, we analyze the behavior of the local observer gain G_i in dependence of the design matrices Q_i and U_i given by noise covariances. Following the properties of the Kalman filter, which are well documented, [38], [45], [46], if for the ith node G_i is chosen according to the solution $\bar{M}_i^{-1}$ of the ARE (17), then if U_i increases while Q_i is fixed G_{io} decreases in magnitude and if Q_i increases while U_i is fixed G_{io}, defined in (58), increases in magnitude. In other words, the more uncertain the plant state, the greater the weight given to the measurements and vice versa; the more uncertain the measurements, the less the weight given to them, or rather greater weight is given to the plant state. This describes the local sensor fusion that fuses the already known state estimate with newly incoming measurement, akin to that of the Kalman filter.

Let us recall properties of the ARE in the following result.

Lemma 3. *By scaling both design matrices Q_i and U_i by some positive scalar $\delta > 0$, for all i, $\mathcal{O}_i \neq \emptyset$, the local observer gain G_i does not change but the distributed observer gain F_i scales with δ for γ fixed.*

Proof: Multiplying the ARE (17) by the scaling gain δ yields

$$\delta\bar{M}_i^{-1}A_{io}^T + A_{io}\delta\bar{M}_i^{-1} + \delta Q_i - 2\delta\bar{M}_i^{-1}C_{io}^T U_i^{-1} C_{io}\bar{M}_i^{-1} = 0, \quad (36)$$

$$(\delta\bar{M}_i^{-1})A_{io}^T + A_{io}(\delta\bar{M}_i^{-1}) + \delta Q_i - 2(\delta\bar{M}_i^{-1})C_{io}^T(\frac{1}{\delta}U_i^{-1})C_{io}(\delta\bar{M}_i^{-1}) = 0. \quad (37)$$

Hence, by multiplying both Q_i and U_i by δ the solution $\bar{M}_i^{-1}$ of the ARE (17) scales as δ. Inserting the scaled terms into (18) we get

$$0 < \alpha_j < \frac{1}{\delta}\frac{w_{min}\lambda_{min}\left(\sum_{i\in\mathcal{D}_j}\bar{M}_i Q_i \bar{M}_i\right)}{w_{max}(p - |\mathcal{D}_j|)\lambda_{max}\left(A_j + A_j^T\right)}, \quad (38)$$

which yields that the upper bound on α_j scales as $1/\delta$ and thereby $\bar{N}_j^{-1}$ scales as δ. Inserting this scaling into (19) we obtain

$$F_i = \gamma T_i^T \begin{bmatrix} \delta\bar{M}_i^{-1} & \mathbf{0} \\ \mathbf{0} & \text{diag}(\delta\bar{N}_j^{-1}) \end{bmatrix} T_i, \quad j \in \bar{\mathcal{O}}_i. \quad (39)$$

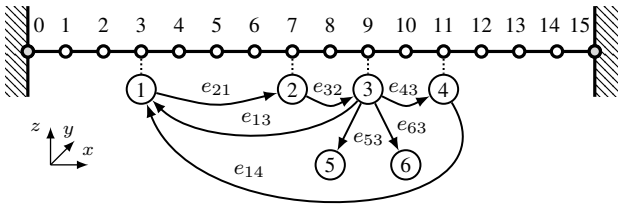

Fig. 1. A beam divided into 15 finite elements with a sensor network consisting of 4 sensing nodes, $\{1, 2, 3, 4\}$, and 2 non-sensing nodes, $\{5, 6\}$.

This shows, that by scaling Q_i and U_i by δ, $\forall i \in \mathcal{V}$ the distributed observer gain F_i scales as δ.

In contrast, this scaling does not affect the the local observer gain G_i because the contributions of M_i^{-1} and U_i^{-1} cancel each other

$$G_i = T_i^T \begin{bmatrix} (\delta\bar{M}_i^{-1})C_{io}(\frac{1}{\delta}U_i^{-1}) \\ \mathbf{0} \end{bmatrix}. \quad (40)$$

■

Remark 11. This has a clear interpretation in the context of our design. The local observer gain G_i effects the local Kalman filter from the history of local measurements and state estimate. If both the process noise Ω and local measurement noise Ξ_i scale equally, the local observer gain G_i will not change but the distributed observer gain F_i will increase, if γ is kept the same. Simply, the more uncertain the measurements for the state-group j the greater weight will be given to the information coming from the network even for non-sensing nodes.

Moreover, the restriction of the upper bound on all α_j to 1 brings an additional degree of freedom in the observer design as it was already mentioned in Remark 8. It separates scaling of the observable and unobservable parts of F_i. From the proof of Lemma 3 it follows that scaling of Ω and Ξ_i by some δ scales only the block of F_i corresponding to the observable subsystem, as long as all $\alpha_j = 1$. This additional functionality can improve overall performance of the estimator, however it applies only to stable systems or unstable systems with $\alpha_{*j_{\max}} > 1, \forall j \in \bigcup_{i=1}^{p}\bar{\mathcal{O}}_i$.

Remark 12. The value of α_j is chosen the same for all nodes not measuring the jth state-group directly to design their F_i. But in fact, α_j is determined by the nodes that do measure this state-group directly, by (18). To be more precise, α_j is determined by the worst sensor sensing state-group j. This means, if we have a faulty measurement somewhere in the network, in average we have more corrupt sources of information, the more the non-sensing nodes will listen to the network. This increases network cohesion and ultimately reduces the steady state error covariances.

VI. Numerical simulations

The proposed distributed observer design is numerically validated on a model of a clamped beam adopted from [42, Section 1.1.4]. The beam is 150 cm long, with a cross-section of 1 cm^2. It is divided into 15 elements, i.e. 14 free and 2 clamped (fixed) nodes as depicted in Fig. 1. Each node has 3

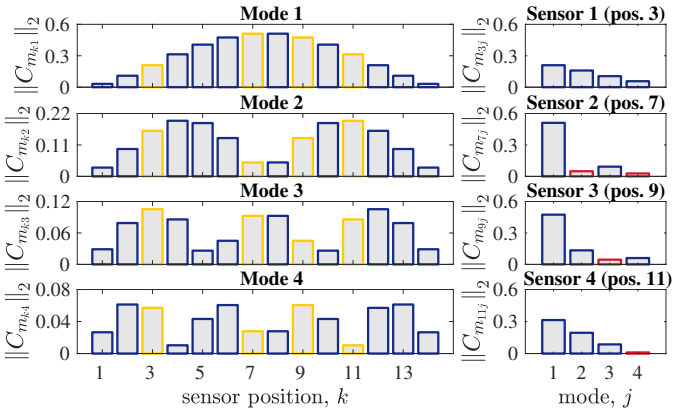

Fig. 2. The 2-norm of the output matrices $C_{m_{kj}}$ for the first four modes j and all possible sensor positions k on the beam on the left and chosen sensor positions on the right.

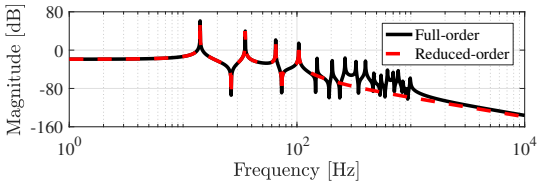

Fig. 3. Frequency response from 6th input to 3rd output.

degrees of freedom (displacement in x and z axis, and pitch in y axis. In general, the clamped beam model represents a mass-spring-damper system which is described in nodal form by a second order matrix differential equation

$$M\ddot{q}(t) + D\dot{q}(t) + Kq(t) = B_o u(t), \tag{41}$$
$$y = C_{oq}q(t) + C_{ov}\dot{q}(t), \tag{42}$$

where $q, \dot{q}$, and $\ddot{q}$ are nodal displacement, velocity, and acceleration vectors in $\mathbb{R}^{42}$, M, D, and K are the mass damping, and stiffness matrices in $\mathbb{R}^{42\times 42}$, $B_o \in \mathbb{R}^{42\times 14}$ is the input matrix and C_{oq}, and C_{ov} are the output matrices in $\in \mathbb{R}^{14\times 42}$. The beam mass and stiffness matrices are given in [42, Appendix C.2]. The damping matrix is given by Rayleigh damping in the form $D = M \cdot 10^{-5} + K \cdot 10^{-6}$. The sensor locations are given by $C_{oq} = I_{14} \otimes c_{oq}$, where $c_{oq} = [0\ 1\ 0]$ and C_{ov} is a zero matrix. For purposes of a proper sensor placement we first evaluate performance of all possible sensor locations. For the distributed observer design we consider zero control input, i.e. $u = 0$.

A transformation to modal form is used to obtain the block diagonal structure of the system required by the design. Following the transformation procedure, described in [42], we obtain the full modal state-space representation

$$\dot{z}(t) = A_m z(t), \tag{43}$$
$$y(t) = C_m z(t), \tag{44}$$

with $A_m = diag(A_{m_j})$ and $C_m = [C_{m_1}, C_{m_2}, \ldots, C_{m_f}]$, where $j = 1, 2, ..., f$ and f represents the number of modal pairs (state-groups) $z_j = [\bar{\omega}_j q_{m_j}\ \dot{q}_{m_j}]^T$ consisting of modal displacement $z_{j_a} = \bar{\omega}_j q_{m_j}$ and modal velocity $z_{j_b} = \dot{q}_{m_j}$. The matrices A_{m_j} are in the form

$$A_{m_j} = \begin{bmatrix} 0 & \bar{\omega}_j \\ -\bar{\omega}_j & -2\zeta_j\bar{\omega}_j \end{bmatrix}, \tag{45}$$

where $\bar{\omega}_j$ is the jth modal frequency and ζ_j is the jth modal damping ratio. Since the plant is a flexible structure, the modal output matrix C_m satisfies Assumption 1.

The model order reduction technique, [42], is used to obtain the reduced model containing the first $l = 4$ dominant modes given by frequencies $\bar{\omega} = [89, 221, 409, 651]^T$ Hz, hence the set of state-groups is $\mathcal{S} = \{1, 2, 3, 4\}$. The output matrix C_m is reduced column-wise to contain only the 4 chosen modes. The 2-norm of the output matrices $C_{m_{kj}}$ for the 4 considered modes $j \in \mathcal{S}$ and all possible sensor positions $k \in \{1, 2, \ldots, 14\}$ is depicted in Fig. 2 on the left. The output matrix is further reduced row-wise by choosing only the sensor locations $3, 7, 9, 11$ for good sensing performance of all 4 modes. A detailed comparison of the 2-norm of output matrices $C_{m_{kj}}$ for chosen sensor locations is shown in Fig. 2 on the right. As discussed in Remark 1, the magnitude of some $C_{m_{kj}}$ is very small for the distributed design, hence one can consider them to be zero as long as the Assumption 2 remains satisfied. The small magnitudes of $C_{m_{kj}}$ for chosen sensor locations appear in Fig. 2 in red color. Observable set for each node is allocated as follows: $\mathcal{O}_1 = \{1, 2, 3, 4\}, \mathcal{O}_2 = \{1, 3\}, \mathcal{O}_3 = \{1, 2, 4\}, \mathcal{O}_4 = \{1, 2, 3\}, \mathcal{O}_5 = \emptyset$ and $\mathcal{O}_6 = \emptyset$. The observability of modes is found to satisfy Assumption 2.

After the model order reduction and sensor placement we obtain the reduced-order model of the beam given by the plant dynamics with process noise, (7), and sensor model with measurement noise, (8). The reduced-order model has $\tilde{A} \in \mathbb{R}^{8\times 8}$ and $\tilde{C} \in \mathbb{R}^{4\times 8}$. Fig. 3 shows a comparison of the amplitude characteristic of frequency response for the nominal plant and the reduced model. The frequency response is calculated by considering an input displacement at node 6 in z direction and measuring a response of a sensor at node 4 in y direction. It is introduced for a better interpretation of the reduced model, however for purposes of this design we do not consider any input.

The communication topology of the sensor network is given in Fig. 1. It consists of four sensing nodes $\mathcal{V}_1 = \{1, 2, 3, 4\}$ contained in an irreducible leader group and two non-sensing nodes $\mathcal{V}_2 = \{5, 6\}$ located in the remainder of the graph, i.e. $\mathcal{V} = \mathcal{V}_1 \cup \mathcal{V}_2$. Note that the topology satisfies Assumption 3. The corresponding adjacency matrix is

$$E = \left[\begin{array}{cccc|cc} 0 & 0 & 1 & 1 & 0 & 0 \\ 1 & 0 & 0 & 0 & 0 & 0 \\ 0 & 1 & 0 & 0 & 0 & 0 \\ 0 & 0 & 1 & 0 & 0 & 0 \\ \hline 0 & 0 & 1 & 0 & 0 & 0 \\ 0 & 0 & 1 & 0 & 0 & 0 \end{array}\right]. \tag{46}$$

The beam model represents a low damped flexible structure with stable poles close to the imaginary axis. For this reason the bounds on the α_j and γ do not restrict the design, i.e. their values can be set arbitrary large. Nevertheless, following the design guidelines from Section V we set $\alpha_j = 1, \forall j$. The

value of γ is chosen later such that the rate of convergence corresponds to the speed of the local observers.

A. Simulation with initial conditions

Functionality of the proposed distributed observer is demonstrated on a simulation of the clamped beam excited only by initial conditions. The plant initial conditions in nodal coordinates are set to zero except the displacement in z direction at 7th position which is set to 0.01. The corresponding initial conditions in modal coordinates are: $z(0) = [2.9, 0, -5.2, 0, -6.2, 0, 21.5, 0]$. Initial conditions of nodes in the sensor network are chosen randomly in appropriate scales. The sensing nodes' measurement noises are WGN with covariance matrix $\Xi = \text{diag}([2, 5, 3, 0.1])\cdot 10^{-6}$. Process noises are also WGN with randomly generated diagonal covariance matrix $\Omega = \text{diag}([6, 10, 10, 6, 18, 14, 8, 8])\cdot 10^{-4}$. The remaining design parameters are: $\alpha = 1$, $\beta = 1$, and $\gamma = 200$.

Out analysis follows three simulated scenarios:

a) General simulation with introduced parameters.
b) Measurement degradation of 4th node, i.e. $\Omega_{44} = 10^{-2}$.
c) Failure of the communication link $4 \to 1$, i.e. $e_{14} = 0$.

In all three investigated cases 2-norm of the state observation error η_{ij}, depicted in Fig. 6, converges to a bounded region given by the magnitude of the process and measurement noises, hence each node $i \in \mathcal{V}$ obtains a full estimate of the plant state vector. These results validate the conclusion of Theorem 2. In general, more dominant modes have better observability, therefore their convergence speed is faster, which is evident from the figures.

a) General simulation: This simulation shows the functionality of the proposed observer. The convergence of the ith node modal estimate $\hat{z}_{ij}$ to the plant modal vector z_j can be seen in Fig. 4. and also in Fig. 6a in form of 2-norm of the estimation error η_{ij}. The comparison of the sensing nodes' measurements with their measurement estimates is given in Fig. 5.

b) Measurement degradation: In case of corrupted measurements of the 4th sensing node, the convergence of the estimator is shown in Fig. 6b. The 4th node obtains the full estimates of the plant state together with the rest of the network in spite of its corrupted measurement. The reason is the judiciously designed distributed observer which for the 4th node takes into consideration the large noise variance of that measurement and thereby imposes small G_4 and large F_4. In other words 4th node assigns much larger confidence to informations from its neighbors than to its corrupted measurement. This also follows from the 2-norms of G_4 and F_4 before and after the measurement degradation, which are $\|G_4\|_2 = 248$, $\|F_4\|_2 = 1$ and $\|G_4\|_2 = 0.44$, $\|F_4\|_2 = 12$, respectively. By its comparison to a general case from Fig. 6a it can be seen, that small noise variance in 4th sensing node provides slight improvement in convergence rate of the estimator.

c) Communication link failure: By failure of the communication link from node 4 to node 1, the redundant sensing node 4 gets disconnected from the irreducible leader group. In this particular case, the rest of the network is not able to obtain information from the 4th node. Since the Assumption 2 remains satisfied the nodes are still able to obtain full estimate of the plant states. Fig. 6c shows that the 4th node estimates the modes faster than other nodes, except for the 4th mode which is in agreement with the network. The small noise variance in the 4th node measurement causes the 4th node to assign larger confidence to its measurements that to information from the network, therefore the 4th nodes estimates of the modes 1, 2, and 3 show faster convergence than the network. On the other hand, the 4th mode is unobservable from the 4th nodes perspective, hence it receives information on that mode from the network. This is in line with the analysis of the observer convergence provided in Section IV. Note that, because there is no other link from the node 4 to the irreducible leader group, failure of this link is identical to the failure of the sensing node 4 from all other nodes' perspective.

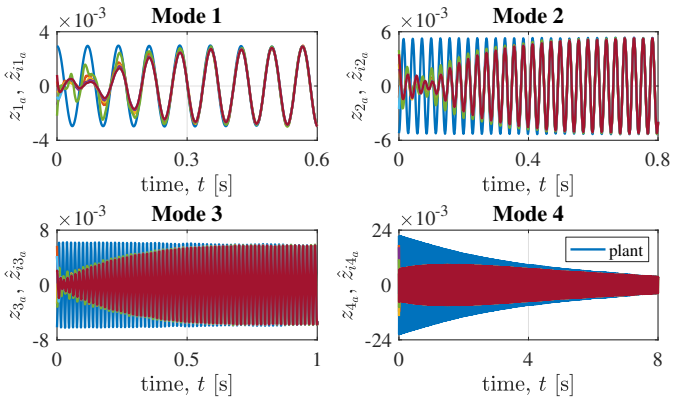

Fig. 4. The plants modal displacements and nodes' estimates, z_{j_a} and $\hat{z}_{ij_a}$, $\forall (i,j), i \in \mathcal{V}, j \in \mathcal{S}$, in time-domain, response to initial conditions.

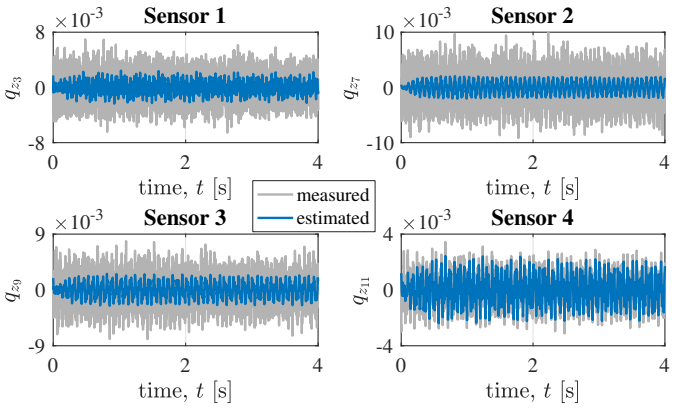

Fig. 5. Comparison of measured and estimated nodal displacement $q_{z_k}, \forall k \in \{3, 7, 9, 11\}$ of the sensing nodes, response to initial conditions.

B. Steady-state simulation

To provide insight into the overall deterioration of precision of nodes' estimates for all three investigated cases from Section VI-A, the plant and the sensor network are simulated in a steady state with zero initial conditions. Fig. 7 shows a comparison of the calculated variances of modal displacement observation errors z_{ij_a}. It can be seen that differences in the variances are negligible, hence the proposed design is found robust to measurement degradation and a link/node failure.

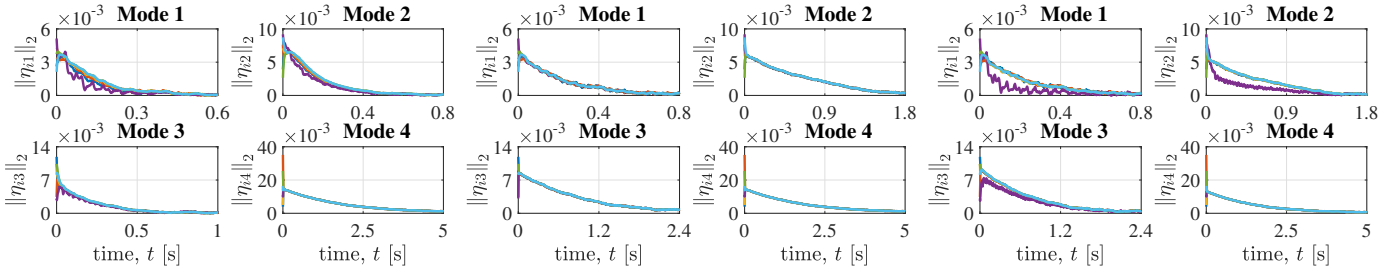

(a) $\Omega_{44} = 10^{-7}$, $e_{14} = 1$ (b) $\Omega_{44} = 10^{-2}$, $e_{14} = 1$ (c) $\Omega_{44} = 10^{-7}$, $e_{14} = 0$

Fig. 6. The 2-norm of the state observation error η_{ij}, $\forall(i,j), i \in \mathcal{V}, j \in \mathcal{S}$, response to initial conditions. Simulation for three cases: a) general case for demonstration of the observer convergence; b) 4th sensor measurement degradation; c) failure of the communication link from node 4 to node 1.

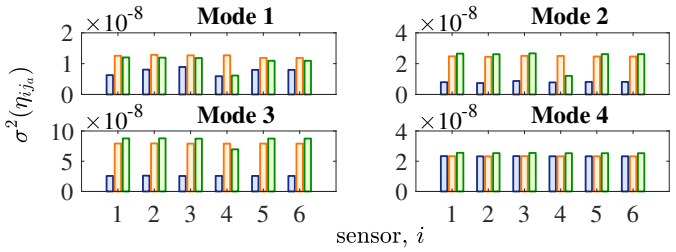

Fig. 7. Variance of modal displacement estimation error η_{ija}, $\forall(i,j), i \in \mathcal{V}, j \in \mathcal{S}$, steady-state simulation for the three cases *a), b)* and *c)*.

VII. Conclusion

In this paper, we propose a distributed Luenberger-like observer design for sensor networks, which considers disturbance acting on states of the plant and noise corrupting the sensor measurements. Observer nodes in the sensor network are designed and implemented in a fully distributed manner based only on their local information and information from their neighbors. The presented distributed observer design exhibits good scalability on large-scale sensor networks and flexibility to integrating new nodes into the network. Additional node redundancy provides robustness to communication link or node failures. The convergence of the state estimates of networked observers to the plant (target) state are rigorously proven. The observer design is thoroughly described and its theoretical analysis is provided. Numerical simulations validate the proposed distributed observer design.

Appendix A

Proof of Theorem 1: Define a Lyapunov function candidate in the quadratic form

$$V = \sum_{i\in\mathcal{V}} w_i \eta_i^T M_i \eta_i, \tag{47}$$

where $w_i > 0$ is the element of the left eigenvector corresponding to zero eigenvalue of the Laplacian matrix L defined in Theorem 1 and $M_i \in \mathbb{R}^{n\times n}$ is a positive definite symmetric matrix to be specified later in the proof. The time-derivative of this Lyapunov function candidate is

$$\dot{V} = \sum_{i\in\mathcal{V}} w_i (\dot{\eta_i}^T M_i \eta_i + \eta_i^T M_i \dot{\eta_i}), \tag{48}$$

$$\dot{V} = \sum_{i\in\mathcal{V}} w_i \eta_i^T \left(M_i(\tilde{A} - G_i C_i \Pi) + (\tilde{A} - G_i C_i \Pi)^T M_i \right) \eta_i + 2 \sum_{i\in\mathcal{V}} w_i \eta_i^T M_i F_i \sum_{j\in\mathcal{V}} e_{ij}(\eta_j - \eta_i). \tag{49}$$

Let $M_i F_i = \gamma I_n$ with $\gamma \in \mathbb{R}^+$. The second term can be rewritten to a quadratic form according to [13] as follows

$$\begin{aligned} 2 \sum_{i\in\mathcal{V}} w_i \eta_i^T M_i F_i \sum_{j\in\mathcal{V}} e_{ij}(\eta_j - \eta_i) = \\ 2\gamma \sum_{i,j} w_i e_{ij} \eta_i^T (\eta_j - \eta_i) = \\ \gamma \sum_{i,j} w_i e_{ij} \eta_i^T (\eta_j - \eta_i) + \gamma \sum_{i,j} w_i e_{ij} \eta_j^T (\eta_i - \eta_j) = \\ - \gamma \sum_{i,j} w_i e_{ij} (\eta_j - \eta_i)^T (\eta_j - \eta_i), \end{aligned} \tag{50}$$

yielding the derivative of the Lyapunov function in the form

$$\begin{aligned} \dot{V} = \sum_{i\in\mathcal{V}} w_i \eta_i^T \left(M_i(\tilde{A} - G_i C_i \Pi) + (\tilde{A} - G_i C_i \Pi)^T M_i \right) \eta_i \\ - \gamma \sum_{i,j\in\mathcal{V}} w_i e_{ij} (\eta_j - \eta_i)^T (\eta_j - \eta_i). \end{aligned} \tag{51}$$

Note, that the second term of the time-derivative of the Lyapunov function (51) is negative semidefinite. It is zero only for the case $\eta_i = \eta_j, \forall(j,i) \in \mathcal{E}$. To show $\dot{V} < 0$ we investigate two cases; first, for $\eta_i = \eta_j, \forall(j,i) \in \mathcal{E}$, the second term vanishes and we show that the first term is then negative definite. Then, for $\exists(j,i) \in \mathcal{E}, \eta_i \neq \eta_j$, we show that the second negative definite term overpowers the first indefinite term.

1) Let $\eta_i = \eta_j, \forall(j,i) \in \mathcal{E}$. The time-derivative of the Lyapunov function then retains only the first term

$$\begin{aligned} \dot{V} = \sum_{i\in\mathcal{V}} w_i \eta_i^T \Big(M_i(\tilde{A} - G_i C_i \Pi) \\ + (\tilde{A} - G_i C_i \Pi)^T M_i \Big) \eta_i. \end{aligned} \tag{52}$$

Define a permutation matrix $T_i \in \mathbb{R}^{n_i \times n_i}$, $T_i^T = T_i^{-1}$, that rearranges the states groups η_{ij} of ith observer node into observable and unobservable ones as follows

$$\hat{\eta}_i = \begin{bmatrix} \eta_{io} \\ \eta_{i\bar{o}} \end{bmatrix} = T_i \eta_i. \tag{53}$$

Applying this transformation, the time-derivative of the Lyapunov function can be written as

$$\begin{aligned} \dot{V} = \sum_{i\in\mathcal{V}} w_i \hat{\eta_i}^T T_i \Big(M_i(\tilde{A} - G_i C_i \Pi) \\ + (\tilde{A} - G_i C_i \Pi)^T M_i \Big) T_i^T \hat{\eta}_i, \end{aligned} \tag{54}$$

$$\begin{aligned} \dot{V} = \sum_i w_i \hat{\eta_i}^T \big(T_i M_i T_i^T (T_i \tilde{A} T_i^T - T_i G_i C_i \Pi T_i^T) \\ + (T_i \tilde{A} T_i^T - T_i G_i C_i \Pi T_i^T)^T T_i M_i T_i^T \big) \hat{\eta_i}^T, \end{aligned} \tag{55}$$

$$\dot{V} = \sum_i w_i \hat{\eta}_i{}^T \left(\hat{M}_i(\hat{A} - \hat{G}_i\hat{C}_i) + (\hat{A} - \hat{G}_i\hat{C}_i)^T \hat{M}_i \right) \hat{\eta}_i, \quad (56)$$

with the state-space matrices of the plant dynamics in the Kalman decomposed form

$$\begin{aligned} \hat{A} = T_i \tilde{A} T_i^{-1} = T_i \tilde{A} T_i^T = \begin{bmatrix} A_{io} & 0 \\ 0 & A_{i\bar{o}} \end{bmatrix}, \\ \hat{C}_i = C_i \Pi T_i^T = \begin{bmatrix} C_{io} & 0 \end{bmatrix}, \end{aligned} \quad (57)$$

and the local observer gain matrix and matrix $\hat{M}_i$ in the form

$$\begin{aligned} \hat{G}_i = T_i G_i = \begin{bmatrix} G_{io} \\ 0 \end{bmatrix}, \\ \hat{M}_i = T_i M_i T_i^T = \begin{bmatrix} \bar{M}_i & 0 \\ 0 & \bar{N}_i \end{bmatrix}, \end{aligned} \quad (58)$$

where $A_{io} = \text{diag}(A_j)$, $j \in \mathcal{O}_i$ and $A_{i\bar{o}} = \text{diag}(A_j)$, $j \in \bar{\mathcal{O}}_i$ are block diagonal matrices with $|\mathcal{O}_i|$ and $|\bar{\mathcal{O}}_i|$ blocks on their diagonal. Similarly, $\bar{N}_i = \text{diag}(N_j)$, $j \in \bar{\mathcal{O}}_i$ is a block diagonal matrix with $|\bar{\mathcal{O}}_i|$ blocks on its diagonal in agreement with the block structure of $A_{i\bar{o}}$. Matrix C_{io} can be interpreted as a row vector consisting of $|\mathcal{O}_i|$ elements (matrices) C_{ij}, $j \in \mathcal{O}_i$. Note that the system matrix $\hat{A}$ in (57) has zero matrices on the off-diagonal blocks because of the Assumption 1 considering observability of a state-group.

We can write the time-derivative of the Lyapunov function as $\dot{V} = \sum_i w_i \hat{\eta}_i^T (J_i + J_i^T) \hat{\eta}_i$ with

$$\begin{aligned} J_i = \begin{bmatrix} \bar{M}_i & 0 \\ 0 & \bar{N}_i \end{bmatrix} \Bigg(\begin{bmatrix} A_{io} & 0 \\ 0 & A_{i\bar{o}} \end{bmatrix} \\ - \begin{bmatrix} G_{io} \\ 0 \end{bmatrix} \begin{bmatrix} C_{io} & 0 \end{bmatrix} \Bigg), \end{aligned} \quad (59)$$

or in an expanded form as follows

$$J_i = \begin{bmatrix} \bar{M}_i(A_{io} - G_{io}C_{io}) & 0 \\ +(A_{io} - G_{io}C_{io})^T \bar{M}_i & \\ 0 & \bar{N}_i A_{i\bar{o}} \\ & +A_{i\bar{o}}^T \bar{N}_i \end{bmatrix}. \quad (60)$$

This transformation allows us to split the time-derivative of the Lyapunov function into two terms representing the contributions of observable and unobservable state-groups separately

$$\begin{aligned} \dot{V} = \sum_i w_i \eta_{io}^T \left(\bar{M}_i(A_{io} - G_{io}C_{io}) + (A_{io} - G_{io}C_{io})^T \bar{M}_i \right) \eta_{io} \\ + \sum_i w_i \eta_{i\bar{o}}^T \left(\bar{N}_i A_{i\bar{o}} + A_{i\bar{o}}^T \bar{N}_i \right) \eta_{i\bar{o}}. \end{aligned} \quad (61)$$

Referring to Theorem 1, let $Q_i \succ 0$ and $U_i \succ 0$ are chosen matrices and the local observer gain is given by $G_{io} = \bar{M}_i^{-1} C_{io}^T U_i^{-1}$, where $\bar{M}_i^{-1}$ is the solution of the ARE (17). Then by using the ARE (17), the first term of the time-derivative of the Lyapunnov function can be simplified

$$\begin{aligned} &\bar{M}_i(A_{io} - G_{io}C_{io}) + (A_{io} - G_{io}C_{io})^T \bar{M}_i = \\ &\bar{M}_i \left((A_{io} - G_{io}C_{io}) \bar{M}_i^{-1} + \bar{M}_i^{-1} (A_{io} - G_{io}C_{io})^T \right) \bar{M}_i = \\ &\bar{M}_i (\bar{M}_i^{-1} A_{io}^T + A_{io} \bar{M}_i^{-1} - 2\bar{M}_i^{-1} C_{io}^T U_i^{-1} C_{io} \bar{M}_i^{-1}) \bar{M}_i = \\ &\qquad \bar{M}_i (-Q_i - \bar{M}_i^{-1} C_{io}^T U_i^{-1} C_{io} \bar{M}_i^{-1}) \bar{M}_i. \end{aligned} \quad (62)$$

Then the time-derivative of the Lyapunov function is

$$\begin{aligned} \dot{V} = \sum_i w_i \eta_{io}^T \bar{M}_i (-Q_i - \bar{M}_i^{-1} C_{io}^T U_i^{-1} C_{io} \bar{M}_i^{-1}) \bar{M}_i \eta_{io} \\ + \sum_i w_i \eta_{i\bar{o}}^T \left(\bar{N}_i A_{i\bar{o}} + A_{i\bar{o}}^T \bar{N}_i \right) \eta_{i\bar{o}}. \end{aligned} \quad (63)$$

By neglecting the negative semi-definite term with $(-\bar{M}_i^{-1} C_{io}^T U_i^{-1} C_{io} \bar{M}_i^{-1})$ we find an upper bound on the time-derivative of the Lyapunov function as

$$\begin{aligned} \dot{V} < -\sum_i w_i \eta_{io}^T \bar{M}_i Q_i \bar{M}_i \eta_{io} \\ + \sum_i w_i \eta_{i\bar{o}}^T \left(\bar{N}_i A_{i\bar{o}} + A_{i\bar{o}}^T \bar{N}_i \right) \eta_{i\bar{o}}. \end{aligned} \quad (64)$$

Finding lower bound on the first term gives

$$\sum_i w_i \lambda_{\min}(\bar{M}_i Q_i \bar{M}_i) \eta_{io}^T \eta_{io} \leq \sum_i w_i \eta_{io}^T \bar{M}_i Q_i \bar{M}_i \eta_{io} \quad (65)$$

Let $\bar{N}_i = \text{diag}(N_j), N_j \in \mathbb{R}^{n_j \times n_j}, j \in \bar{\mathcal{O}}_i$. Denote $R_j = N_j A_j + A_j^T N_j$, then the time-derivative of the Lyapunov function is

$$\begin{aligned} \dot{V} < -\sum_{i \in \mathcal{V}} w_i \left(\sum_{j \in \mathcal{O}_i} \lambda_{\min}(\bar{M}_i Q_i \bar{M}_i) \eta_{ij}^T I_{n_j} \eta_{ij} \right) \\ + \sum_{i \in \mathcal{V}} w_i \left(\sum_{j \in \bar{\mathcal{O}}_i} \eta_{ij}^T R_j \eta_{ij} \right). \end{aligned} \quad (66)$$

Let us recall that here $\eta_i = \eta_j, \forall (j,i) \in \mathcal{E}$, which implies that all corresponding state-groups of all nodes are equal, i.e. $\eta_j^* = \eta_{1j} = \eta_{2j} = \cdots = \eta_{pj}, \forall j \in \mathcal{S}$. This allows us to rewrite the time-derivative of the Lyapunov function into the form $\dot{V} = \sum_{j \in \mathcal{S}} \eta_j^{*T} E_j \eta_j^*$ where

$$E_j < -\sum_{i \in \mathcal{D}_j} w_i \lambda_{\min}(\bar{M}_i Q_i \bar{M}_i) I_{n_j} + \sum_{i \in \bar{\mathcal{D}}_j} w_i R_j, \quad (67)$$

with sum over state-groups instead of sum over agents and vice versa. For $\dot{V} < 0$, as state-groups are dynamically independent, $E_j \prec 0$ has to be satisfied by each state-group j. The second sum in E_j is indefinite while the first sum is negative definite. To allow $\dot{V} \prec 0$, every state-group has to be observable by at least one agent to have at least one negative definite term in E_j. Note that this property is guaranteed by Assumption 2.

Using the definition $N_j = \alpha_j I_{n_j}$ from Theorem 1 we derive an upper bound on matrix E_j as follows

$$\begin{aligned} E_j \leq -w_{min} \sum_{i \in \mathcal{D}_j} \lambda_{\min}(\bar{M}_i Q_i \bar{M}_i) \\ + (p - |\mathcal{D}_j|) \alpha_j w_{max} \lambda_{max} \left(A_j + A_j^T \right). \end{aligned} \quad (68)$$

Choosing α_j as in (18), $E_j \prec 0$, thus $\dot{V} < 0$ for the investigated case when $\eta_i = \eta_j, \forall (j,i) \in \mathcal{E}$.

2) Let now $\exists (j,i) \in \mathcal{E}, \eta_i \neq \eta_j$. Define a Kronecker product $\mathbf{W} = W \otimes I_n$, $W = \text{diag}(w_i)$ and a block diagonal matrix $H = \text{diag}(M_i(\tilde{A} - G_i C_i \Pi))$, $i \in \mathcal{V}$. Rewriting the derivative of the Lyapunov function (51) to the matrix form gives

$$\begin{aligned} \dot{V} = \eta^T \left(\mathbf{W} \big(H + H^T \big) \right) \eta \\ - \gamma \eta^T \left((WL + L^T W) \otimes I_n \right) \eta. \end{aligned} \quad (69)$$

The first term of (69) is generally indefinite while the second term is negative definite. Finding upper and lower bounds on these two terms we get

$$\begin{aligned} \dot{V} \leq w_{max} \lambda_{max} \big(H + H^T \big) \|\eta\|^2 \\ - \gamma \lambda_{min>0} (WL + L^T W) \|\eta\|^2 \end{aligned} \quad (70)$$

Hence the derivative of the Lyapunov function is negative definite for

$$\gamma > w_{max} \frac{\lambda_{max}\big(H + H^T\big)}{\lambda_{min>0}(WL + L^T W)}. \tag{71}$$

For sufficiently large γ, $\dot{V} < 0$ for the second investigated case $\exists (j,i) \in \mathcal{E}, \eta_i \neq \eta_j$.

Hereby we showed that the time-derivative of the Lyapunov function candidate (47) is negative definite. Hence the nodes' estimation dynamics (10) is stable in the sense that nodes' states always converge to the plant state. This concludes the proof. ■

REFERENCES

[1] J. Lunze, *Control theory of digitally networked dynamic systems*. Heidelberg: Springer, 2014.

[2] A. Bemporad, M. Heemels, and M. Johansson, *Networked Control Systems, Lecture Notes in Control and Information Sciences*. London: Springer, 2010, vol. 406.

[3] F.-Y. Wang and D. Liu, *Networked Control Systems*. London: Springer, 2008.

[4] J. Lee, B. Bagheri, and H. A. Kao, "A Cyber-Physical Systems architecture for Industry 4.0-based manufacturing systems," *Manufacturing Letters*, vol. 3, pp. 18–23, 2015.

[5] S. K. Khaitan and J. D. McCalley, "Design techniques and applications of cyberphysical systems: A survey," *IEEE Systems Journal*, vol. 9, no. 2, pp. 350–365, 2015.

[6] R. Baheti and H. Gill, "Cyber-physical Systems, The Impact of Control Technology," *IEEE Control Systems Society*, 2011.

[7] C. Godsil and G. Royle, *Algebraic Graph Theory*. New York: Springer, 2001.

[8] J. Fax and R. Murray, "Information Flow and Cooperative Control of Vehicle Formations," *IEEE Transactions on Automatic Control*, vol. 49, no. 9, pp. 1465–1476, 2004.

[9] R. Olfati-Saber and R. M. Murray, "Consensus problems in networks of agents with switching topology and time-delays," *IEEE Transactions on Automatic Control*, vol. 49, no. 9, pp. 1520–1533, 2004.

[10] R. Olfati-Saber, J. A. Fax, and R. M. Murray, "Consensus and Cooperation in Networked Multi-Agent Systems," *Proceedings of the IEEE*, vol. 95, no. 1, pp. 215–233, 2007.

[11] W. Ren, R. W. Beard, and E. M. Atkins, "Information Consensus in Multivehicle Cooperative Control," *IEEE Control Systems Magazine*, vol. 27, no. 2, pp. 71–82, 2007.

[12] H. Zhang, F. L. Lewis, and A. Das, "Optimal Design for Synchronization of Cooperative Systems: State Feedback, Observer and Output Feedback," *IEEE Transactions on Automatic Control*, vol. 56, no. 8, pp. 1948–1952, 2011.

[13] H. Zhang, F. L. Lewis, and Z. Qu, "Lyapunov, Adaptive, and Optimal Design Techniques for Cooperative Systems on Directed Communication Graphs," *IEEE Transactions on Industrial Electronics*, vol. 59, no. 7, pp. 3026–3041, 2012.

[14] K. Hengster-Movric and F. Lewis, "Cooperative observers and regulators for discrete-time multiagent systems," *International Journal of Robust and Nonlinear Control*, vol. 23, no. 14, pp. 1545–1562, 2013.

[15] K. K. Oh, M. C. Park, and H. S. Ahn, "A survey of multi-agent formation control," *Automatica*, vol. 53, pp. 424–440, 2015.

[16] A. Bidram, F. L. Lewis, and A. Davoudi, "Distributed control systems for small-scale power networks: Using multiagent cooperative control theory," *IEEE Control Systems*, 2014.

[17] I. Akyildiz, Weilian Su, Y. Sankarasubramaniam, and E. Cayirci, "A survey on sensor networks," *IEEE Communications Magazine*, vol. 40, no. 8, pp. 102–114, 2002.

[18] G. Cooray, "The Kuramoto Model," Tech. Rep., 2008.

[19] S. Wasserman and K. Faust, *Social Network Analysis, Methods and Applications*. Cambridge: Cambridge University Press, 1994.

[20] Z. Qu, *Cooperative Control of Dynamical Systems*. London: Springer, 2008.

[21] F. L. Lewis, H. Zhang, K. Hengster-Movric, and A. Das, *Cooperative Control of Multi-Agent Systems*. London: Springer, 2014.

[22] J. W. Tukey and N. Wiener, "The Extrapolation, Interpolation and Smoothing of Stationary Time Series with Engineering Applications." *Journal of the American Statistical Association*, vol. 47, pp. 319–321, 1952.

[23] N. Levinson, "The Wiener (Root Mean Square) Error Criterion in Filter Design and Prediction," *Journal of Mathematics and Physics*, vol. 25, no. 1-4, pp. 261–278, apr 1946.

[24] R. E. Kalman, "On the general theory of control systems," *IEEE Transactions on Automatic Control*, vol. 4, no. 3, pp. 110 – 110, 1959.

[25] D. G. Luenberger, "Observing the State of a Linear System," *IEEE Transactions on Military Electronics*, vol. 8, no. 2, pp. 74–80, 1964.

[26] J. L. Speyer, "Computation and Transmission Requirements for a Decentralized Linear-Quadratic-Gaussian Control Problem," *IEEE Transactions on Automatic Control*, vol. 24, no. 2, pp. 266–269, 1979.

[27] B. Rao and H. Durrant-Whyte, "Fully decentralised algorithm for multisensor Kalman filtering," *IEE Proceedings D - Control Theory and Applications*, vol. 138, no. 5, p. 413, 1991.

[28] B. Rao, H. Durrant-Whyte, and J. Sheen, "A Fully Decentralized Multi-Sensor System For Tracking and Surveillance," *International Journal of Robotics and Research*, vol. 12, no. 1, pp. 20–24, 1993.

[29] R. Olfati-Saber, "Distributed Kalman Filter with Embedded Consensus Filters," *Proceedings of the IEEE Conference on Decision and Control*, vol. 2005, pp. 8179–8184, 2005.

[30] R. Olfati-Saber and J. S. Shamma, "Consensus Filters for Sensor Networks and Distributed Sensor Fusion," *Proceedings of the IEEE Conference on Decision and Control*, pp. 6698–6703, 2005.

[31] D. P. Spanos, R. Olfati-saber, and R. M. Murray, "Dynamic consensus on mobile networks," *Proceedings of the IFAC World Congress*, 2005.

[32] X. Zhang, K. Hengster-Movric, M. Sebek, W. Desmet, and C. Faria, "Consensus-based distributed sensor fusion over a network," in *Proceedings of the IEEE Conference on Control Technology and Applications*, 2017.

[33] R. Olfati-Saber, "Distributed Kalman filtering for sensor networks," *Proceedings of the IEEE Conference on Decision and Control*, pp. 5492–5498, 2007.

[34] ——, "Kalman-Consensus filter: Optimality, stability, and performance," *Proceedings of the IEEE Conference on Decision and Control*, pp. 7036–7042, 2009.

[35] H. Ji, F. L. Lewis, Z. Hou, and D. Mikulski, "Distributed information-weighted Kalman consensus filter for sensor networks," *Automatica*, vol. 77, pp. 18–30, 2017.

[36] T. Kim, H. Shim, and D. D. Cho, "Distributed Luenberger observer design," in *Proceedings of the IEEE Conference on Decision and Control*, 2016.

[37] X. Zhang, K. Hengster-Movric, and M. Šebek, "Distributed Observer and Controller Design for Spatially Interconnected Systems," *IEEE Transactions on Control Systems Technology*, vol. PP, no. 99, pp. 1–13, 2017.

[38] F. L. Lewis, L. Xie, and D. Popa, *Optimal and Robust Estimation: With an Introduction to Stochastic Control Theory, Second Edition*. Boca Raton: CRC Press, 2007.

[39] H. Zhang, Z. Li, Z. Qu, and F. L. Lewis, "On constructing Lyapunov functions for multi-agent systems," *Automatica*, vol. 58, pp. 39–42, 2015.

[40] K. Hengster-Movric, M. Sebek, and S. Celikovsky, "Structured Lyapunov Functions for Synchronization of Identical Affine-in-control AgentsUnified Approach," *Journal of the Franklin Institute*, vol. 353, no. 14, pp. 3457–3486, 2016.

[41] J. W. Brewer, "Kronecker Products and Matrix Calculus in System Theory," *IEEE Transactions on Circuits and Systems*, vol. 25, no. 9, pp. 772–781, 1978.

[42] W. K. Gawronski, *Advanced Dynamics and Active Control of Structures*. New York: Springer, 2004.

[43] P. J. Antsaklis and A. N. Michel, *A Linear Systems Primer*. Boston: Birkhäuser, 2007.

[44] R. A. Horn and C. R. Johnson, *Matrix Analysis*. Cambridge: Cambridge University Press, 1985.

[45] D. Simon, *Optimal State Estimation: Kalman, H, and Nonlinear Approaches*. Hoboken: John Wiley & Sons, 2006.

[46] A. H. Jazwinski, *Stochastic Processes and Filtering Theory*. New York and London: Academic Press, 1970.

8. DISTRIBUTED ADAPTIVE CONSENSUS PROTOCOLS

Štefan Knotek, Kristian Hengster-Movric, and Michael Sebek, **Distributed adaptive consensus protocol with decaying gains on directed graphs**, *6th IFAC Workshop on Distributed Estimation and Control in Networked Systems*, Tokyo, Japan, September, 2016. IFAC-PapersOnLine 49 (22), pp. 355-360, 2016

Štefan Knotek, Kristian Hengster-Movric, Michael Šebek, **Distributed adaptive consensus protocol with Laplacian eigenvalues estimation**, 21st International Conference on Process Control (PC), 2017, pp. 269-273, 2017

The following two conference papers investigate the possibilities of using adaptive consensus protocols on directed graphs in which the only remaining requirement for centralized information in the synchronizing region based designs is avoided through adaptation the coupling constant. In particular, the coupling constant in the synchronizing region designs, required for single-agent design, is often found to depend on the global graph topology which is not known to each/any single-agent. Distributed adaptation protocols are supposed to, in a way, overcome this obstacle by providing that information to all single-agents dynamically. Those results were first presented on the 2016 *Necsys* conference, and 2017 *Process Control* conference. Results are applicable, in principle, to all designs based on synchronizing region methods, which would, in turn, make them indeed fully distributed.

The first section presents a distributed adaptive consensus protocol that solves the cooperative regulator problem for multi-agent systems with general linear time-invariant dynamics networked on directed, strongly connected communication graphs. This protocol addresses the problems of recent distributed adaptive consensus protocols with large or unbounded coupling gains. These problems are solved by introducing a novel coupling gain dynamics that allows the coupling gains to synchronize and decay to some estimated value. Unlike the static consensus protocols, which require the knowledge of the smallest real part of the non-zero Laplacian eigenvalue to design their coupling gain, the proposed adaptive consensus protocol does not require any centralized information. It can be therefore implemented on agents in a fully distributed fashion.

The second section addresses distributed consensus problem for multi-agent systems with general linear time-invariant dynamics and undirected connected communication graphs. A distributed adaptive consensus protocol is found to solve problems of existing adaptive consensus protocols related to different, generally large and possibly unbounded coupling gains. This protocol guaranties ultimate boundedness under all conditions, however for an asymptotic stability, a proper estimation of reference values for coupling gains is required. In this work, we propose an algorithm for the estimation of this coupling gain reference. The algorithm is based on a distributed estimation of Laplacian matrix eigenvalues. In comparison to previously proposed algorithm based on the interval halving method, this algorithm offers robustness to change of the network topology. In addition, it decouples the estimation from the consensus protocol; hence it does not influence stability properties of the adaptive consensus protocol.

Distributed Adaptive Consensus Protocol with Decaying Gains on Directed Graphs ⋆

Štefan Knotek, Kristian Hengster-Movric and Michael Šebek

Department of Control Engineering, Czech Technical University, Prague, Czech Republic (e-mail: stefan.knotek@fel.cvut.cz)

Abstract: In this paper we present a distributed adaptive consensus protocol, that solves the cooperative regulator problem for multi-agent systems with general linear time-invariant dynamics and directed, strongly connected communication graphs. The protocol addresses the problems of recent distributed adaptive consensus protocols with large or unbounded coupling gains. These problems are solved by introducing a novel coupling gain dynamics that allows the coupling gains to synchronize and decay to some estimated value. Unlike the static consensus protocols, which require the knowledge of the smallest real part of the non-zero Laplacian eigenvalues to design the coupling gain, the proposed adaptive consensus protocol does not require any centralized information. It can be therefore implemented on agents in a fully distributed fashion.

Keywords: cooperative control, adaptive control, multi-agent systems.

1. INTRODUCTION

In past few decades an increasing demand for the cooperation of multiple interconnected systems initiated a great progress made in the design of distributed controllers for networked multi-agent systems. The inspiration came from the collective animal behaviour such as schooling of fish, flocking of birds, herding of quadrupeds and swarming of insect.

The designs of distributed controllers were motivated by the previously developed theoretical results in the centralized control. When the centralized controller is used for the control of a network of agents, the controller views it as a single complex system, therefore the complexity of the centralized controller increases with the complexity of the network. In most applications the centralized controller can not observe the full state information due to communication constrains between agents. Moreover, centralized controller might fail when the network topology changes, e.g. an agent or an edge is added or dropped. Therefore the distributed control approach was developed for the control of the multi-agent systems. It handles all drawbacks of the centralized approach and enjoys many advantages, such as robustness, flexibility and scalability.

The basic distributed consensus protocols for formation control in networked multi-agent systems are introduced by Fax and Murray (2004), Olfati-Saber and Murray (2004), Olfati-Saber et al. (2007) and Ren et al. (2007). Various approaches of design of distributed controllers on directed communication graphs are summarized by Zhang et al. (2012). The passivity based design of cooperative controllers is introduces by Arcak (2007). A unified viewpoint on design of consensus regulator on directed graph topologies using the synchronizing region is introduced by Li et al. (2010). The design of distributed controllers and observers using state or output-feedback in continuous and discrete-time is considered by Zhang et al. (2011), Zhang et al. (2012) and Hengster-Movric and Lewis (2013).

The static consensus protocols, e.g. by Li et al. (2010) and Zhang et al. (2011) are very popular in the community because of their well developed and simple controller design. However, because the centralized information (knowledge of the graph topology) is required by each agent by the design, they are not fully distributed.

The recently developed adaptive consensus protocols by Li et al. (2013) and Li et al. (2015) propose a solution to this problem. Since they do not rely on any centralized information, the distributed controllers of agents can be implemented independently without using any global information. Nevertheless the benefit from distributiveness suffers from the high control effort and weak robustness.

In Knotek et al. (2016) we present an adaptive consensus protocol to solve the cooperative regulator problem on undirected graphs. The protocol introduces a novel coupling gain dynamics that forces the coupling gains to synchronize and decay to some estimated value. This solves the above mentioned problems of recent adaptive consensus protocols. In this paper we expand these results to solve the cooperative regulator problem on directed strongly connected communication graphs.

This paper is structured as follows. Section 2 introduces the basic notation and graph preliminaries used throughout the paper. Section 3 states the problems that are being solved by the novel adaptive consensus protocol presented in Section 4. Numerical simulations of the introduced protocol are given in Section 5. Section 6 concludes the paper.

⋆ This work was supported by the Grant Agency of the Czech Technical University in Prague, grant No. SGS16/232/OHK3/3T/13.

2. PRELIMINARIES

In this paper the following notations and definitions are used. $\mathbb{R}^{m\times n}$ denotes the set of $m \times n$ real matrices. A matrix $M = \text{diag}(v)$ for $v \in \mathbb{R}^n$ denotes $\mathbb{R}^{n\times n}$ diagonal matrix with elements of the vector v on the diagonal. Positive (semi)-definite symmetric matrix is denoted by $M \succ (\succeq)0$.

A directed graph is given by $\mathcal{G} = (\mathcal{V}, \mathcal{E})$, where $\mathcal{V} = \{v_1, \ldots, v_N\}$ is a nonempty finite set of nodes and $\mathcal{E} \subset \mathcal{V} \times \mathcal{V}$ is a set of arcs. An arc is an ordered pair of nodes (v_j, v_i), $v_j \neq v_i$, where v_j is a child node and v_i is a parent node, i.e. the information flows from node v_i to node v_j. A directed path of length N from node v_1 to node v_N is an ordered set of distinct nodes $\{v_1, \ldots, v_N\}$ such that $(v_l, v_{l+1}) \in \mathcal{E}$ for all $l \in [1, N-1]$. A directed graph is strongly connected if there exist a directed path from every node to every other node. In the sequel, we assume the graph $\mathcal{G}$ to be directed, strongly connected and simple, i.e. there are no repeated edges or self-loops $(v_i, v_i) \notin \mathcal{E}, \forall i$.

The adjacency matrix $E = [e_{ij}] \in \mathbb{R}^{N\times N}$ associated with the graph $\mathcal{G}$ is defined by $e_{ij} > 0$ if $(v_j, v_i) \in \mathcal{E}$, otherwise $e_{ij} = 0$. Let the degree matrix $D = [d_{ij}] \in \mathbb{R}^{N\times N}$ be a diagonal matrix given by $d_{ii} = \sum_{j\neq i} e_{ij}$. Then the graph Laplacian matrix is defined by $L = D - E$. Denote $p \in \mathbb{R}^N$ the left eigenvector of L, such that $p^T L = 0$.

3. MOTIVATION

Consider a graph $\mathcal{G}$, that consists of N identical agents with general LTI dynamics

$$\dot{x}_i = Ax_i + Bu_i, \quad i = 1, \ldots, N \tag{1}$$

where $x_i \in \mathbb{R}^n$ is the state, $u_i \in \mathbb{R}^m$ is the input, and $A \in \mathbb{R}^{n\times n}$ and $B \in \mathbb{R}^{n\times m}$ are constant matrices. The matrix A is not necessarily stable but the pair of matrices (A, B) is assumed to be stabilizable.

The goal is to design a control law to solve the cooperative regulator problem in the sense of $\lim_{t\to\infty} ||x_j - x_i|| = 0$, $\forall i, j = 1, \ldots, N$ without requiring any centralized information. An adaptive control approach proposes a possible solution to this problem.

There has been several proposed distributed adaptive consensus protocols. The adaptive consensus protocol introduced in Li et al. (2013) solves the cooperative regulator problem on undirected connected graphs. The more recent adaptive consensus protocol by Li et al. (2015) solves the cooperative tracking problem on directed graphs containing a spanning tree with the leader as the root node. The distributed adaptive consensus protocols do not require any global information of a communication graph, therefore they are fully distributed. Nevertheless they introduce also several drawbacks.

Since their coupling gain dynamics contains a quadratic term the coupling gain derivative is a monotonically increasing function and the coupling gain values rise as long as there is some error in states between agents. The farther the initial conditions of the agents, the higher the final values of the coupling gains. The coupling gains might therefore reach higher values than it is needed for the network stability. The coupling gains are decoupled, therefore they end up with different final values and the network gets unbalanced, i.e. the agents react differently to the input signal.

Assuming some noise in state measurements, the coupling gains would permanently rise until they reach some physical bound. Therefore the coupling gains could be just statically set to the boundary value and the adaptive consensus protocol would not be necessary.

To solve the cooperative regulator problem on directed strongly connected graphs and address the above mentioned difficulties, we introduce a novel adaptive control protocol, that allows coupling gains to decay and synchronize.

4. ADAPTIVE CONSENSUS PROTOCOL

Let each agent implement a control input in the form

$$u_i = c_i K \sum_{j=1}^{N} e_{ij}(x_j - x_i), \quad i = 1, \ldots, N \tag{2}$$

where $c_i \geq 0$ is the time-varying coupling gain associated with an i-th agent. The i-th agent dynamics is given by

$$\dot{x}_i = Ax_i + c_i BK \sum_{j=1}^{N} e_{ij}(x_j - x_i). \tag{3}$$

Let each agent implement the coupling gain dynamics

$$\dot{c}_i = \sum_{j=1}^{N} e_{ij}(x_j - x_i)^T \Gamma (x_j - x_i) + \sum_{j=1}^{N} e_{ij}(c_j - c_i) - \ell(c_i - \kappa_i) \tag{4}$$

where $\ell > 0$ is a constant, $\kappa_i \geq 0$ is a constant estimated by the i-th agent and $\Gamma \in \mathbb{R}^{n\times n}$ is the adaptation-gain matrix.

The gain matrices K and Γ are designed by the LQR method. Let $Q \in \mathbb{R}^{n\times n}$ and $R \in \mathbb{R}^{m\times m}$ be positive definite symmetric matrices, then

$$K = R^{-1} B^T P \tag{5}$$

$$\Gamma = PBK \tag{6}$$

where the positive definite symmetric matrix $P \in \mathbb{R}^{n\times n}$ is the unique positive definite solution of the algebraic Riccati equation (ARE)

$$0 = A^T P + PA + Q - PBR^{-1}B^T P. \tag{7}$$

The introduced adaptive consensus protocol (2, 4) is motivated by Li et al. (2013) and Li et al. (2015), however there are several major differences. The coupling gains are associated with each agent as by Li et al. (2015) and not each interconnection as by Li et al. (2013), but the protocol is more similar to Li et al. (2013). This leads to qualitative changes in the network interactions.

The coupling gain dynamics (4) is not a monotonically increasing function as it was in Li et al. (2013) and Li et al. (2015). It consists of three main terms. The first term on the right-hand side $\sum_j e_{ij}(x_j - x_i)^T \Gamma (x_j - x_i)$ is the non-negative quadratic term motivated by the coupling gain dynamics from Li et al. (2013). Its purpose is to push the coupling gains to higher values until the states get synchronized. The second term on the right-hand side

$\sum_j e_{ij}(c_j - c_i)$ synchronizes the coupling gains and thereby solves the above mentioned difficulties with different and to some extent high coupling gains. The third term on the right-hand side $-\ell(c_i - \kappa_i)$ pushes the coupling gains to κ_i and by this solves the problem with generally high gains. The value of κ_i is estimated by an estimation algorithm. The decay rate ℓ determines the strength of the convergence of the coupling gain c_i to the value of κ_i.

The proper estimation of κ_i is required for the exponential stability of the network dynamic (3, 4). Not estimating κ_i and just setting it to zero would mean that the solution of the network dynamics ends up in a bounded set. This worst case behaviour guarantees that the states of agents can not get arbitrarily far apart from each other and provides time for the estimation of κ_i. The value of κ_i is estimated by an estimation algorithm from the network trajectory. This is thoroughly discussed in the next sections.

In the sequel, we derive the network dynamics (3, 4) and investigate its stability. First we define a general network dynamics (8, 9). Then step by step by modifying the general network dynamics (adding new terms to the coupling gain dynamics) we derive the introduced network dynamics (3, 4). In each step we investigate the stability of the obtained network dynamics. These results we use to conclude the stability of the network dynamics (3, 4).

4.1 General network dynamics

Assume the general network dynamics (3, 4) with $\ell = 0$

$$\dot{x}_i = Ax_i + c_i BK \sum_{j=1}^{N} e_{ij}(x_j - x_i) \tag{8}$$

$$\dot{c}_i = \sum_{j=1}^{N} e_{ij}(x_j - x_i)^T \Gamma (x_j - x_i) + \sum_{j=1}^{N} e_{ij}(c_j - c_i) \tag{9}$$

where decay term $-\ell(c_i - \kappa_i)$ that pushes the coupling gain value c_i to the value of κ_i is omitted.

Assume that the general network dynamics starts with different initial states and different initial coupling gains of all agents. Consider agents with unstable but stabilizable dynamics. If the coupling gains are small the general network dynamics might be unstable and the states of agents might diverge. The adaptive term is positive while there is some error in states of agents, therefore it pushes the coupling gains to higher values. At the same time the coupling gain synchronization term pushes the coupling gains towards each other to synchronize. When the coupling gains rise sufficiently high the general network dynamics becomes stable and the states of agents start to synchronize. When the states of agents get synchronized the adaptive term is zero. If the coupling gains are not synchronized yet the synchronization term synchronizes the coupling gains and they get steady at some common final value. Note that since the coupling gains are non-negative real numbers the coupling gain synchronization term can not push them to negative values.

Starting with agents having a stable dynamics, the general network dynamics behaves the same as in the previous case except that it is always stable because it is stable for any coupling gain values. Note that the control law just speeds up the synchronization of the states of agents. Since all agents end up in one common equilibrium the control law does not need to be implemented to reach consensus.

From the previous analysis, one expects that the states of agents synchronize and the values of the coupling gains rise and synchronize to some finite value for all initial conditions, i.e. the general network dynamics is globally asymptotically stable. This result is confirmed by the simulations.

Note that by the asymptotic stability of a network we mean the stability with respect to the collective dynamics of agents in the sense of $||x_j - x_i|| \to 0$ as $t \to \infty$, $\forall i, j$. Same holds for the exponential stability with addition, that convergence $||x_j - x_i|| \to 0$ as $t \to \infty$, $\forall i, j$ is faster than some exponential function.

The work on the proof of the global asymptotic stability of the general network dynamics (8, 9) is currently in progress therefore we introduce just an idea of the proof. Define the virtual leader $x_0 = \sum_i p_i x_i$ and the virtual tracking error $\delta_i = x_i - x_0$. Assume the coupling gain dynamics (4) with $\ell = 0$, then the network error dynamic is

$$\dot{\delta}_i = A\delta_i + c_i BK \sum_{j=1}^{N} e_{ij}(\delta_j - \delta_i) - \sum_{k=1}^{N} p_k c_k BK \sum_{j=1}^{N} e_{kj}(\delta_j - \delta_k) \tag{10}$$

$$\dot{c}_i = \sum_{j=1}^{N} e_{ij}(c_j - c_i) + \sum_{j=1}^{N} e_{ij}(\delta_j - \delta_i)^T \Gamma (\delta_j - \delta_i). \tag{11}$$

Consider a Lyapunov function candidate

$$V = \sum_{i=1}^{N} p_i \delta_i^T P \delta_i + \sum_{i=1}^{N} p_i (c_i - \alpha)^2 \tag{12}$$

where α is some positive constant. The time-derivative of the Lyapunov function candidate along the trajectory of the network error dynamics (10, 11) is

$$\dot{V} = \delta^T [P_1 \otimes (A^T P + PA) - \alpha (P_1 L + L^T P_1) \otimes \Gamma] \delta - c^T P_1 L v - \frac{1}{2} c^T (P_1 L + L^T P_1) c. \tag{13}$$

where $P_1 = \mathrm{diag}(p)$, $\delta = (\delta_1^T, \ldots, \delta_N^T)^T$ is the vector of virtual tracking errors, $c = (c_1, \ldots, c_N)^T$ is the vector of time-varying coupling gains and $v = (v_1, \ldots, v_N)^T$ is the vector of quadratic forms given by $v_i = \delta_i^T \Gamma \delta_i$. To prove that the general network dynamics (8, 9) is globally exponentially stable it has to be shown, that for every initial condition there exists α such that $\dot{V} \leq 0$.

The general network dynamics (8, 9) synchronizes the coupling gains to one common value that is lower than the final value of the largest coupling gain without using the coupling gain synchronization. This is found to solve the problems of the recent adaptive consensus protocols Li et al. (2013) and Li et al. (2015) with different and partially large gains. Nevertheless the general network dynamics inherits the problem with unbounded coupling gains. Therefore we modify the general network dynamics to allow coupling gains to decay and introduce the uniformly ultimately bounded network dynamics (14, 15).

4.2 Bounded network dynamics

Assume the coupling gain dynamics (4) with $\kappa_i = 0$, $\forall i$, then the network dynamic is given by

$$\dot{x_i} = Ax_i + c_i BK \sum_{j=1}^{N} e_{ij}(x_j - x_i) \tag{14}$$

$$\dot{c_i} = \sum_{j=1}^{N} e_{ij}(x_j - x_i)^T \Gamma (x_j - x_i) + \sum_{j=1}^{N} e_{ij}(c_j - c_i) - \ell c_i. \tag{15}$$

This network dynamics consists of the general network dynamics (8, 9) and an additional decay term $-\ell c_i$ in the coupling gain dynamics that pushes the values of the coupling gains to zero.

Consider agents with unstable but stabilizable dynamics. Assume that the network dynamics (14, 15) starts with different initial states and different initial coupling gains of all agents. Note that the network dynamics might be unstable because of small coupling gains. Then the adaptive term overpowers the decay term therefore the coupling gains start to rise. When the coupling gains rise sufficiently high the network becomes stable and the states of agents synchronize. When the states of agents get close to each other the decay term overpowers the adaptive term and the coupling gains start to decay to zero. Decreasing coupling gains slowly destabilize the network dynamics. When the coupling gains decay sufficiently low the network becomes unstable and the states of agents start to diverge. With the states far from each other the adaptive term again overpowers the decay term and the cycle repeats. Hence one expects oscillatory behaviour of the network trajectory in some set. The term that synchronizes the coupling gains apparently does not have any influence on this oscillatory behaviour. The simulations of the network dynamics (14, 15) from Section 5 confirm the boundedness of its solution.

If the agents are stable then also the network dynamics is stable. The states of agents converge to the equilibrium point and thereby synchronize, therefore the consensus protocol is not necessary. Applying the adaptive consensus protocol one expects faster convergence to consensus. Let the network dynamics start with different initial states and initial coupling gains of agents. The coupling gains start to rise because the adaptive term overpowers the decay term. The states of agents are pushed towards each other to synchronize by the adaptive consensus protocol. When the states of agents get close to each other the decay term overpowers the adaptive term and the coupling gains start to decay to zero. At the same time the states of agents synchronize and the coupling gains tend to zero therefore the states end up synchronized in the equilibrium point and the coupling gains end up being zero.

The work on the proof of the boundedness of the solution of the network dynamics (14, 15) is currently in progress therefore we introduce just the possible sketch of the proof. Define the coupling gain transformation $z_i = c_i - \beta$, where β is some positive constant. Then the network error dynamics (14, 15) in the new coordinates (δ_i, z_i) is

$$\dot{\delta_i} = A\delta_i + z_i BK \sum_{j=1}^{N} e_{ij}(\delta_j - \delta_i) + \beta BK \sum_{j=1}^{N} e_{ij}(\delta_j - \delta_i)$$

$$- \sum_{k=1}^{N} p_k z_k BK \sum_{j=1}^{N} e_{kj}(\delta_j - \delta_k) \tag{16}$$

$$\dot{z_i} = \sum_{j=1}^{N} e_{ij}(\delta_j - \delta_i)^T \Gamma (\delta_j - \delta_i) + \sum_{j=1}^{N} e_{ij}(z_j - z_i) - \ell z_i - \ell\beta. \tag{17}$$

This network dynamics consists of some nominal dynamics and the non-vanishing perturbation term $-\ell\beta$, therefore consider it as the perturbed nominal dynamics. First it has to be shown, that the nominal dynamics is globally exponentially stable and the Lyapunov function and its time derivative are bounded. Then, since the non-vanishing perturbation term is bounded, following (Khalil, 1996, Lem. 5.2) it can be shown, that the perturbed nominal dynamics (16, 17) is uniformly ultimately bounded.

The boundedness of the network dynamics (3, 4) is an important property. It says that for $\kappa_i = 0$, $\forall i$, the solution of the network dynamics is uniformly ultimately bounded, i.e. in the worst case the solution ends up being bounded.

Having uniform ultimate boundedness is necessary, but not sufficient for a practical implementation of the protocol. For that reason we introduce the full form of the proposed coupling gain dynamics (4). In comparison to the coupling gain dynamics (15) it contains an additional term $\ell\kappa_i$, that can cancel effects of the non-vanishing perturbation term $-\ell\beta$ from (17).

Consider the coupling gain dynamics (4), then the network error dynamics reads

$$\dot{\delta_i} = A\delta_i + z_i BK \sum_{j=1}^{N} e_{ij}(\delta_j - \delta_i) + \beta BK \sum_{j=1}^{N} e_{ij}(\delta_j - \delta_i) \tag{18}$$

$$\dot{z_i} = -\ell z_i + \ell\kappa_i - \ell\beta + \sum_{j=1}^{N} e_{ij}(z_j - z_i) + \sum_{j=1}^{N} e_{ij}(\delta_j - \delta_i)^T \Gamma (\delta_j - \delta_i). \tag{19}$$

Increasing the κ_i, effects of non-vanishing perturbation term are continuously reduced until the condition $\kappa_i = \beta$, $\forall i$ is met. If $\kappa_i \geq \beta$, $\forall i$ the non-vanishing perturbation term is cancelled, the dynamics reduces to the case of nominal dynamics and it gets globally exponentially stable.

4.3 Estimation of κ_i

Now we have to properly estimate the value of κ_i to reach global exponential stability of the network dynamics (3, 4). We require sufficiently high value of κ_i to guarantee global exponential stability but at the same time we want the value as low as possible to minimize the control effort.

To estimate the value of κ_i we propose an algorithm based on the interval halving method. The idea is to increase the value of κ_i as long as the trajectory of the network dynamics oscillates, i.e. it is uniformly ultimately bounded. When the network trajectory oscillates the non-vanishing perturbation term is present in the dynamics. To cancel this term the value of κ_i has to rise until the non-vanishing

perturbation term is cancelled and the network dynamics gets globally exponentially stable. The oscillating trajectory implies oscillating coupling gain, therefore the coupling gain c_i is sampled by some sampling frequency f_s and recorded in some time window Δt. The highest and the lowest recorded values are averaged and this average is then used as a new κ_i. This process is repeated all the time. The coupling gain c_i and the trajectory of the network dynamics stop to oscillate when the network dynamics becomes globally exponentially stable. Then also the κ_i reaches the steady state value.

Note that the sampling frequency f_s has to be chosen according to the Nyquist-Shannon sampling theorem. The sampling rate must exceed $2f_{max}$ and the time window $\triangle t$ must be greater than $1/f_{min}$, where f_{max} and f_{min} are the highest and the lowest frequency in the system. The decay-rate and the size of the non-vanishing perturbation are determined by the positive constant ℓ. The decay term can be interpreted as a filtration term therefore the constant ℓ influences also the frequency and the amplitude of oscillations of the coupling gain c_i.

To handle the noise acting on state measurements the value of κ_i is updated only if the difference between the maximal and minimal recorded coupling gain values is greater than some predefined dead-zone. Note that the dead-zone influences just the estimation of κ_i therefore it does not harm the stability of the network. The solution of the network dynamics is uniformly ultimately bounded and with a properly chosen dead-zone corresponding to the measured noise it remains uniformly ultimately bounded however it approaches the exponential stability as close as the dead-zone, and thus the noise, allow.

The simulations verify the theoretical results on the proposed adaptive consensus protocol with the interval-halving estimation algorithm.

5. SIMULATIONS

This section shows the simulations of the proposed adaptive consensus protocol (2, 4) with agents described by linear double integrator dynamics

$$\dot{x_i} = \begin{bmatrix} 0 & 1 \\ 0 & 0 \end{bmatrix} x_i + \begin{bmatrix} 0 \\ 1 \end{bmatrix} u_i, \quad x_i = \begin{bmatrix} x_{i_1} \\ x_{i_2} \end{bmatrix}, \quad \forall i. \qquad (20)$$

The interval-halving algorithm for the estimation of κ_i is configured to the time window $\triangle t = 5s$ and the sampling frequency $f_s = 10$Hz. The initial value of κ_i, $\forall i$ is set to zero. Initial conditions of the agents are

$$x_{i_1}(0) \in \langle -10, 10 \rangle, \quad x_{i_2}(0) = 0, \quad c_i(0) = 0, \quad \forall i. \quad (21)$$

The uniform ultimate boundedness of the solution of the network dynamics (3, 4) for $\kappa_i = 0$, $\forall i$ is shown by simulations in Figure 1. The algorithm for estimation of κ_i was not used and κ_i was just statically set to zero. The simulation on a circular communication graph consisting of 50 agents is situated on the top of the figure and the simulation on a communication graph consisting of two interconnected circles each with 25 agents is situated on the bottom. The topology of the communication graph with two interconnected circles is shown in Figure 4.

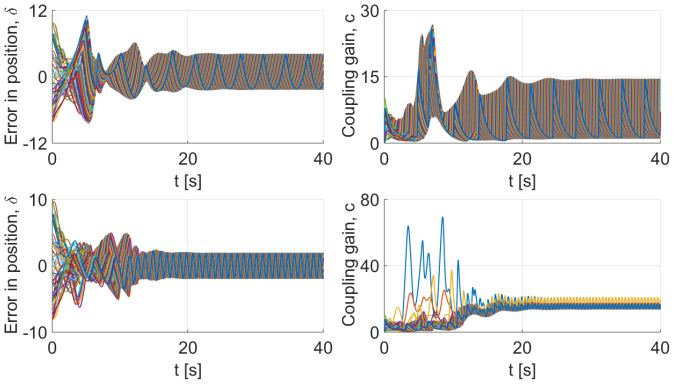

Fig. 1. Simulations of the proposed protocol without estimation of κ_i, for $\kappa_i = 0$, $\forall i$. The simulation of 50 agents on a circular topology is shown on the top and the simulation of two interconnected circles each with 25 agents is shown on the bottom.

In following simulations the final coupling gain value is compared to the minimal coupling gain value required by the static consensus protocol. The static consensus protocol implements the input in the form of (2), but instead of c_i it uses just one coupling gain c for all agents. To guarantee stability by the static consensus protocol the coupling gain value has to satisfy

$$c \geq \frac{1}{2 \min \Re(\lambda_i)} \qquad (22)$$

where $\min \Re(\lambda_i)$ is the smallest non-zero real part of the eigenvalues of the Laplacian matrix L.

Simulations of the proposed protocol with the interval-halving estimation algorithm for the estimation of κ_i are shown in Figure 2. The simulation on a circular graph consisting of 50 agents is situated on the top of the figure. In the first few seconds of the simulation the response is uniformly ultimately bounded because of the low coupling gain values. As the coupling gain values rise the network reaches cooperative stability and states synchronize. The coupling gains reach steady state value 61.2 while the calculated lower bound on the coupling gain required by static consensus protocols is 63.4. The simulation on a graph consisting of two interconnected circles each with 25 agents is situated on the bottom of the figure. The topology of the communication graph is shown in Figure 4. The steady state value of the coupling gains reach 15.4 while the calculated lower bound on the coupling gain for the static consensus protocol is 16.

Figure 3 shows the simulations of the proposed protocol with and without noise acting on the state measurements. The simulations have been done on the circular graph consisting of 10 agents. The steady state value of the coupling gains is 3.2 without noise and 5.5 for the case with noise, respectively. The static consensus protocol require the coupling gain value to be greater than 2.6. Since the coupling gain values end in a bounded set and they do not permanently rise as they do in Li et al. (2013) and Li et al. (2015), the proposed protocol with the interval-halving estimation algorithm is found robust to the noise acting on states.

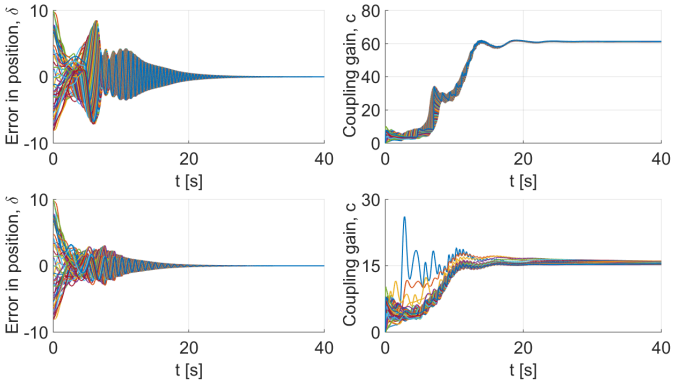

Fig. 2. Simulations of the proposed protocol on a circular graph consisting of 50 agents on the top and on a graph consisting of two interconnected circles each with 25 agents on the bottom, respectively.

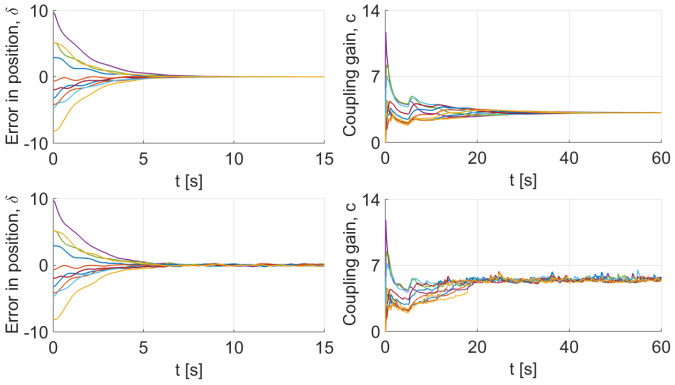

Fig. 3. Comparison of the protocol simulated on a circular topology consisting of 10 agents on the top without and on the bottom with the noise acting on states.

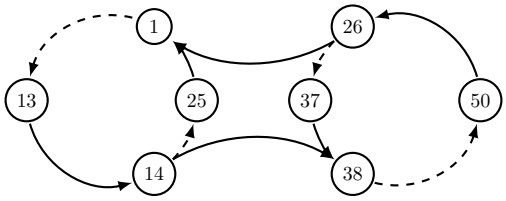

Fig. 4. The communication graph of two interconnected circles each with 25 agents.

6. CONCLUSION

We presented a novel distributed adaptive consensus protocol, that solves the cooperative regulator problem on directed, strongly connected communication graphs. The protocol introduces a novel coupling gain dynamics, that forces the coupling gains to synchronize and converge to some estimated value. This solves the problems of recent adaptive consensus protocols with high gains and consequently large control effort. The value to which the coupling gains converge is estimated by the estimation algorithm based on the interval-having method.

The simulations of the proposed adaptive consensus protocol verify the theoretical results. Due to decay term, the coupling gains in some situations attain lower values than conventional algorithms. The protocol is found robust to the noise in state measurements unlike the recent adaptive protocols whose gains would permanently rise.

The work on the proofs of the global asymptotic stability of the general network dynamics (8, 9) and the uniform ultimate boundedness and the global exponential stability of the network dynamics (14, 15) for different κ_i is still ongoing. The investigation of relation between the decay rate ℓ and the parameters (time window Δt and sampling frequency f_s) is the task of the future research.

REFERENCES

Arcak, M. (2007). Passivity as a design tool for group coordination. *IEEE Transactions on Automatic Control*, 52(8), 1380–1390. doi:10.1109/TAC.2007.902733.

Fax, J. and Murray, R. (2004). Information Flow and Cooperative Control of Vehicle Formations. *IEEE Transactions on Automatic Control*, 49(9), 1465–1476.

Hengster-Movric, K. and Lewis, F. (2013). Cooperative observers and regulators for discrete-time multiagent systems. *International Journal of Robust and Nonlinear Control*, 23(14), 1545–1562. doi:10.1002/rnc.2840.

Khalil, H.K. (1996). *Nonlinear Systems*. Prentice-Hall, Upper Saddle River, NJ, 2nd edition.

Knotek, S., Hengster-movric, K., and Sebek, M. (2016). Distributed adaptive consensus protocol with decaying gains. URL `http://aa4cc.dce.fel.cvut.cz/members-publications/49`.

Li, Z., Duan, Z., Chen, G., and Huang, L. (2010). Consensus of Multiagent Systems and Synchronization of Complex Networks: A Unified Viewpoint. *IEEE Transactions on Circuits and Systems I: Regular Papers*, 57(1), 213–224.

Li, Z., Ren, W., Liu, X., and Fu, M. (2013). Consensus of Multi-Agent Systems With General Linear and Lipschitz Nonlinear Dynamics Using Distributed Adaptive Protocols. *IEEE Transactions on Automatic Control*, 58(7), 1786–1791.

Li, Z., Wen, G., Duan, Z., and Ren, W. (2015). Designing fully distributed consensus protocols for linear multi-agent systems with directed graphs. *IEEE Transactions on Automatic Control*, 60(4), 1152–1157.

Olfati-Saber, R., Fax, J.A., and Murray, R.M. (2007). Consensus and Cooperation in Networked Multi-Agent Systems. *Proceedings of the IEEE*, 95(1), 215–233.

Olfati-Saber, R. and Murray, R.M. (2004). Consensus problems in networks of agents with switching topology and time-delays. *IEEE Transactions on Automatic Control*, 49(9), 1520–1533.

Ren, W., Beard, R.W., and Atkins, E.M. (2007). Information Consensus in Multivehicle Cooperative Control. *IEEE Control Systems Magazine*, 27(2), 71–82.

Zhang, H., Lewis, F.L., and Das, A. (2011). Optimal Design for Synchronization of Cooperative Systems: State Feedback, Observer and Output Feedback. *IEEE Transactions on Automatic Control*, 56(8), 1948–1952.

Zhang, H., Lewis, F.L., and Qu, Z. (2012). Lyapunov, Adaptive, and Optimal Design Techniques for Cooperative Systems on Directed Communication Graphs. *IEEE Transactions on Industrial Electronics*, 59(7), 3026–3041.

Distributed adaptive consensus protocol with eigenvalue estimation

Štefan Knotek, Kristian Hengster-Movric and Michael Šebek

Abstract— **This paper addresses distributed consensus problem for multi-agent systems with general linear time-invariant dynamics and undirected connected communication graphs. A distributed adaptive consensus protocol is found to solve problems of existing adaptive consensus protocols related to different, generally large and possibly unbounded coupling gains. This protocol guaranties ultimate boundedness under all conditions, however for an asymptotic stability, a proper estimation of reference values for coupling gains is required. In this work, we propose an algorithm for the estimation of the coupling gain reference. The algorithm is based on a distributed estimation of the Laplacian eigenvalues. In comparison to the previously proposed algorithm based on the interval halving method, this algorithm offers robustness to change of the network topology. In addition, it decouples the estimation from the consensus protocol, hence it does not influence stability properties of the adaptive consensus protocol.**

I. INTRODUCTION

In last two decades, a great effort has been made in distributed control and estimation in formations of mobile robots, satellites and vehicles. The inspiration came from the natural behaviour of swarms, flocks and schools. Connecting the graph theory, describing the topological structure of a network, and control theory, the basic consensus protocols for formation control in networked multi-agent systems are introduced in [1], [2], [3] and [4].

Previously developed theoretical results in control of single-agent system motivated the designs of recent distributed controllers and observers. For example the passivity-based design of cooperative controllers for cooperation and synchronization of multi-agent systems is described in [5]. A unified viewpoint on design of consensus regulator on directed graph topologies using the synchronizing region is introduced in [6]. The design of cooperative regulators and observers using state or output-feedback in continous and discrete-time is considered in [7], [8] and [9].

The static consensus protocols presented in [6], [7] and [8] use a feedback coupling gain that satisfies a bound calculated from the smallest non-zero real part of Laplacian eigenvalues. The graph structure has to be known to calculate this bound. Therefore centralized information is required by each agent.

Distributed adaptive consensus protocols propose a solution to this problem on undirected connected graphs [10] as well as on directed graphs having a spanning tree with leader as a root node [11]. These protocols do not rely on any centralized information, therefore they can be implemented by each agent separately without using any global information. The protocols guarantee cooperative stability, however the benefits from adaptability suffer from possibly large control effort and lack of robustness to noise.

To avoid these drawback, a novel distributed adaptive consensus protocol is developed. Firstly, it was designed to solve the cooperative regulator problem on undirected connected communication graphs [12]. This work was later extended to directed graphs having a spanning tree [13]. The protocol is fully distributed, therefore it does not require any centralized information. The lack of centralized information is compensated by its estimation. The protocol runs an algorithm for estimation of reference values for coupling gains. If the reference values are estimated properly, the network of agents is asymptotically stable. On the other hand the solution of the network dynamics is ultimately bounded.

In this paper, we introduce an algorithm for proper estimation of coupling gains' references. The algorithm is based on distributed estimation of Laplacian eigenvalues presented in [14] and [15]. Each agent implements this algorithm and estimates the smallest non-zero eigenvalue of the Laplacian matrix. This values is then used to calculate the coupling gain required for the asymptotic stability of the network. The algorithm offers better robustness to change of the network topology than the previously introduced estimation algorithm based on the interval halving method. Moreover, it decouples the estimation of coupling gains' references from the adaptive consensus protocol, thereby maintains the stability property of the adaptive consensus protocol.

This paper is organized as follows. Section II introduces the basic notation and graph preliminaries used throughout the paper. Section III introduces the problems addressed by the adaptive consensus protocol with the novel estimation algorithm. The adaptive consensus protocol is presented in Section IV. Section V introduces the novel algorithm estimating the eigenvalues of Laplacian matrix. Numerical simulation are given in Section. VI. Section VII concludes the paper.

II. PRELIMINARIES

Through this paper the following notations and definitions are used. $\mathbb{R}^{m\times n}$ denotes the set of $m \times n$ real matrices. Denote $\mathbf{1}_N$ as a column vector with N entries, all equal to one. A vector $v = 0$ has all entries equal to zero. A matrix $M = \mathrm{diag}(v)$ for $v \in \mathbb{R}^n$ denotes $\mathbb{R}^{n\times n}$ diagonal matrix with elements of v on the diagonal. The smallest and the largest eigenvalue of a matrix M are denoted by $\sigma_{\min}(M)$ and $\sigma_{\max}(M)$, respectively. Positive (semi)-definite symmetric matrix is denoted by $M \succ (\succeq)0$. The sum over all agents

All authors are with the Faculty of Electrical Engineering, Czech Technical University in Prague. e-mail: stefan.knotek@fel.cvut.cz

This work was supported by the Grant Agency of the Czech Technical University in Prague, grant No. SGS16/232/OHK3/3T/13.

is denoted by $\sum_i$ for $i = 1, \ldots, N$ when it is not stated directly.

An undirected graph is given by $\mathcal{G} = (\mathcal{V}, \mathcal{E})$, where $\mathcal{V} = \{v_1, \ldots, v_N\}$ is a non-empty finite set of vertices and $\mathcal{E} \subset \mathcal{V} \times \mathcal{V}$ is a set of edges. An edge is a pair of nodes (v_i, v_j), $v_i \neq v_j$, representing that agents i and j can exchange information between them. In sequel, the graph $\mathcal{G}$ is assumed to be undirected, connected and simple.

The adjacency matrix $E = [e_{ij}] \in \mathbb{R}^{N \times N}$ associated with the graph $\mathcal{G}$ is defined by $e_{ij} = e_{ji} > 0$ if $(v_i, v_j) \in \mathcal{E}$, otherwise $e_{ij} = e_{ji} = 0$. Define the vector of node degrees as $d = E\mathbf{1}_N$, and the degree matrix as $D = \text{diag}(d)$. Then the graph Laplacian is defined by $L = D - E$.

III. PROBLEM STATEMENT AND MOTIVATION

Consider a group of N identical agents. Each agent is described by a general LTI dynamics

$$\dot{x}_i = Ax_i + Bu_i, \quad i = 1, \ldots, N, \tag{1}$$

where $x_i \in \mathbb{R}^n$ is the agents state, $u_i \in \mathbb{R}^m$ is the agents input, and $A \in \mathbb{R}^{n \times n}$ and $B \in \mathbb{R}^{n \times m}$ are constant matrices. The matrix A does not need to be stable but the pair of matrices (A, B) is assumed stabilizable. The communication topology of the network of agents is given by an undirected graph $\mathcal{G}$, that is assumed connected.

Our goal is to synchronize the states of agents in the sense of $\lim_{t \to \infty} ||x_j - x_i|| = 0, \forall i, j$ without requiring any centralized information. There has been developed many adaptive consensus protocols that can reach this goal. However, all these adaptive consensus protocols suffer from several drawbacks. They are:

- different final coupling gain values,
- higher final coupling gain values,
- week robustness to noise.

Our recent work [12], [13] present a novel adaptive consensus protocol that avoids these drawback and solves the cooperative regulator problem on undirected conected communication graphs [12], later extended to directed strongly connected communication graphs [13].

In this paper, we are going to extend the results on undirected connected graphs [12] by proposing a new method for estimation of coupling gain values.

IV. DISTRIBUTED ADAPTIVE CONSENSUS PROTOCOL

Let each agent implements an adaptive control law [12], [13] given by a control input and a coupling gain dynamics

$$u_i = c_i K \sum_j e_{ij}(x_j - x_i), \quad i = 1, \ldots, N, \tag{2}$$

$$\dot{c}_i = \sum_j e_{ij}(x_j - x_i)^T \Gamma (x_j - x_i) + \sum_j e_{ij}(c_j - c_i) - \ell(c_i - \kappa_i), \tag{3}$$

where $\ell > 0$ is a constant, $c_i > 0$ is the coupling gain associated with the i-th agent and $\kappa_i \geq 0$ is a coupling gain reference estimated by the i-th agent.

The gain matrices K and Γ are designed by LQR method. Let $Q = Q^T \in \mathbb{R}^{n \times n}$ and $R = R^T \in \mathbb{R}^{m \times m}$ be positive definite symmetric matrices, then

$$K = R^{-1} B^T P, \tag{4}$$

$$\Gamma = \Gamma^T = PBK = PBR^{-1}B^T P, \tag{5}$$

where matrix $P \succ 0$ is the unique solution of the algebraic Riccati equation

$$A^T P + PA - PBR^{-1}B^T P = -Q. \tag{6}$$

The task of the coupling gain dynamics (3) is to adapt the coupling gains c_i. It consists of three main terms. The first term on the right hand side pushes the coupling gains to higher values until the states of agents get synchronized. The second term on the right hand side synchronizes the coupling gains. The third term on the right hand side pushes the coupling gain c_I to its reference κ_i. The value of the reference κ_i is estimated by an estimation algorithm. The strength of the third term is determined by the positive constant ℓ.

The estimation algorithm determines the stability of the network of agents implementing the adaptive control law (2, 3). Each agent runs this algorithm to estimate its own coupling gain reference κ_i. Since the coupling gain c_i is pushed to its reference κ_i by the coupling gain dynamics (3), each agent estimates its own coupling gain. For small values of κ_i below some bound $\kappa_i < \beta$ the network dynamics is ultimately bounded and the agent's trajectories oscillate. For large values of κ_i bigger than this bound $\kappa_i \geq \beta$, the network dynamics is asymptotically stable and the agents reach consensus. Note that the ultimate boundedness is the worst case scenario that guaranties stability albeit bounded. This property provides sufficient time for the estimation of κ_i.

With increasing κ_i increases also c_i and thereby the control effort. Hence, the aim of the estimation algorithm is to estimate proper κ_i, that is sufficiently high to reach asymptotic stability of the network but at the same time as low as possible to minimize the control effort.

In the next section we present an estimation algorithm for estimation of κ_i. We discuss its benefits and drawback, and provide a comparison with previously proposed algorithm.

V. EIGENVALUE ESTIMATION ALGORITHM

The main contribution of this paper is an estimation algorithm for estimation of the coupling gain reference κ_i. The algorithm is based on the estimation of Laplacian eigenvalues proposed in [14], [15]. Each agent estimates the Laplacian eigenvalues by performing an algorithm with the following updating rule

$$\begin{aligned} \dot{p}_i(t) &= \sum_{j \in \mathcal{N}_i(t)} q_i(t) - q_j(t), \\ \dot{q}_i(t) &= \sum_{j \in \mathcal{N}_i(t)} p_i(t) + p_j(t), \end{aligned} \tag{7}$$

where $p_i, q_i \in \mathbb{R}$ are artificial states of i-th agent.

The network implementing the updating rule can be described by a time-varying autonomous linear system

$$\begin{bmatrix} \dot{p}(t) \\ \dot{q}(t) \end{bmatrix} = \mathcal{A}(t) \begin{bmatrix} p(t) \\ q(t) \end{bmatrix}, \tag{8}$$

where

$$\mathcal{A}(t) = \begin{bmatrix} \mathbf{0}_N & -L(t) \\ L(t) & \mathbf{0}_N \end{bmatrix}, \tag{9}$$

and $\mathbf{0}_N \in \mathbb{R}^{N \times N}$ is the matrix of zeros.

Since $\mathcal{A}$ is a skew symmetric matrix, all its eigenvalues are on the imaginary axis. Moreover, the eigenvalues of $\mathcal{A}$ can be derived from the eigenvalues of the Laplacian matrix L.

Lemma 1 ([14], Thm. 1)**.** *Consider an undirected graphs $\mathcal{G}$ given by a Laplacian matrix L. Let $\mathcal{A}$ be given as in (9). Then for every eigenvalue of Laplacian matrix L there is a complex pair of eigenvalues of matrix $\mathcal{A}$*

$$\lambda_{\mathcal{A}}, \bar{\lambda}_{\mathcal{A}} = \pm\lambda_L. \tag{10}$$

From Lemma 1 follows, that each state p_i and q_i follow an oscillating trajectory, that is a linear combinations of sinusoid oscillating at frequencies given by the Laplacian eigenvalues. Note, that by change of the network topology the trajectories remain continuous only the phase and the module of the signal change. Using a Fast Fourier Transformation (FFT), each agent can independently estimate the eigenvalues of the Laplacian matrix. The smallest non-zero estimated eigenvalues is then used to calculate the new κ_i. The formula for calculation of κ_i was adopted from the stability condition of a static consensus protocol.

Consider a control law with the control input (2) and one static common coupling gain c, i.e. the coupling gain dynamic (3) is neglected and the coupling gains c_i are replaced by only one static coupling gain c. A static consensus protocol presented in [7] and [8] is obtained. Following from [7, Thm. 1], a static consensus protocol is globally asymptotically stable if

$$c \geq \frac{1}{2\lambda_{\min>0}(L)}. \tag{11}$$

One could expect, that having one coupling gain separately for each agents does not change the conclusion on stability. If each c_i satisfy (11), then the network of agents should be asymptotically stable. The estimation algorithm uses this conclusion to determine the new value of κ_i as

$$\kappa_i = \frac{1}{2\lambda_{\min>0}(L)}. \tag{12}$$

If the agents correctly estimate the smallest non-zero eigenvalue of the Laplacian matrix the network of agents should be globally asymptotically stable. Note, that this eigenvalue might be unobservable for some agents or some agents might catch some other bigger eigenvalue instead of the smallest non-zero one. It this case the adaptive control protocol (2, 3) still guarantees ultimate boundedness of the solution. The network of agents will be stable but the agents' trajectories might oscillate.

To estimate κ_i, each agent performs the estimation algorithm consisting of following steps:

1) At the beginning $t = 0$ generate the initial conditions $p_i, q_i \in \{-1, 1\}$.
2) Perform the state updating rule (7).
3) In a time window $\triangle t$ estimate the frequencies of sinusoids of its artificial state p_i or q_i. The values of the estimated frequencies correspond to the eigenvalues of the Laplacian matrix.
4) Use the smallest non-zero estimated eigenvalue to calculate the new κ_i from (11).

Previously proposed estimation algorithm based on the interval halving method represents a low-pass filter that can handle only fast disturbances in the network. Change of the network topology, like for instance adding an agent, generates an abrupt changes in the local neighbourhood errors, what results in increase of the values of κ_i and thereby also c_i. This estimation algorithm is therefore not robust to change of the network topology.

Moreover, the interconnection of the estimation algorithm and the adaptive consensus protocol creates an additional artificial feedback in network dynamics. This interconnection appears to be stable, however to prove analytical stability is not an easy task. The approach we propose in this paper decouples the control and estimation dynamics. Hence the adaptive consensus protocol and the Laplacian eigenvalue estimator can be designed separately and their interconnection does not create any artificial feedback in the network.

VI. SIMULATION RESULTS

The adaptive control protocol (2, 3) has been simulated on a graph $\mathcal{G}$ consisting of agents described by linear double integrator dynamics

$$\dot{x_i} = \begin{bmatrix} 0 & 1 \\ 0 & 0 \end{bmatrix} x_i + \begin{bmatrix} 0 \\ 1 \end{bmatrix} u_i, \quad x_i = \begin{bmatrix} x_{i_1} \\ x_{i_2} \end{bmatrix}, \quad \forall i. \tag{13}$$

For comparison, both estimation algorithm are implemented to estimate κ_i. The interval-halving estimation algorithm uses the time window $\triangle t_1 = 5s$ and the sampling frequency $f_{s1} = 10$Hz. The eigenvalue estimation algorithm uses the sampling frequency $f_{s2} = 1$Hz. The positive constant ℓ was set to 1 in both cases. Initial conditions of the agents are

$$x_{i_1}(0) \in \langle -10, 10 \rangle, \quad x_{i_2}(0) = 0, \quad c_i(0) = 0, \quad \forall i. \tag{14}$$

The simulations of the control protocol (2, 3) with the previously proposed interval-halving estimation algorithm and with the current eigenvalue estimation algorithm κ_i are situated on the top and bottom of the figures, respectively.

The simulations on the circular graph consisting of 50 agents are shown in Figure 1. The proposed protocol implemented with the interval-halving estimation algorithm reaches lower coupling gains with preserving stability. The distributed eigenvalue estimation algorithm estimates the eigenvalues in the first 100 seconds. During this period $\kappa_i = 0$, $\forall i$. The smallest estimated non-zero eigenvalues is then used for calculation of κ_i. After 100 second the consensus is reached. The higher oscillating coupling gains

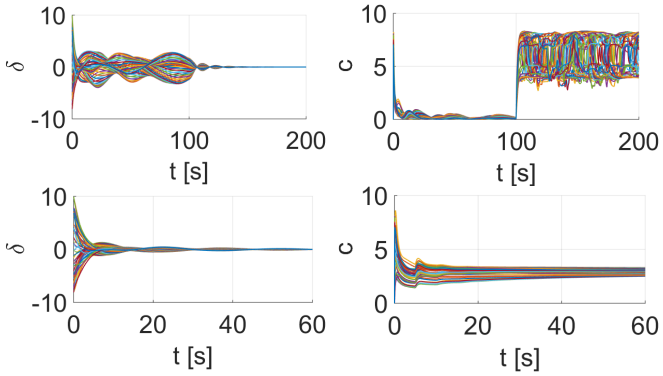

Fig. 1: Simulation of 50 agents on a circular topology.

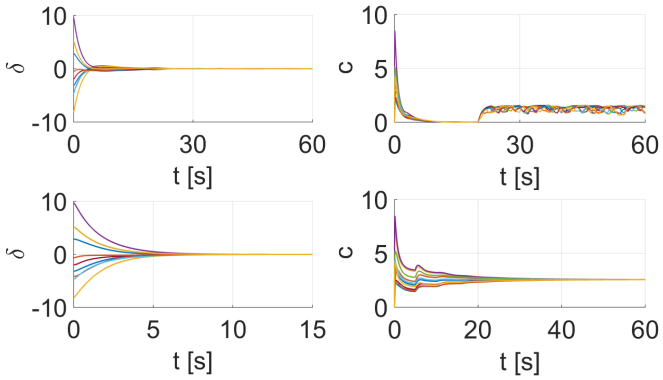

Fig. 2: Simulation of 10 agents on a circular topology assuming noise in state measurements.

come from the poor accuracy in the eigenvalue estimation. To increase accuracy longer estimation time period is required.

Assuming small noise acting on states, the responses of 10 agents in circular topology are shown in Figure 2. The distributed eigenvalue-estimation approach uses estimation period of 20 seconds. From the figure it follows that the proposed protocol implemented with both approaches is robust to noise acting on states.

Figure 3 shows the response to the change in the network topology. At the time instance of 30 seconds the graph topology was switched from the circular graph of 4 synchronized agents to the path graph and 5-th agent was connected to the end of path. The distance of 5-th agent from the rest of the network was chosen to be 10. The protocol implemented with interval-halving estimation algorithm detected slight increase of the coupling gains. This happened because of the abrupt change in the network triggered by insertion of an agent. The eigenvalue estimation algorithm adapted to the change in the network by estimated the new smallest non-zero Laplacian eigenvalue. Therefore, it was found robust to change in the network topology.

VII. CONCLUSION

In this paper we extend the results on distributed adaptive consensus protocol [12] by proposing a novel algorithm for estimation of the reference value κ_i for the coupling gain c_i. The coupling gains' references are then used by the

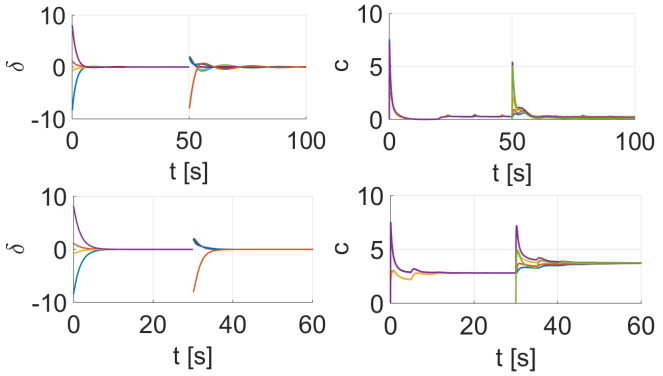

Fig. 3: Simulation of 5 agents by change in a graph topology.

adaptive consensus protocol to reach asymptotic stability of the network.

The estimation algorithm is based on the distributed estimation of Laplacian eigenvalues presented in [14], [15]. It contains a local updating rule to generate a signal oscillating at frequencies corresponding to eigenvalues of the Laplacian matrix. The FFT is then applied at this oscillating signal to obtain the estimates of Laplacian eigenvalues. The smallest non-zero estimated eigenvalue is then used to calculate the coupling gain reference κ_i.

An advantage of this estimation algorithm is, that it can adjust the coupling gains to the network topology. This allows the adaptive consensus protocol to be used on switching networks. Additionally, the algorithm decouples the estimation of the coupling gains' references from the control law, thus it does not influence the conclusions on the stability of the adaptive consensus protocol.

REFERENCES

[1] J. Fax and R. Murray, "Information Flow and Cooperative Control of Vehicle Formations," *IEEE Transactions on Automatic Control*, vol. 49, no. 9, pp. 1465–1476, 2004.

[2] R. Olfati-Saber and R. M. Murray, "Consensus problems in networks of agents with switching topology and time-delays," *IEEE Transactions on Automatic Control*, vol. 49, no. 9, pp. 1520–1533, 2004.

[3] R. Olfati-Saber, J. A. Fax, and R. M. Murray, "Consensus and Cooperation in Networked Multi-Agent Systems," *Proceedings of the IEEE*, vol. 95, no. 1, pp. 215–233, 2007.

[4] W. Ren, R. W. Beard, and E. M. Atkins, "Information Consensus in Multivehicle Cooperative Control," *IEEE Control Systems Magazine*, vol. 27, no. 2, pp. 71–82, 2007.

[5] N. Chopra and M. W. Spong, "Passivity-Based Control of Multi-Agent Systems," *Advances in Robot Control, from everyday physicsto human-like movements*, pp. 107–134, 2006.

[6] Z. Li, Z. Duan, G. Chen, and L. Huang, "Consensus of Multiagent Systems and Synchronization of Complex Networks: A Unified Viewpoint," *IEEE Transactions on Circuits and Systems I: Regular Papers*, vol. 57, no. 1, pp. 213–224, 2010.

[7] H. Zhang, F. L. Lewis, and A. Das, "Optimal Design for Synchronization of Cooperative Systems: State Feedback, Observer and Output Feedback," *IEEE Transactions on Automatic Control*, vol. 56, no. 8, pp. 1948–1952, 2011.

[8] H. Zhang, F. L. Lewis, and Z. Qu, "Lyapunov, Adaptive, and Optimal Design Techniques for Cooperative Systems on Directed Communication Graphs," *IEEE Transactions on Industrial Electronics*, vol. 59, no. 7, pp. 3026–3041, 2012.

[9] K. Hengster-Movric and F. Lewis, "Cooperative observers and regulators for discrete-time multiagent systems," *International Journal of Robust and Nonlinear Control*, vol. 23, no. 14, pp. 1545–1562, 2013.

[10] Z. Li, W. Ren, X. Liu, and M. Fu, "Consensus of Multi-Agent Systems With General Linear and Lipschitz Nonlinear Dynamics Using Distributed Adaptive Protocols," *IEEE Transactions on Automatic Control*, vol. 58, no. 7, pp. 1786–1791, 2013.
[11] Z. Li, G. Wen, Z. Duan, and W. Ren, "Designing fully distributed consensus protocols for linear multi-agent systems with directed graphs," *IEEE Transactions on Automatic Control*, vol. 60, no. 4, pp. 1152–1157, 2015.
[12] S. Knotek, "Fully distributed adaptive consensus protocol with bounded gains," in *Proceedings of the International Student Conference on Electrical Engineering*, 2016.
[13] S. Knotek, K. Hengster-movric, and M. Sebek, "Distributed adaptive consensus protocol with decaying gains on directed graphs," in *Proceedings of the IFAC Workshop on Distributed Estimation and Control in Networked Systems*, 2016.
[14] M. Franceschelli, A. Gasparri, A. Giua, and C. Seatzu, "Decentralized laplacian eigenvalues estimation for networked multi-agent systems," *Proceedings of the IEEE Conference on Decision and Control*, pp. 2717–2722, 2009.
[15] ——, "Decentralized estimation of Laplacian eigenvalues in multi-agent systems," *Automatica*, vol. 49, no. 4, pp. 1031–1036, 2013.

9. KRISTIAN HENGSTER MOVRIC, PhD, 16.2.1986

Kristian Hengster Movrić, PhD. hengskri@fel.cvut.cz

Born in Zagreb, Croatia, 16.2. 1986; address, Taborska 32, Praha 4 Nusle, CZ

H-index: **5** (WoS, Scopus)

Degrees

- **University of Texas at Arlington (UTA), Texas, US (August 2009 – August 2013)**

Degree: **Ph.D**. in Electrical Engineering

Ph.D. Dissertation: "*Cooperative Control of Multi-agent Systems; Stability, Optimality and Robustness*".

- **University of Zagreb, (FER UniZg) Croatia (October 2004 - July 2009)**

Degree: **M.S.** in Electrical Engineering (**dipl. ing.**)

M.S. Thesis: "*Formation Control of Moving Objects Based on Bell-shaped Field Functions*".

Research - projects and posts held

- **University of Zagreb, Croatia, College of Electrical Engineering and Computing**

  Student (dipl.ing) (October 2004-July 2009)

  - Worked primarily on automation and control of formations, potential field control
  - Collaborated on topics involving financial market modelling

- **University of Texas at Arlington Research Institute (UTARI) and EE Dept, UTA, Arlington, Texas**

  Research Assistant (August 2009 – August 2013)

  Worked under following grants:

  - 'Supervisory Control and Nonlinear Motion Control of Networked Autonomous Teams', Army Research Office (ARO) grant W91NF-05-1-0314,
  - 'Trust Based Collaborative Control for Teams on Communication Networks', Air Force Office of Scientific Research (AFOSR) grant FA9550-09-1-0278,
  - 'Adaptive Dynamic Programming for Real-Time Cooperative Multi-Player Games and Graphical Games', NSF grant ECCS-0801330,

  as a team member, researcher in distributed control of multi-agent systems. In particular, pertinent research topics were

  - Discrete-time multi-agent system distributed synchronization control; novel geometric technique is introduced to guarantee discrete-time multi-agent system synchronization.
  - Discrete-time distributed observer design; distributed observation in discrete-time is investigated together with its potential use in distributed dynamic regulator design for multi-agent system synchronization.

- Optimal control of multi-agent systems, performance criteria are found for distributed linear cooperative consensus and synchronization control.
- Extending classical results to multi-agent systems having heterogeneous agents and multi-agent systems with disturbances.
- Output cooperative feedback for consensus, synchronization and optimal output feedback

- **Czech Technical University in Prague, FEL, Department of Control Technology**

  Postdoctoral fellow (October 2013-2016)

  Worked on distributed micromanipulation and dielectrophoresis, supported by the European social fund within the framework of realizing the project „Support of inter-sectoral mobility and quality enhancement of research teams at Czech Technical University in Prague“, CZ.1.07/2.3.00/30.0034. Period of the project´s realization 1.12.2012 – 30.6.2015.

  Collaborated in the capacity of Supervisor Specialist of one PhD student on the project ARRAYCON, European Commission Research Executive Agency, Marie Curie Actions- Networks for Initial Training-project 605087.

  In 2016 successfully applied for the junior project with GAČR, (Grantova Agentura Češke Republice-Czech Republic Granting Agency), project 16-35493Y for the period 2016-2018, to research applications of multi-agent sensors and actuators for estimation and control of large-scale distributed parameter systems.

  In particular, pertinent research topics were

  -Distributed parameter systems, distributed estimation, sensor fusion, distributed control

  -Synchronization in presence of communication delays

  -Output synchronization of heterogeneous agents, H_{oo} output synchronization, cooperative multi-player graphical games

  Assistant Professor (April 2016-present)

  Serves also as the Academic Coordinator for the SpaceMaster program, a liaison from CTU to the SpaceMaster consortium, representing CTU at regular Consortium meetings and closing ceremonies. Organized the SpaceMaster closing ceremony in Prague, October 2017. In addition to that organized Consortium meetings on October 27th and 28th. Organized and moderated the Scientific Workshop, an event taking place along the main commencement ceremony.

Teaching

- Teaching Assistant for **Mathematics 1**, **Mathematics 2** and **Signals and Systems**, at Faculty of Electrical Engineering, University of Zagreb, 2006-2009
- Teaching Assistant for numerous undergraduate and graduate courses: **Control Systems, Circuit Theory, Electronics, Linear Systems, Distributed Decision and Control** at Electrical Engineering College, University of Texas at Arlington, 2009-2013.
- Occasionally thought classes in **Control Theory**, **Linear Systems**, and **Nonlinear Systems** at the EE College, UTA, 2009-2013.
- Served as a supervisor to a visiting scholar **Chen Zhimin** at UTA in Spring 2013
- Thought graduate level **Optimal Control** at CTU in Spring semester, 2014

- Introduced PhD level course **Cooperative Control of Multi-agent Systems** into curriculum at CTU in Autumn 2014, https://moodle.dce.fel.cvut.cz/course/view.php?id=73
- Organized and thought the MS. level course **Dynamics and Control of Networks** at CTU in Autumn 2017, https://moodle.fel.cvut.cz/course/view.php?id=1628
- Thought specific lectures and prepared exercises in the master's level course **Space Engineering** (B3M37KIN),

  https://www.fel.cvut.cz/cz/education/bk/predmety/47/49/p4749406.html
- Served as a Supervisor Specialist for two Ph.D. students **Xueji Zhang** and **Štefan Knotek** at CTU in Autumn 2014-Spring 2015. Xueji Zhang successfully defended his PhD in May 2018; Stefan Knotek finished his study period and is progressing in research and publications towards his eventual defence.

Research topics of interest

Topics of broad interest: Automation & Control Systems, Control Theory, Physical systems-modelling and control, Ordinary Differential Equations, Partial Differential Equation, Dynamical Systems, Differential Geometry, Differential Topology, General Topology, Classical Mechanics, Electromagnetism

Main results achieved in: Distributed Control, Complex Systems, Dynamical Systems, Optimal Control

Honors and Awards:

- Recipient of *state scholarship, from the Ministry of Education*, University of Zagreb, 2004-2009
- Awarded *Rector's Prize*, for the research work, University of Zagreb, 2009
- Recipient of *STEM Doctoral Fellowship*, UT Arlington, 2009
- Inducted into *Golden Key Honor Society*, UT Arlington Chapter, 2010
- Second place prize, *N.M. Stelmakh Outstanding Student Research Award*, University of Texas at Arlington, 2013
- Dean's Summer Fellowship awarded for Summer 2013

Research visits:

Short visit to United States in July 2014 with a PhD student Jiri Zemanek from CTU. Visit included University of Maryland, DC, University of California at Santa Barbara and Rochester Institute of technology, where the work done by our group in Prague was presented to potential collaborators. The purpose of the visit was establishing connections with researchers in the field of dielectrophoresis.

Regular stays with the Department of Electronic Systems and Information Processing (ZESOI), Faculty of Electrical Engineering and Computing, University of Zagreb, as a collaborator on the project *ASYRMEA*, in the period 2016-2018

Languages: English, German, Italian, Croatian, conversational French

LIST OF PUBLICATIONS 2018

Books (1)

1. Frank L. Lewis, Hongway Zhang, Kristian Hengster-Movric, and Abijit Das, *Cooperative Control of Multi-Agent Systems: Optimal Control and Adaptive Control*," Springer-Verlag, 2014.

Book Chapters (1)

1. Kristian Hengster-Movric and Michael Sebek, Synchronizing Region Approach for Identical Linear Time-Invariant Agents", *Control of Complex Systems - Theory and Applications*, Ch. 18, Elsevier, pp. 519-548, 2016.

Journal papers (12)

1. Tomislav Petkovic, Kristian Hengster-Movric, Patricius' Phenomenological Theory of Tides and its Modern Relativistic Interpretation, *SYNTHESIS PHILOSOPHICA* 42 vol. 2., 2006. pp. 255–266.
2. Zvonko Kostanjcar, Kristian Hengster-Movric, Branko Jeren, Model of discrete dynamics of asset price relations based on minimal arbitrage principle, *Central European Journal of Physics*, June 2011, vol 9, issue 3, pp. 865-873.
3. Kristian Hengster-Movrić, Stjepan Bogdan, Ivica Draganjac, Multi-agent Formation Control Based on Bell-shaped Potential Functions, *Journal of Inteligent and Robotic Systems-JIRS*, 2010, vol. 58, no. 2., pp 165-189. DOI: 10.1007/s10846-009-9361-7.
4. Kristian Hengster-Movric, Keyou You, Frank.L: Lewis, Lihua Xie, Synchronization of discrete-time multi-agent systems on graphs using Riccati design, *Automatica*, Feb 2013, vol. 49, no. 2, pp. 414-423. DOI: 10.1016/j.automatica.2012.11.038.
5. Kristian Hengster-Movric, Frank Lewis, Cooperative observers and regulators for discrete-time multiagent systems, *International Journal of Robust and Nonlinear Control*, May 11, 2012, DOI: 10.1002/rnc.2840
6. Kristian Hengster-Movric, Frank Lewis, Cooperative Optimal Control for Multi-agent Systems on Directed Graph Topologies, *IEEE Transactions on Automatic Control*, 2013, DOI: 10.1109/TAC.2013.2275670
7. Kristian Hengster-Movric, Frank L. Lewis**,** Michael Sebek, Distributed Static Output-feedback Control for State Synchronization of Multi-agent Systems, *Automatica* 53(2015), pp. 282–290.
8. Kristian Hengster-Movric, Frank L. Lewis, Michael Sebek, Tomas Vyhlidal, Cooperative synchronization control for agents with control delays: A synchronizing region approach, *Journal of the Franklin Institute*, 2015
9. Kristian Hengster-Movric, Michael Sebek, Sergej Celikovsky, Structured Lyapunov functions for synchronization of identical affine-in-control agents—Unified approach, *Journal of the Franklin Institute* 353 (14), pp. 3457-3486, 2016
10. Xueji Zhang, Kristian Hengster-Movric, Michael Sebek, Wim Desmet, Cassio Faria, Distributed observer and controller design for spatially distributed systems, *IEEE Transactions on Control Systems Technology*, 1-13, 2017

11. Farnaz A. Yaghmaie, Kristian Hengster Movric, Frank L. Lewis, Rong Su, Michael Sebek, H_∞-output regulation of linear heterogeneous multiagent systems over switching graphs, *International Journal of Robust and Nonlinear Control* 28 (13), pp. 3852-3870, 2018
12. Martin Gurtner, Kristian Hengster-Movric, Zdenek Hurák, Green's function-based control-oriented modeling of electric field for dielectrophoresis, *Journal of Applied Physics* 122 (5), 054903, 2017

Conference papers(9)

1. Kristian Hengster-Movric, Stjepan Bogdan, Ivica Draganjac: Formation Control Based on Adaptive Bell-shaped Potential Functions. *ECMR 2009*, pp. 141-146.
2. Kristian Hengster-Movric, Stjepan Bogdan, Ivica Draganjac, Bell-shaped potential functions for multi-agent formation control in cluttered environment, *Mediteranean Conference on Control and Automation - MED 2010*, DOI: 10.1109/MED.2010. 5547604
3. Kristian Hengster-Movric, Keyou You, Frank L. Lewis, Lihua Xie: Synchronization of discrete-time multi-agent systems on graphs using H_2-Riccati design. *CCA 2012*, pp. 439-444.
4. Kristian Hengster Movric, Synchronizing Region Approach to Identical LTI System State Synchronization Distributed Control; Continuous and discrete-time systems, state, output-feedback and delays, *Process Control Conference, June 2015*, Štrbske Pleso Slovakia.
5. Farnaz A. Yaghmaie, K. Hengster-Movric, Frank L. Lewis, Rong Su, Michael Sebek, Output H_∞ synchronization of heterogeneous linear multi-agent systems via a distributed output-feedback, *IEEE 55th Conference on Decision and Control (CDC)*, pp. 2677-2682, 2016
6. Xueji Zhang, Kristian Hengster-Movric, M. Šebek, Distributed observer and controller design for state-output decomposed systems, *IEEE Conference on Control Applications (CCA)*, pp. 450-455, 2016
7. Xueji Zhang, Kristian Hengster-Movric, and Michael Šebek, Wim Desmet, and Cassio Faria, Consensus-based distributed sensor fusion over a network, *2017 IEEE Conference on Control Technology and Applications*, pp. 674-679, 2017
8. Štefan Knotek, Kristian Hengster-Movric, and Michael Sebek, Distributed adaptive consensus protocol with decaying gains on directed graphs, *6th IFAC Workshop on Distributed Estimation and Control in Networked Systems*, Tokyo, Japan, September, 2016. IFAC-PapersOnLine 49 (22), pp. 355-360, 2016
9. Štefan Knotek, Kristian Hengster-Movric, Michael Šebek, Distributed adaptive consensus protocol with Laplacian eigenvalues estimation, 21st International Conference on Process Control (PC), 2017, pp. 269-273, 2017